UNIVERSITA' DEGLI STUDI DI UDINE

CORSO DI DOTTORATO DI RICERCA IN
SCIENZE BIOMEDICHE E BIOTECNOLOGICHE

CICLO XXV

FUNCTIONAL REGULATION AND NON-CANONICAL ROLES OF DNA REPAIR PROTEINS IN MAMMALIAN CELLS

Dottorando: GIULIA ANTONIALI

Relatore: prof. GIANLUCA TELL

ANNO ACCADEMICO 2012/2013

1 Table of contents

2 Preface

Apurinic/apyrimidinic Endonuclease 1 / Redox factor 1 (APE1/Ref-1) is a multifunctional and an essential protein in mammals [1]. It plays an essential role in cellular response to oxidative stress conditions [2] and contributes to maintenance of the genome integrity [3]. It is expressed ubiquitously and at high levels in tumor cells, approximately 4×10^7 molecules per cell [4][5], albeit the intracellular localization pattern can be heterogeneous among different tissues [6]. Its acronym reflects its, at least, dual nature: apurinic/apyrimidinic (AP) endonuclease, or APE1, was first discovered as a major constituent of the base excision repair (BER) pathway [7] that copes with DNA damages induced by oxidative and alkylating agents, including chemotherapeutics [8]. Ref-1, the acronym for redox effector factor-1, refers, instead, to APE1 transcriptional regulatory activity in modulating gene expression through a redox-based co-activating function on several transcription factors involved in cancer promotion and progression [9-11]. These two activities are split into two functionally independent domains of the protein itself: the N-terminal portion of the protein, which contains a bipartite nuclear localization signal (NLS), is devoted to the transcriptional co-activating function; on the other hand, the C-terminal domain exerts the endonuclease activity on DNA abasic sites. The latter domain is highly conserved; conversely, the N-terminal region presents wider variability among different organisms, being more conserved in mammals and thus suggesting a recent acquisition during evolution.

Due to its emerging role as a new target for chemotherapy, comprehension of the functional regulation of this pleyotropic protein represents a scientific frontier in translational medicine.

Over the past two decades, knowledge of the biological functions, mechanisms of action, interactions and regulation of the protein APE1/Ref-1 has grown exponentially. It has been shown that APE1/Ref-1 participates in multiple cellular processes that are not only confined to DNA repair and maintenance of genome stability. Notably, this concept is emerging as a new paradigm in the DNA repair field. Emerging evidences have indeed pointed out that also other DNA repair enzymes may play important roles in transcriptional regulation of genes suggesting that nucleic acid processing enzymes are more strategically promiscuous than originally thought.

Beside its dual nature as a DNA repair enzyme and as a redox factor, several other functions have been indeed discovered for APE1/Ref-1.

Recent findings demonstrated that APE1/Ref-1 N-terminal portion also interacts with different proteins involved in ribosome biogenesis, pre-mRNA maturation/splicing and ribonucleotide catabolism, highlighting an unexpected role of APE1/Ref-1 in RNA metabolism [12][13]. In addition, at least two independent studies have shown that APE1/Ref-1 cleaves abasic RNA *in vitro* and *in vivo* [14], as well as a specific coding region of c-*myc* mRNA *in vitro,* likely influencing the expression of the oncogene in cells [15]. Accordingly, APE1/Ref-1 has been proposed as a main candidate factor in the abasic RNA cleansing process, explaining some of the activities exerted by APE1/Ref-1 on gene expression through post-transcriptional mechanisms.

Another interesting, though yet poorly investigated, function of APE1/Ref-1 was discovered during investigation of trans-acting factors that act as Ca^{2+}-dependent repressor of the parathyroid hormone (PTH) gene by binding to the negative Ca^{2+} responsive elements (nCaRE) in its promoter [16]. Expression of the PTH gene is down-regulated in response to an increase in intracellular calcium concentration, which is mediated by two DNA sequences, i.e. nCaRE-A and nCaRE-B, which were first discovered in the promoter of PTH and later in other promoters including APE1 promoter itself. Subsequently, further experiments have demonstrated that APE1 requires other factors, such as heterogeneous ribonucleoprotein L (hnRNPL) [17], Ku antigen (KuAg) [18] and PARP-1 [19] to stably bind nCaRE elements. It was also shown that APE1/Ref-1 affinity for nCaRE elements is enhanced when p300/CBP acetylates protein Lys6 and Lys7 residues as a result of an increase in extracellular Ca^{2+} concentration [20].

At present, information is still inadequate regarding the molecular mechanism responsible for the coordinated control of APE1/Ref-1 several activities. Regardless of transcriptional control, the fine-tuning of the multiple functions of this essential protein may reside on its post-translational modifications (PTM) and on the modulation of its interactions with other proteins under different conditions. While for some PTMs a functional role has been proposed (i.e. acetylation at Lys6/7 and Lys27/31/32/35 and ubiquitination at Lys24/25/27) [21] the identity of proteins that interact and modulate APE1/Ref-1 biological functions is still under investigation.

Several reports indicated that deregulation of APE1/Ref-1 in both expression and subcellular localization is associated to different tumorigenic processes [22]. Different studies have also shown a correlation between high level of APE1/Ref-1 and tumor resistance against chemotherapeutic drugs and ionizing radiation, implying that APE1/Ref-1 enhances repair and survival of these tumor cells [23], and, furthermore, other studies have demonstrated that subcellular distribution of APE1/Ref-1 has also been linked to tumor aggressiveness. For these reasons, APE1/Ref-1 is actually considered a promising and powerful pharmacological target. However, APE1/Ref-1 is a

pleiotropic protein playing a critical role not only in DNA repair but also in regulating apoptosis, cell proliferation and an adaptive cell response to oxidative stress. Therefore, the question remains to understand the relative importance of attenuation of APE1's repair or transcriptional functions by small molecule inhibitors as a potential approach for reversing drug resistance. Thus, dissecting the molecular mechanism underlying APE1/Ref-1 regulation and functions in mammalian cells is extremely interesting especially for the translation relevance in the field of molecular medicine.

3 Synopsis

Apurinic/apyrimidinic Endonuclease 1 / Redox factor 1 (here after referred to as APE1) is a multifunctional protein contributing to genome stability, through its central role in the BER pathway of DNA lesions, caused by oxidizing and alkylating agents. It also plays a role in gene expression regulation, as a redox co-activator of several transcription factors and in RNA metabolism. Another interesting and yet poorly characterized function for this non-canonical DNA repair protein is associated to its ability to bind to negative calcium responsive elements (nCaRE) of some gene promoters, thus acting as a transcriptional regulator. Since nCaRE sequences are located within ALU repeats, transposable elements that occupy at least one tenth of the human genome, many other functional nCaRE sequences could exist and play a role in the transcriptional regulation of genes. However, at present, specific information concerning an accurate number and the identity of genes containing these sequences within their own promoter are still evanescent, as well as the knowledge of how these elements plays an active biological function. Thus, the quest for functional nCaRE sequences on human genome would provide new insights on APE1 multifunctional roles and, in particular, it would identify new potential genes whose expression may be regulated by APE1 through nCaRE binding opening new hypothesis for understanding the functional link existing between DNA repair and transcriptional regulation.

The present work is devoted to address this issue and is focused on the characterization of the molecular mechanisms responsible for APE1 binding to nCaRE sequences and its relevance in DNA-damage induced transcriptional regulation of genes during cell response to genotoxic damage.

To this aim, a bioinformatic analysis systematically looking for functional nCaRE sequences within the human genome has been performed by filtering expression profile data of genes resulting deregulated upon APE1 knockdown. This analysis revealed the presence of multiple nCaRE sequences in genes deregulated upon APE1 silencing and conserved in mouse genome. Among the list of genes, whose expression is potentially regulated by APE1, attention was focused on the deacetylase sirtuin1 (SIRT1) due to its relevant involvement in cell stress, including senescence, apoptosis, tumorigenesis and, in particular, its role in the cell response to genotoxic agents through its deacetylating activity on APE1 N-terminal domain. Through a multidisciplinary approach, based on SPR, limited proteolysis, ChIP and gene reporter assays, it has been found that the APE1 N-terminus is required for the stable binding to nCaRE elements present within

SIRT1 promoter. APE1 was demonstrated to be part of a multi-protein complex, that includes hOGG1, Ku70 and RNA Pol II, which is quickly recruited on SIRT1 promoter upon oxidative damage playing a central role in the regulatory function of SIRT1 gene expression.

These findings show that recruitment of repair enzymes to the transcription initiation site of the SIRT1 promoter occurs during early cell response to oxidative stress. All together, our data underline the importance of APE1 during the transcriptional initiation process, in positively promoting transcription of genes under genotoxic conditions. Our findings provide a general model unveiling BER enzymes involvement in controlling specific gene expression at the transcriptional level.

4 Introduction

4.1 DNA repair pathways

The genome of eukaryotic cells is permanently exposed to endogenous and exogenous DNA-damaging agents. DNA damage resulting from endogenous agents includes oxidation by reactive oxygen species (ROS) generated from normal metabolic processes, alkylation by agents such as *S*-adenosylmethionine, adduct formation resulting from attack by reactive carbonyl species formed during lipid peroxidation, hydrolytic depurination leading to the formation of abasic sites, or deamination of bases [24]. Exogenous agents, instead, comprise different environmental insults (chemicals, carcinogens, UV light), chemotherapeutic agents, and radiation damage [25]. If not repaired, DNA damage can result in mutations, diseases and cell death [26]. However, organisms have evolved several DNA-repair pathways to promptly correct the DNA damage preventing genome instability and mutagenesis. Each repair pathway is directed to specific types of damage and a given type of damage can be targeted by several pathways. Figure 1 reported the major DNA repair pathways which are mismatch repair (MMR), nucleotide excision repair (NER), base excision repair (BER), homologous recombination repair (HR), and non-homologous end joining (NHEJ) [23][27][28] (Figure 1). Distinct DNA damage is repaired by different pathways and mechanisms, however, overlap and interaction between the various pathways and, in addition, some overlap in mechanisms can occur. Knowledge about the number of DNA-repair proteins and factors involved in the cellular response to DNA damage, as well the regulatory networks that are induced by persistence of DNA damage in the cell, is increasing as more and more information is obtained [29]. Interaction of different DNA-repair pathways and mechanisms furnish the most efficient defense for the cell to prevent genomic instability. Several diseases has been reported to be associated with defects in DNA repair, including Xeroderma pigmentosum, Cockayne syndrome, trichothiodystrophy, Werner syndrome, and Bloom syndrome [30][31].

The description of each DNA repair pathways is far from my intention, for a comprehensive reviews on each DNA-repair pathway the reader is directed to [32-38] and to the following link for an updated information on the individual repair proteins http://sciencepark.mdanderson.org/labs/wood/dna_repair_genes.html [29]. What follow is instead an overview of BER pathway to provide a context for understanding the role of APE1 protein in DNA repair.

The BER pathway is responsible for the repair of DNA damage arising from alkylation, deamination, or oxidation of bases [39]. Alkylation of bases arises from exposure to either endogenous agents such as *S*-adenosylmethionine or exogenous agents, including environmental and chemotherapeutic agents, whereas deamination of cytidines and adenines occurs spontaneously. Oxidative damage can result from ROS generated by normal cellular processes, in addition to environmental or chemotherapeutic agents.

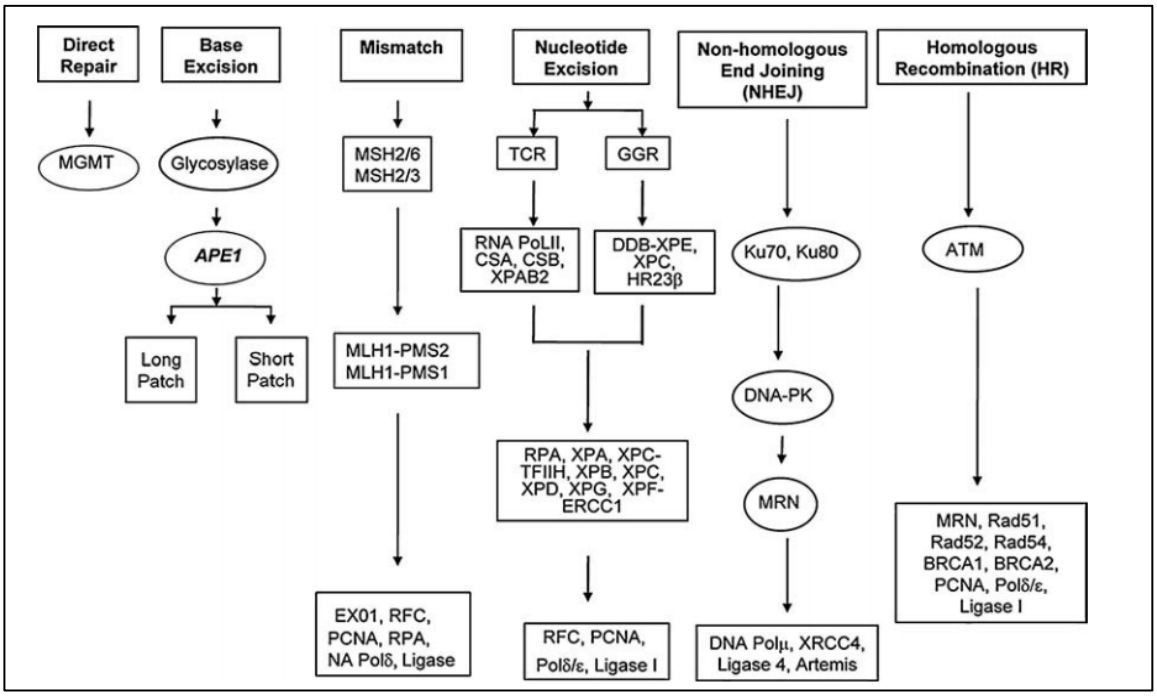

Figure 1 - Schematic overview of DNA-repair pathway.
Genome stability is maintained by several DNA-repair pathways, including direct repair (DR), base-excision repair (BER), nucleotide-excision repair (NER), mismatch repair (MMR), homologous recombination (HR), and non-homologous end joining (NHEJ). (Image from Luo M. *et al*., *Antiox. Redox Signal*., 2010)

4.2 Oxidative DNA damage and its repair in mammalian cells

The genome content of eukaryotic cells is constantly subjected to reactive oxygen species (ROS) exposure. ROS are formed during a variety of biochemical reactions and cellular functions which can be derived from the external environment, but predominantly from endogenous byproducts of respiration [40]. Another major source of ROS production is represented by phagocytic NADPH oxidases during inflammatory responses and by non-phagocytic NADPH oxidases, as determined in different cell systems [41]. ROS are also produced by cellular oxidase in response to different external insults including environmental chemicals and chemotherapeutic drugs, ultraviolet (UV) light or ionizing radiation.

In its ground state, molecular oxygen (O_2) is relatively unreactive. However, during normal metabolic activity O_2 is capable of generating harmful reactive excited states such as free radicals and derivatives. All ROS are extremely reactive and can cause molecular damage, leading to cell death [42]. All the intermediate oxygen species can interact with i) proteins, ii) lipids and iii) nucleic acids to cause several damages [43].

Exposure of nucleic acids to reactive species may result in strand breakage, nucleic acid-protein crosslinking, and nucleic base modification. Base modification, crosslinking of DNA-DNA and DNA-proteins, sister chromatid exchange, and single- or double-strand breakage may lead to block of transcription, translation, and DNA replication [44]. Therefore it is not surprising that ROS-induced genome damage has been implicated in number of diseases, including cardiovascular dysfunction, arthritis, and cancer, as well as in the aging process and aged-related neurodegenerative disorders.

The most abundant oxidative genome damage product is oxidation of purines leading to various chemical modifications: the highly mutagenic guanine derivate 8-hydroxyguanine (8-oxoG) and the formamidopyrimidines (FapyG and FapyA) (Figure 2). The common oxidized pyrimidines are the thymine glycol (TG) and 5-hydroxyuracil (5-OHU); the latter is generated via oxidative deamination of C. Except for TG, these abnormal bases do not block DNA replication but could be mutagenic if not correctly recognized and repair. For example, the miscoding effect of 8-oxoG lesion is due to DNA polymerase activity which inserts adenine opposite to 8-oxoG, resulting in G:C to A:T transition mutations, therefore generating a DNA base mutation. The less common oxidized base lesions such as 8-oxoA, 5-formylU and 5-OHC could be also mutagenic.

All these described oxidized base are recognized by different DNA glycosylases, which remove the damaged nitrogenous base by cleaving the N-glycosylic bond and generating an abasic (AP) site while leaving the sugar-phosphate backbone intact. This reaction represents the initiation step of the BER pathway.

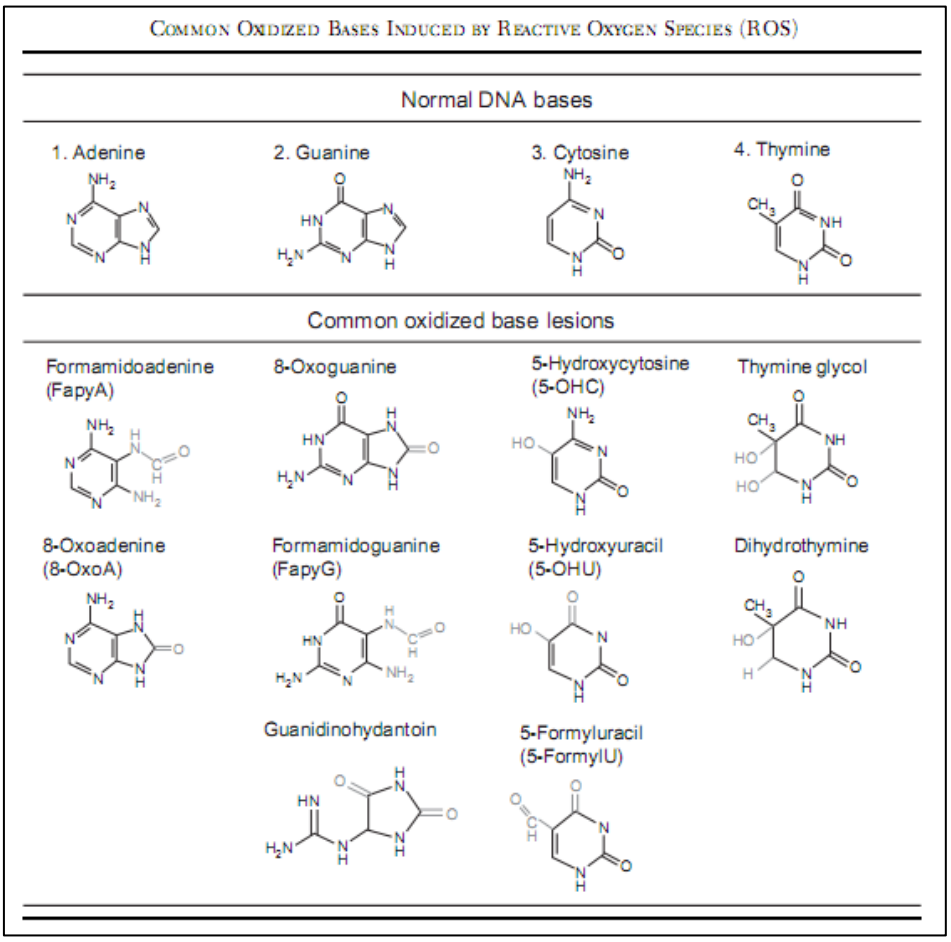

Figure 2 - Chemical structures of the four canonical bases and of the oxidized nucleotides processed by the BER pathway.
Oxidative modifications are shown in gray. (Image from Hegde M.L. *et al*., *Prog Mol Biol Transl Sci*., 2012)

4.3 The Base Excision Repair pathway

Damage to mammalian genomes, induced by a variety of ROS includes a plethora of oxidative damaged bases, abasic sites and DNA single-strand breaks (SSBs). It is generally estimated that more than 10^4 base lesions and SSBs are induced daily in a mammalian cell genome [45]. These base lesions and SSBs are typically repaired via the evolutionarily conserved DNA base excision repair (BER) pathway.

BER is primarily responsible for repairing non-helix distorting base lesions produced by alkylation, oxidation or deamination of bases [46]. The currently accepted model for the core BER pathway reveals the presence of five distinct and coordinated enzymatic steps, as reported in Figure 3 [28]. The BER pathway is initiated by the removal of oxidated, alkylated or deaminated bases through enzymes called DNA glycosylases. Cells contain several DNA glycosylases, each of them exhibiting a specific substrate spectrum. Glycosylases catalyzes the hydrolysis of the N-glycosidic bond of the damaged nucleoside, the damaged base is released and an AP site is created. An AP

site can also occur spontaneously and represents damage itself. Glycosylases are of two types, monofunctional and bifunctional. Monofunctional glycosylases [*e.g.*, *N*-methyl purine DNA glycosylase (MPG or AAG)] excise the damaged base to generate an AP site, which is successively processed by the multifunctional AP endonuclease, APE1. Bifunctional glycosylases such as the human 8-oxoguanine DNA glycosylase (hOGG1), human endonuclease VIII–like DNA glycosylase (NEIL1-3), and *E. coli* endonuclease III (NTH) glycosylase have an intrinsic AP lyase function [47][48] that cleaves the sugar-phosphate backbone 3′ to the AP site. The resulting AP site is processed by APE1, which hydrolyzes the phosphodiester backbone immediately 5' to the AP site, creating 3' OH and 5' deoxyribose phosphate (5' dRP) termini. At this step, the resulting single-strand break (SSB) can be processed by either two pathways, the “short-patch” (SP-BER), where a single nucleotide is replaced, or the “long-patch” BER (LP-BER) where several new nucleotides are synthesized by a DNA polymerase. In SP-BER, the one-nucleotide gap is filled by DNA Polymerase β (Pol β) which incorporates a nucleotide and its deoxyribophosphodiesterase (dRPase) activity removes the 5′ moiety and uses the 3' OH terminus to insert the correct base. In LP-BER pathway a segment or flap of three to eight nucleotides surrounding the AP site is displaced, followed by insertion of the correct nucleotides by DNA polymerase *δ, ε*, or *β*, along with proliferating cell nuclear antigen (PCNA) and replication factor-C (RF-C). After resynthesis, flap endonuclease 1 (FEN1) removes the displaced strand. Finally a DNA ligase, DNA ligase III/XRCC1, can complete the repair process and restore the integrity of the helix by sealing the single-stranded DNA nick. Beside these enzymes, a number of accessory proteins are also involved, such as the scaffold protein X-ray cross-complementation group 1 (XRCC1), and the poly(ADP-ribose) polymerase 1 (PARP-1) which is an enzyme capable of immediately binding to an incised AP site, recruiting other BER proteins and increase overall process efficiency [49].

All the steps of the BER pathway must be finely orchestrated both from thermodynamic and the kinetic point of view, to provide an accurate repair of the damage base. In this context, APE1 plays a crucial role since evidences from reconstituted systems and from cell extracts suggest that, besides providing the AP endonuclease activity, APE1 contributes also to the coordination of the different BER steps by interacting directly or indirectly with other BER enzymes and with other repair pathways. APE1 can interact with different glycosylases (OGG-1, MYH, MPG), with Pol β, with XRCC1, which in turn stimulates APE1 endonuclease activity, or with FEN1, directly stimulating its activity [6]. Due to its ability to recruit different protein factors, APE1 can be considered as one of the key elements capable of aggregating together different proteins

to form large DNA-repair factories. The molecular basis of the specificity of these interactions, as well as their biological significance, remains to be largely determined.

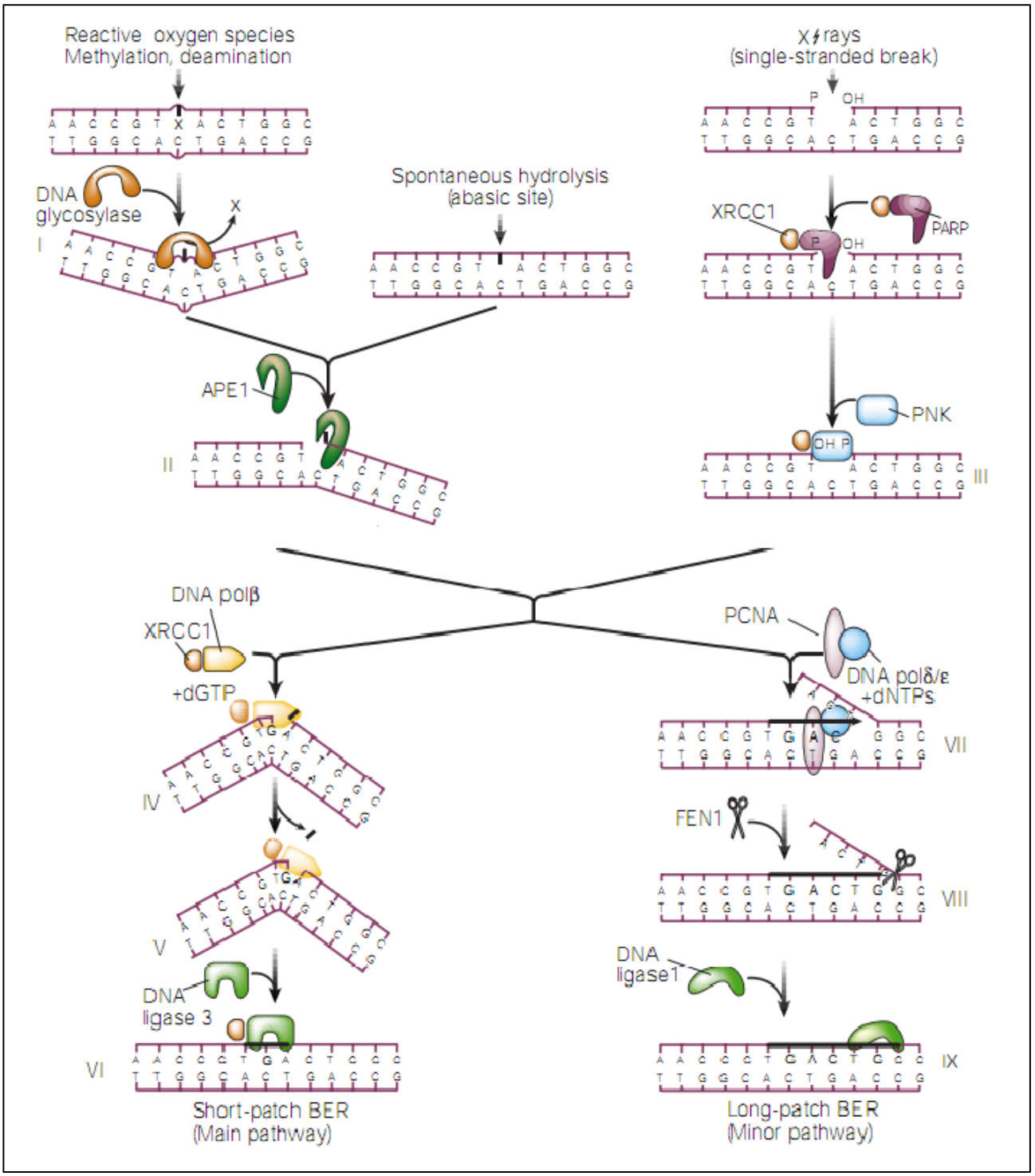

Figure 3 - Schematic representation of BER pathway illustrating both short- and long-BER pathway. (Image from Hoeijmakers J., *Nature,* 2001)

4.3.1 Proteins involved in BER

DNA Glycosylases

DNA glycosylases (DG) catalyze the first step of BER pathway. Individual base lesions are recognized by distinct DNA glycosylases. These classes of enzymes flip the damaged base out of the double helix, while leaving the sugar-phosphate backbone intact, creating an apurinic/apyrimidinic site (AP). Eleven different mammalian glycosylases have been characterized so far, which can be broadly divided into two different mechanistic subclasses: the monofunctional or “pure” glycosylases and the bifunctional glycosylases (Table 1). Monofunctional glycosylases have only glycosylase activity, whereas bifunctional glycosylases also possess AP lyase activity that permits them to cut the phosphodiester bond of DNA, creating a single-strand break without the need for an AP endonuclease. The peculiarity of DNA glycosylases is the specific recognition of different damaged bases. Lesion recognition, particularly in chromatin of mammalian which is highly condensed, poses a serious challenge for DNA glycosylases which has not been extensively understand. Analysis of crystal structure of DNA glycosylase have revealed that the mechanism of base lesion excision involved the flipping of the damaged base out of the double helix into the DG active site pocket. DNA glycosylases bind to the minor groove of DNA, kinking it at the site of damage, and flip the lesion nucleotide out of the major groove of DNA. Only those lesions that could accommodate in the active pocket after nucleotide flipping are removed. To cleave the N-glycosidic bond, monofunctional glycosylases use an activated water molecule to attack the anomeric carbon of the substrate. Bifunctional glycosylases, instead, use an amine residue as a nucleophile to attack the same carbon, going through a Schiff base intermediate. While the high-resolution structures of a number of DNA glycosylases provided important information about the mechanism of action of glycosylases towards its specific substrates, it remains still elusive how DNA glycosylases are coordinated with the enzymes that follow them in the BER pathway. It is likely that protein-DNA interaction surfaces play a large role coupled to protein-protein interactions and steric displacements.

Based on structural similarity, glycosylases are grouped into four structural subfamilies and inside these into more groups based on the specificity to substrate and subcellular localization. The UDG and AAG families contain small, compact glycosylases, whereas the MutM/Fpg and HhH-GPD families comprise larger enzymes with multiple domains [50].

Table 1 - The mammalian DNA glycosylases and their specificity towards different substrates. (Table from Vascotto C. and Fishel M., Academic Press, 2012)

Glycosylase	Enzyme	Substrate	Type
UNGs	UNG	U	Monofunctional
	TDG	U:G, T:G	
	SMUG1	U, OHmeU	
HhH	MBD4	U:G and T:G in CpG sites	Monofunctional
	OGG1	8-oxoG:C, faPyA, faPyG	Bifunctional
	MYH	A:8oxoG	Monofunctional
	NTH1	TG, DHU, faPy	Bifunctional
H2TH	NEIL1	faPyA, faPyG, DHU, TG, 8-oxoG	Bifunctional
	NEIL2	5-OHU, DHU	
	NEIL3	Unknown	Bifunctional?
AAG	AAG	3-meA, 7-meG, hypoxanthine	Monofunctional

AP Endonucleases

Removal of damaged base by DNA glycosylases leads to the formation of AP sites, which can also arise spontaneously. Moreover, AP sites could be generated as a results of free radicals and alkylating agents that promote the release of bases by introducing base modifications that destabilize the N-glycosylic bond [45]. In the BER pathway, cleavage of baseless sites in DNA is performed by an AP endonuclease. The major human AP endonuclease is APE1 protein (also known as Ref-1 or HAP1), a homolog of bacterial Exonuclease III [51]. The fundamental role of this enzyme is highlighted by genetic studies demonstrating that nullizygous mice for APE1 gene result in early stage embryonic lethality (E5 to E9) and attempts to isolate stable APE1-knockout cell lines were totally unsuccessful [52]. Moreover, downregulation of APE1 expression levels in human cells through RNAi leads to AP site accumulation, reduced cell proliferation and triggering of apoptosis [53]. APE1, in a Mg^{2+}-dependent manner, is able to recognize an AP site and cleave the phosphodiester bonds 5' to the AP site, leaving a 3'-hydroxyl group and 5'-deoxyribose phosphate (dRP) termini flanking the nucleotide gap (see also 4.5.2) [54].

In addition to its crucial role in the BER pathway, APE1 also exerts other different functions within the cells: it works as a redox protein stimulating the DNA binding activity of several transcription factors that are known to be involved in cancer promotion and

progression. Reader is redirected to chapter 4.5 for full comprehensive annotations of all APE1 activities and functions.

DNA Polymerases

Excision of a damaged base and subsequent processing of AP site by APE1 endonuclease results in an intermediate containing a 3'-hydroxyl, which represents the suitable priming strand for the resynthesis operated by a DNA polymerase and a 5'-dRP that must be removed prior to completion of repair by a DNA ligase [55]. In the SP-BER, where a single nucleotide is removed and replaced, both DNA resynthesis and removal of the blocking 5'-dRP residue are carried out by Pol β a member of the X family of polymerases together with Pol σ, Pol λ, Pol μ and terminal deoxynucleotidyl transferase (TdT). The polymerase activity is located in the C-terminal domain of Pol β, while in the N-terminal resides the dRP lyase activity [56]. Pol β lacks any intrinsic proof-reading activity and the error frequency of short-patch base excision repair in mammalian cell extracts has been calculated to be of the order of $5\text{-}10 \times 10^{-4}$. Due to its essential function in BER pathway and therefore in the maintenance of genome integrity, overexpression of Pol β has been correlated with a number of cancer types, whereas deficiencies in Pol β result in hypersensitivity to alkylating agents, induced apoptosis, and chromosomal breaking [57][58].

As discussed above, Pol β removes the blocking 5'-dRP moiety through a β-elimination reaction, after the insertion of the nucleotide. However, if the dRP formed after incision of AP endonuclease is refractory to dRP lyase activity and therefore cannot be processed by Pol β, then a polymerase switch may occur with Pol δ and Pol ε continuing the strand synthesis with displacement of the DNA strand ahead of the polymerase. In this case, the repair is re-routed through the PCNA-dependent long-patch pathway in which between 2 and 8 nucleotides are removed and replaced [59].

DNA Ligases

The sealing of the nick with 3'OH and 5'P termini is operated by a DNA ligase ATP-dependent that utilizes the energy of phosphoanhydride hydrolysis to make a phosphodiester bond [60]. In human cells, two DNA ligases have been implicated in BER: DNA ligase I (Lig I) and DNA ligase III (Lig III). Lig I plays an essential role in DNA replication where it is active in joining Okazaki fragments [61]; however, Lig I has also been implicated in several DNA repair pathways including BER pathway [62]. Indeed, human cell lines containing a partially inactive Lig I exhibit hypersensitivity to such DNA-

damaging agents as ionizing radiation and alkylating agents, supporting the notion of a crucial role for Lig I enzyme in BER pathway and in particular in long-patch repair [63][64].

In mammals, DNA ligase III is present in two isoforms, Lig IIIα and Lig IIIβ. However, it is DNA Lig IIIα that has a crucial role in BER pathway as demonstrated by the fact that this enzyme was originally purified in complex with XRCC1 [65] and further analysis unveiled the biological relevance of this protein:protein interaction in short-patch BER [66].

4.3.2 Scaffold proteins involved in BER pathway

All the enzymes discussed above constitute the core of BER pathway and are sufficient to reconstitute BER *in vitro*. However, several other accessory proteins are involved in BER *in vivo* and although they do not exert a specific enzymatic activity, they provide a scaffold for the core BER enzymes. XRCC1 and PARPs are other key factors with direct roles in BER.
XRCC1 participates in BER as a scaffold to recruit BER proteins at AP site. It has been demonstrated that physically interacts with different proteins such as NEILs, APE1, Pol β and Lig IIIα. Relevance of XRCC1 is evidenced by the fact that its knockout results in embryonic lethality [67].

PARPs proteins act as a sensor of single strand break. PARPs constitute a superfamily with regulatory functions in various cellular processes. PARP-1 and PARP-2 are the ones implicated in BER pathway. They are activated by SSB when they transfer ADP-ribose moiety from NAD to a variety of proteins including themselves. However, PARPs direct involvement in BER pathway has not been fully characterized. It is likely that the main role of PARP-1 may be related to histone poly(ADP)-ribosylation, a modification that could facilitate the access of BER enzymes to the site of damage, or to recruitment of XRCC1 and Pol β through their interaction with automodified PARP-1 itself [68].

Other proteins have also been described to be involved in the process of BER: the proliferating cell nuclear antigen (PCNA) and the heterotrimer constituted by Rad9, Rad1 and Hus1, named 9-1-1. The first protein, PCNA, is required during LP-BER as support for Pol δ [69]. 9-1-1, as well PCNA, has been demonstrated to interact with and stimulate many BER proteins such as MYH, NEIL1, TDG, APE1, Pol β, FEN1 and Lig I, suggesting their involvement in replication-associated BER.

4.3.3 Complexity of BER pathway

An *in vitro* complete nuclear BER requires only four or five enzymes. Until recently, in fact, BER was believed to be the simplest among the DNA repair pathways. However, recent studies have revealed that BER is much more complex, involving a network of distinct cell cycle-dependent as well as genome region-specific repair sub-pathways and could also involve non-BER proteins.

Several non-canonical proteins have been demonstrated to participate in BER, even if their *in vivo* functions are yet to be fully unraveled. The list of non-BER proteins includes: YB-1, which has been shown to interact with NEIL2 [70], NTH1 and APE1 [71]; NEIL2 was also found to interact with hnRNP-U, a RNA-binding protein [72]; HMGB1 has been implicated in single strand break repair involving Pol β [73]; the tumor suppressor p53 was also shown to play a role in DNA damage repair through the binding of APE1 and Pol β [74]. The list of these non-BER proteins is still growing, highlighting the paradigm that BER *in vivo* is far more complex than *in vitro* repair. The observation and the characterization of the BER interactome which involves multiprotein interactions and complexes has led to a new paradigm where complete repair occurs in the BER complex (BERosome) [75]. The initial prevailing view of BER mechanism, based on co-crystal structure analysis of substrate-bound BER proteins, proposed that BER comprises a sequence of steps with individual repair enzymes carrying out reactions independently of one another. Since recent studies shown that BER enzymes stably interact with most downstream repair components, this initial view of BER as 'hand-off' or 'passing the baton' process has been revisited by Hedge *et al*. who proposed, rather, a new BER paradigm in which collaboration of multiple proteins in a coordinated fashion involving dynamic protein-protein interactions enhances repair efficiency. Although *in vivo* role of 'hand-off' versus interactome modes of repair is not yet clear, Hedge *et al*. proposed that preformed BER complexes predominantly repair endogenous base lesions, while repair via hand-off mechanism by sequential recruitment could occur with induced DNA damage. Further characterization of the dynamics of BERosomes is required to unravel the repair processes.

4.4 DNA repair enzymes and their involvement in gene regulation

A growing body of evidences points out that several DNA repair enzymes of BER pathway exert non-canonical functions that differ from the "orthodox" activity in maintenance of genome stability. Current reports indicate indeed the participation of

numerous DNA repair enzymes in other cellular processes distinct to DNA repair. This is an emerging paradigm observed for many proteins belonging to DNA repair pathways. Among these enzymes, for example, many papers have reported the relevance and involvement of PARP proteins and APE1 in multiple steps of gene regulation. PARP-1 and PARP-2 were originally described in connection to DNA repair and in physiological and pathophysiological processes associated with genome maintenance. PARP-1's enzymatic activity is stimulated dramatically by the binding of PARP-1 to damaged DNA and hence, most studies of PARP-1 to date have focused on its role in DNA repair and cell death pathways. Following DNA damage, PARP-1 protein located near the damaged region binds DNA breaks, activating the catalytic site, and begins to transfer ADP-ribose groups to the chromatin proteins located in the immediate vicinity. The modified proteins are released from the DNA, allowing repair enzymes to access the damaged region. However, rather than simply functioning as a repair enzyme, PARP-1 has been shown to be necessary for viability and to organize the chromatin structure of nucleoli, heterochromatin, and other sequences during development and under physiological condition evidencing its involvement in multistep events for regulated activation of gene transcription [76-79]. Recent reports have also identified important rearrangements in gene expression upon knockdown of PARP-2 suggesting the emerging transcriptional roles of this DNA-repair protein [80].

APE1, another critical enzyme in the BER pathway, is emerging as a key factor in multiple aspects of DNA and RNA metabolism. APE1 acts as the predominant AP site incision enzyme in mammalian cells. Genetic knockout of APE1 in mice causes postimplantation embryonic lethality [1][52] and any attempt to isolate stable APE1-knockout cell lines has been so far unsuccessful, underlining that APE1 is essential for cell viability. The essentiality of APE1 for mammalian cells seems to be mainly due to its DNA-repair activity in BER pathways [2]. However, attempts to restore this activity in cells not expressing APE1 by using the yeast homologous Apn1 [2], which lacks the redox-transcriptional activation domain, or an APE1 mutant lacking the acetylation sites but not the DNA-repair activity [81], were unsuccessful. These observations indicate that essentiality of APE1 may be due to its pleiotropic biological effects rather than merely to its DNA- repair activity. Previous works that combined mRNA expression profiling and proteomic analysis to determine the molecular changes associated with APE1 loss-of-expression were in agreement with this notion [53]. This approach has indeed identified that APE1 acts as a hub in coordinating different and vital functions in mammalian cells including cell growth, apoptosis, intracellular redox state, mitochondrial function, and cytoskeletal structure. Therefore, despite the central role played by APE in the BER pathway, APE1 is to be considered as a pleiotropic protein playing also a critical role in

the regulation of apoptosis, cell proliferation and an adaptive cell response to oxidative stress. The following chapter is dedicated to an update review describing the molecular basis for the multifunctional roles of this protein.

4.5 APE1: not only a DNA repair enzyme

Human APE1 was first cloned by Demple and colleagues in 1991 and successively, the same group also characterized its enzymatic activity on AP site-containing DNA [51]. One year later, Xanthoudakis and Curran described a protein which stimulated AP-1 DNA-binding activity through the conserved Cys residues in Fos and Jun and named this protein Ref-1, acronym of Redox Effector Factor-1. They also suggested that the newly identified protein may represent a novel redox component of the signal transduction processes that regulated eukaryotic gene expression [82]. It turned out that the two groups independently identified the same protein and described its endonuclease and redox functions which are exerted by two functionally independent domains.

4.5.1 APE1 structure and domain organization

The APE1/Ref-1 protein is 318 amino acids in length and has a MW of ~ 37 kDa. The structure of the human APE1 consists of two symmetrically related domains with similar topology and has a significant structural similarity to both bovine DNase I and its *E. coli* homologue Exonuclease III. APE1/Ref-1 is a globular alpha/beta protein consisting of two domains: N-terminal domain core residues 44-136 and 295-318; C-terminal domain core residues 137-260. Each domains is made up of a six-stranded beta-sheet surrounded by an alpha-helix which pack together to form a four layered α/β sandwich with overall dimensions of 40x45x40 Å (Figure 4) [83].

Besides these two structural domains of the protein, three functionally independent domains can be distinguished: i) the first 33–35N-terminal unstructured sequence is essentially involved in protein–protein interaction and is important for the RNA-binding activity of the protein [84] and the modulation of its catalytic activity on abasic DNA [5][85]; ii) the redox domain which spans the region between amino acids 35 and 127; and iii) the DNA repair domain which spans the C-terminal domain of the protein from about residue 161 onwards. Furthermore, whereas APE1 C-terminal domain involved in AP endonuclease activity is conserved from bacteria to humans, the redox function is unique to mammals. In fact, APE1 and *E. coli* Exonuclease III, the major AP endonuclease found within *E. coli*, are closely related in terms of structure and with also very similar endonuclease active sites. The sequence identity between APE1 and Exonuclease III is 27.7%. The most obvious structural difference between human APE1 and Exonuclease III is an additional 62 N-terminal residues found only in APE1. Within this N-terminal region of APE1 is a nuclear localization sequence. However, addition of

N-terminal residues alone does not confer redox activity; zebrafish APE1 includes a similar N-terminal addition but lacks redox activity [86].

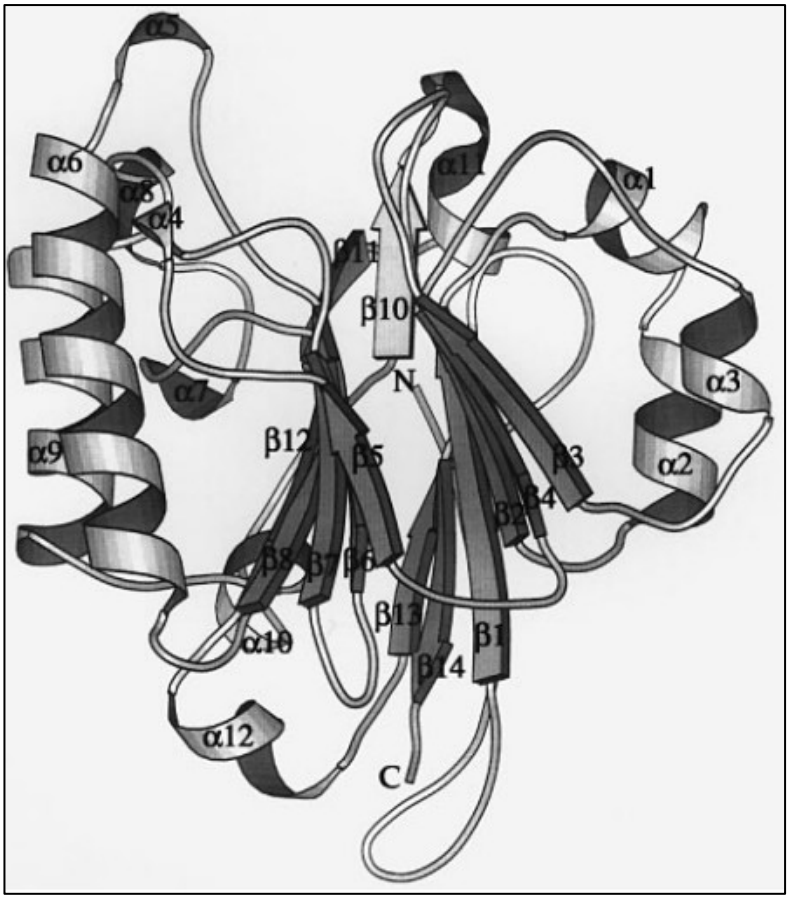

Figure 4 - Ribbon representation of the APE1 structure.
An α/β-sandwich is formed by the packing of two six-stranded β-sheets surrounded by α-helices, with strand order β3-β4-β2-β1-β14-β13 and β5-β6-β7-β8-β12-β9 from domains 1 and 2, respectively. The α-helices and β-strands are numbered sequentially from the N-terminus. (Image from Gorman MA *et al*., *EMBO J*., 1997)

C-term domain exerts APE1 endonuclease activity

This domain is responsible for APE1 endonuclease activity. The active site, which lies in a pocket at the top of the α/β sandwich, consists of several critical residues (His309, Glu96, Asp283, Thr265, Tyr171, Asn68, Asp210, Asp70, Asn212) determined by site-directed mutagenic studies [83][87]. Within the active site, at least one divalent ion (Mg^{2+}) is present bound to Glu96 and it is an essential cofactor critical for high level of AP endonuclease activity [88]. It has been postulated that APE1 orients a rigid pre-formed DNA binding face and penetrates the DNA helix from both the major and the minor grooves, stabilizing an extra-helical conformation for the target abasic deoxyribose and excluding any normal DNA nucleotide. Interactions between APE1 and DNA are preferentially at the strand containing the abasic site involving the phosphates at 5' and 3'. Met270 inserts through the minor groove to pack against the orphan base. Meanwhile,

Arg177 inserts through the DNA major groove and delivers a hydrogen bond to the AP site 3' phosphate. Together, Arg177 and Met270 effectively lock APE1 onto AP-DNA. The catalytic process implicated is still under investigations since there is not consolidate view concerning the hypothetical catalytic mechanism.

N-term domain is responsible for redox regulation

Recent data pointed out that two distinct regions has to be considered when looking at APE1 N-terminal domain. The first 33-35 amino acid region consists of a structural disordered segment which is essential for the interaction with other proteins and harbors sites for post-translational modifications [75]. The region comprised between residues 43 and 65 is, instead, necessary for APE1 redox transcriptional co-activation activity. APE1 acts in a redox mode, reductively activating several oxidized transcription factors. In this process, APE1 controls transcriptional regulation of gene expression by enhancing the DNA binding activity of proteins like p53 [10], AP-1 [82], HIF-1α [89], NF-κB [90], CREB [91], Egr-1 [9]. The structural data indicate that this region forms an extended loop which lies across the β-strands β13 and β14 making a number of hydrogen bond and salt bridge interactions with the globular core of the molecule. Cys65 is the key residue implicated in the redox activity of the APE1 together with Cys93 [88]. Cys65 is located into a hydrophobic pocket away from the central β sheet and is not accessible to solvent suggesting that Cys65 is unable to directly interact with residues from other proteins unless APE1 may undergo a conformational change, which involves exposure of Cys65 and creates a binding site that will accommodate the different transcription factors [86]. However, factors capable of stimulating this conformational rearrangement are still under investigations. A redox-independent mode of action by APE1 on transcription factors activities has also been hypothesized, as in the case of p53 [92], subsequently extended to AP-1 [93].

N-term domain: functions of a disordered terminal extension

Recent experimental evidences have demonstrated that the non-conserved N-terminal segment of the human APE1, absent in the *E.coli* prototype Xth, consists of an unstructured domain [94]. Long disordered segments are a common features recently observed for a large percentage of proteins under physiological conditions. Such disordered tails were also shown to be more common in DNA binding proteins than in other proteins, particularly in the ones that are involved in target sequence binding that includes early repair proteins and transcription factors [95][96]. It is likely that their

structural flexibility and plasticity provides major functional advantages. Commonly used disordered prediction tool (PONDR and PrDOS) were used to compare the secondary structure of human and bacterial early BER proteins and correlated them with their available structural information [75]. This analysis showed that mammalian DNA glycosylases are endowed with an unique structural feature absent in their homologs in lower organisms because of the presence of a non-conserved extension at N or C terminus (Figure 5). hNEIL1 contains an extended disordered region spanning about 100 residues in the C-terminus which is absent in *E. coli* Nei-like protein. Similar comparison of predicted structures of human DNA glycosylases NTH1, MYH and their *E. coli* prototypes Endonuclease III and MutY, respectively, indicates that both hNTH1 and hMYH have extended disordered tails at the N-terminus that are absent in the *E. coli* enzymes. Similarly, the N-terminal disordered region present in hAPE1 is absent in Xth, its *E. coli* prototype. The size range of disordered extension is almost between 50-100 residues. In the case of human APE1 consists of approximately 65 residues being the most disordered.

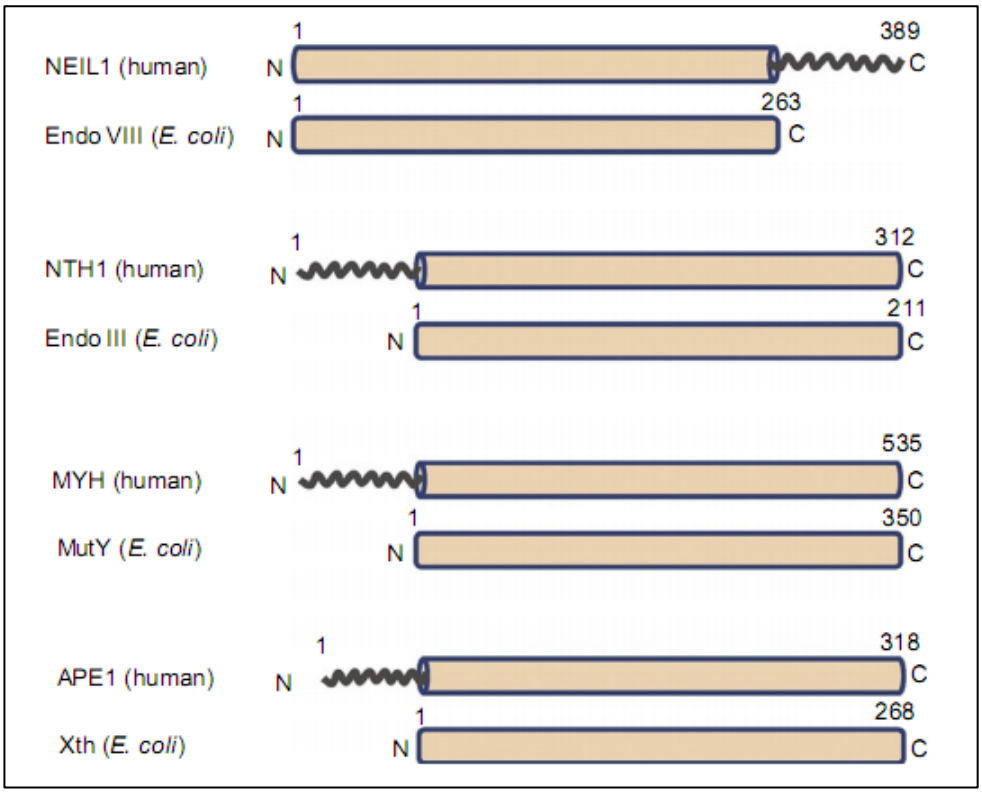

Figure 5 - Disordered terminal extensions in human early BER proteins as compared to their *E. coli* prototypes. (Image from Hegde M.L. *et al.*, *Prog Mol Biol Transl Sci.*, 2012)

These disordered regions are essential for their biological functions including damage sensing, protein-protein interactions, repair regulation via post-translational modifications and nuclear localization signal (NLS). The unique presence of disordered

segments in eukaryotic proteins but not in the prokaryotic counterparts, with the highest degree of disorder in mammals, suggests its evolutionary development. The disorder segment provides advantage of limiting molecular size as complexity increases, by providing common interface for multiprotein binding and sites of modifications. Thus disorder regions may help higher organisms to limit protein size and to reduce intracellular crowding.

4.5.2 APE1 canonical functions

APE1/Ref-1 is a master regulator of cellular response to oxidative stress conditions. Its acronym reflects its dual nature: APE1 is a major constituent of the Base Excision Repair (BER) pathway of DNA lesions generated as a consequence of oxidant-induced base damages and highly contributes to the maintenance of the genome stability; Ref-1, the acronym for redox effector factor-1, refers to its redox abilities exerted on different redox-regulated transcription factors (TFs) during adaptive cellular response to oxidative stress (Figure 6) [97]. Therefore, beside APE1 crucial role in the maintenance of genome stability as the major apurinic/apyrimidinic endonuclease in mammalian cells, its involvement in redox signalling and in the regulation of gene expression suggest that APE1 is to be considered as a multifunctional protein with hallmarks that transcend the classical activities of a DNA repair enzyme. Non-canonical functions of APE1 are represented by its transcriptional repressor activity through binding of particular regulatory sequences, the negative calcium responsive elements (nCaRE) and by the recently unsuspected function in RNA metabolism. APE1 was demonstrated to bind RNA acting as a cleansing factor of abasic RNA. Furthermore, a recent paper demonstrated that APE1 may control *c-myc* expression by cleaving its mRNA [15].

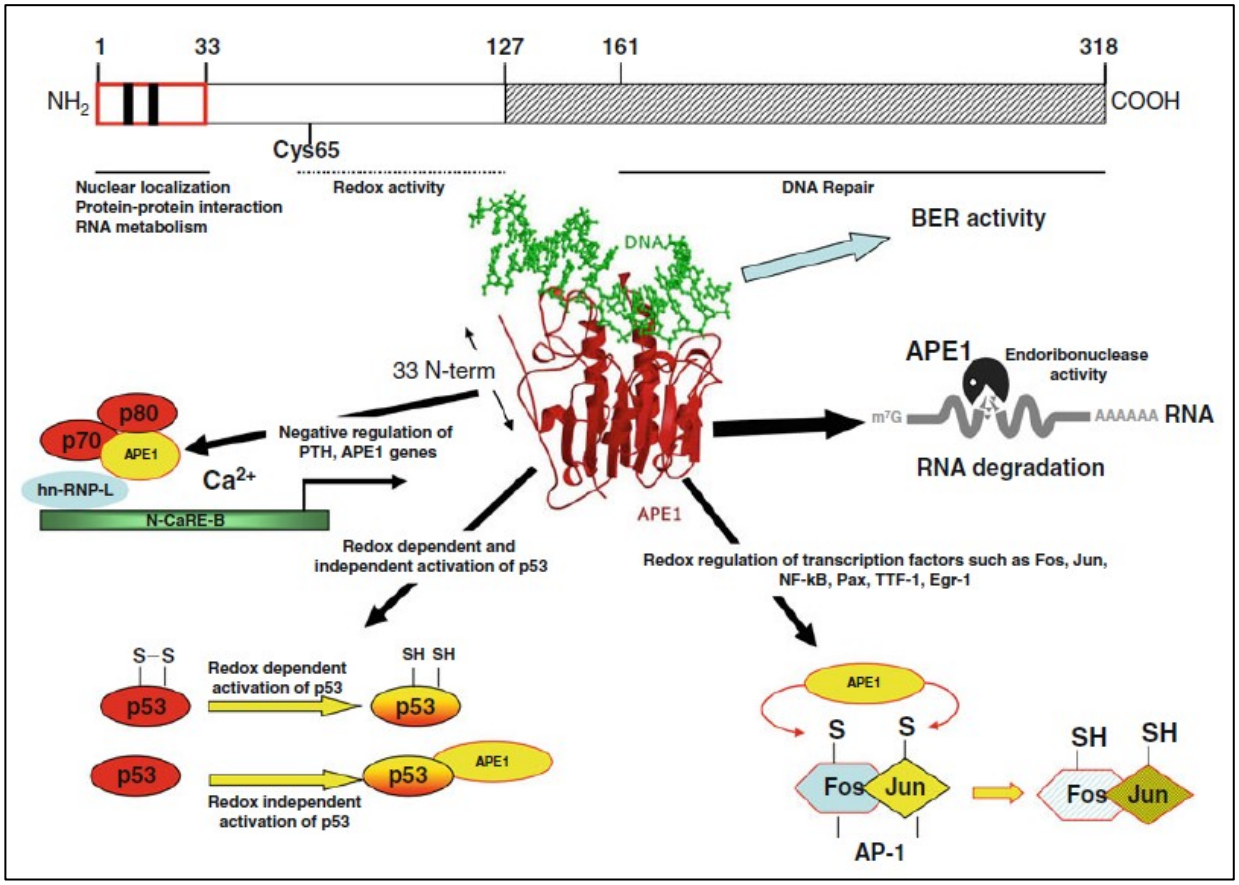

Figure 6 - The many different functions of APE1.
Above, the schematic organization of the human APE1 structure reporting some critical residues. Ribbon representation of the APE1 structure and the main function of APE1 are reported. (Image from Tell G. *et al.*, *Cell. Mol. Life Sci.*, 2010)

Base excision repair

APE1 hydrolyzes the phosphodiester backbone immediately 5′ to an AP site to produce 3′ OH group and 5′ deoxyribose-5-phosphate [98]. After the removal of this blocking group via dRP lyase activity of DNA polymerase β, the repair DNA synthesis is followed by DNA ligase action which restores genome integrity [99]. Oxidized base-specific DNA glycosylases have intrinsic AP lyase activity and cleave the DNA strand 3′ to the AP site [100]. The resulting 3′ blocking group is removed by APE1 in the next step of repair [48]. APE1's 3′ phophodiesterase activity is also involved in repairing DNA single-strand breaks with 3′ blocking group directly generated by ROS [101]. Unrepaired AP sites lead to DNA strand breaks, apoptosis, and increases cytotoxicity [102]. Thus, the DNA repair function of APE1 protects the cell from both endogenous and exogenous DNA damage. All APEs have dual activities as an endonuclease and a 3′phosphodiesterase [98]. However, mammalian APE1's endonuclease activity is quite strong relative to its 3′ exonuclease/phosphodiesterase activity [48][98][103]. Furthermore, unlike *E. coli* Xth with potent 3′ phosphatase/phosphodiesterase activities,

the mammalian APE1 has extremely weak 3′ phosphatase activity that would be required to remove 3′ phosphate directly generated by ROS or due to AP lyase activity of mammalian glycosylases, NEIL1 and NEIL2 [104][103]. APE1 also coordinates BER as an assembly factor by interacting with downstream BER protein such as DNA Polymerase β, X-ray cross-complementing-1 (XRCC1), proliferating nuclear antigen (PCNA), and flap endonuclease (FEN1) [105-107]. Due to its ability to recruit different protein factors, APE1 can be considered as one of the key element in the BER pathway.

Redox regulation of transcription factors

Reactive oxygen species represent a danger for all aerobic organisms since elevated levels of ROS can damage lipids, protein, carbohydrates and nucleic acids. Of notice the observation that sub-toxic levels of ROS could lead to a variation of intra/extracellular redox balance that can result in an alternation of gene expression. The molecular mechanism at the basis of this regulation is exerted through the modulation of transcription factors (TFs) activity. In particular, the redox status of reactive Cys residues, located within the DNA-binding domain of some TFs, may control the transcriptional activity of the TFs itself. APE1 has been identified as a protein capable of nuclear redox activity, inducing the DNA binding activity of several transcription factors, such as AP-1 [82], NF-κB [90], Myb [91], PEBP2 [108], HLF [109], NF-Y [110], Egr-1 [9][111], HIF-1α [89], ATF/CREB family [91], p53 [10][112][113], and Pax proteins [114-116]. In each case, this effect was accomplished by maintaining the cysteine residues of the TFs in the reduced state, through a redox cycle in which the thioredoxin (Trx) would restore the reduced form of APE1 [117-120]. It has been shown that APE1 Cys65 is the redox-active site of the protein [86][121]. Since Cys65 is located inside the 3-D model structure of the protein [83][87], the redox regulation may implicate the occurrence of unfolding or conformational change of APE1 to allow interaction with redox-sensitive TFs.

Recently, a novel mechanism by which APE1 may regulate DNA binding activity of various transcription factors has been proposed. Ando K. *et al.* discovered a novel activity of APE1 termed “redox chaperone activity” by which APE1 promotes reduction of TF cysteine residues by other reducing molecules, such as GSH and thioredoxin [122]. This chaperone activity seems to be mediated by direct interactions between APE1 and target transcription factor (Figure 7).

In conclusion, this APE1 redox and the redox chaperone activities are crucial to preserve the cell from the genotoxic insults due to increased ROS concentration. However, since APE1 could modulate several TFs belonging to different classes with

opposing effects on cell biology, further works are required to comprehend the mechanism responsible for targeting this APE1 activity in response to a specific stimulus.

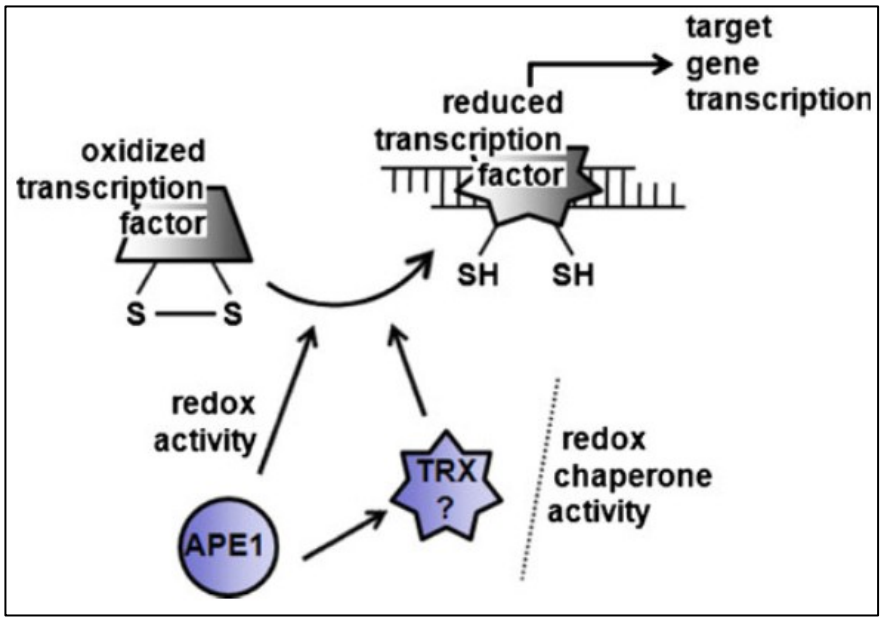

Figure 7 - Schematic representation of APE1 redox and redox-chaperone activities.
APE1 is responsible for the reduction of oxidized cysteines within DNA-binding domain or regulatory domain of a number of transcription factors. (Image from Tell G. *et al.*, *Cell. Mol. Life Sci.*, 2010)

Inhibition of RAC1-mediated intracellular ROS production by APE1

In recent years, numerous evidences have suggested that reactive oxygen species (ROS) can induce a number of functional changes either deleterious or adaptive in the eukaryotic cells. ROS, in fact, are known to play a dual role in biological systems, since they can be either deleterious or beneficial to living systems. Beneficial effects of ROS involve physiological roles in cellular responses such as during organism's defense against infectious agents and as second messengers of cellular signalling systems. As concern this latter case, several evidences have demonstrated that functional triggering of membrane-bound receptors (such as those for TSH, CD40L, ATP, IL-2, etc.) can lead to APE1 functional activation through intracellular generation of sublethal doses of ROS [6]. Noteworthy is the observation that APE1 is also directly responsible in endothelial cells for the control of the intracellular ROS levels through its inhibitory effect on Rac1, the regulatory subunit of a membrane nonphagocytic NADPH oxidase system [123][124]. This enzyme, composed of multiple membrane-associated (Mox and p22phox) and cytosolic components (p67phox, p47phox, and Rac1), catalyzes the transformation of the molecular oxygen to the superoxide anion by transferring an electron from the substrates

NADH or NADPH [125]. Activation of NADPH Oxidase results in generation of ROS, which are important in the host defense against infection [126] and in vascular cell function. The Rac1 protein has been shown to play a critical role in the assembly and activation of NADPH oxidase in the neutrophil form of the enzyme complex. RAC1 is a small GTP binding protein belonging to the Ras superfamily. The exact mechanism by which RAC1 is involved in the activation of the vascular NADPH oxidase remains unclear [127]; however, it seems that one of the oxidase complex subunits, p67phox, could be sequestered by p40phox. RAC1 binding to p67phox could result in the disruption of p67phox/p40phox association, allowing NADPH oxidase activation [128]. Endothelial cells, subjected to TNFα treatment or hypoxia/reoxygenation (H/R), respond activating NADPH oxidase in a RAC1 dependent manner. Angkeow P. *et al.* discovered that APE1 overexpression in an endothelial cell line could prevent oxidative stress induced by TNFα or H/R, even if the molecular mechanism was not characterized. The authors hypothesized that APE1 could interfere with RAC1 activation, presumably perturbing either an activation (GEF) or inactivation (GAP) process of RAC1 (Figure 8). Moreover, since it has been reported that NADPH oxidase, RAC1 and oxidative stress are related to regulation of cell motility and cell adhesion, thus, through the ability of controlling RAC1 mediated ROS production, APE1 could play also a fundamental role in regulating actin network organization in endothelial cells. However, further experiments are required to understand these aspects. Very recently, an interesting evidence concerning the ability of APE1 to control intracellular ROS levels has been obtained shedding lights on the molecular mechanism involved. Zou G.M. and Maitra A. found that human pancreatic cancer PANC1 cell lines treated with E3330, which is a specific inhibitor of APE1 redox activity [129], displayed an increased ROS levels [130]. In this work the authors did not investigate the molecular mechanism; however since pancreatic cells express NADPH oxidase [131], thus it could be speculated that E3330 could influence the pathway involving RAC1. Therefore, it is possible that APE1 could exert a redox-like activity also in cytoplasm or that the RAC1 inhibition could be attributable to APE1 redox activity, therefore one of its substrates should be a factor involved in RAC1 activation/inactivation cycle. Further experiments are required to better clarify these mechanisms, which are still unknown.

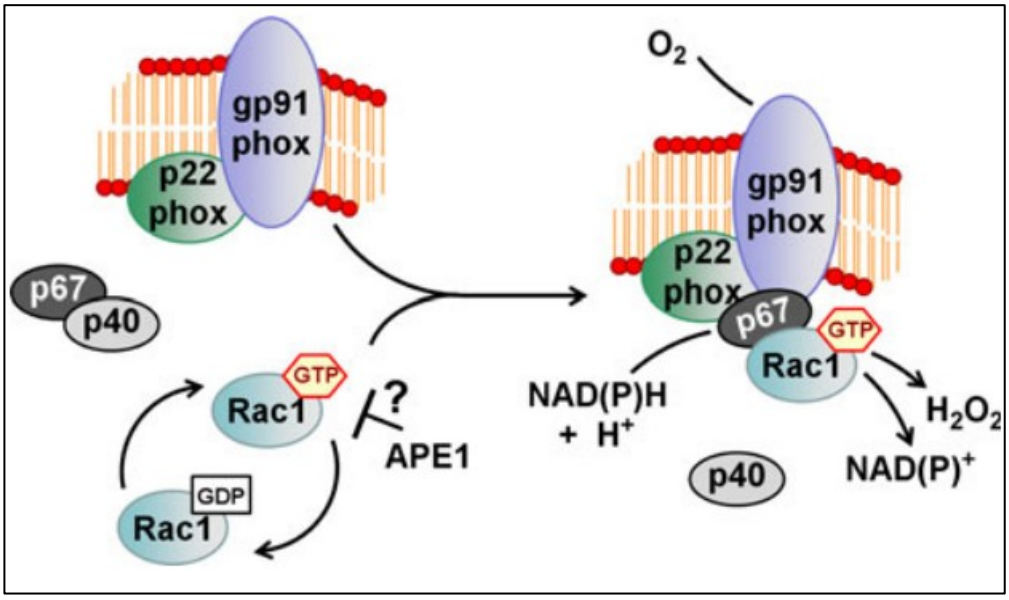

Figure 8 - Role of APE1 in intracellular ROS production control.
APE1 is capable of inhibiting intracellular H_2O_2 production, through modulation of a Rac1-regulated NADPH oxidase. (Image from Tell G. *et al.*, *Cell. Mol. Life Sci.*, 2010)

4.5.3 APE1 non-canonical functions for a DNA repair protein

Role of APE1 in RNA metabolism

There is a growing body of evidences that links DNA repair proteins to RNA metabolism. The mechanism by which cells cope with damaged RNA is currently unknown. However, specific surveillance mechanism is needed to remove damaged molecules of RNA that can impair protein synthesis. Barzilay *et al*. were the first to demonstrated APE1 RNase H-activity [132]. They showed that APE1 binds with relatively low affinity to undamaged single- and double-stranded nucleic acid substrates (RNA and DNA) but does not exhibit general nuclease activity against them. However, their findings let hypothesize a possible involvement of APE1 in RNA metabolism. Subsequently, it has been suggested that APE1 can also bind to RNA molecules *in vivo* [6] and it was found to be associated with protein factors involved in ribosome assembly and RNA maturation within cytoplasm [13][17][71] suggesting a direct involvement of APE1 in RNA metabolic pathways.

Very recently, Berquist BR *et al.* discovered that APE1 possesses the ability to cleave AP sites within ssRNA molecules which depends on molecule conformation [14]. This finding further supports the idea that APE1 serves as a “cleansing” factor for oxidatively damaged abasic RNA. It is known that RNA is oxidized to a greater extent than cellular DNA by treatment with H_2O_2 [133] and that oxidized RNA molecules are

present in huge amounts in brains from Alzheimer patients [134]. Although the biological relevant question is whether the formation of abasic RNA molecules is a spontaneous or guided process, the results propose APE1 as an ideal candidate for a novel RNA cleansing process [12][14]. Furthermore, in line with this hypothesis, very recently, Barnes *et al*. [15] identified APE1 as the endonuclease capable of cleaving a specific region of the *c-myc* mRNA *in vitro* therefore influencing *c-myc* mRNA level and half-life in cells. Altogether, these results clearly demonstrate that APE1 acts on RNA molecules and is involved in RNA metabolism. Further studies are needed to verify if APE1 role in controlling mRNA expression is mRNA-specific or if APE1 cleaves other types of RNA hence affecting a broad range of cellular function.

APE1 transcriptional activity through nCaRE binding

Another intriguing function of APE1 as a *trans*-acting factor was discovered when APE1 was identified as one of the regulatory proteins that bind to the negative calcium responsive elements, nCaRE-A and nCaRE-B, in the intracellular calcium $[Ca^{2+}]_i$–dependent downregulation of the human parathyroid hormone (PTH) gene [16]. An increase in hematic PTH concentration mobilizes Ca^{2+} from the storage tissues [135]: high levels of extracellular calcium inhibit PTH transcription with a negative feedback mechanism which involves the binding of the trans-acting complex to the nCaRE sequences [136][137]. Subsequently, other nCaRE elements were identified on the promoter sequences of other genes, like renin [138] and APE1 itself [139]. Thus, experimental observations suggest that APE1 could down-regulate its own gene and this negative feedback mechanism would represent the first example of such a transcriptional self-regulatory mechanism for a DNA repair enzyme.
The reader is directed to chapter 4.8 for further details concerning sequence and function of nCaRE element.

4.6 Modulation of APE1 different functions

APE1 is a multifunctional protein that exerts several different and in some ways antithetic functions within cells: APE1 is indeed correlated with cell survival but, at the same time, with proapoptotic pathway as well. The regulatory functions of the different APE1 activities must be therefore fine-tuned. This could be implemented via at least three different mechanisms: (i) increase in APE1's level after transcriptional activation; (ii) re-localization of APE1 from the cytoplasm to the nucleus; and (iii) modulation of APE1's

post-translational modifications (PTMs). Together with PTMs, changes in the interactome of APE1 could target it towards a specific biological function.

4.6.1 APE1 transcriptional regulation

The gene encoding the APE1/Ref-1 protein spans 2.6 kbp and maps to chromosome 14 bands q11.2–12 in the human genome [140][141]. The complete gene consists of four introns and five exons, the first of which is untranslated. The APE1/Ref-1 promoter lacks a TATA box and, as many TATA-less genes [142], has multiple transcription start sites clustered around 130 bp upstream from the first splice junction, though the assignment of the major site is disputed. The functional basal promoter is approximately 300 bp and is located in a CpG island [141][143][144]. Several potential recognition sites has been reveled by *in silico* analyses: Sp-1, USF, CREB, ATF and AP-1 [6][141]. However, as suggested by results of independent groups, AP-1 putative binding site seems not to exert any effect [141][145]. APE1 transcription is tightly coordinated with the cell cycle [146]: the mRNA levels increase before the onset of DNA synthesis, continue to rise during the S-phase of cell cycle and depend on a specific DNA element, which can be bound by Sp1 transcription factor. As shown in Figure 9, APE1 promoter bears two distinct Sp1 binding sites, the first located close to the CCAAT box (Sp1-1), and the second located downstream of the transcription start site (Sp1-2). While Sp1-1 site is involved in basal gene expression, the Sp1-2 site is required for cell cycle coordinated APE1 gene transcription [146]. More recently, downregulation of APE1 expression by p53 has been suggested. No p53 binding sites were revealed by *in silico* analysis; however it was hypothesized that p53 was indirectly recruited to APE1 promoter although the exact mechanism is still not clear. Zaky *et al*. proposed that p53 could physically interact with Sp1 bound to Sp1-1 element, inhibiting basal APE1 gene transcription [147]. This study suggests an intriguing hypothesis concerning an inverse relationship between the pro-apoptotic factor p53 and the expression of pro-survival factor APE1. The tumor resistance to chemotherapy observed in certain malignancies could be associated with an increase APE1 gene expression when p53 gene is mutated or downregulated.

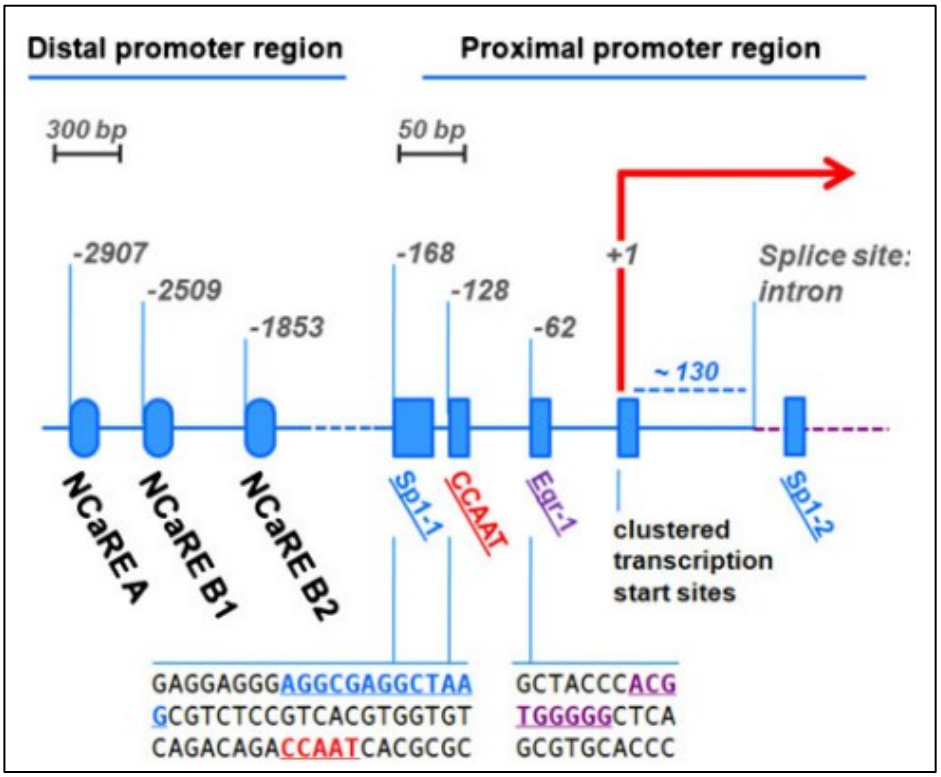

Figure 9 - Schematic representation of APE1 gene promoter region.
In the distal promoter region (between -3,000 and -1,000 bp relative to the transcription start site) there are three nCaRE elements; in the proximal promoter region (between -500 and +200 relative to the transcription start site), there are two Sp1 binding elements, an Egr-1 binding site and a CCAAT box. Moreover, several other putative binding sites for other transcription factors are also reported. (Image from Tell G. *et al*., *Cell. Mol. Life Sci*., 2010)

APE1 expression is stimulated with hormones, such as TSH [148], or upon oxidative stress. Subtoxic doses of ROS strongly increase APE1 mRNA levels in different cell lines [149-151]. However, the molecular mechanism of ROS-induced transcriptional activation of APE1 is still under investigation. Two reports provided important indications about APE1-inducible transcriptional regulatory mechanisms; much work still remains to be done. By performing transfection experiments on CHO cells, Grosch and Kaina [152] identified a CREB binding site (CRE) approximately 600 bp upstream of APE1 transcription start site. They discovered that this element is bound by a complex of ATF2 and c-Jun and it is required for APE1 induction by ROS. Successively, it has been characterized a specific sequence on APE1 promoter, which could be directly bound by Egr-1 and that is involved in ROS inducible APE1 gene transcription [153].

Finally, the upstream region of the promoter contains also negative regulatory elements: one negative calcium responsive element-A type (nCaRE-A) sequence and two nCaRE-B type sequences: B1 and B2 [139]. Deletion of the nCaRE-A sequence does not repress a reporter gene, suggesting that it may not be important for negative regulation. Conversely, the nCaRE-B2 element represses expression of the reporter

gene and interacts with APE1/Ref-1 to form complexes. These data suggest that APE1/Ref-1 can autoregulate by binding to its own promoter and inhibiting transcription.

4.6.2 Post-translational modifications

Post-translational modifications represent a quick and usually reversible way to regulate protein activities or functions. Concerning APE1 protein, knowledge of PTMs affecting APE1 function has grown exponentially in the last decade [3][21]. Several PTMs have been described occurring *in vitro*, but only a few having a function *in vivo*: acetylation, phosphorylation, ubiquitination, S-nitrosation, proteolytic cleavage of the N-terminal 33 amino acids domain and redox regulation, which is at the basis of APE1 redox activity (Figure 10). A detailed discussion of critical PTMs on APE1 can be found in Busso *et al*.'s review [21].

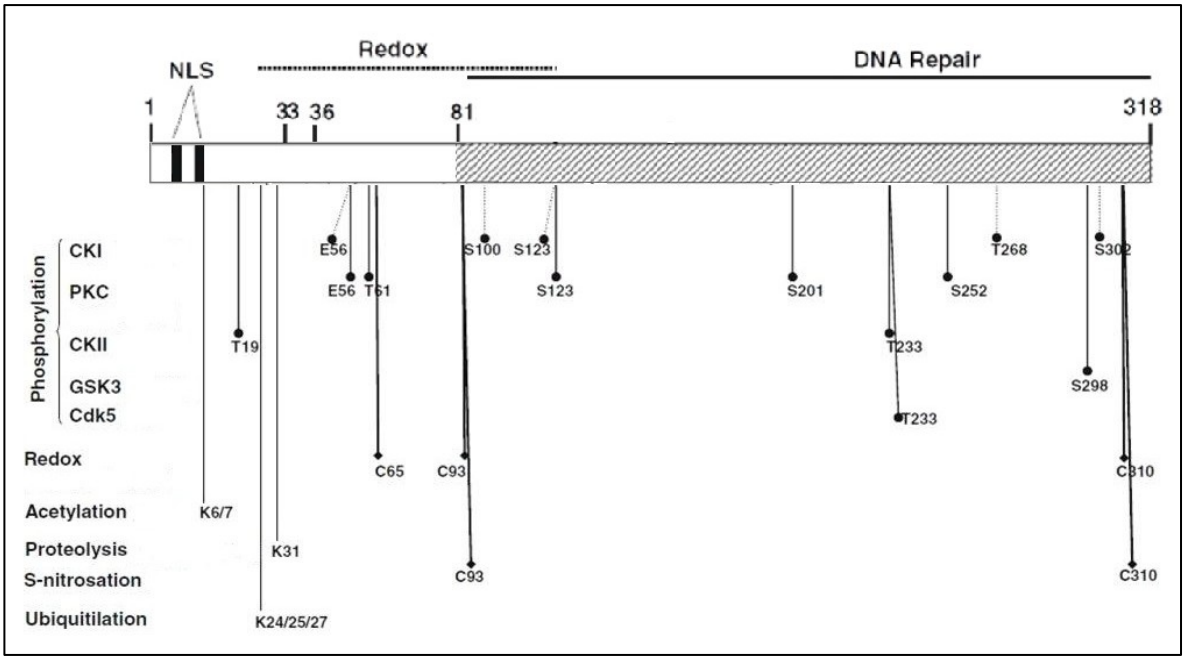

Figure 10 - Schematic representation of the PTM acceptor sites on APE1 sequence. (Adapted image from Tell G. *et al*., *Cell. Mol. Life Sci*., 2010)

Phosphorylation

APE1 has several putative phosphorylation sites for different kinases, like Casein Kinase 1 and 2 (CK-I and CK-II), Glycogen Synthase Kinase 3 (GSK-III) and Protein Kinase C (PKC). Yacoub *et al*. showed that *in vitro* phosporylation of APE1 by CK-II (at residues 19T, 123S, or 233T) inhibited endonuclease activity [154]; moreover, *in vivo* CK-II mediated phosphorylation of APE1 was also suggested, even if not directly shown [155]. However, *in vivo* experiments performed using CK-II specific inhibitors didn't

confirm *in vitro* results. *In vitro* PKC phosphorylation exerted no effect on the endonuclease activity of APE1, but was able to increase its redox activity, since it was found to enhance the *in vitro* binding of c-Fos and c-Jun to AP-1 binding elements. In agreement with these findings, *in vivo* studies by Hsieh *et al*. showed that, under oxidative stress conditions capable of stimulating PKC activity, APE1 phosphorylation level increased, stimulating its redox activity [156]. Despite the potential significance of APE1 phoshorylation, its biological relevance has not been investigated further.

Acetylation

APE1 acetylation has been studied fairly extensively. In 2004, Bhakat *et al*. [20] showed that APE1 was acetylated by histone acetyl transferase (HAT) p300. The same group achieved to generate an antibody specific to acetylated APE1 and confirmed its endogenous presence *in vivo* [71]. APE1 has 29 lysines, however, up to date, only lysines K6 and K7 have been identified as target of acetylation. Acetylation of these two lysine residues was associated to an increase APE1 DNA binding activity to nCaRE sequences, followed by repression of PTH gene in parathyroid cells and presumably of APE1 gene itself in different cell types.

More recently, our group observed that other Lys residues within the APE1 N-terminal domain, K24, K27, K31, K32, and K35, may undergo *in vivo* acetylation under basal conditions. Fantini *et al.* have previously demonstrated that these residues are crucial for APE1 interaction with rRNA and NPM1 and for modulating its catalytic activity on abasic DNA through regulation of product binding [85]. Very recently, we also demonstrated that K27, K31, K32, K35 are acetylated during genotoxic stress condition influencing APE1 subnuclear distribution [5] (see list of papers published during PhD course). In particular, we showed that genotoxic-induced acetylation of K27-35 determines APE1 relocalization out of the nucleoli thus influencing DNA repair activity and cell proliferation. We demonstrated that cells expressing a specific K-to-A multiple mutant are APE1 nucleolar deficient and are more resistant to genotoxic treatment accordingly to an augmented APE1 enzymatic activity on DNA. Of interest, we also found that the charged status of K27-35 modulates acetylation at K6/K7 residues through a mechanism regulated by the sirtuin 1 (SIRT1) deacetylase. We found that SIRT1 is able to bind and possibly deacetylate APE1 K27-35 residues and that its ability to efficiently deacetylate APE1 K6/7 residues relies on the presence of positive charges at K27-35 suggesting the existence of a cross-talk between the charged state of K27-35 and the acetylation status of K6/7.

If p300 has already been established as the main enzyme responsible for APE1 acetylation *in vivo*, less information are available about the process of APE1 deacetylation. Bhakat KK *et al.* were the first to suggest the involvement of a class I HDAC enzymes [20]. Recently, Yamamori T. *et al.* showed that acetylated APE1 may undergo deacetylation by means of a class III HDAC enzyme: SIRT1 [157]. Yamamori T. *et al*. demonstrated that SIRT1 deacetylates lysines 6 and 7 both *in vitro* and *in vivo*. Genotoxic insults stimulate lysine acetylation of APE1 which is antagonized by transcriptional upregulation of SIRT1. Activation of SIRT1 promotes binding of APE1 to the BER protein X-ray cross-complementing-1 (XRCC1) suggesting that SIRT1 plays a vital role in maintaining genome stability.

Ubiquitination

Ubiquitin is a highly conserved 76 amino acids polypeptide that can be covalently attached to target proteins in a three step-enzymatic reaction involving E1, E2 and E3 ubiquitin ligases [158]. The attachment of a single ubiquitin to a target protein can alter its function or localization [159]; the tandem attachment of multiple ubiquitin to form a polyubiquitin chain can also alter function or localization, however it usually marks the substrate for degradation by the 26S proteasome. Busso C.S. *et al.* were the first to demonstrate that APE1 is target of ubiquitination *in vivo*. They discovered that the E3 ligase MDM2 (murine double minute 2) can carry out the APE1 ubiquitination reaction both *in vitro* and *in vivo*, and showed that the target site should be one among the residues K24, K25 and K27 [160]. MDM2 is the most important negative regulator of the p53 tumor suppressor. Under basal conditions, MDM2 ubiquitinates p53 protein through direct interaction and addresses it to proteosomal-mediated degradation pathway. Upon genotoxic stress, MDM2-p53 interaction is prevented through multiple mechanisms such as phosphorylation and acetylation of p53, or induction of ARF expression, which is in turn able to sequester MDM2 in the nucleolus. Even if MDM2 is by far the most crucial regulator for p53, it is able to recognize and ubiquitinate other substrates, such as histone H2B [161], protein component of hnRNP K [162] and FOXO4 [163]. In later years, Busso *et al.* further deepen into APE1 ubiquitination process and reported that there is a delicate balance between ubiquitination and phosphorylation of APE1. They demonstrated indeed that ubiquitination activity of MDM2 is increased for T233E APE1, a mimicry of phospho-T233 APE1. They showed that monoubiquitinated APE1 was present in the nucleus and through global gene expression profiles with or without induction of a ubiquitin-APE1 fusion gene they also suggested that monoubiquitination enhanced the gene suppression activity of APE1.

However, even if evidences of APE1 ubiquitination *in vivo* were obtained, much work has to be done in order to understand many unclear aspects concerning the occurrence of this PTM. In fact, despite the observation of Busso and co-workers of MDM2 involvement, very recently Meinsenberg *et al*. using an *in vitro* ubiquitylation assay, purified the human E3 ubiquitin ligase UBR3 as a major enzyme that polyubiquitylates APE1 at multiple lysine residues clustered on the N-terminal tail [164].

4.6.3 Proteolytic cleavage

APE1 was found to undergo a very peculiar proteolytic PTM, which generates a protein lacking the first N-terminal 33 or 35 amino acids. First *in vivo* evidences of such a PTM were reported by Yoshida A *et al*., who purified a 34-kDa, Mg^{2+} dependent endonuclease, from apoptotic human promyelocytic leukemia HL-60 cells treated with etoposide [165]; only 5 years later, the same group discovered that this enzyme was just a truncated form of APE1, lacking a N-terminal portion spanning 33 amino acids (NΔ33APE1) obtained by an unidentified trypsin-like enzyme, activated by caspase-3 during apoptosis [166].

Successively, the truncated form of APE1 was discovered to be also involved during a granzyme-induced caspase-independent type of apoptosis. Granzymes are serine proteases, released by cytotoxic T cells and natural killer cells, whose function is to induce cell death within virus-infected cells [167]. Granzyme A (GzmA) activates a caspase-independent cell death pathway with morphological features of apoptosis. Single-stranded DNA damage is initiated when the endonuclease NM23-H1 becomes activated to nick DNA after granzyme A cleaves its inhibitor, SET. SET and NM23-H1 reside in an endoplasmic reticulum-associated complex (the SET complex) that translocates to the nucleus in response to superoxide generation by granzyme A [168]. Fan *et al*. reported APE1 binds to GzmA and is contained in the SET complex. GzmA cleaves APE1 after Lys31 and destroys its known oxidative repair functions. In this way, GzmA may block cellular repair and force apoptosis [169]. An APE1 role within the SET complex in preventing HIV autointegration was also recently demonstrated [170]. It has been suggested that the formation of the truncated form of APE1 protein could be induced during different cell death pathways, and could exert a nuclear function by contributing to the accumulation of single strand breaks on DNA molecules. However, some aspects still remain to be elucidated concerning NΔ33APE1 function. In fact, it is known from early studies on different APE1 deletion mutants, that the NΔ33APE1 keeps both redox and AP endonuclease activities [121], without acquiring a general nuclease activity. Furthermore, it is to be clarified the mechanism by which NΔ33APE1 could be

translocated to the nucleus of the apoptotic cell since the truncated protein lacks both nuclear localization signals, previously identified by Jackson E.B. *et al.* [171]. Since it has been associated with cell death, this peculiar irreversible APE1 PTM is extremely intriguing but unfortunately several studies are needed to solve many questions regarding the identification of the protease, of the stimuli that induces such PTM, and the effects of this modification on APE1 subcellular localization and function.

S-nitrosation

S-nitrosation is a ubiquitous redox-related modification of cysteine thiols by nitric oxide. S-nitrosation has been implicated in the regulation of gene transcription [172], enzymatic activity [173], and protein intracellular trafficking [174].

Qu J. *et al*. discovered that APE1 can undergo S-nitrosation at Cys93 and Cys310 after S-nitroglutathione treatment and this PTM can induce a complete exclusion of APE1 from cell nucleus [175]. APE1 can inducibly translocate from nucleus to cytoplasm in response to nitric oxide stimulation. The mechanism of nuclear export is not the canonical one, since it resulted to be Exportin1-independent, and requires further analysis. Since the alteration of APE1 subcellular localization may result in defects in DNA repair and redox APE1 functions, this finding may establish a novel role for APE1 in NO-related physiological and pathological processes. Moreover, it has been reported that redox modification of Cys310 of APE1 can repress its AP endonuclease activity [176]. Thus it is reasonable to expect that also NO may exert influence on APE1 DNA repair function through S-nitrosation of this site. Very recently, it has been demonstrated that the augmented APE1 S-nitrosation induced its cytoplasmatic relocalization in various lung cancer promoting malignancy via NF-κB activation by p53 aberration and resulting in poor outcome in non-small cell lung cancer (NSCLC). These results underline the importance of S-nitrosation in determining APE1 cytoplasmatic distribution that has been observed in some human tissues. However, it remains to clarify which stimuli and which transduction pathways could lead to NO production and induce a nuclear exclusion of APE1.

4.7 Modulating APE1 activities as a cancer therapeutic approach

APE1 relevance in normal and tumor cell survival is demonstrated by the fact that knocking out APE1 gene induces either activation of apoptosis in differentiated cells [81] or developmental failure during embryogenesis [177]. Thus, due to the fundamental role played by APE1 within cells, it was then hypothesized its involvement in human

pathologies. Accumulating evidences have demonstrated that the heterogeneity of APE1 expression pattern is associated to different pathologies conditions ranging from metabolic to differentiative disorders, including cancer and neurodegenerative diseases. Upregulation or dysregulated APE1 expression has been found in a variety of cancers including prostate, pancreatic, ovarian, cervical, germ cell tumor, rhabdomyosarcoma and colon [23][129]. Elevated APE1 levels are typically associated with aggressive proliferation, increased resistance to therapeutic agents, and poor prognosis [26]. Anomalous intracellular localization of APE1 is also be correlated with human cancer. Generally, APE1 is mainly localized in the nucleus while in several carcinomas a nuclear, cytoplasmatic, and nuclear/cytoplasmatic staining was observed [178]. This peculiar localization correlates with aggressiveness and prognosis of the tumor. In fact, in tumors where APE1 expression is mainly nuclear there is always a positive correlation with better prognostic features; while an APE1 cytoplasmatic localization, as observed in hepatocellular carcinoma, is associated with a significant lower degree of differentiation and with a shorter survival time. Furthermore, several studies have shown that decreasing APE1 levels by using specific anti-sense oligonucleotides and siRNA leads to the blockage of cell growth and to an increase of cellular sensitivity to DNA-damage agents such as methylmethanesulfonate (MMS), H_2O_2, bleomycin, temozolomide (TMZ) and gemcitabine [179-182].

Considering that APE1 expression appears to be linked to chemoresistance, APE1 is altered in a variety of cancers as well as in multiple myeloma [183], and, in addition, given that APE1 plays an important role in the tumor microenvironment through the regulation of HIF-1α both in normal and cancer-associated endothelial cell function, APE1 represents a promising target for pharmacological treatment. However, it still debates whether the enhanced sensitivity to cytotoxic agents observed when APE1 functions are blocked is solely due to the loss of APE1 DNA repair activity or also due to the loss of its transcriptional regulatory function or both. Efforts to determine the effects of inhibiting either the redox or repair function of APE1 are ongoing.

A list of published APE1 inhibitors of DNA repair or redox function is reported below (Figure 11). A description of all the compounds is far beyond my scope, for an exhaustive reviewed of APE1 inhibitors, the readers is redirected to [23][184].

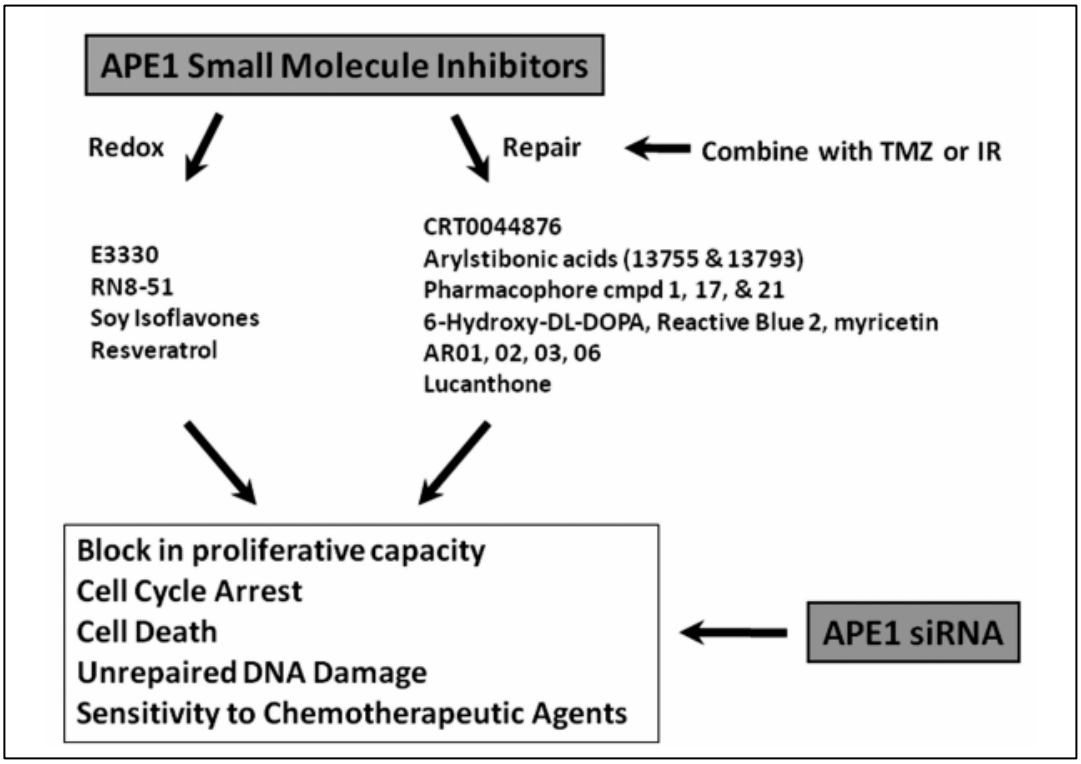

Figure 11 - Published inhibitors of each function are listed below as well as the effects of APE1 siRNA on tumor cell viability and function. (Adapted image from Vascotto C. and Fishel M., Academic Press, 2012)

Briefly, as concern the blockade of APE1 DNA repair activity, this will result in an accumulation of DNA damage, especially if paired with a chemotherapeutic agent that generates DNA base damage leading to tumor cell death. It is well clear that since both short- and long-patch BER pathways contribute to the maintenance of genomic integrity in cells, manipulation of the processing of these pathways has the potential to shift the balance from repair to apoptosis or cell death, a favorable outcome in tumor cells. Many chemotherapeutic agents kill cancer cells by damaging their DNA, therefore inhibiting the action of BER in cancer cells could render them more sensitive to these agents. Several chemotherapeutic agents generate lesions that are subject to BER pathway, including TMZ, melphalan, thiotepa, methyl-lexitropsin (Me-lex), dacarbazine/procarbazine, and streptozotocin [26]. More recently, it has become clear that some chemotherapeutic agents generate ROS secondary to their primary mechanism of action. BER proteins are the predominant mechanism to cope with the oxidative DNA damage. Chemotherapeutics such as platinum-based drugs, anthracyclines, i.e. daunorubicin, doxorubicin, and paclitaxel generate ROS, indicating that BER may play a role in cellular response to these drugs even though they have not been considered to generate single base lesions. Another frequent treatment modality in cancer is ionizing radiation (IR) and BER is one of the DNA repair pathways that contributes to the repair of the DNA damage generated.

Small molecule inhibitors have been identified for several other DNA-repair enzymes, including MGMT, poly ADP-ribose polymerase (PARP1), ataxia–telangiectasia mutated kinase (ATM kinase) and DNA PKCs [26]. Inhibitors of DNA repair of APE1 are under development. They can be distinguished in two classes of molecules: molecules like methoxyamine (MX) which binds to aldehyde in the AP site on DNA and stops APE1 in performing its endonuclease activity, and small molecules that would directly bind to APE1 and inhibit activity on AP site-containing DNA (Figure 11).

Inhibition of APE1's redox activity in promoting cancer cell death and inhibition of tumor cell growth is a novel approach that has been unexplored to date. The redox activity of APE1 affects the DNA binding activity of several crucial transcription factors in cancer survival and growth signaling pathways. Transcription factors including HIF-1α, p53, NF-κB, CREB, and AP-1 have all been implicated in major aspects of cancer survival, including angiogenesis and tumor promotion and progression. Therefore, targeting APE1's redox activity would render these transcription factors unable to bind to DNA, thereby halting tumor cell signaling of angiogenesis and uncontrolled growth and possibly impairing the tumor's ability to respond to hypoxia and nutrient deprivation and thereby sensitize the tumor to chemotherapeutic agents.

The most selective and well-characterized APE1 redox inhibitor is the naptho-quinone compound, E3330 (2E-3-[5-(2,3dimethoxy-6-methyl-1,4-benzoquinolyl)]-2-nonyl-2-propenoic acid). Previous studies demonstrated that the quinone derivative E3330 selectively inhibited NFκB-mediated gene expression without affecting any other regulatory steps such as phosphorylation or translocation to the nucleus [185]. Successively, it has been demonstrated that E3330 blocks the redox function of APE1 with AP-1 as the downstream target *in vitro,* as well as after the treatment of ovarian cancer cells with E3330 [186]. Additionally it has been found that E3330 blocks APE1 redox activity with HIF-1α and other downstream transcription factors. This demonstrates that the redox inhibition is not specific for the downstream target. Although E3330 blocks the redox function of APE1, it has no effect on APE1-repair endonuclease activity or BER activity of an AP site. Kelley's group has extensively characterized the effect of E3330 on APE1 redox activity in cancer cell lines and endothelial cells as well as developing more potent analogs (RN8-51) demonstrating a new role of APE1 in angiogenesis, and inhibition of APE1 redox function by E3330 abrogates this role [186]. E3330 also has been shown to inhibit the growth of pancreatic cancer cell lines, an effect that is enhanced under hypoxic conditions [187], as well as pancreatic cancer–associated endothelial and endothelial progenitor cells [181].

In addition to E3330, a number of natural products reported to affect either directly or indirectly the redox function of APE1 in cells were recently reviewed [26][188]. Among

those, soy isoflavones [189][190] and resveratrol [191][192] have reported activity against the redox activity of APE1 (Figure 11). Soy isoflavones, a component in soybeans, are thought to have potential as chemopreventive agents in prostate cancer [193]. Resveratrol was shown to inhibit both the endonuclease activity of APE1 and the DNA-binding activities of AP-1 in cellular extracts, presumably through inhibition of APE1 redox function. However, there are conflicting reports regarding this compound's efficacy for inhibition of APE1, since it has not been corroborated by others, nor it has been shown to be effective at levels that are physiologically relevant.

Thus, collectively all these data demonstrated that targeting APE1 DNA repair activity and/or redox function will have important implications for human health and cancer therapeutic development.

4.8 nCaRE sequences: features and functioning of a negative regulative mechanism

Okazaki and co-workers firstly identified and characterized a pair of negative regulatory elements between 2.4 and 3.6 kbp upstream the transcription start site of the human parathyroid hormone (hPTH) gene [16]. They evidenced the negative regulatory function of these elements showing a reduced chloramphenicol acetyltransferase (CAT) activity when transfecting various types of cultured cells (BHK, CV1 and NIH3T3) with a fusion plasmid containing the 4.7 kilobase pairs of the 5'-flanking portion of the hPTH gene linked to CAT-coding sequence. Further deletion analyses clearly revealed that there were two separate upstream DNA elements in the hPTH gene promoter responsible for the negative regulation observed and gel retardation experiments, performed with nuclear extract from BHK or CV1 cells, demonstrated that both these elements were bound by common nuclear factors. Successively, the same authors, through Southwestern cloning were able to identify APE1 as one of the proteins involved in the specific binding of these sequences [136]. In particular, they also showed that hPTH gene suppression was dependent to extracellular calcium concentration levels demonstrating that higher Ca^{2+} concentration increased APE1 binding activity to these sequences. Since this mechanism of negative regulation depends on extracellular calcium levels, these sequences were called nCaRE standing for negative calcium-responsive element.

After the first evidence of a negative regulation mechanism for PTH, Okazaki *et al*., showed that the expression of other genes was negatively regulated by extra-cellular calcium through the analogous nCaRE sequence [194]. Searching for the DNA sequence homologous to the nCaRE-PTH, by using the EMBL gene bank, they found that other five genes bear DNA sequences that were identical or very similar to the nCaRE-PTH in their 5'-flanking regions: the mouse myeloperoxidase, the human ATP synthase beta subunit, the human endogenous retrovirus-like sequence (HuERS-P1-2) 5'-LTR, the rat vasopressin and the rat atrial natriuretic polypeptide (ANP).

Atrial natriuretic peptide (ANP) hormone is released by atrial myocytes in response to high blood pressure which acts to reduce the water, sodium and adipose loads on the circulatory system, thereby reducing blood pressure [195]. Okazaki *et al*. demonstrated that the rat ANP gene, was negatively regulated in the heart by extracellular calcium by using an *in vivo* infusion system comparing by Northern blot analysis the level of ANP mRNA obtained from the heart rat infused with calcium-free solution to that infused with calcium-containing solution [194]. Furthermore, transfection of BHK cells with a reporter

gene containing the nCaRE element found on ANP promoter confirmed that this DNA functions as a negative calcium-responsive DNA element.

Hence, the presence of nCaREs in the regulatory region of APE1 gene itself has been showed suggesting a possible mechanism for its own homeostatic regulation [139]. Analysis of APE1 sequence promoter revealed the presence of three nCaRE sequences: one nCaRE-A type sequence which is identical in 11 out of 13 internal bases to the element 1 of the PTH gene and two nCaRE-B sequences, denoted nCaRE-B1 and nCaRE-B2, with a 2 base pair gap, and a gap along with a mismatch relative to the element 2 of the PTH gene, respectively. Analysis of APE1 promoter activity by transient expression of the luciferase reporter gene in human HeLa and TK6 cells displayed that only the two nCaREB-like sequences were responsible for inhibiting reporter gene expression while no repression of luciferase reporter was observed for nCaRE-A, suggesting that this element may not be essential for the negative regulation of APE1. Competitive electrophoretic mobility shift assay with HeLa nuclear extract indicated that the nCaRE sequences of the APE1 and PTH genes were recognized by the APE1 polypeptide. These results suggested that the APE1 gene may regulate its own expression product. However, conversely to the original work of Okazaki in which the expression of PTH was affected by altering extracellular Ca^{2+} level in parathyroid cells, in this work, Izumi *et al*., did not show if APE1 protein binds to its promoter in a Ca^{2+}–dependent fashion.

In later years, Fuchs *et al*. identified the molecular mechanism by which the human renin gene is negatively regulated in chorio-decidual cells by calcium increase in the same way as described for PTH, through APE1 binding to nCaRE [138].

Renin, also known as angiotensinogenase, is an aspartic acid protease secreted by juxtaglomerular cells of kidneys, that participates in the body's renin-angiotensin system (RAS) that mediates extracellular volume (i.e., that of the blood plasma, lymph and interstitial fluid) and arterial vasoconstriction thus regulating the body's mean arterial blood pressure [196].

Analysis of the human renin proximal promoter led to the identification of a nCaRE element (-1781bp), which is identical to the region of the PTH promoter. Transfection experiments in renin-expressing chorio-decidual cells demonstrated the transcriptional functionality of the human renin promoter nCaRE. Validation of the involvement of nCaRE in the negative regulation of human renin came also by additional analysis in which mutation of nCaRE, as performed in the PTH promoter by Okazaki [16], suppressed sensitivity of the renin promoter to the increase in intracellular calcium. Gel shift assays confirmed that also in chorio-decidual cells the nuclear factor involved in nCaRE sequence binding is APE1, and furthermore, immunohistochemistry localization

of APE1 in chorio-decidual cells allowed suggesting that an increase in Ca^{2+} concentration induces the translocation of Ref-1 from the cytoplasm to the nucleus.

4.8.1 Molecular features of nCaRE sequences

The sequence of the two nCaRE elements originally found by Okazaki *et al.* were determined exposing the DNA-protein mixtures to DNase I and analyzing the footprints of the retarded bands after electrophoresis [16]. In Figure 12 are shown the footprinting results of Okazaki and the relative sequence composition of the two elements. They showed that several regions present in element 1 and one region in element 2 were protected from DNase I digestion. These sites present in AT-rich regions of the element 1 and in a cluster of 17 thymidines in the element 2. The sequence of the most clearly delineated footprinting on the element 1 is GCATACACAA. The protected region in the element 2 consists of 12 palindromic bases in a 15-residue sequence, TGAGA(AGG)GTCTCA; the three bases in the parentheses were not protected from DNase I digestion. These two sequences were then distinguished as nCaRE-A (element 1) and nCaRE-B (element 2). Okazaki *et al*. demonstrated other peculiarities of these elements which were both bound by the same nuclear complexes: nCaRE-A functions as a negative transcriptional element when present in both orientations on PTH promoter, while nCaRE-B functions only in the native orientation. Furthermore, when the 4 thymidines preceding the palindromic nCaRE-B are removed, this oligonucleotide does not bind to APE1 protein-complex anymore suggesting that not only the palindrome but also these thymidine-rich sequences play important roles in the negative gene regulation.

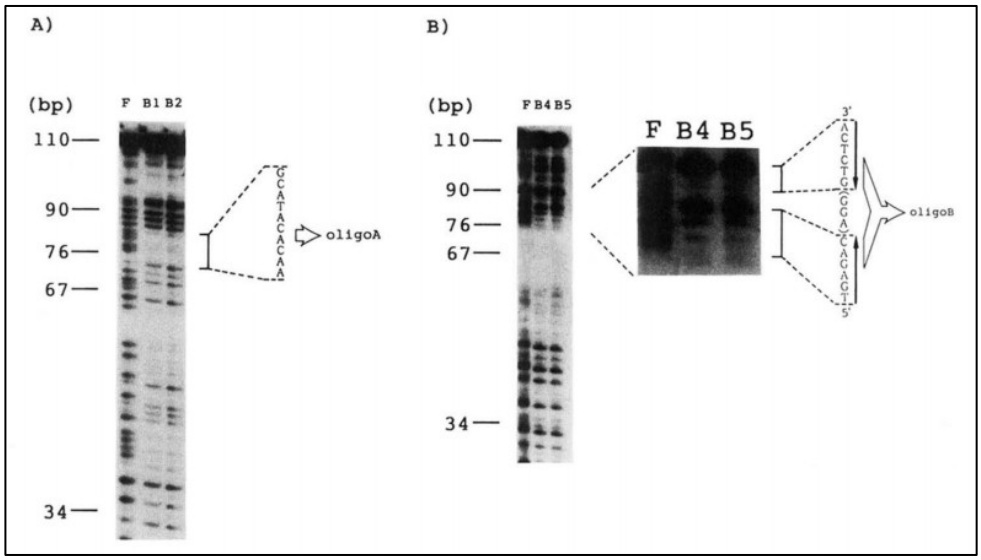

Figure 12 - DNase I footprinting analysis of nCaRE element found on PTH promoter.
Original footprinting analysis of element 1 (A) and element 2 (B) performed by Okazaki *et al*.. DNA sequences protected from DNase I digestion are indicated on the right side of each gel. (Image from Okazaki T. *et al*., *J. Biol. Chem.*, 1991)

After the first discovery of nCaRE sequences in PTH gene promoter, other nCaRE elements were described [19][139][138]. Figure 13 reports the three nCaRE elements found on APE1 promoter which are not identical in bases composition with respect to those found in the PTH promoter as shown by the alignments [139]. The nCaRE-B element identified within the APE1 promoter where denoted nCaRE-B1 and nCaRE-B2 to distinguish them from that of PTH. Both nCaRE-B1 and nCaRE-B2 are bound by APE1 and are responsible for inhibiting reporter gene expression. This finding denotes that even in the presence of a variation in the nCaRE sequence, APE1 binding is still possible and therefore it means that this type of binding is not only sequence-dependent but could involve also a recognition mediated by the secondary structure adopted by these elements.

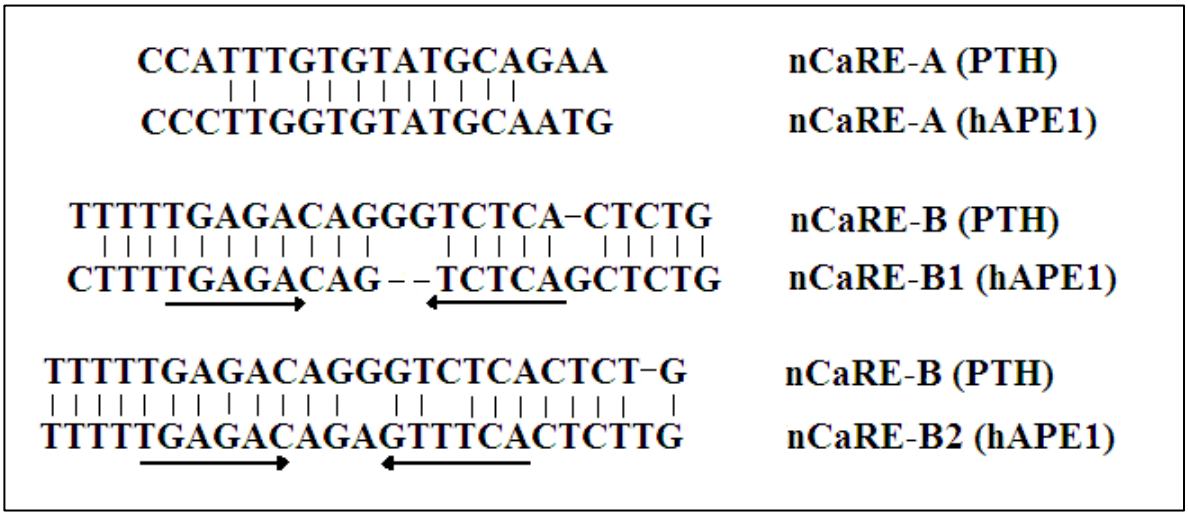

Figure 13 - Characterization of nCaRE sequences found on APE1 promoter.
Sequence similarity of nCaRE sequences found on PTH and APE1 promoters. Arrows within nCaRE-B's indicate inverted repeats. (Modified imagine from Izumi T. *et al*., *Biochemistry*, 1996)

4.8.2 Origin of nCaRE elements in an ALU-Repeat

In 1995 McHaffie and Ralston evidenced the origin of the nCaRE-B sequences in an ALU-repeat thus suggesting that other nCaRE elements might also exist, raising the possibility that nCaRE binding may be a common mechanism by which extracellular calcium regulates gene transcription [197].

ALU repeats belong to SINE (short interspersed nucleotide elements) family of repetitive sequences. Detailed sequence analysis of the structure of ALU element RNAs has indicated that the ALU elements were ancestrally derived from the retrotransposition of the small cytoplasmic 7SL RNA, a component of the signal recognition particle [198]. The event of reverse-transposition of a copy of the 7SL RNA is an evolutionarily recent event that coincided with the radiation of primates in the past 65 million years [199].

When McHaffie *et al*. analyzed the 7SL RNA sequence, they found an nCaRE "core" sequence in reverse orientation lying immediately upstream of the poly-A tail. They envisaged a mechanism by which nCaRE-B is derived from retrotransposition of 7SL RNA and forms an integral part of many ALU elements. Figure 14 describes how during the process of reverse transcription, poly-T residues are added adjacent to the nCaRE core. If the insertion of the ALU into the genome occurs in the opposite orientation, this does not result in a functional nCaRE.

ALU elements have been broadly classified into three subfamilies: Old (ALU Js), Middle (ALU S) and the Youngest (ALU Ys) [200][201]. Beside nCaRE, ALUs have been shown to harbor a number of other regulatory sites [202]. Table 2 displays the positional conservation of the regulatory sites across all subfamilies in which they are represented.

The regulatory elements are most abundant in the middle subfamilies and least represented in the younger ALUs. Very interestingly, nCaRE are present in older and middle ALUs but poorly represented in the younger as well as polymorphic ALUs. This is very curious since nCaRE are also present in ancestral progenitor of ALU, the 7sl RNA.

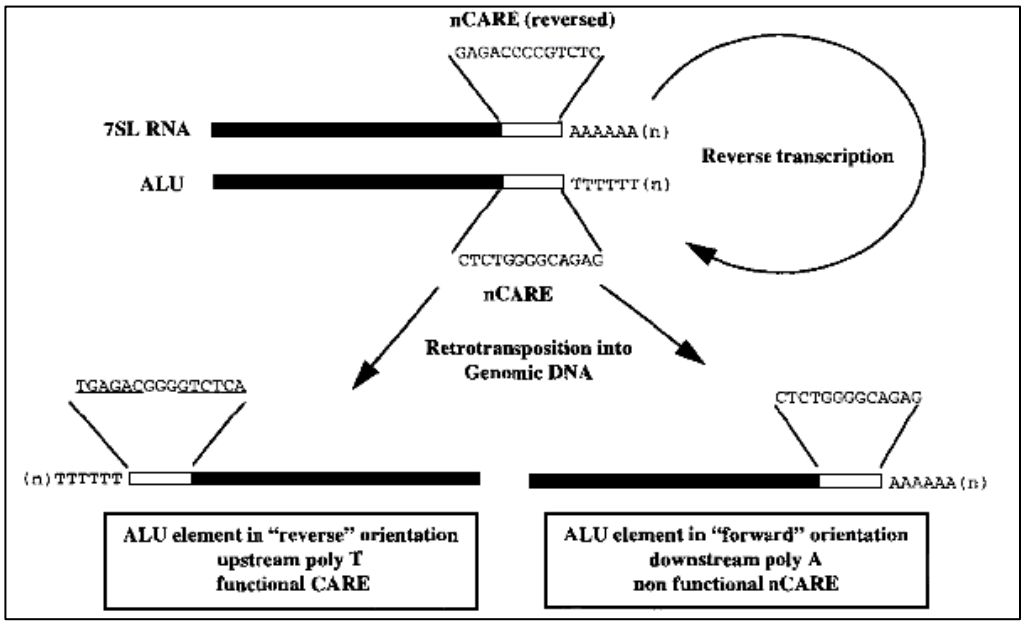

Figure 14 - Suggested mechanism of ALU formation from 7SL RNA retrotransposition.
Described is the proposed sequence of events whereby the 7SL RNA is reverse transcribed and reinserted into genome in reverse orientation, giving rise to an nCaRE element at the 5' end of an ALU repeat. (Image from McHaffie G.S. and Ralston S.H. *Bone*, 1995)

Another intriguing features of ALU is that their distribution has been shown to be non-random in the human genome [203-205] and increasing evidences show that these elements are implicated in different functions such as transcription, translation, response to stress, nucleosome positioning and imprinting. A retrospective analysis of putative functional sites of various evolutionary aged ALU, such as the RNA pol III promoter elements, pol II regulatory elements like hormone responsive elements and ligand-activated receptor binding sites, demonstrated a progressive loss of the RNA pol III transcriptional potential with concomitant accumulation of RNA pol II regulatory sites [202]. Moreover, it has been observed a significant over-representation of ALUs harboring these sites in promoter regions of signaling and metabolism suggesting that ALU elements, through retrotransposition, could distribute functional and regulatable promoter elements, which in the course of subsequent selection might be stabilized in the genome. In this way ALUs could thus have contributed to evolution of novel regulatory networks of preexisting gene in primate genome.

Table 2 - Position of regulatory sites analyzed in ALU repeats in various subfamilies. (Shankar R. *et al*., *BMC Evol. Biol*., 2004)

Family	A-box	B-box	AML	MPO	CETP	Rec	API	ERE	RARE	TRE	nCaRE	LXR
Jb	5	76	48	48	47	22	13/221	80	57–76	-67	289	
Jo	5	76	48	48	47	22	13/221	80	66	-67	289	224–240
Sx	5	76	48	48	47	22	13	80	60	-67	289	237–250
Sc	5	76	48	48	47	22	13/267	80	68	-67	289	
Y	5	76	48	48	47	22		80		-67	289	
Yb8	5	76	48	48	47	22	13/270	80	60–66	-67	289	230–240
POLY	5	76	48	48	47	22	13/267	80	60	-67	289	

4.8.3 Proteins involved in nCaRE recognition

Through Southwestern cloning, Okazaki *et al*. demonstrated the presence of APE1 in the nCaRE binding complex; however, they also suggested that APE1 alone could not explain all the features of nCaRE-binding activity postulating the existence of another nuclear protein(s) that could cooperate with APE1 for functional binding. This was particularly evident from gel shift assay in which they revealed two nCaRE-protein complexes when using smaller amounts of HeLa nuclear proteins (6-15 µg) [136]. The lower retarded complex co-migrated with APE1-nCaRE complex. In this condition, addition of recombinant APE1 protein to the HeLa nuclear proteins increased the binding of both nCaRE-protein complexes at almost the same positions. Since APE1 alone could not produce the slower migrating complex, Okazaki *et al*. suggested that APE1 may form a heterodimer with another nuclear protein to efficiently bind to nCaREs.

By the employment of oligonucleotide affinity column and amino acid microsequencing, in a later work, the group of Okazaki identified another partner of nCaRE binding: the Ku Antigen (KuAg) [18]. The Ku antigen is a heteromeric (Ku70/Ku80) protein that participates in multiple nuclear processes from DNA repair to V(D)J recombination to telomere maintenance to transcriptional regulation and serves as a DNA binding subunit and allosteric regulator of DNA-dependent protein kinase [206-209].

Chung *et al*. demonstrated that both subunits of KuAg, p70 and p80, interact with the N-terminal portion of APE1 to bind nCaRE-A sequence. In particular they evidenced that KuAg binds to nCaRE-A in a cooperative manner with APE1, giving rise to a reinforced binding specificity, respect to the less stringent binding observed for the purified KuAg alone. Electromobility shift assay (EMSA) showed the formation of two migrating complexes bound to nCaRE-A. Differential silencing of p70 and p80, allowed to demonstrate that there are two distinct steps in the formation of these two complexes in which p70 and p80 act separately. At first, APE1 and p80, but not p70, take part in the formation of the complex with higher molecular weight; then, there is shift to a second

complex in which p70 cooperates with APE1. Notably, this second complex with a higher mobility contained both the subunits and the reassociation of these both subunits of KuAg was predicted to be essential for the transcriptional suppression mediated by Ca^{2+} since an abrogation nCaRE-mediated transcriptional repression by Ca^{2+} was observed only in the case of combined silencing of both p70 and p80.

Similarly to the situation of nCaRE-A-binding complex, which was shown to include APE1 together with KuAg protein, Kuninger *et al*., utilizing DNA affinity chromatography, eluted the protein hnRNP-L bound to nCaRE-B2 sequence in association with APE1 [17]. Heterogeneous nuclear ribonucleoprotein L (hnRNP-L) belongs to hnRNP family, which consists of about 20 members that are stably associated with heterogeneous nuclear RNAs, pre-mRNAs, which required extensive post-transcriptional processing to generate mature mRNAs [210]. hnRNP complexes were described to be involved in the formation, packaging, processing, and function of mRNA. Identification of this protein bound to nCaRE sequence was therefore completely unexpected even if different studies suggested broader and unrelated functions for hnRNP proteins, e.g. in transcriptional regulation of gene expression and other cellular processes[211][212]. hnRNP-L binding with nCaRE-B2 sequence was verified by EMSA analysis and by reconstitution of the nCaRE-B2 binding activity. Consistent with data reported by Okazaki, recombinant protein alone displayed a weak binding activity toward nCaRE-B. However, this binding was increased in presence of HeLa nuclear extract suggesting that some other component are required for the ideal complex formation. Furthermore, Kuninger *et al*., demonstrated by GST-pull down assay, that the interaction between APE1 and hnRNP-L was not dependent on the presence of nCaRE elements indicating that these proteins could be complexed *in vivo* in the absence of the nCaRE-B2 oligo. The hnRNP-L polypeptide contains a stretch of basic amino acids similar to those found in the transcription factors HLF, c-Fos and c-Jun. The N-terminal redox domain of APE1 has been shown to be required for reductive activation of these transcription factors at specific, conserved cysteine residues in these proteins [213][214]. It has been proposed that this region may function as an interaction domain that mediates the coupling of hnRNP-L and APE1 without implicating a reductive activation of hnRNP-L, as the conserved cysteine in hnRNP-L is replaced by arginine. This would involve an interaction of the N-terminal region of APE1 with a region near the C-terminus of hnRNP-L. This model is consistent with the interaction between APE1 and Ku70/Ku86, which has been shown by Chung *et al*. [18] to require the N-terminal region of APE1, i.e. the region encompassing the redox domain. Chung *et al*. identified a sequence, AALCR, corresponding to residues 395–399 in Ku70, which is involved in this interaction. This is

compatible with Kuninger's proposal that this region may function as a common protein–protein interaction domain for APE1.

The inability of the recombinant APE1 alone to bind to nCaRE-A or nCaRE-B in the PTH promoter indicated a requirement for additional factors in the complexes. Later studies demonstrated that APE1 binding to nCaRE sequences on PTH promoter is influenced not only by other proteins but also by the acetylation status of APE1 itself [20]. Treatment with Ca^{2+} significantly increased APE1 acetylation in BHK-21 cells, which could explain the original observation that an increase in Ca^{2+} enhanced the binding activity of BHK-21 cell extract for nCaRE-B [136]. Bhakat *et al*., indeed, showed that APE1 is acetylated *in vivo* and *in vitro* by the transcriptional co-activator p300 which is activated by Ca^{2+}. Mass spectrometric analysis confirmed APE1 acetylation and indicated that this modification occurs preferentially on Lys 6 and Lys 7 in APE1 N-terminal domain. They observed an increased HAT activity of p300 upon Ca^{2+} treatment and suggested CAM kinase IV as the kinase responsible for Ca^{2+}-dependent activation of p300 HAT. Acetylation of APE1 at Lys6/7 by p300 resulted in an increased APE1 binding to nCaRE-B on PTH promoter. Moreover, the authors found that APE1 immunoprecipitates with class I HDACs (HDACs 1-3) and the acetylation status of APE1 is not essential for the stable binding of the two proteins. Interaction of APE1 with HDAC 1-3 could at least partially explain how APE1 acts as a transcriptional repressor. Based on their results, Bhakat *et al*. proposed a model for Ca^{2+}-dependent repression of the PTH gene. APE1, present partly as the APE1-HDAC complex *in vivo*, is unacetylated. A rise in Ca^{2+} increases the HAT activity of p300, which then acetylates APE1. Acetylation stimulates association of APE1 with its partner hnRNP-L, and binding to nCaRE-B in the PTH promoter. This promoter-bound repressor complex turns off PTH transcription by deacetylating histones in the promoter region. Finally, deacetylation of AcAPE1 by HDAC in the nCaRE complex reduces APE1's affinity for hnRNP-L (and possibly other proteins) in the nCaRE-B complex; subsequent release of APE1 from the complex leads to restoration of transcription. Thus the negative feedback regulation is mediated by the acetylation/deacetylation cycle of APE1.

Another described APE1 partner of nCaRE binding is Poly (adenosine diphosphate-ribose) polymerase 1 (PARP-1) which was identified by Bhattacharyya *et al*. in the context of gastric epithelial cell (GEC) infected by *Helicobacter pylori* [19]. Bhattacharyya *et al*. evidenced a negative calcium responsive element (nCaRE-B) in the human *Bax* promoter. Bax (Bcl-2–associated X protein), is a protein of the Bcl-2 gene family that promotes apoptosis by competing with Bcl-2. Upon initiation of apoptotic signaling, Bax undergoes a conformation shift which determines its shuttling from the cytoplasm where, under basal condition it is found, to the outer mitochondrial membrane where it can

induce the release of cytochrome c and other pro-apoptotic factors from the mitochondria, leading to activation of caspases. *H. pylori* infection enhances Bax expression [215] determining GEC death which can finally be the cause of gastritis, duodenal and gastric ulcer and gastric cancer [216]. Bhattacharyya *et al*. provided evidences that, in the context of *H. pylori* infected GEC, APE1 manifests antiapoptotic properties suppressing bax expression through the binding of nCaRE sequence on bax promoter (Figure 15).

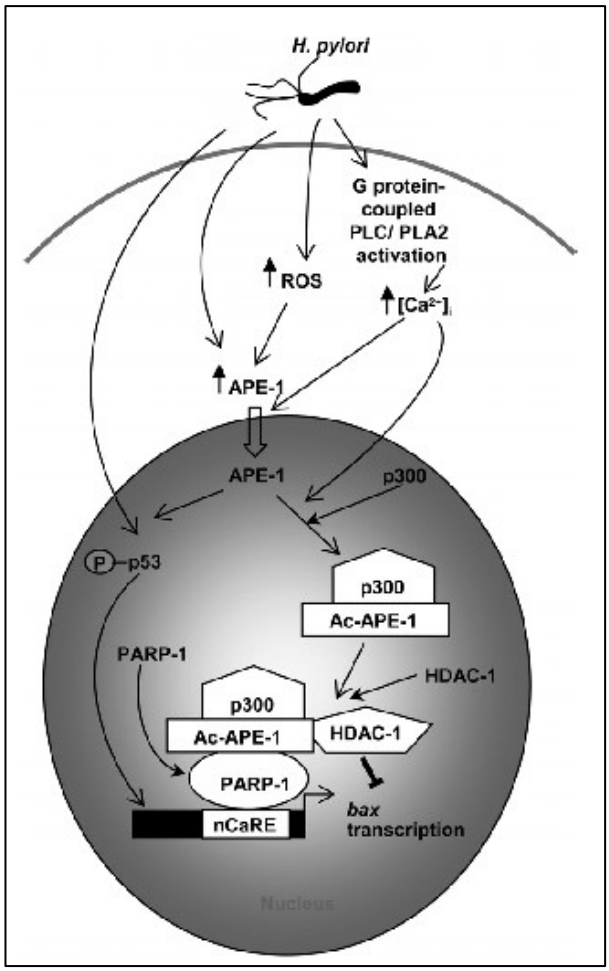

Figure 15 - APE1 acetylation suppresses *H. pylori*-mediated apoptosis in GEC by negative regulation of Bax transcription.
H. pylori infection induces an increase in Ca^{2+} which promotes nuclear translocation of APE1. Ca^{2+} and ROS promote p300 binding to nuclear APE1 leading to APE1 acetylation. ac-APE1 binds to the nCaRE present in the Bax promoter and attracts HDAC-1 thus repressing Bax transcription mediated by p53; PARP-1 recruits the repressor complex to the Bax nCaRE. (Image from Bhattacharyya A. *et al*., *Gastroenterology*, 2009)

In particular, in this work it has been proposed that *H. pylori* infection of GEC induces an increase in the intracellular levels of Ca^{2+} which in turn augment APE1 acetylation at Lys 6/7 by p300 increasing APE1 binding to bax nCaRE leading to a reduced bax expression. Repression of bax transcription is due to the formation of a multiprotein repressor

complex. They reported that PARP-1 binds directly to nCaRE-B on bax promoter and recruits the acetylated APE1 (ac-APE1)/HDAC-1 repressor complex. Further studies are needed to demonstrate that PARP-1 binding to nCaRE is specific for GEC or occurs in all cell types.

5 Results

Data reported in this chapter have been the subject of a submitted publication: Antoniali *et al*., *SIRT1 gene expression upon genotoxic damage is regulated by APE1 through nCaRE-promoter elements*

5.1 Bioinformatic searching for nCaRE sequence-containing genes reveals SIRT1 gene as a novel candidate target of APE1 regulation

Systematic searching for functional nCaRE sequences on human genome would provide new insights into APE1 multifunctional roles and in particular it could help in defining new genes whose expression may be potentially regulated by APE1 through nCaRE binding. To this aim, bioinformatic analysis for the systematic retrieval of functional nCaRE sequences in the human genome was carried out filtering through biological data obtained in our previous work, in which changes of gene expression profile, associated with the loss of APE1 expression, were analyzed through microarray analysis [53]. Here, I developed a method that integrates different approaches aiming to address the problem on a whole genome scale while minimizing the number of false positives. To this purpose, classical DNA pattern matching studies were integrated with independent information on gene regulation. Three main sources for data filtering were used: i) functional annotation data collected in GO; ii) gene expression data derived from the microarray profile of APE1 knock-down HeLa cells [53]; iii) human-mouse gene sequence comparisons. In fact, both expression data and functional annotation database are known to provide a wealth of information about co-regulation. This is of particular interest, since co-regulated genes likely share similar transcriptional regulatory mechanisms. At the same time, comparison with orthologous gene promoters highlighted sequences retained during evolution, whose conservation suggests their potential functionality. As a final result, a set of genes that passed the previously mentioned filters were obtained and might be considered *bona fide* as candidates co-regulated through nCaRE sequences (Figure 16A).

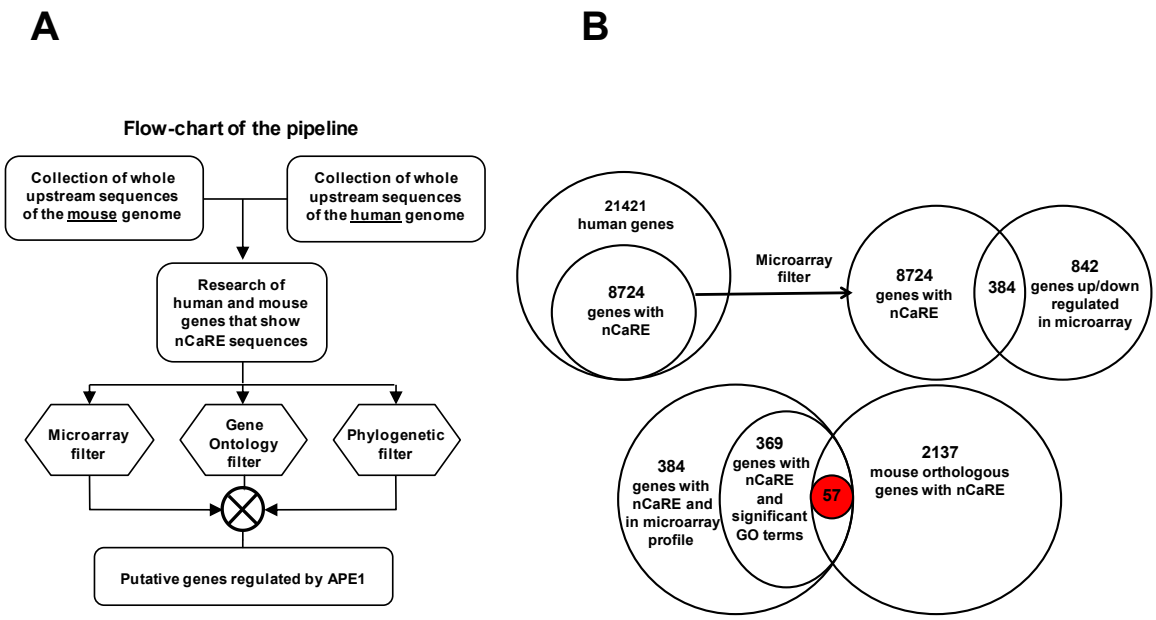

Figure 16 - Bioinformatic research of nCaRE sequences on human genome.
Panel A. Schematic representation of the pipeline steps used for the identification of putative nCaRE elements within the human genome.
Panel B. Results obtained from the application of the different filters. *Upper panel*, data derived from alignment research of nCaRE sequences on human gene promoters and the subsequent cross-check with microarray data. *Bottom panel*, final results deriving from the combined Gene ontology and phylogenetic footprinting analyses.

Experimentally, 6000 bp upstream regions of all human and mouse protein coding genes were collected. The extension of the chosen region was based on the knowledge of the localization of previously identified nCaRE elements [16][138][139]. Although nCaRE elements seem to be active also at downstream regions [139], I focused only on the upstream sequence of human genes; in a near future, I plan to extend this approach also to downstream and intron regions. Retrieved promoters were then analysed for the presence of nCaRE-B elements using Glsearch as program for local alignment [217]. 8724 human genes were found to contain one or more nCaRE matches within their promoters; similarly, 2173 matches were retrieved in the mouse genome. We then cross-checked candidate genes with gene expression data obtained from APE1 knock-down cells [53], thus verifying some evidences of co-expression between genes carrying nCaRE elements. Through this analysis, 384 common genes were identified in the two datasets (Figure 16B). Then, I considered the GO annotations of these 384 genes, searching for statistically significant common annotations. In general, a GO annotation term was considered to be significantly overexpressed when the corresponding *p*-value (not corrected for multiple testing) was lower than 1E-4. Through this approach, it has been observed a strong over-representation of terms related to RNA processing and metabolism, in accordance to our previous studies [53]. All the significant associations between genes and GO terms are reported in Supplementary Table 4 in Appendix. Finally, the "phylogenetic footprinting filter" was applied to evaluate whether the

significant fraction of the genes, obtained through the GO filter, shares homologous genes, containing nCaRE related sequences in the upstream region, with the mouse gene dataset. As a final result, 57 genes were extracted that may be considered *bona fide* candidates bearing the putative nCaRE sequences within their regulatory elements. The complete list of the 57 genes retrieved is reported in Supplementary Table 5 in Appendix. Finally, a functional enrichment analysis was performed to unveil if the 57 genes found are involved in common biological processes. This examination showed that candidate genes were associated with processes related to gene expression, activation or increment of the extent of transcription from an RNA polymerase II promoter (Figure 17 and Supplementary Table 6 in Appendix). Among these 57 genes, several are involved with DNA repair process and cellular response to external stimuli and DNA damage, e.g. SWI/SNF related, matrix associated, actin dependent regulator of chromatin, subfamily a, member 4 (SMARCA4), sirtuin 1 (SIRT1), valosin-containing protein (VCP), multiple endocrine neoplasia I (MEN1), structural maintenance of chromosomes protein 6 (SMC6), early growth response 1 (EGR-1) and APE1 itself. Particular attention was focused on SIRT1, a NAD-dependent histone deacetylase belonging to the class III of the sirtuin family because it occurs most frequently among the functional enriched categories (see Supplementary Table 6 in Appendix) and based on the recent demonstration of a functional involvement of this enzyme in the deacetylation of some K residues in the N-terminal region of APE1 [5][157](see also list of papers published during PhD). The latter information and the data derived from our bioinformatic analysis, led us to hypothesize the existence of an auto-regulatory loop between APE1 and SIRT1.

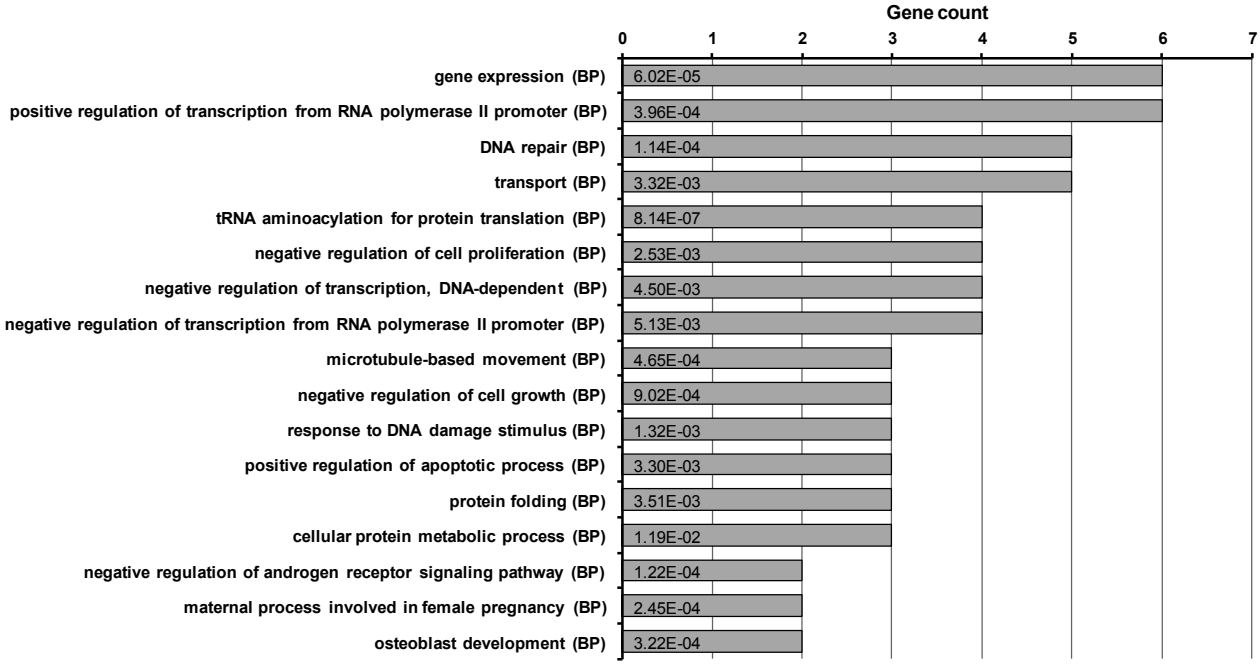

Figure 17 – GeneCodis functional enrichment analysis of the 57 putative genes bearing nCaRE sequences performed according to biological process.
The histogram reported the list of the first seventeen co-occurrence terms. On the horizontal axis it is shown the number of genes for each category together with the statistical significance. For clarity only the most representative functional categories are reported. See Supplementary Table 6 in Appendix for the complete list.

5.2 APE1 binds the nCaRE sequences present in the human SIRT1 promoter

In order to prove the functional relevance of the nCaRE sequences identified in the human SIRT1 promoter, I first tested *in vitro* the ability of APE1 to specifically bind to these elements. Thus, EMSA analyses were performed using different APE1 recombinant proteins and two double stranded (ds) oligonucleotides containing the SIRT1 nCaRE elements corresponding to the sequences found at -2701 (SIRT1-A) and -1754 bp (SIRT1-B) from the transcription start site (TSS), respectively (Figure 18A). Full length human wild type APE1 ($APE1^{WT}$), the N-terminal APE1 deletion mutant ($APE1^{N\Delta33}$) and the homologous APE1 from zebrafish (zAPE1) expressed in *E. coli* were used to this purpose. As clearly demonstrated by the EMSA analyses, only the $APE1^{WT}$ protein was able to stably bind both the nCaRE sequences (Figure 18B, lanes 2 and 6), while a complete absence of retarded complex was observed in the case of the truncated $APE1^{N\Delta33}$ form (Figure 18B, lanes 3 and 7). These findings underlined the importance of the first 33 amino acids present at APE1 N-terminus for the proper binding of the protein to nCaRE sequences. A similar poor DNA binding activity was also evident in the case of zAPE1 (Figure 18B, lanes 4 and 8), which bears a non-related N-terminal domain [85]. All together, these results suggest that the phylogenetically evolved N-terminal domain is essential for a stable interaction between APE1 and the nCaRE sequences; in this

context, it is conceivable that K residues present within this region, and acquired during phylogenetic evolution in mammals [85][86][218], may play a major role in protein binding to these DNA elements.

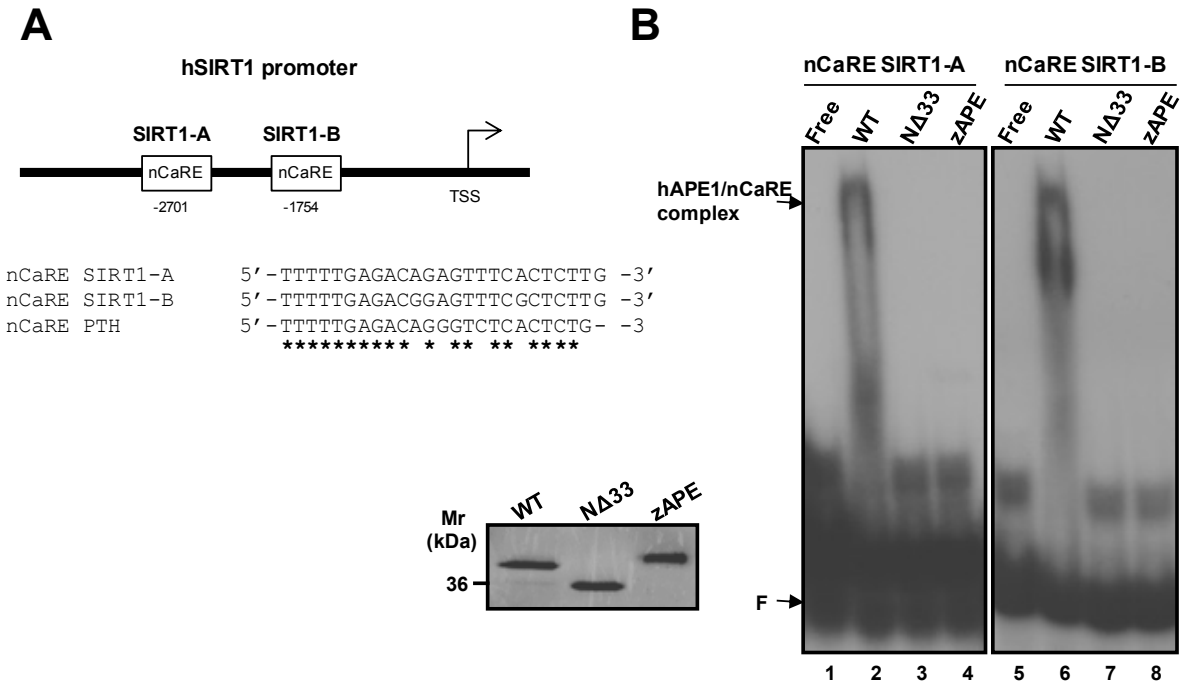

Figure 18 - APE1 N-terminal domain is essential for APE1 binding to nCaRE sequences contained in the human SIRT1 promoter.
Panel A. Schematic representation and multiple sequence alignment of two candidate nCaRE-B-like sequences identified in human SIRT1 gene promoter with the nCaRE sequence found on the human PTH promoter.
Panel B. EMSA analysis with ds oligonucleotides corresponding to nCaRE SIRT1-A and SIRT1-B sequence challenged with $APE1^{WT}$, $APE1^{N\Delta33}$ and zAPE1. Reactions were performed with 2.5 pmol of oligonucleotide and 10 pmol of purified $APE1^{WT}$ (lanes 2, 6), $APE1^{N\Delta33}$ (lanes 3, 7) and zAPE1 (lanes 4, 8). Lanes 1 and 5 represent probe alone; F shows the position of the free oligonucleotide probe. Specific APE1/nCaRE interaction is indicated by the arrow. Coomassie staining of the purified recombinant proteins challenged in EMSA is shown on the left.

Then the affinity of APE1 for nCaRE sequences was estimated through Surface Plasmon Resonance (SPR) analysis (Figure 19). SPR analyses were performed in collaboration with the Institute of Biostructures and Bioimaging, National Research Council of Naples, Italy. Biotinylated versions of the nCaRE or polyT sequences were immobilized onto a streptavidin chip to be used as ligands in SPR assays. $APE1^{WT}$ and $APE1^{N\Delta33}$ were then analyzed for their DNA binding activity. When testing $APE1^{WT}$ as analyte, a K_D value of 3.90±0.08 μM was measured [218]; corresponding kinetic parameters are shown in Table 3. Conversely, when using $APE1^{N\Delta33}$, any SPR signal variation was observed (data not shown), in accordance with the EMSA analysis (Figure 18B). This result confirmed that the APE1 region 1-33 is essential for a stable interaction with these DNA elements. As DNA-repair enzyme APE1 has an intrinsic ability to bind DNA in a sequence-independent manner, and independent observations clearly pointed to a role of the nucleic acid secondary structure in positively modulating this activity [218],

the protein capacity to bind a single-stranded 24-mer oligo-dT (here called polyT) was also evaluated. A K_D value of 308±3 μM was measured in the case of $APE1^{WT}$, while no binding was observed for $APE1^{N\Delta33}$ (Figure 19 and

Table **3**), in agreement with EMSA analysis. These experiments indicated that APE1 poorly recognizes an oligonucleotide formed by stretch of thymidines, having a non-structured conformation, thus confirming that this protein may bind to DNA with different affinities and that the oligo-dT sequence may be used in EMSA analysis as non-specific competitor.

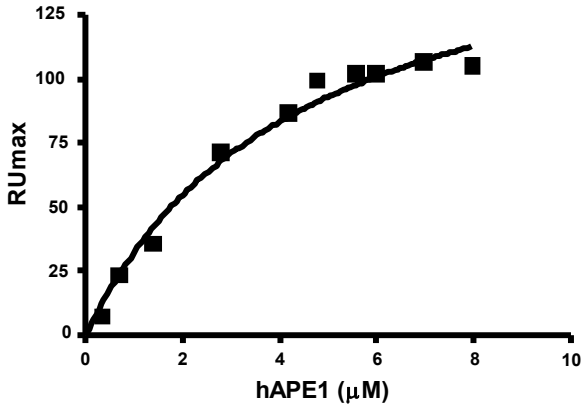

Figure 19 - Sequence specificity of APE1 binding to wild type nCaRE motif.
SPR analysis on the hAPE1–nCaRE interaction. Recombinant hAPE1 and biotinylated nCaRE SIRT1-B were used as analyte and ligand, respectively. Plot of RUmax from each binding vs. hAPE1 concentrations (0.5-8 μM); data were fitted by non-linear regression analysis.

Table 3 - Dissociation constant and kinetic parameter values as determined for hAPE1 by SPR analysis.

Ligand	Ka (Ms 10^5)	Kd (1/s)	K_D (μM)
SIRT1-B nCaRE	0.270	0.105	3.90±0.08
SIRT1-B mutated	0.0198	0.236	119±8
polyT	0.00364	0.112	308±3

EMSA analysis on APE1 binding activity to the nCaRE sequences showed a poor affinity for recombinant APE1; therefore, I tested whether additional factors present in nuclear extracts of cells may increase the protein binding affinity to its nucleotide target. To this aim, further EMSA analyses were performed with HeLa cells nuclear fractions, confirming that a nuclear activity able to specifically bind nCaRE sequences was indeed present (Figure 20A). The high affinity complex measured even using much lower

amounts of APE1 (0.63 pmol, as estimated separately [5]) with respect to that obtained with the recombinant purified protein alone (10 pmol) (Figure 18B), suggested that additional factors are required for an efficient APE1 binding to SIRT-1 nCaRE sequences. To demonstrate the presence of APE1 in the retarded complex observed in Figure 20A, I used nuclear extracts obtained from a HeLa lines (CL.3) where endogenous APE1 protein expression has been previously knocked-down through stable shRNA transfection [13]. As apparent from lane 3 in Figure 20A, an overall reduction of the intensity of the retarded nCaRE-bound complex was observed, similarly to what occurred also for the clone expressing $APE1^{N\Delta 33}$ (lane 5). Nuclear extracts obtained from HeLa cells reconstituted with ectopic $APE1^{WT}$ (lane 4) showed the same amount of the bound complex as the control cell clone expressing a scrambled shRNA vector (indicated as SCR-1). Pre-incubation of the nuclear extract from the SCR-1 clone with an anti-APE1 antibody resulted in the formation of a super-shifted complex (Figure 20B, lane 3); this complex was absent when a non-related antibody was used (lane 6), clearly demonstrating that APE1, present in the nuclear cell extract, is involved in the recognition of the nCaRE elements of the SIRT1 promoter. The reduced intensity of the retarded complex band upon APE1 silencing or in the reconstituted cells expressing $APE1^{N\Delta 33}$ (Figure 20A), as well as the lower apparent electrophoretic mobility of the protein-DNA retarded complex when using nuclear extracts in place of the recombinant purified protein (Figure 18B), suggested that APE1 may be part of a multi-protein complex. Since Ku70 antigen protein was already demonstrated to bind nCaRE sequences in complex with APE1 [18], the HeLa nuclear extract was incubated with an antibody against the Ku70 antigen; the reaction was then subjected to EMSA analysis. The formation of a super-shifted complex was evident (Figure 20B, lane 4). Concurrent presence of APE1 and Ku70 in the same retarded complex was confirmed by performing a simultaneous pre-incubation with antibodies against these proteins (Figure 20B, lane 5). Overall, these data demonstrated that APE1 must be part of a multi-protein complex containing Ku70 to elicit its high-affinity binding potential to the nCaRE sequences present on SIRT1 promoter.

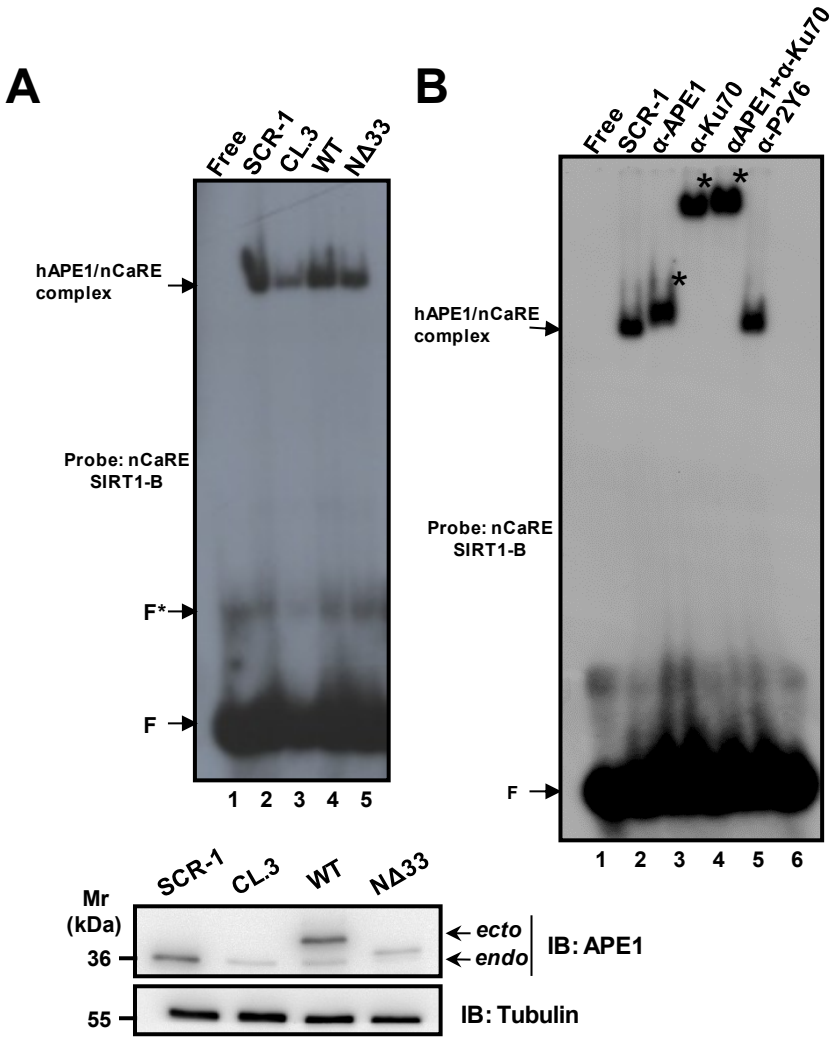

Figure 20 - APE1 is part of a nuclear protein complex which binds to SIRT1 nCaRE sequence.
Panel A. EMSA analysis with nuclear extracts from reconstituted cells on nCaRE SIRT1-B. 2.5 pmol of ds oligonucleotide corresponding to nCaRE SIRT1-B were incubated with 5 µg of HeLa nuclear extract of different clones: control clone, $APE1^{SCR-1}$ (lane 2), clone silenced for APE1, $APE1^{CL.3}$ (lane 3), clone where the expression of APE1 is reconstituted with $APE1^{WT}$ (lane 4) or with $APE1^{N\Delta33}$ (lane 5). Lane 1 correspondes to probe alone; F shows the position of the free oligonucleotide probe. Specific APE1/nCaRE interaction is indicated by the arrow. Western blotting analysis with APE1 antibody of the nuclear cell extracts reveals the silencing of endogenous APE1 ($APE1^{CL.3}$), when compared with control clone transfected with the empty vector ($APE1^{SCR-1}$) and that expression the ectopic flagged $APE1^{WT}$ and $APE1^{N\Delta33}$. Tubulin was used as protein loading control.
Panel B. 2.5 pmol of ds oligonucleotide corresponding to nCaRE SIRT1-B were incubated with HeLa nuclear extract from $APE1^{SCR-1}$ clone alone (lane 2) or pre-incubated with monoclonal antibody against APE1 (lane 3) or/and with an antibody against Ku-70 (lanes 4 and 5). Lane 6 corresponds to $APE1^{SCR-1}$ nuclear extract incubated with an aspecific antibody (α-P2Y6). Lane 1 is probe alone; F shows the position of the free oligonucleotide probe. Specific APE1/nCaRE interaction is indicated by the arrow. Asterisk indicates super-shift.

5.3 nCaRE sequences may fold into a cruciform-like structure that is recognized by the N-terminal portion of APE1

nCaRE element consists of a palindromic sequence that can possibly fold into self-complementary hairpins (Figure 21A). *In silico* analyses performed with mFold program were suggestive of the capacity of these elements to fold into cruciform-like structures. To evaluate whether nCaRE sequences can fold into cruciform duplexes and to specifically assess if APE1 binding to the SIRT1 nCaRE elements may depend on such secondary structures formation, footprinting analyses were performed by using the T7 endonuclease I. This is a structure-sensitive enzyme that specifically recognizes conformationally-branched DNA and Holliday structures or junctions [219-221]. Footprinting data supported the hypothesis of the existence of a secondary structure for the nCaRE-B sequences (Figure 21A). In particular, these experiments showed the predominant occurrence of two bands (10 and 19 nt in length) in the product digestion, which corresponded to a cutting site close to the predicted loop and immediately adjacent to the predicted stem (Figure 21A, arrows). Interestingly, pre-incubation of the nCaRE oligonucleotide with APE1 impairs T7 endonuclease digestion (Figure 21A, lane 4). Consistent with these observations, EMSA analysis demonstrated that digestion of the nCaRE oligonucleotide with T7 endonuclease affects APE1 binding to this element but conversely, when APE1 was first incubated with the nCaRE probe and then digested with T7 endonuclease, the binding was not affected. These data were suggestive for a protective role of APE1 to T7 endonuclease action, strongly supporting the hypothesis that these proteins may compete for the same binding site on the nCaRE-B sequences (Figure 21B).

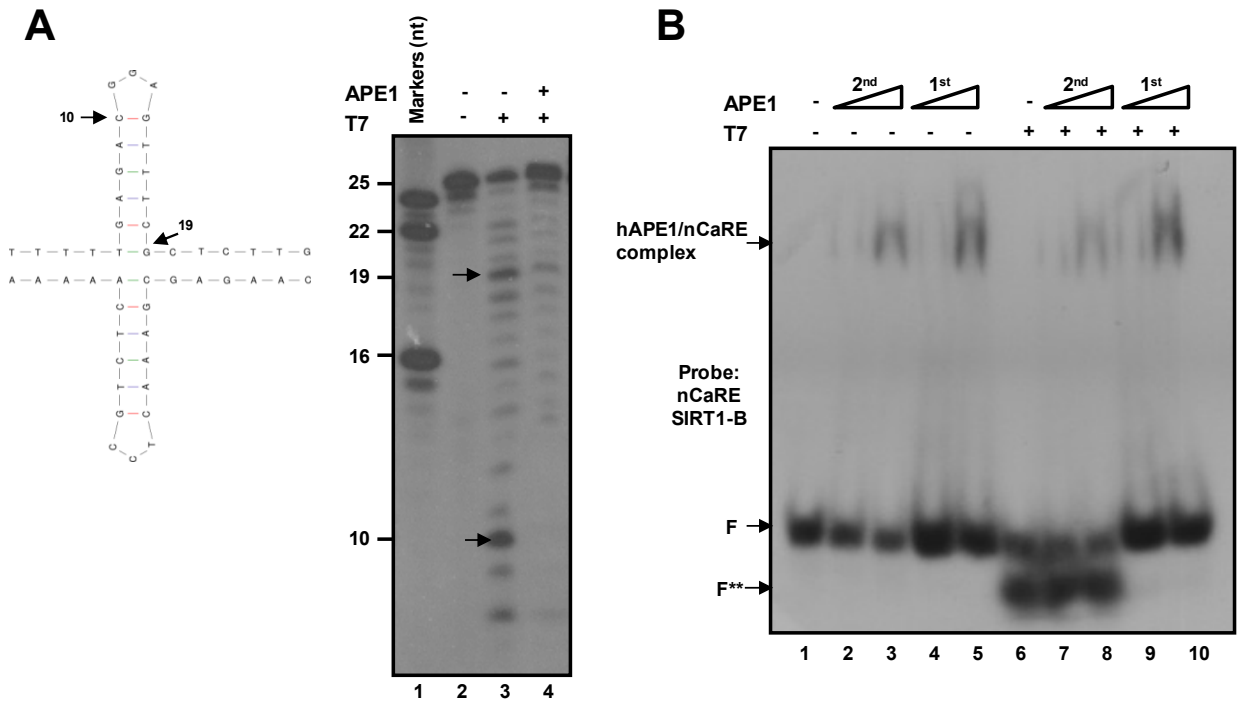

Figure 21 - APE1 recognizes structured nCaRE sequence.
Panel A. *Left*, cruciform structure of nCaRE SIRT1-B double-stranded oligonucleotide as predicted using mFold web server program. Arrows indicate the position and the length of the estimated cleavege sites by T7 endonuclease; *Right*, T7 endonuclease I footprinting analyisis. 2.5 pmol of ds oligonucleotide corresponding to nCaRE SIRT1-B were pre-incubated (lane 4) or not (lane 3) with 35 pmol of APE1 recombinant protein for 15 min at 37°C in EMSA binding buffer, then 5U of T7 endonuclease I were added to each reaction.
Panel B. EMSA analysis of APE1 binding to nCaRE sequence after digestion with T7 endonuclease or after pre-incubation with APE1 and subsequent digestion with T7 endonuclease. 2.5 pmol of ds oligonucleotide corresponding to nCaRE SIRT1-B were first digested with T7 endonuclease at 37°C, for 1 h, and subsequently incubated with increasing amounts of recombinant APE1 (10 or 30 pmol) at 37°C, for 15 min (lanes 7, 8). Alternatively, 2.5 pmol of nCaRE probe were first incubated with APE1 at 37°C, for 15 min, and sequentially digested with T7 endonuclease at 37°C, for 1 h (lanes 9, 10). Lane 1 is probe alone; 1st and 2nd indicate if APE1 incubation with the probe was performed temporally before (1st) or after (2nd) T7 digestion; F shows the position of the free oligonucleotide probe. F** indicates the T7 endonuclease-digested probe. Specific APE1/nCaRE interaction is indicated by the arrow.

To corroborate structural data obtained for SIRT1 nCaREB sequence with T7 endonuclease, the same experiment was performed with another enzyme, the mung bean nuclease (MB)[222], a single-strand specific endonuclease, typically used for the removal of hairpin loops during cDNA synthesis (Figure 22). In accordance to T7 endonuclease analysis, digestion of SIRT1 nCaREB oligonucleotide with mung bean nuclease prevents APE1 binding. EMSA analysis evidenced that the retarded band, ascribable to nCaRE-APE1 complex, decreased when a time-course mung bean digestion was performed previous to APE1 incubation (Figure 22A) and, similarly to what observed for T7 endonuclease, when APE1 was firstly incubated with the nCaRE probe and then digested with mung bean nuclease, the binding was not altered (Figure 22B).

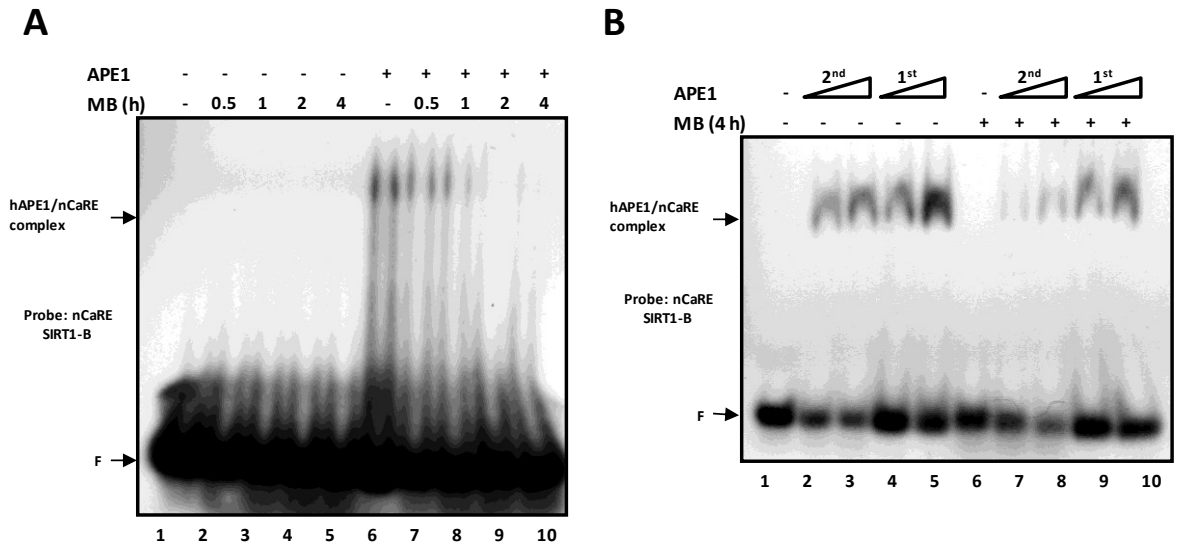

Figure 22 - EMSA analysis of APE1 binding to SIRT1 nCaRE sequence after mung bean digestion.
Panel A. 2.5 pmol of ds oligonucleotide corresponding to nCaRE SIRT1-B were digested with mung bean endonuclease at 30°C for the indicated period of time. The reactions then were incubated at 37°C with 10 pmol of recombinant APE1 protein for additional 15 min. Lane 1 is probe alone; F shows the position of the free oligonucleotide probe. Specific APE1/nCaRE interaction is indicated by arrow. Panel B. APE1 and mung bean endonuclease compete for the same nCaRE binding site. EMSA analysis of APE1 binding to nCaRE sequence after digestion with mung bean endonuclease or after preincubation with APE1 and subsequent digestion with mung bean. 2.5 pmol of ds oligonucleotide corresponding to nCaRE SIRT1-B were first digested with mung bean endonuclease at 30°C for 4 h and subsequently incubated with increasing amounts of recombinant APE1 (10, 30 pmol) at 37°C for 15 min (lanes 7, 8). Alternatively, 2.5 pmol of nCaRE probe were first incubated with APE1 at 37°C for 15 min and sequentially digested at 30°C for 4 h with mung bean endonuclease (lanes 9, 10). Lane 1 is probe alone; 1st and 2nd indicate if APE1 incubation with the probe was performed temporally before (1st) or after (2nd) mung bean digestion; F shows the position of the free oligonucleotide probe. Specific APE1/nCaRE interaction is indicated by arrow.

The first 33 N-terminal amino acids of APE1 are required for protein binding to nCaRE sequences (Figure 18). In order to investigate the role of this protein portion on APE1 ability of binding to these DNA sequences, the APE1-nCaRE complex was subjected to combined limited proteolysis-mass spectrometry experiments, according to previous studies realizing a differential probing of accessible amino acids in isolated and complexed proteins [223][224]. These analyses were performed in collaboration with the Proteomics & Mass Spectrometry Laboratory, ISPAAM of Naples by Dr. Andrea Scaloni. When limited proteolysis experiments were carried out on recombinant APE1 protein in the absence or presence of its target nCaRE oligonucleotide, differential peptide maps were obatained, which were exploited to infer the residues present at the complex interface [225]. Interpretation of the results was based on the concept of "shielding" from proteolytic attack. In particular, limited proteolysis experiments were carried out on a time-course basis on isolated APE1, protein complexed with SIRT1 nCaRE-B oligonucleotide and protein complexed with PTH nCaRE oligonucleotide [194]; the latter was used as control. Data interpretation was rationalized according to the X-ray crystallographic APE1 structures reported so far [83][226].

Panels A and D of Figure 23 show the time-course LC-ESI-MS analysis of the endoprotease AspN digestion on isolated APE1, as carried out by using an enzyme/substrate of 1:500 w/w. Under these experimental conditions, APE1 remained partly undigested, showing that its native conformation is susceptible to proteolysis at a unique, likely flexible site. After 5 min, only the peptide pair 1-17 and 18-321 was detected (Figure 23A), and no further fragments were released after 60 (Figure 23D) and 120 min (data not shown) (Supplementary Table 7 in Appendix). As previously reported [225], the definition of the primary cleavage sites was inferred by the identification of the complementary peptides released by a single proteolytic event occurring on the intact protein. According to these criteria, non-complexed APE1 was preferentially cleaved at D18 present within the unstructured protein N-terminal domain. When the APE1-SIRT1 nCaRE-B oligonucleotide complex was analyzed under the same conditions, no proteolytic fragments resulting from D18 cleavage were released even after 60 min (Figure 23, panel A and E) (Supplementary Table 7 in Appendix), demonstrating a tighter conformation of the complex and a DNA-shielding effect for D18. A very reduced digestion at this site was observed only after incubation for 120 min (data not shown). A similar condition was verified also for the APE1-PTH nCaRE oligonucleotide complex, which showed absent or practically negligible proteolysis at D18 after 5 and 60 min, respectively (Figure 23, panel C and F). These results clearly demonstrate that after APE1 interaction with DNA, D18 is no longer accessible to the protease action. Thus, it may be hypothesized that this residue occurs at the protein-nCaRE oligonucleotide complex interface.

The different accessibility of the basic residues in isolated APE1 and in its complex with nCaRE oligonucleotides was similarly probed with trypsin, used at 1:5000 w/w enzyme/substrate (Supplementary Table 7 in Appendix). LC-ESI-MS analysis of the proteolytic fragments released from the isolated protein led to the identification of the complementary peptide pairs 1-9, 10-321 and 1-10, 11-321 already after 5 min of reaction, which were generated by single hydrolytic events at K9 and K10, respectively. Additional products resulting from fragment subdigestions were also observed, but they did not provide information on further accessible amino acids. These results confirmed that APE1 N-terminal portion is very flexible and highly exposed to the protease action. Conversely, appreciable hydrolysis of recombinant APE1 following protein interaction with SIRT1 nCaRE-B or APE1-PTH nCaRE oligonucleotides was observed at K9 only after 60 min of reaction (Supplementary Table 7 in Appendix). Due to the nature of the proteolytic products observed, these experiments confirmed the masking effect of both oligonucleotides over the non-structured protein N-terminal region.

Further experiments were then carried out with broader-specificity proteases, such as chymotrypsin and elastase. In the first case, limited proteolysis of isolated APE1 (enzyme/substrate of 1:1000 w/w) generated only a complementary peptide pair, namely 1-114 and 115-321, which identified L114 as the primary cleavage site (Supplementary Table 7 in Appendix). Additional products resulting from fragment subdigestions were also observed, but they did not provide information on further accessible amino acids. According to X-ray crystallographic data, this residue is exposed on the molecular surface of the globular APE1 domain. No significant differences were observed on a time-course basis when peptide maps were characterized for both APE1-nCaRE oligonucleotide complexes (Supplementary Table 7 in Appendix). In fact, both peptides 1-114 and 115-321 were detected within the APE1-SIRT1 nCaRE-B and APE1-PTH nCaRE oligonucleotide products after 5 and 15 min, respectively, similarly to the non-complexed protein sample. These data excluded any involvement of L114 in binding to the nCaRE elements and further confirmed the suitability of the strategy used here.

When elastase digestion of isolated APE1 was carried out using an enzyme/substrate of 1:1000 w/w, only two peptide pairs (1-12, 13-321, and 1-14, 15-321) were detected after 5 min of reaction, whereas an additional pair (1-20, 21-321) was observed after 15 min (Supplementary Table 7 in Appendix). These data demonstrated that non-complexed APE1 was preferentially cleaved at A12, A14 and L20. When the recombinant APE1-SIRT1 nCaRE oligonucleotide and APE1-PTH nCaRE oligonucleotide complexes were analyzed under the same conditions, different proteolytic patterns were obtained, which proved preferential cleavage site at L20, as demonstrated by the identification of the complementary peptides 1-20 and 21-321 after 30 min of reaction (Supplementary Table 7 in Appendix). These results clearly demonstrated that, following complex formation, A12 and A14 are no longer accessible to elastase, whereas L20 is still partially exposed to the protease action.

The overall results of the limited proteolysis experiments for recombinant APE1 are summarized in (Supplementary Table 7 in Appendix), from which a number of general considerations can be driven concerning the native protein. Preferential cleavage sites, occuring in isolated APE1, gathered into a specific region of the protein, the most exposed segment being the unstructured N-terminal domain, which contained 6 hydrolysis sites (K6, K7, A9, A11, D15 and L17). A further hydrolyzed peptide bond was located within the globular APE1 domain (L111). Interestingly, no other cleavage sites were detected in other protein regions, although exposed on the molecular surface. After complex formation, a marked protection effect exerted by nCaRE oligonucleotides was observed, as demonstrated by the large decrease in the number of proteolytic sites

present in the N-terminal region (from 6 to 1), thus confirming the involvement of this APE1 portion in binding to these DNA elements.

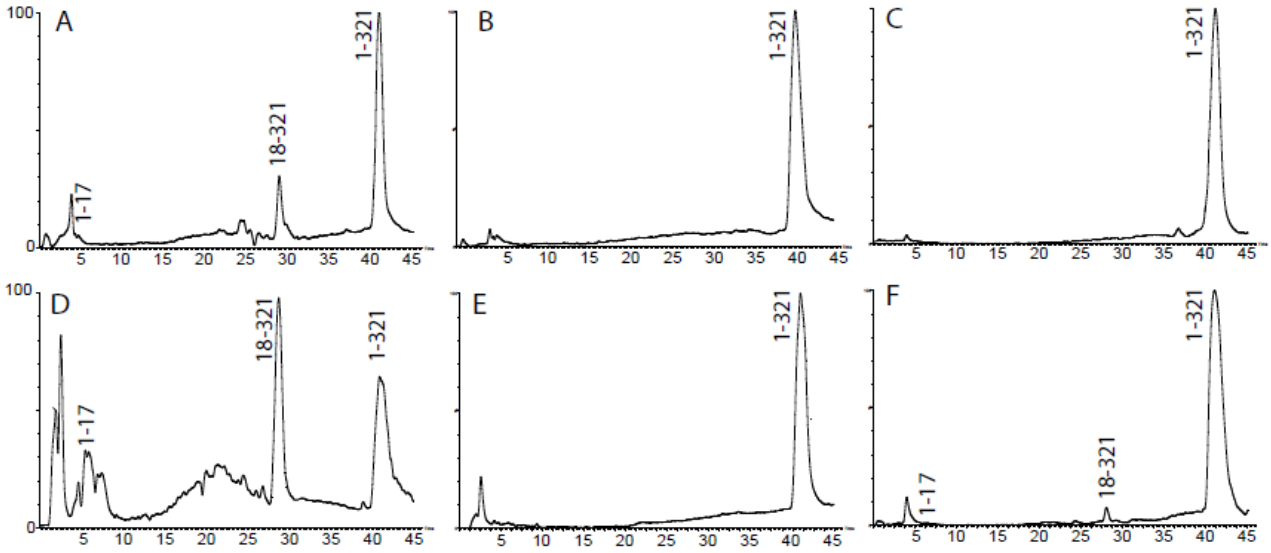

Figure 23 - Topology of the APE1-nCaRE complex: the APE1 N-terminal domain is involved in this binding. Comparative limited proteolysis experiments on isolated or DNA-complexed APE1. Time-course analysis of simultaneous trials performed on non-complexed recombinant APE1 (A, D), recombinant APE1-SIRT1 nCaRE-B complex (B, E) or recombinant APE1-PTH nCaRE complex (C, F) are shown. LC-ESI-MS profiles from samples taken at 5 (A-C) and 60 min (D-F) are reported. Identified peptides are reported on the corresponding chromatographic peaks; 1-321 denotes the intact protein.

5.4 APE1 regulates SIRT1 expression at the promoter level

To determine whether the observations obtained *in vitro*, regarding APE1 binding to nCaRE sequences, have any relevance *in vivo*, I examined the APE1 occupancy of the nCaRE sequence in the SIRT1 promoter through chromatin immunoprecipitation (ChIP) analyses. To this purpose, HeLa cells were co-transfected with a human SIRT1 promoter-containing plasmid [157] and FLAG-tagged APE1^{WT}- or APE1$^{N\Delta33}$-expressing plasmids. The amount of immunoprecipitated SIRT1 promoter was significantly enriched in APE1^{WT}-transfected cells, when compared with that obtained from control cells transfected with the empty vector alone (Figure 24A). As expected, APE1$^{N\Delta33}$-transfected cells had a remarkable reduction, even though not complete, in the amount of immunoprecipitated SIRT1 promoter. A similar degree of reduction was also observed when ChIP analysis was performed by using a SIRT1 promoter bearing a mutated sequence within the nCaRE motif (Figure 24B), whose reduced specificity was previously assessed through SPR analysis (

Table **3**). These experiments revealed that the mutation introduced in the nCaRE-B sequence significantly reduced the APE1 binding to DNA, lowering the affinity of the complex by a 30-fold factor (K_D = 119 ± 3 μM). Competitive EMSA analyses were in agreement with these findings. In fact, addition of the unlabeled nCaRE ds oligonucleotide resulted in an almost complete elimination of bound complex formation. On the other hand, competition with the unlabeled mutant nCaRE oligo (nCaRE-mut) caused only a slight reduction of the nCaRE-binding complex, in agreement with ChIP and SPR data, and supporting the notion of a sequence-dependent binding specificity (data not shown). Altogether, these results confirmed our *in vitro* observations (Figure 18, Figure 19 and Figure 20) and support the notion that, under basal conditions, APE1 is

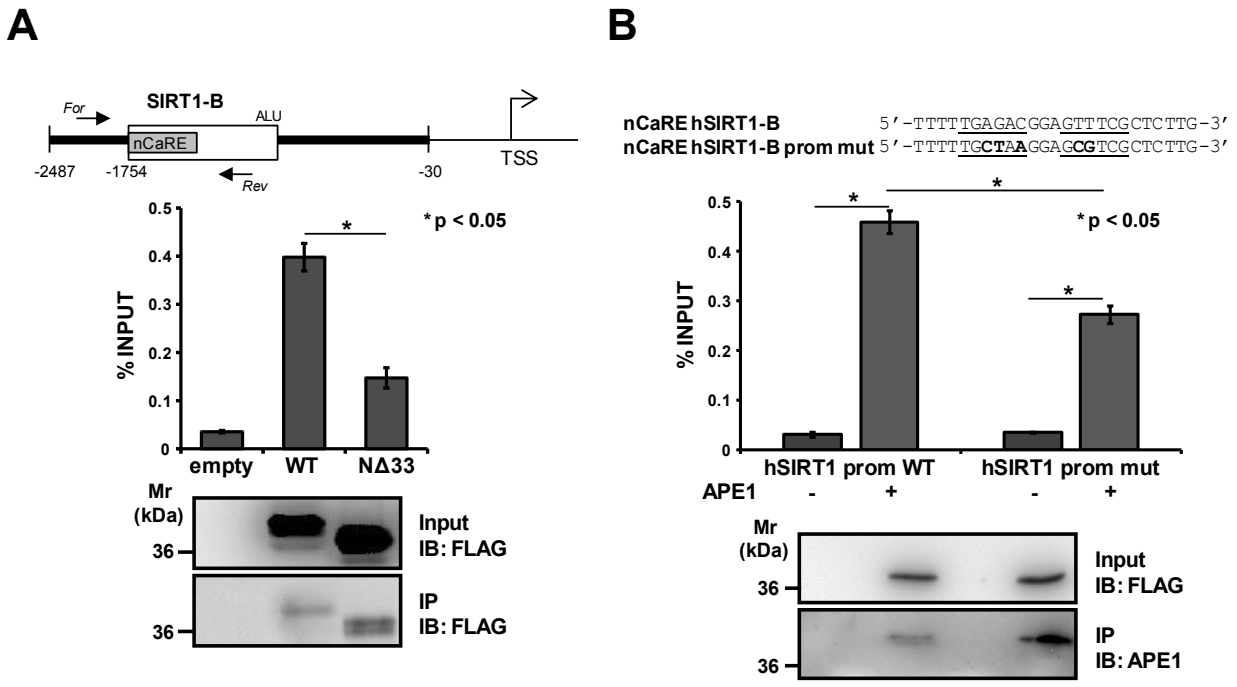

associated with the nCaRE-B sequence within the SIRT1 promoter also *in vivo*, possibly as part of a multiprotein complex.

Figure 24 - APE1 is constitutively associated with nCaRE sequence in SIRT1 human promoter.
Panel A. ChIP assay for *in vivo* association of APE1 and nCaRE sequence on human SIRT1 promoter. *Upper panel*, schematic representation of the human SIRT1 promoter used for HeLa transfection which included the nearest nCaRE sequence from TSS (nCaRE SIRT1-B). *For* and *Rev* arrows indicated the position of the RT-PCR primer designed for the quantification of the human SIRT1 nCaRE sequence bound to APE1. *Middle panel*, ChIP assay for APE1-nCaRE sequence association. HeLa cells were co-trasfected with both human SIRT1 promoter and with vector expressing $APE1^{WT}$, $APE1^{N\Delta33}$-FLAG tagged, or the empty vector as ChIP negative control. The values reported were calculated as fold percentage of the amount of immunoprecipitated nCaRE DNA relative to that present in total input chromatin. Data were further normalized to the amount of immunoprecipitated protein. The significance of sample average difference observed was estimated by Student's t test. * *p*-value < 0.05. *Bottom panel*, Western blotting analysis was performed on total cell extracts (input) and on immunoprecipitated material (IP) with specific antibody for FLAG and APE1. IB: immunoblot.
Panel B. ChIP analysis on mutated human SIRT1 promoter. *Upper panel*, base composition of the nCaRE sequence of human SIRT1 promoter (-1754 bp from TSS) and of the the mutated sequence used for site-directed mutagenesis. Divergent sequences in the mutant nCaRE are bold. *Middle panel*, HeLa cells were co-transfected with empty vector or with vector expressing $APE1^{WT}$ and, alternatively, with wild type hSIRT1 promoter or hSIRT1 promoter carrying a

mutation on its nCaRE-B sequence. The histogram represents the amount of hSIRT1 promoter sequence that was immunoprecipitated. Data are presented as percent of input and were normalized to the amount of APE1 immunoprecipitated, as evaluated by Western blotting analysis (*bottom panel*). Statistical tests were performed with Student's t test. * *p*-value < 0.05.

Then the functional relevance of APE1 on SIRT1 promoter activation was checked by performing promoter-reporter assays. HeLa cells were co-transfected with a luciferase reporter vector bearing the SIRT1 promoter and APE1^{WT} FLAG-tagged vector to evaluate if APE1 binding to SIRT1 promoter may play a role in SIRT1 transcriptional regulation (Figure 25A). SIRT1 promoter-reporter assays showed that there was a significant increase in the luciferase signal detected in the presence of APE1, compared to that of the promoter alone. Therefore, I decided to evaluate the effect of APE1 silencing on endogenous SIRT1 mRNA expression levels through an inducible shRNA knock-down strategy [53]. Endogenous APE1 knockdown (CL.3) caused a significant reduction in the SIRT1 endogenous expression levels (Figure 25B), which was rescued in cells reconstituted with a siRNA resistant APE1 cDNA expression plasmid (WT). These data demonstrated the positive effect of APE1 on SIRT1 transcriptional activation in accordance with our previous observations on gene expression profiling analysis [53], where a reduced expression of SIRT1 in APE1 knocked-down HeLa cells was apparent.

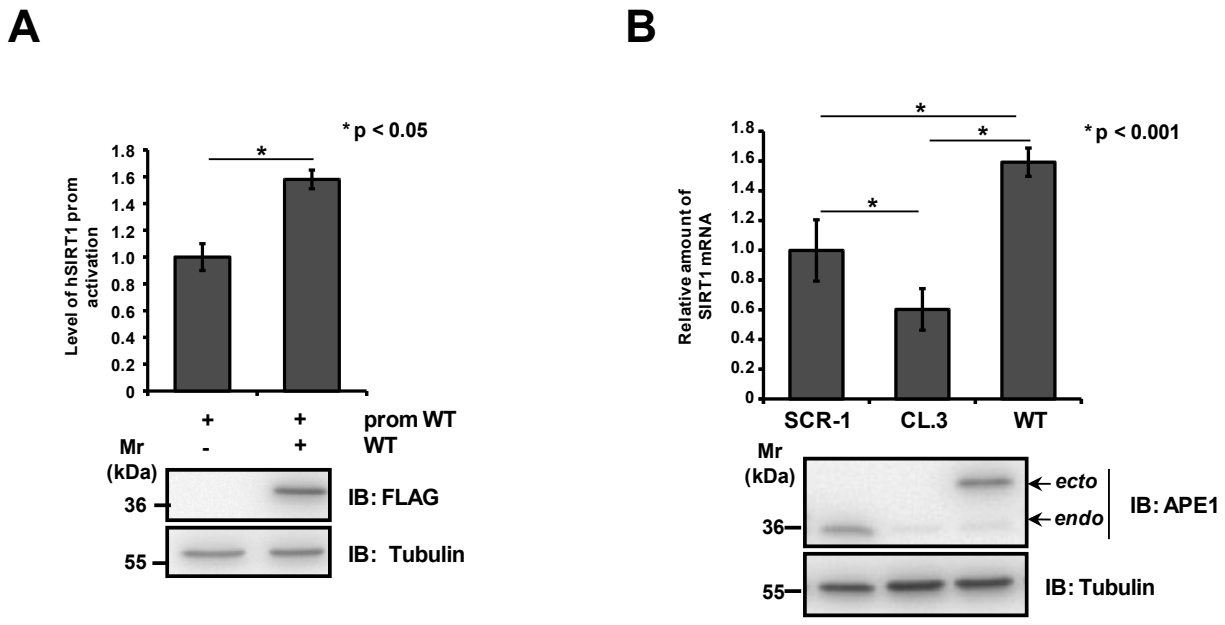

Figure 25 - APE1 positively regulates SIRT1 expression at the promoter level.
Panel A. hSIRT1 promoter is activated in presence of APE1. *Upper panel*, reporter assay with hSIRT1 firefly reporter vector co-trasfected with APE1^{WT} FLAG-tagged vector. Firefly luciferase activity observed was normalized to renilla luciferase activity. *Bottom panel*, Western blotting analysis for the normalization of protein levels. Tubulin protein level was used to normalize samples.
Panel B. Analysis of SIRT1 mRNA level with Q-PCR in clones expressing APE1^{WT} or APE1 silenced (CL.3) cells. *Upper panel*, data shown in the histogram are normalized to the amount of GPDH. Statistical tests were performed with Student's test. A *p*-value < 0.001 was considered as statistically significant (*). *Bottom panel*, Western blotting analysis on protein extract of clones showing the suppression of endogenous APE1 expression, upon ten days of treatment with doxycycline. Tubulin protein level was used to normalize samples.

5.5 Oxidative stress induces SIRT1 transcription via recruitment of BER enzymes

In order to better understand the transcriptional function exerted by APE1 through the binding to nCaRE sequences, we investigated if APE1's positive role on SIRT1 transcription could rely on its enzymatic activity on DNA. First, it has been observed that under basal conditions APE1 does not present endonuclease activity on the SIRT1 nCaRE-B sequence, as assessed through an oligonucleotide cleavage assay (

Figure **26**A). APE1 cleavage at any site on cruciform nCaRE sequence should lead to a site-specific single-stranded break that can be detected by the appearance of an extra fragment in the cleavage assay. Even using increasing amount of purified recombinant APE1 protein we did not detect any nuclease activity that, on the contrary, was readily visible when using a radiolabeled 26-mer ds oligonucleotide containing a tetrahydrofuran mimicking an AP site (here referred as THF) [14]. Substitution of the guanine residue at position 12, within the predicted loop of the nCaRE-B sequence, with a THF residue, resulted instead in efficient APE1 cleavage activity on the nCaRE-B sequence. This activity depends on the APE1 catalytic function, since the catalytically inactive APE1^{E96A} mutant [227] was unable to efficiently cleave the same substrate (

Figure **26**B).

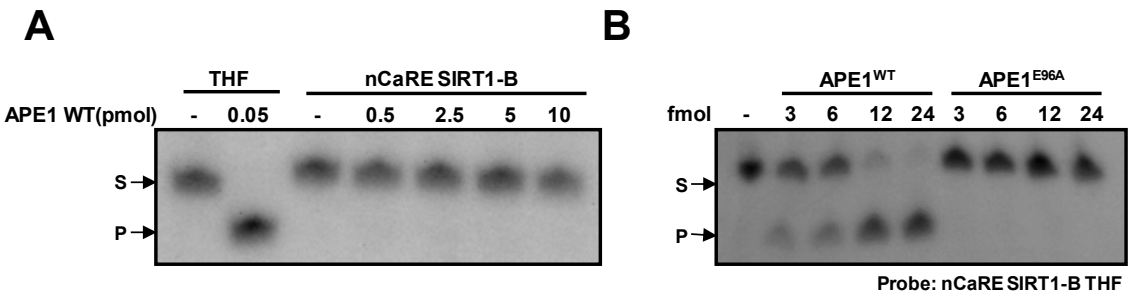

Figure 26 - APE1 cleaves SIRT1 nCaRE sequence only in the presence of an AP site within its structure.
APE1 endonuclease activity on ds nCaRE SIRT1-B radiolabeled oligonucleotide was tested by using an AP endonuclease activity assay. A radiolabeled ds THF-containing deoxyoligonulceotide (THF) was used as control. Reactions were performed as described in *Materials and Methods* with 2.5 pmol of each probe and increasing amounts (pmol) of recombinant APE1^{WT} protein; they were stopped after 15 min of incubation, at 37°C. The conversion of the radiolabeled THF-containing oligonucleotide substrate (S) to the shorter product (P) was evaluated on a denaturing 20% polyacrylamide gel. The corresponding gel image of the enzymatic reactions is shown. Panel A. Under basal condition, APE1 doesn't cleave the nCaRE SIRT1-B oligonucleotide. Panel B. APE1 AP endonuclease activity on ds nCaRE SIRT1 radiolabeled oligonucleotide containing a THF site. nCaRE SIRT1-B THF-containing probe were incubated with increasing amounts of recombinant APE1^{WT} protein or a catalytic inactive APE1 mutant (APE1^{E96A}).

Prompted by these findings, it has been hypothesized that the APE1 positive function observed on SIRT1 promoter may be ascribed to APE1 catalytic activity on nCaRE sequences; this phenomenon can be exerted after specific stimuli, such as oxidative stress, which can lead to abasic site formation on nCaRE sequences. It is well known that SIRT1 expression and function are regulated by external stressors, including the exposure to genotoxic agents [157][228][229]. I therefore measured the SIRT1 transcription after oxidative stress conditions, such as that generated by H_2O_2 exposure. First, I demonstrated that SIRT1 promoter activation was increased by H_2O_2 treatment in a concentration-dependent fashion (Figure 27A).

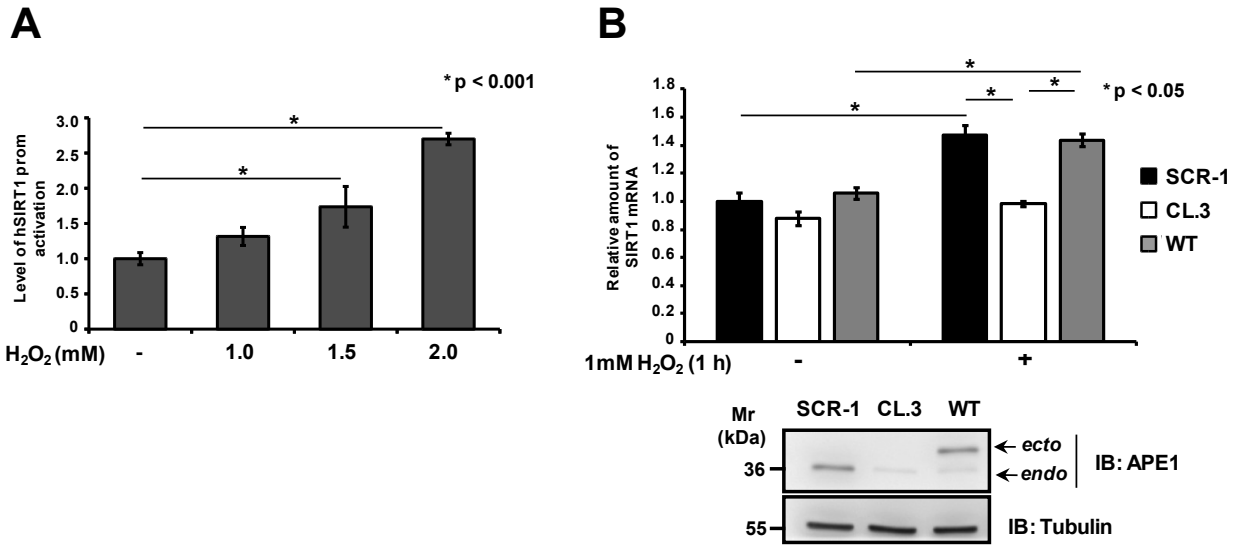

Figure 27 - H_2O_2 increases SIRT1 promoter activity which is mediated by APE1.
Panel A. Reporter assay with HeLa cells transfected with hSIRT1 firefly reporter vector and challenged with increasing doses of H_2O_2, for 1h, as indicated. Firefly luciferase activity observed was normalized to renilla luciferase activity. A *p*-value < 0.001 was considered as statistically significant (*).
Panel B. Q-PCR analysis of SIRT1 mRNA levels in clones expressing $APE1^{WT}$ or APE1 silenced cells $APE1^{CL.3}$ after 1 mM H_2O_2 treatment, for 1 h. Data shown in the histogram are normalized to the amount of GAPDH. The significance of sample average difference observed was estimated by Student's t test. A *p*-value < 0.05 was considered as statistically significant (*). Western blotting analysis on the protein extracts described in the upper panel. Tubulin protein level was used to normalize samples.

Next, it has been examined the effect of APE1 silencing or re-expression on SIRT1 transcriptional activation in HeLa cell clones upon H_2O_2-treatment (Figure 27B). The control (SCR-1), the APE1-silenced (CL.3) and the $APE1^{WT}$ cell clones were treated with 1 mM H_2O_2 for 1 h. SIRT1 mRNA levels were then evaluated by Q-PCR analysis and compared with untreated clones. Upon oxidative treatment, SIRT1 mRNA resulted significantly increased and, notably, this response was higher in the presence of $APE1^{WT}$ protein, whereas it was lower in the case of APE1 knocked-down expressing cells. The residual activation of SIRT1 mRNA expression, which was apparent also in APE1 knocked-down cells, might be ascribable to the presence of remaining endogenous APE1

protein and/or to the existence of further limiting factors as already speculated [17-19]. I confirmed the general relevance of our model by testing further hypothetical APE1 target genes containing an nCaRE element in their promoters and resulted dysregulated in APE1-kd cell model (Figure 16). To this aim, the expression levels, upon H_2O_2-treatment, of the Early growth response protein 1 (EGR-1) and Eukaryotic translation initiation factor 4E-binding protein 1 (EIF4EBP1), in the HeLa cell inducible-kd (CL.3) and in the reconstituted cell model (WT) used here, were evaluated by Q-PCR analysis (Figure 28). Similar results were also obtained when challenged cells with another genotoxic agent, methyl methanesulfonate (MMS) whose DNA-induced damages are repaired through BER [230] (Figure 29). These data, showing inducible expression of these genes dependent on APE1 expression similar to that observed in the case of SIRT1, were suggestive of a general mechanism of gene activation upon DNA damage that involves APE1 binding to nCaRE elements.

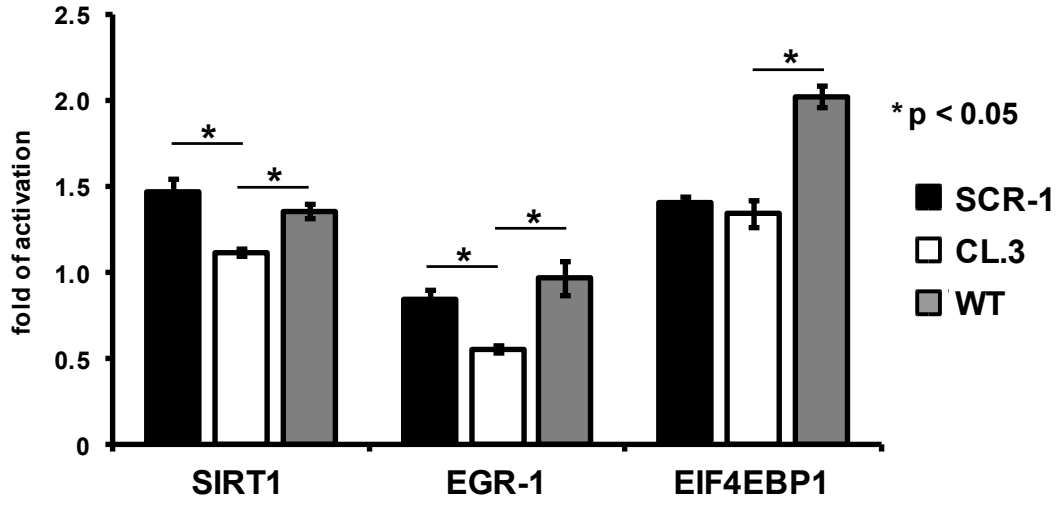

Figure 28 – APE1 regulates gene transcription upon oxidative stress condition.
Q-PCR analysis of SIRT1, EGR-1 and EIF4EBP mRNA levels in clones expressing $APE1^{WT}$ or APE1 silenced cells $APE1^{CL.3}$ after 1 mM H_2O_2 treatment, for 1 h. Data shown in the histogram are reported as fold of activation after H_2O_2 treatment and normalized to the amount of GAPDH. The significance of sample average difference observed was estimated by Student's t test. A *p*-value < 0.05 was considered as statistically significant (*).

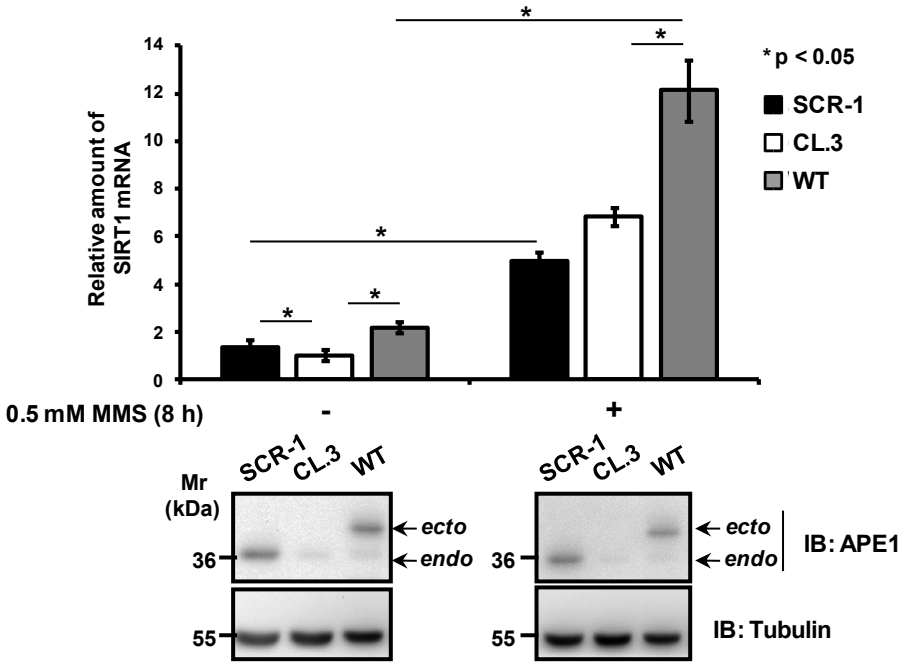

Figure 29 - MMS treatment induces SIRT1 transcription.
Analysis of SIRT1 mRNA level with Q-PCR in clones expressing APE1^{WT} or APE1 silenced cells APE1$^{CL.3}$ after 0.5 mM MMS treatment for 8 h. Data shown in the histogram are normalized to the amount of GAPDH. The significance of sample average difference observed was estimated by Student's t test. A p-value < 0.05 was considered as statistically significant (*). Below, Western blotting analysis on protein extract of clones used. Tubulin protein level was used to normalize sample.

To find a relationship between SIRT1 transcription induced by oxidative stress and the APE1 regulatory activity on the nCaRE sequences located within the promoter, I studied the dynamics of oxidative repair enzymes recruitment on the SIRT1 nCaRE-B sequence at early time upon H_2O_2 treatment. DNA base oxidation determines the formation of 8-oxoG, which is recognized by the DNA glycosylase OGG1. This enzyme initiates the BER pathway by removing the 8-oxoG lesion, which is further processed by APE1 that cleaves the apurinic site. To assess the dynamics of the nCaRE sequence occupation on the SIRT1 promoter by these enzymes upon oxidative stress, I performed a time-course ChIP analysis on the SIRT1 nCaRE-B sequence after 1 mM H_2O_2 treatment (Figure 30 and Supplementary Figure 33 in Appendix). I immunoprecipitated SIRT1 nCaRE-B sequence with antibodies against 8-oxoG, OGG1 and APE1. It has been observed that the signal of 8-oxoG reached its pleteau promptly, 10 min upon H_2O_2 treatment and subsequently decreased, concomitantly with the accumulation of OGG1, that is recruited immediately later (15 minutes), in accordance with the BER processes. The occupancy by APE1 follows the OGG1 recruitment, consequently. To demonstrate a direct link between DNA repair and SIRT1 transcriptional initiation, the recruitment of RNA polymerase II (RNPII) on SIRT1 promoter was checked. Under basal condition, it has been observed that RNPII was found with relatively low abundance on the nCaRE

sequence; conversely, the polymerase was progressively recruited as soon as the oxidative stress began (15 min after H_2O_2 treatment). Successively (at 40 min after H_2O_2 addition), RNAPII was again recruited on the SIRT1 promoter. This oxidatively induced recruitment of RNPII to the SIRT1 promoter, in concert with the observation that APE1 immunoprecipitated with RNPII with an increased interaction resembling approximately the kinetics observed during ChIP analysis, suggested that oxidative stress could be a trigger for SIRT1 transcriptional activation (Figure 31).

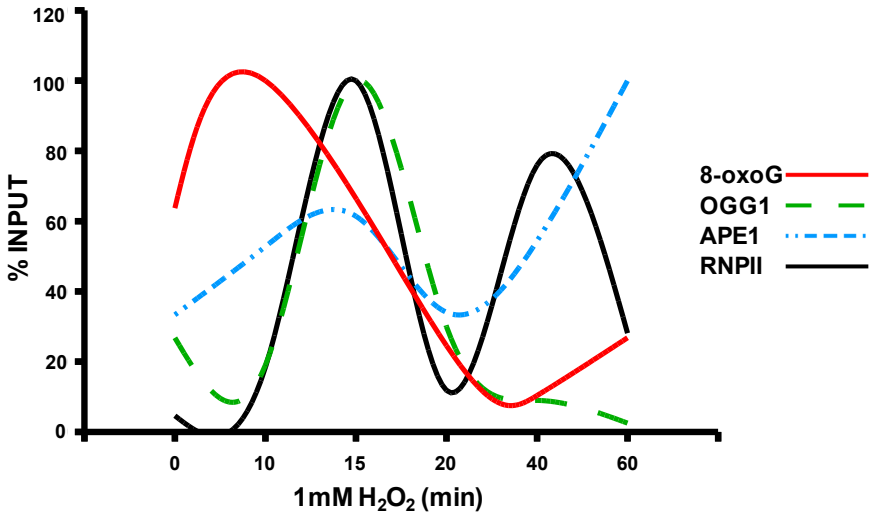

Figure 30 - Recruitment of DNA repair proteins at SIRT1 promoter after H_2O_2 treatment.
Histogram reports the trend of four independent ChIP analyses relative to the accumulation of 8-oxoGs, OGG1, APE1 and RNA polymerase II protein on the SIRT1 promoter after H_2O_2 treatment. HeLa cells were co-transfected with empty vector or with a vector expressing $APE1^{WT}$ and hSIRT1 promoter and challenged with 1 mM H_2O_2, for different times (as reported). Data are presented as percent of input and were normalized to the quantity of DNA immunoprecipitated by α-tubulin (α-tub). See Supplementary Figure 33 for detailed information.

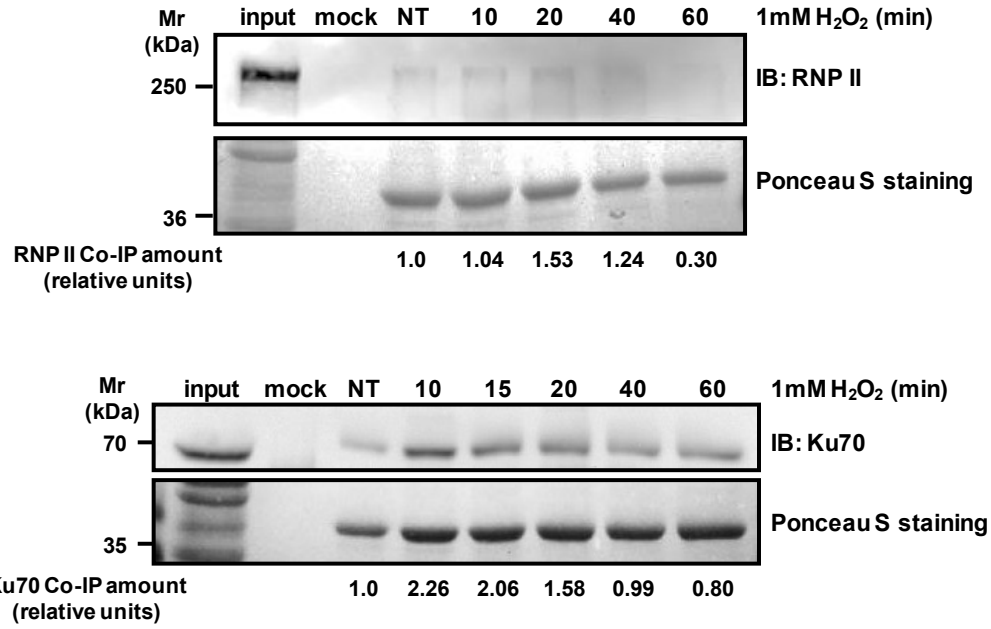

Figure 31 - Time-course interaction of RNA Polymerase II and Ku70 with APE1 after H_2O_2 treatment.
HeLa cells were transfected with a plasmid expressing $APE1^{WT}$ and challenged with 1 mM H_2O_2, for different times (as reported). Immunoprecipitated material and whole cell lysate were separated onto SDS-PAGE, immunoblotted and analyzed for their Ku70 (*upper panel*) and RNA Polymerase II (*bottom panel*) content, as associated with APE1 after H_2O_2 stimulus. Ponceau S staining was used for loading control. Normalized co-immunoprecipitated amounts of Ku70 and RNA Polymerase II are indicated under each relative bar. Mean values of two independent experiments are reported for Ku70.

It could be envisioned a mechanism in which H_2O_2 determines an oxidation of the guanine at the nCaRE sequence, thus recruiting components of the base excision repair system: OGG1 and APE1, together with proteins involved in nCaRE binding such as Ku70. When recruited to theSIRT1 promoter, APE1 (through its endonuclease activity) produces nicks on the nCaRE sequence, thus favouring the DNA relaxation necessary for the formation of chromatin loops that bring RNAPII at the transcription start site (Figure 32); the latter enzyme in turn can initiate transcription. Further work is required to fully circumstantiate this model for the induced transcriptional regulation of SIRT1 gene upon genotoxic conditions.

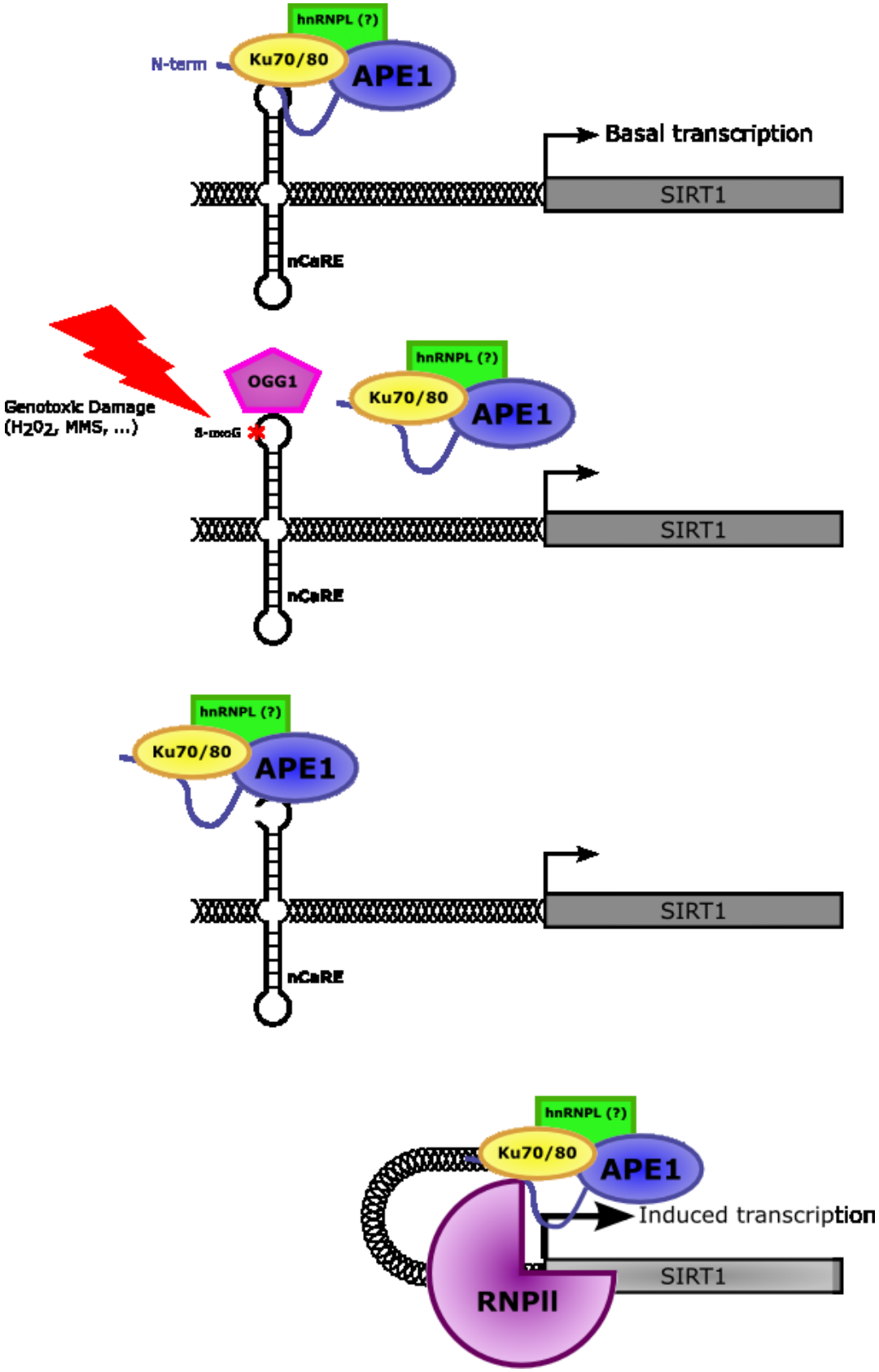

Figure 32 - Mechanistic model for the role of APE1 in oxidatively mediatated SIRT1 transcription. The model has been simplified for clarity. See Discussion for a detailed description.

6 Discussion

After its cloning by independent groups, at first as a DNA repair enzyme [51][7] and then as a redox co-activator protein [82], a number of papers have described the APE1 functions, elucidating its involvement in several biological contexts. As the main apurinic/apyrimidinic endonuclease in mammalian cells, APE1 is classically renowned for its essential function as a DNA repair enzyme in the BER pathway. Beside this crucial role in the maintenance of the genome stability, APE1 was recently demonstrated to be also involved in redox signaling and in the regulation of gene expression [97][231], supporting the notion that it is a multifunctional protein, with features that go beyond the classical activities of a DNA-repair enzyme. Notably, its multifunctional nature ascribes APE1 as an ideal candidate protein that links together DNA damage sensing/repair and transcriptional regulation of genes during cell response to genotoxic damage. Among these non-canonical activities, another interesting APE1 function is represented by its ability to bind the nCaRE sequence of some gene promoters, thus acting as a transcriptional regulator. Okazaki's group was the first that identified two nCaRE sequences within the PTH gene promoter [16]. The presence of these elements was also described in the regulatory region of few other genes, such as the human APE1 [139], the rat atrial natriuretic polypeptide [194], the human renin [138] and the bax ones [19]. Beside these few genes, no further evidences have been provided so far. However, since nCaRE elements are present within ALU repeats that are widely distributed throughout the expressed genome, it is expected that APE1 could potentially regulate the expression of a large number of genes in particular under genotoxic stress condition.

Here, it has been performed an unbiased investigation on the whole human genome, searching for putative genes whose transcription may be mediated through APE1 ability to bind nCaRE elements. Bioinformatic analyses revealed a number of genes potentially regulated by APE1, which are involved in several pathways related to gene expression (Figure 16). Among the 57 candidate genes retrieved from our bioinformatic analysis, I chose to study the human deacetylase sirtuin1 (SIRT1) that bears two nCaRE elements in its promoter.

SIRT1 is the human homolog of yeast Sir2 (silent information regulator 2) and belongs to a novel family of histone deacetylase. Sir2 is involved in gene silencing, telomere position effects, and cellular aging [232]. SIRT1 is the most conserved mammalian NAD(+)-dependent protein deacetylase that has emerged as a key metabolic sensor in various metabolic tissues. In response to different environmental stimuli, SIRT1

directly links the cellular metabolic status to the chromatin structure and the regulation of gene expression, thereby modulating a variety of cellular processes such as energy metabolism and stress response. SIRT1 activation leads to the deacetylation of several metabolic transcription factors such as PPAR gamma coactivator (PGC)-1α, FOXOs, and p53 which in turn prompt mitochondrial biogenensis and oxidative metabolism.

Remarkable interest in SIRT1 was due to recent articles showing that this deacetylase controls the acetylation status of APE1 Lys6/7 [157] and Lys27/31/32/35 [5]. Recently and during this work of Thesis, our lab have demonstrated that these particular APE1 lysines may undergo acetylation during cell response to genotoxic treatment [85]. Yamamori *et al*. were the first to demonstrate SIRT1 deacetylase activity on APE1 N-terminal lysine residues. They showed that the deacetylase activity exerted by SIRT1 on APE1 Lys6/7 is important in modulating APE1 DNA-repair function by regulating the kinetics of its interaction with other enzyme involved in BER. Successively, I also demonstrated the ability of SIRT1 to deacetylate Lys27-35 modulating APE1 subnuclear distribution and therefore coordinating its enzymatic functions in BER pathway (see also list of papers published during PhD course). Taken together these evidences, it has been hypothesized the existence of a possible autoregulatory loop that can be established between the two proteins: APE1 should modulate SIRT1 expression that, in turn, may regulate APE1 functions through deacetylation.

To investigate the APE1 transcriptional regulatory function on SIRT1 expression, I first examined APE1 ability to bind the nCaRE sequences found in the SIRT1 promoter. Through different *in vitro* approaches, it has been showed that APE1 is able to bind SIRT1 nCaRE sequences (Figure 18, Figure 19 and Figure 23). In particular, through EMSA assays and limited proteolysis analyses I originally demonstrated that the APE1 N-terminal domain is essential for the proper binding of these elements. The essential role of this protein domain in DNA-binding is remarkable, particularly if we consider the phylogenesis of the nCaRE elements and that of the APE1 N-terminal region. nCaRE sequences are present within ALU repeats, which belong to SINE (short interspersed nucleotide elements) family of repetitive sequences that originally derived from the reverse transposition of 7SL RNA. This event took place in the genome of an ancestor of Supraprimates [199]; therefore, these repetitive elements have been found exclusively in primates [233], scandentians [234] and rodents [235], all members of the placental mammalian clade Supraprimates (Euarchontoglires) [236]. Similarly, current information regarding the sequence homology of the APE1 N-terminal domain across species, have pointed out the recent phylogenetic acquisition of this region. Sequence conservation of this domain is very high in mammals but almost absent in other organisms with the exception of *Danio rerio*, *Dyctostelium* and *Drosophila*. Accordingly, it could be

envisioned that once ALU elements appeared in primates and were stabilized in their genomes, progressively losing their transcriptional potential, these organisms needed to evolve novel mechanisms to cope with the acquired RNA pol II regulatory sites present within ALU region. The concomitant acquisition of the APE1 N-terminal domain in mammals could explain new modulatory functions towards these DNA elements. The observation that specific K residues (i.e. K24-27) within this reduced APE1 portion seem to be required for the correct binding of nCaRE (data not shown) is in nice accordance with this hypothesis. The zebrafish homologous of APE1, which shares with the human protein less than 40% of the N-terminal aminoacidic sequence and that lacks two out of five K residues in this region [218], is indeed no longer able to stably bind these nCaRE sequences (Figure 18). Similar results were also obtained when using an human recombinant APE1 mutant protein bearing specific K to A multiple substitution at K27/K31/K32/K35, in which the positive charges at amino acid side chain has been removed to mimic a condition similar to that exerted by K acetylation (data not shown).

APE1 N-terminal domain is required for the stable binding to the nCaRE elements, even though it is not sufficient. EMSA analysis, performed with the nuclear extracts of HeLa cells expressing the deletion form of APE1, indeed demonstrated that APE1 is certainly part of a multiprotein complex, being not the limiting factor in the binding reaction. As already speculated by Okazaki and also reported in later works, the binding affinity observed for the multiprotein complex is higher with respect to that detected when using purified APE1 protein alone (Figure 18). This suggested that other factors are necessary and cooperate with APE1 to fully exert this function, confirming previous observations [17][18]. The two subunits of Ku antigen (Ku70 and Ku80) were among the protein factors already described by Chung *et al.* to be involved in the specific binding of nCaRE-A sequences[18]. Here, it has been demonstrated that Ku70 binding is not exclusively limited to the nCaRE-A elements, since I identified this protein in the complex that binds to the nCaRE-B sequence of SIRT1. The Ku heterodimer is a main component of the non-homologous end-joining (NHEJ) pathway repairing DNA double-strand breaks (DSBs), which are generally produced upon extensive oxidative and IR damage to DNA [237]. The X-ray crystal structure of Ku demonstrated that this protein is able to recognize DSBs and to initiate NHEJ pathway by virtue of its donut-shaped structure. Both Ku subunits encircle the DNA molecule and are inter-connected over an extensive binding surface. The peculiar structure of Ku allows recognition and tight binding to DSBs, together with the recruitment of DNA-PKcs and other factors to form the active protein kinase complex DNA-PK that facilitates processing and ligation of the broken ends [238][239]. Its involvement in the nCaRE binding is not clear, but emerging evidences underline the biological role of its non-canonical functions [240]. Several reports have

indeed demonstrated Ku importance in the transcription process. Initial reports identified Ku as a transcriptional factor that directly bound to sequence-specific promoter elements [241]; other works reported instead Ku association with RNA polymerase II sites [242] and its direct association, by itself and as part of DNA-PK complex, with RNA polymerase II complex affecting the transcriptional apparatus [243-246]. Starting from these observations, I envisage that Ku70 association with nCaRE elements could therefore further facilitate APE1 binding, especially after DNA damage, since it has been observed an increased interaction between the two proteins upon an oxidative stress condition (Figure 31). It also cannot be exclude that Ku could recruit the catalytic component of DNA-PK to nCaRE element providing a mechanism for targeting kinase to the transcription complex.

Here, it has also been better characterized the topology of the APE1-nCaRE complex. The palindromic nature of nCaRE-B sequences was already described by Okazaki *et al.*. Authors suggested the possible involvement of a dimeric nuclear protein in this process [16]. Here, it has been suggested that the SIRT1 nCaRE-B, due to its palindromic sequence, can potentially fold into a cruciform-like structure; I also demonstrated that APE1 binding activity toward these elements strongly relies on the secondary conformation adopted by the oligonucleotide, as already established for other DNA and RNA substrates (Figure 21 and Figure 22)[218]. The employment of structure-specific nucleases, such as the T7 [219][220][221] and the mung bean nucleases [222], allowed me to suggest the formation of a cruciform-like structure also for the SIRT1 nCaRE sequence and to demonstrate that APE1 binds to the SIRT1 nCaRE sequence at the predicted loop. Formation of similar cruciform-forming palindromic sequences has been already described in eukaryotic cells and their biological consequences has been related to different processes, including regulation of transcriptional events when present in close proximity of gene promoters [247-251]. We therefore hypothesize a similar mechanism for SIRT1 transcriptional regulation, which should imply APE1 binding to cruciform-structured nCaRE sequences. However, the requirement of a specific recognition motif also cannot be excluded since mutations in the SIRT1 nCaRE sequence, determining only a partial disruption of the oligonucleotide secondary structure, did not affect totally APE1 binding activity *in vivo* (Figure 24B).

I further deepened into APE1 transcriptional function on SIRT1 promoter. It has been found that APE1 positively affects SIRT1 gene transcription. Although APE1 was implicated in the repression of PTH gene transcription in a Ca^{2+}-dependent fashion, I observed that APE1 overexpression activated the SIRT1 promoter (Figure 24) apparently through a Ca^{2+}-independent mechanism. This unexpected positive function on the transcription of a nCaRE-containing promoter was also reported in other works where

authors suggested that the role of the nCaRE sequences in the context of different promoters and cells conditions could affect nCaRE activity [138][20]. Interestingly, I noticed that the positive effect exerted by APE1 was particularly pronounced during oxidative stress, through its binding to nCaRE sequences (Figure 27). Treatment with H_2O_2 leads to an activation of the SIRT1 promoter that determines an increase of the corresponding transcription in an APE1-dependent fashion. This positive transcriptional effect was also observed when we looked at the expression of other genes that present nCaRE elements in their promoters (Figure 28), thus corroborating the hypothesis of a general mechanism of SIRT1 activation upon DNA damage that involves functional activation of APE1. These findings are in line with previous data from Yamamori *et al*. demonstrating that the genotoxic insult augments SIRT1 expression and, therefore, its deacetylase activity on APE1 K6/7, favoring APE1 binding to XRCC1 [157]. Interestingly, these authors evidenced that a decrease of APE1 acetylation at later times after oxidative treatment is usually accompanied by SIRT1 up-regulation. All together, these findings are in accordance with a model of a positive autoregulatory loop between the two proteins. Thus, SIRT1 seems to be involved in a feedback mechanism that shuts off the cellular response mediated by APE1 acetylation [157].

Avvedimento and co-workers suggested that DNA oxidation could trigger positive transcription in the context of Myc-mediated transcription through the involvement of BER enzymes, including APE1 [252][253]. A mechanistic link between DNA damage and repair machinery in regulated gene transcription was also suggested by Ju *et al*. who evidenced a signal-dependent activation of gene transcription after site-specific dsDNA break formation operated by the DNA topisomerase IIβ [254]. Similarly, it has been speculated that the APE1 positive effect observed on SIRT1 transcription might depend on APE1 endonuclease activity over the nCaRE elements present within SIRT1 promoter. Here, it has been proposed a model where oxidative-mediated DNA repair and gene transcription are linked together (Figure 32). During oxidative stress conditions, DNA oxidation determines the formation of 8-oxodeoxyguanine (8-oxoG) lesions, which are recognized and processed by enzymes of the BER pathway, including APE1. In this model, the oxidative burst is an early event essential for the formation of a productive transcription initiation complex, which relies on the initial recruitment of BER enzymes. The nicks introduced at the chromatin level by APE1, during 8-oxoG removal, might promote the local relaxation required for the formation of chromatin loops moving closer the active form of RNA polymerase II to the TSS of the gene, as previously recruited by APE1 on nCaRE sequence, turning on the transcription. My data, therefore, can be generalized into a regulatory model for all those genes that contain nCaRE elements. Accordingly, a new hypothesis can be proposed for the molecular activation of specific

genes during early response to DNA damage that links together DNA-repair enzymes and transcriptional regulation effectors. An oxidative base modification is introduced by oxidative stress condition in a key sequence involved in transcriptional complex formation, i.e. nCaRE. APE1 represents the key factor involved in this peculiar mechanism of transcriptional activation because potentially it can link its two functions; the DNA repair domain of the molecule is required for removal of the oxidative-induced base oxidation product, while the redox effector domain plays an important role in transcriptional complex assembly. As a first step toward exploring this possibility, the present study tested the hypothesis that APE1 is a component of the oxidative-inducible transcriptional complex binding to the nCaRE element of SIRT1 gene. Since among the identified genes bearing nCaRE sequences in their promoter, several other genes are associated with cellular response to DNA damage, further studies will unveil the relevance of this model and its general value.

7 Materials and methods

7.1 Bioinformatic analysis

All human and mouse DNA sequences were retrieved from the Ensembl database (release 56) (http://www.ensembl.org/) by using a dedicated program written in Perl that collects entries from this archive. A sequence window that contains 5' genomic DNA of every gene coding for a protein was selected. This region extends from 6000 bp upstream and 1000 bp downstream of each transcriptional start site. Gene Ontology (GO) annotations were obtained from Ensembl database by using the data mining tool BioMart (http://www.ensembl.org/) [255]. Human and mouse promoter regions were scanned for significant similarities to nCaRE by using Glsearch as program for local alignment (available in the Fasta3 program package)[217]. Glsearch was chosen because it calculates an alignment that is global in the query and local in the library. The following nCaRE sequences were used as query [139]:

Name	Sequence (5’ to 3’)
nCaRE-B (PTH)	TTTTTGAGACAGGGTCTCACTCTG
nCaRE-B1 (APE1)	TTTTGAGACAGTCTCAGCTCTG
nCaRE-B2 (APE1)	TTTTGAGACAGAGTTTCACTCTTG

Alignments were computed with Altschul and Gish's statistical estimates, which are more suitable for searching of short query sequences (-z 3 option) [256]. Only those promoter genes that showed one or more matches for nCaRE sequences were selected, allowing up to two mismatches in the case of human genome and up to three mismatches in the case of mouse one; in fact, in the latter case, most alignments were found with three mismatches. From mouse promoter genes that contained nCaRE elements, only orthologous man/mouse genes were retrieved, as obtained from the BioMart Ensembl database. For the microarray filter, human genes selected from alignment search were cross-checked with microarray data obtained from the gene expression profile of HeLa cells silenced for APE1 by RNA interference [53]. GO filter identified co-regulated human genes, as determined by microarray analysis, studying the prevalence of their GO annotation terms. This analysis was obtained by using a Perl program kindly provided by Caselle and coworkers [257], which performs an exact Fisher’s test based on hypergeometric distribution to determine whether the term appears in the set significantly more often than what expected by chance. This program uses four

different entries: i) a file containing the whole GO database structure (OBO version 1.2, available at http://www.geneontology.org/); ii) the list of genes from whole human genome; iii) a list of all genes with all the GO terms associated with them (as obtained from Ensemble-BioMart); iv) the set of genes to be tested. Phylogenetic footprinting analysis consisted in the last selection from significant data obtained from GO filter of that genes also present in the mouse orthologous dataset.

7.2 Gene annotations co-occurrence analysis

Gene identies corresponding to the list of 57 putative genes regulated by APE1 were submitted to GeneCodis (http://genecodis.cnb.csic.es/), a web-based tool for the ontological analysis [258-260], selecting *Homo Sapiens* as the source for annotations and 'Biological Process' as the Gene Ontology category to perform the gene annotation co-occurrence analysis.

7.3 Cell culture and transient transfection experiments

HeLa cells were grown in Dulbecco's modified Eagle's medium (Invitrogen) supplemented with 10% fetal bovine serum (Euroclone, Milan, Italy), 100 U/ml penicillin and 10 µg/ml streptomycin sulfate. One day before transfection, cells were seeded in 10-cm plates at a density of 3×10^6 cells/plate. Cells were then transiently transfected with plasmids of interest by using Lipofectamine 2000 reagent (Invitrogen), according to the manufacturer's instructions. Cells were harvested 48 h after transfection.

7.4 Inducible APE1 knock-down and generation of APE1 knock-in cell lines

Inducible silencing of endogenous APE1 and reconstitution with mutant proteins in HeLa cell clones was performed as already described [53][13]. For inducible shRNA experiments, doxycycline (1 µg/ml) (Sigma) was added to the cell culture medium and cells were grown for 10 days.

7.5 Plasmids and expression of recombinant proteins

Plasmid containing the human SIRT1 promoter was kindly provided by Dr. Irani, University of Pittsburgh, USA. This plasmid consists of a fragment of the human SIRT1 promoter (–1266 to +137 relative to transcription start site) cloned into the pGL4.1 firefly luciferase reporter vector (Promega) [157]. The human SIRT1 promoter carrying the

mutation at nCaRE sequences was generated with a Site-Directed Mutagenesis Kit (Stratagene), using the following primers:
SIRT1-B mut for 5'-
TCATCTAGGTTTTATTTATATATTTTTTTGCTAAGGAGCGTCGCTCTTGCTGCCCAGG
CTGGTGTG-3' and SIRT1-B mut rev5'-
CACACCAGCCTGGGCAGCAAGAGCGACGCTCCTTAGCAAAAAAATATATAAATAAAA
CCTAGATGA-3'.

Expression and purification of recombinant proteins from *E. coli* were performed as previously described [85][13].

7.6 Antibodies and Western blotting analysis

For Western blotting analyses, the indicated amounts of cell extracts were resolved in 10% SDS-PAGE and transferred to nitrocellulose membranes (Schleicher & Schuell). Membranes were blocked with 5% w/v non-fat dry milk in PBS containing 0.1% v/v Tween 20 and probed with the monoclonal anti-FLAG antibody (Sigma), the monoclonal anti-Ku70 (Santa Cruz), the monoclonal anti-RNA polymerase II (Abcam) and the monoclonal anti-APE1 antibody [53]; blots were developed by using the ECL enhanced chemiluminescence procedure (GE Healthcare) or Western Lightning Ultra (Perkin Elmer). Data normalization was performed by using a monoclonal anti-tubulin antibody (Sigma). Blots were quantified by using a Chemidoc XRS video densitometer (Bio-Rad).

7.7 Secondary structure predictions

Potential secondary structures for nCaRE SIRT1-B oligonucleotide were determined by using the mFold Web Server program available at (http://mfold.rna.albany.edu/?q=mfold). Structure predictions were run by setting the program parameters as close as possible to the conditions used in binding assays (i.e. 37°C and 50 mM monovalent cation).

7.8 Chromatin immunoprecipitation (ChIP) Analysis

ChIP assay was performed by using a protocol described previously [5]. 5×10^6 HeLa cells in 10-cm dishes were transiently co-trasfected with the human SIRT1 promoter plasmid or the mutated one and $APE1^{WT}$ or $APE1^{N\Delta33}$ FLAG-expressing plasmids. Before harvesting, cells were fixed with 1% formaldehyde for 10 min, at 37°C, to allow reversible cross-linking of proteins. After 2 washes with PBS, cells were scraped

with 1 ml of ice-cold PBS supplemented with 1x Protease inhibitor cocktail (Sigma), 0.5 mM phenylmethylsulfonyl fluoride (PMSF), 1 mM NaF, 1 mM Na_3VO_4 and clarified by centrifugation at 7,000 *g*, at 4°C, for 5 min. Cells were then lysed in 300 µl of 50 mM Tris-HCl pH 7.4, 150 mM NaCl, 1 mM EDTA and 1% w/v Triton X-100, completed with the same inhibitors quoted above. Chromatin preparations were sonicated (Bioruptor® Diagenode, Liege, Belgium) into fragments with an average length of 0.5–1 kb; after centrifugation at 12,000 *g* for 10 min, at 4°C, supernatants were diluted 10 fold in 0.01% SDS, 1.1% Triton X-100, 1.2 mM EDTA, 16.7 mM Tris-HCl pH 8.1 and 167 mM NaCl, added with protease inhibitors. Immunoprecipitation was performed by using the anti-FLAG® M2 Affinity Gel (Sigma). To reduce nonspecific background, 0.4 µg of Salmon Sperm DNA (Sigma) and 1 µg of BSA (Sigma) were added. Samples were then placed in a roller shake for 3 h and centrifuged at 8,000 x *g*, at 4°C, for 1 min. Supernatants were discarded and the resin was washed with 1 ml of Low Salt Immune Complex Wash Buffer (0.1% SDS, 1% Triton X-100, 2 mM EDTA, 20 mM Tris-HCl pH 8.1 and 150 mM NaCl), High Salt Immune Complex Wash Buffer (0.1% SDS, 1% Triton X-100, 2 mM EDTA, 20 mM Tris-HCl pH 8.1 and 500 mM NaCl), LiCl Immune Complex Wash Buffer (0.25 M LiCl, 1% NP-40, 1% deoxycholate, 1 mM EDTA, 10 mM Tris-HCl pH 8.1) and with two washes with TE buffer (10 mM Tris-HCl pH 8.0, 1 mM EDTA) for 5 min, at room temperature, with rotation. Immune complexes were eluted two times by adding 250 µl of Elution Buffer (1% SDS and 0.1 M $NaHCO_3$), incubated 15 min, at room temperature, and the two elution fractions combined. Elutes were added with 20 µl of 5 M NaCl and heated at 65°C, for 4 h, to reverse the formaldehyde cross-links. Released DNA was digested by incubation with a solution consisting of 2 µl of proteinase K (10 mg/ml) (Sigma), 10 µl of EDTA 0.5 M and 20 µl of Tris-HCl pH 6.5, for 1 h, at 45°C. Digested DNA was extracted with 24:1 v/v phenol/isoamyl alcohol and then precipitated with ethanol. Precipitated samples were resuspended in 50 µl of H_20 and analyzed by qRT-PCR with an ABI PRISM7000 instrument.

The human SIRT1 promoter containing the nCaRE SIRT1-B sequence was amplified by qRT-PCR with CFX96 Real-Time System (Bio-Rad), according to the manufacturer's protocol. The following primers were used: nCaREB_for 5'-CACCAATCAACCCCTCAT-3' and nCaREB_rev 5'- CACCAATCAACCCCTCAT-3', which amplified a region of 136 bp. DNA was amplified in 96-well plates using primers for nCaREB_for and nCaREB_rev using the 2X iQ™ SYBR® Green Supermix (Bio-Rad) (100 mM KCl, 40 mM Tris-HCl pH 8.4, 0.4 mM of each deoxynucleoside triphosphate [dNTP], 50 U/ml iTaq DNA polymerase, 6 mM $MgCl_2$, SYBR green I, 20 nM fluorescein, and stabilizers) and 10 µM of the specific sense and antisense primers, in a final volume of 15 µl for each well. Each analysis was performed in triplicate. As negative control, a sample

without template was used. The cycling parameters were: i) denaturation at 95°C, for 10 s; ii) annealing/extension at 60°C, for 30 s (repeated 40 times). In order to verify the specificity of the amplification, a melting-curve analysis was performed, immediately after the amplification protocol. The results of the qRT-PCR assay for each sample were reported as percent of ng of immunoprecipitated nCaRE DNA relative to that present in total input chromatin, using an absolute standard curve (0.002, 0.02, 0.2, 2, 20, 200 and 2000 pg of hSIRT1 promoter-plasmid standard).

7.9 Preparation of nuclear cell extracts

Nuclear protein extracts were prepared as described earlier [261]. Briefly, cells were harvested and then centrifuged at 2,000 *g* for 10 min at 4°C. Supernatant was removed, and the pellet was resuspended in buffer A (10 mM Tris-HCl [pH 7.5], 1.5 mM MgCl2, and 10 mM KCl supplemented with 1x protease inhibitor cocktail, 0.5 mM PMSF, 1 mM NaF and 1 mM Na_3VO_4) at a cell density of $3x10^7$ cells/ml and incubated on ice for 10 min. The nuclei were collected by centrifugation at 2,000 *g* for 10 min at 4°C and then resuspended in buffer B (20 mM Tris-HCl [pH 7.5], 0.42 M KCl, 1.5 mM MgCl2, 20% [vol/vol] glycerol supplemented with 1x protease inhibitor cocktail, 0.5 mM PMSF, 1 mM NaF, and 1 mM Na3VO4) and rotated for 30 min at 4°C. The suspension was centrifuged at 15,000 *g* for 30 min at 4°C. The protein concentration was determined using Bio-Rad protein assay reagent.

7.10 Electrophoretic Mobility Shift Assay (EMSA) analysis

APE1 binding to nucleic acids was assessed as already described [85], with some modifications. Briefly, the indicated amount of recombinant proteins or 5 µg of the reported nuclear extract were incubated at 37°C for 15 minutes with 250 pmol of unlabeled poly(dT), or 250 ng of sonicated salmon sperm DNA (Sigma). 2.5 pmol of ^{32}P-labeled double-stranded (ds) oligonucleotides were then added and incubated for additional 15 min and further separated onto a native 6% w/v polyacrylamide gel at 150 V, for 4 h. When performing super-shift assays, 5 µl of monoclonal anti-APE1 [53], anti-Ku-70 (sc-12729, Santa Cruz Biotechnology, Inc.) or anti-P2Y6 (Alomone Labs) were pre-incubated with HeLa nuclear extract from APE1^{SCR-1} clone at 4°C, for 3 h.

Oligonucleotides used for EMSA were the following:

Name	Sequence (5' to 3')
nCaRE SIRT1-A	For TTTTTGAGACAGAGTTTCACTCTTG
	Rev CAAGAGTGAAACTCTGTCTCAAAAA

nCaRE SIRT1-B	For TTTTTGAGACGGAGTTTCGCTCTTG
	Rev CAAGAGCGAAACTCCGTCTCAAAAA
Poly(dT)	For TTTTTTTTTTTTTTTTTTTTTTT

7.11 T7 endonuclease I footprinting

Footprinting analysis on nCaRE sequence were conducted using T7 endonuclease I. Briefly, 5'-^{32}P-end-labeled nCaRE-B was digested with 5U of T7 endonuclease I at 37°C, for 1h. The reaction mixtures were then loaded and separated for 2h onto a denaturing 8M urea sequencing gel. After separation, the gel was incubated for 30' in a 10% methanol and 10% acetic acid solution for 30' and then wrapped in Saran wrap and exposed to film for autoradiograpy.

7.12 Determination of AP endonuclease activity

Determination of APE1 AP endonuclease activity was performed using an oligonucleotide cleavage assay, as described previously [13]. The indicated amount of recombinant APE1 protein was incubated with a 5'-^{32}P-end-labeled 26 mer ds oligonucleotide containing a single tetrahydrofuranyl (here called THF) artificial AP site at position 14, which is cleaved to a 14-mer in the presence of AP endonuclease activity. Alternatively, a 5'-^{32}P-end-labeled ds nCaRE SIRT1-B oligonucleotide or a 5'-^{32}P-end-labeled ds nCaRE SIRT1-B oligonucleotide, bearing a single tetrahydrofuranyl residue at position 12 (bolded) nCaREB2 5'- TTTTTGAGACG**G**AGTTTCGCTCTTG -3' (Integrated DNA Technologies) were used.

7.13 Reporter assays

For reporter assay experiments, we used a human SIRT1 promoter plasmid allowing for promoter activity measurements upon luciferase assay, as already described [157]. To this purpose, 2.5x10^4 HeLa cells were seeded in a 96-well plate and co-transfected with 15 ng of human SIRT1 promoter, 0.3 ng of a constitutive renilla reporter plasmid and 75 ng of a vector expressing FLAG-tagged APE1 protein. When performing luciferase assays upon H_2O_2, cells were challenged with increasing amounts of H_2O_2 in serum-free medium for 1h, at 37°C, and then firefly and renilla luciferase activities were measured 24 h after the treatment by using the Dual-Glo Luciferase assay system (Promega), according to manufacturer's recommendations. Firefly activity was

normalized to renilla activity to correct for differences in transfection efficiency. Results are from triplicate experiments.

7.14 Q-PCR

Total RNA from cell lines was extracted with the SV Total RNA isolation System kit (Promega). One microgram of total RNA was reverse transcribed using the iScript cDNA synthesis kit (Bio-Rad), according to the manufacturer's instructions. qRT-PCR was performed with a CFX96 Real-Time System (Bio-Rad) using iQ™ SYBR® Green Supermix (Bio-Rad). Primer sequences for human SIRT1 were those reported in [157]. Human GAPDH was used as internal control; sense, 5'-CCCTTCATTGACCTCAACTACATG -3'; antisense 5'-TGGGATTTCCATTGATGACAAGC -3'. The cycling parameters conditions are identical to those reported for ChIP analysis.

7.15 Surface Plasmon Resonance (SPR) analysis

SPR analysis was performed at Institute of Biostructures and Bioimaging, National Research Council of Naples, Italy. Real time binding assays were performed on a Biacore 3000 SPR instrument (GE Healthcare). Biotinylated ds oligonucleotides were immobilized on a SA-chip at the desired level, as result of their injection at a concentration of 500 nM in HBS (20 mM Hepes, 150 mM NaCl, 3.4 mM EDTA, and 0.005% v/v P20 surfactant, 0.1 mM tris(2-carboxyethyl)phosphine), at 10 µL/min as flow rate. Flow cell 2 contained 100 RU of poly(dT); flow cell 3 and 4 contained 77 and 60 RU of nCaRE SIRT1-B2 and nCaRE SIRT1-B2 mut respectively, and flow cell 1 (with streptavidin) was left blank to be used as a reference surface. APE1 and its deletion mutant APE1$^{N\Delta 33}$ were serially diluted in running buffer to the indicated concentrations and injected at a flow rate of 20 µL/min for 4.5 min, at 20°C. Disruption of any complex that remained bound after a 3-min dissociation was achieved by using an injection of 1 M NaCl at 20 µL/min, for 1 min. BIAevaluation analysis package version 4.1 (GE Healthcare) was used to subtract blank signal, and to evaluate kinetic and dissociation constants. Kinetic parameters were estimated assuming a 1:1 binding model and using version 7 4.1 Evaluation Software (GE Healthcare). An affinity steady state model was applied to fit the RUmax data versus proteins concentrations and fitting was performed with GraphPad Prism v4.00 [85].

7.16 Limited proteolysis and LC-ESI-MS analysis

Limited proteolysis and LC-ESI-MS analysis were performed at the Proteomics & Mass Spectrometry Laboratory, ISPAAM of Naples, Italy.

Suitable experimental conditions were chosen by testing proteolysis with different enzyme/substrate values; no preventive removal of DNA was performed. Thus, limited proteolysis experiments on recombinant APE1 were conducted in 50 mM NH_4HCO_3, pH 7.5 (reaction buffer) at 37°C, by using an enzyme to substrate ratio ranging from 1:500 to 1:5000 w/w. Three identical aliquots of APE1 (500 pmol) were combined with reaction buffer or DNA nCaRE ds oligonucleotides (PTH and nCaRE SIRT1-B) (5:1 mol DNA/protein) dissolved in reaction buffer to generate samples (100 µl final volume each), which were incubated for 15 min at 37°C, before protease addition. After digestion starting, the extent of proteolysis was monitored on a time-course basis by sampling 10 µl of the mixture at time intervals ranging from 5 to 120 min. Reaction samples were immediately quenched with 5% formic acid and then frozen in dry-ice before LC-ESI-MS analysis.

APE1 digests were analyzed with Q-TOF Premier mass spectrometer (Waters, Milford, MA) equipped with a nanospray source. Peptide mixtures were separated on an Atlantis C_{18} column (100 µm x 100 mm, 3 µm), using a linear gradient ranging from 30 to 60% acetonitrile in 1% formic acid, over a period of 50 min, at a flow rate of 800 nl/min. Spectra were acquired in the *m/z* 650-2500 range. Data were processed by using the MassLynx software (Waters). Mass calibration was performed by means of the multiply charged ions from horse heart myoglobin (Sigma). Depending on polypeptide size, mass values have been reported as monoisotopic or average values. Observed mass values were assigned to specific polypeptides by using the Paws software (Proteometrics Inc.), based on APE1 sequence and selectivity of the protease used for protein digestion.

7.17 Statistical analyses

Statistical analyses were performed by using the Excel (Microsoft, Redmond, WA) data analysis program for Student's t test analysis. $P < 0.05$ was considered as statistically significant.

8 References

[1] Xanthoudakis S, Smeyne RJ, Wallace JD & Curran T. The redox/DNA repair protein, Ref-1, is essential for early embryonic development in mice. *Proc. Natl. Acad. Sci. U.S.A.* (1996) 93: p. 8919–8923.

[2] Fung H & Demple B. A vital role for Ape1/Ref1 protein in repairing spontaneous DNA damage in human cells. *Mol. Cell* (2005) 17: p. 463–470.

[3] Tell G, Quadrifoglio F, Tiribelli C & Kelley MR. The Many Functions of APE1/Ref-1: Not Only a DNA Repair Enzyme. *Antioxid. Redox Signal.* (2008) 11(3) : p. 601-620.

[4] Chen DS, Herman T & Demple B. Two distinct human DNA diesterases that hydrolyze 3'-blocking deoxyribose fragments from oxidized DNA. *Nucleic Acids Res.* (1991) 19: pp. 5907-5914.

[5] Lirussi L, Antoniali G, Vascotto C, D'Ambrosio C, Poletto M, Romanello M, Marasco D, Leone M, Quadrifoglio F, Bhakat KK, Scaloni A & Tell G. Nucleolar accumulation of APE1 depends on charged lysine residues that undergo acetylation upon genotoxic stress and modulate its BER activity in cells. *Mol. Biol. Cell* (2012) 23: pp. 4079-4096.

[6] Tell G, Damante G, Caldwell D & Kelley MR. The intracellular localization of APE1/Ref-1: more than a passive phenomenon?. *Antioxid. Redox Signal.* (2005) 7: p. 367–384.

[7] Robson CN & Hickson ID. Isolation of cDNA clones encoding a human apurinic/apyrimidinic endonuclease that corrects DNA repair and mutagenesis defects in E. coli xth (exonuclease III) mutants. *Nucleic Acids Res.* (1991) 19: p. 5519–5523.

[8] Chen J & Stubbe J. Bleomycins: towards better therapeutics. *Nat. Rev. Cancer* (2005) 5: pp. 102-112.

[9] Huang RP & Adamson ED. Characterization of the DNA-binding properties of the early growth response-1 (Egr-1) transcription factor: evidence for modulation by a redox mechanism. *DNA Cell Biol.* (1993) 12: p. 265–273.

[10] Gaiddon C, Moorthy NC & Prives C. Ref-1 regulates the transactivation and pro-apoptotic functions of p53 in vivo. *EMBO J.* (1999) 18: p. 5609–5621.

[11] Tell G, Pellizzari L, Cimarosti D, Pucillo C & Damante G. Ref-1 controls pax-8 DNA-binding activity. *Biochem. Biophys. Res. Commun.* (1998) 252: p. 178–183.

[12] Tell G, Wilson DM3 & Lee CH. Intrusion of a DNA repair protein in the RNome world: is this the beginning of a new era?. *Mol. Cell. Biol.* (2010) 30: pp. 366-371.

[13] Vascotto C, Fantini D, Romanello M, Cesaratto L, Deganuto M, Leonardi A, Radicella JP, Kelley MR, D'Ambrosio C, Scaloni A, Quadrifoglio F & Tell G. APE1/Ref-1

interacts with NPM1 within nucleoli and plays a role in the rRNA quality control process. *Mol. Cell. Biol.* (2009) 29: p. 1834–1854.

[14] Berquist BR, McNeill DR & Wilson DM. Characterization of abasic endonuclease activity of human Ape1 on alternative substrates, as well as effects of ATP and sequence context on AP site incision. *J. Mol. Biol.* (2008) 379: p. 17–27.

[15] Barnes T, Kim W, Mantha AK, Kim S, Izumi T, Mitra S & Lee CH. Identification of Apurinic/apyrimidinic endonuclease 1 (APE1) as the endoribonuclease that cleaves c-myc mRNA. *Nucleic Acids Res.* (2009) 37: pp. 3946-3958.

[16] Okazaki T, Zajac JD, Igarashi T, Ogata E & Kronenberg HM. Negative regulatory elements in the human parathyroid hormone gene. *J. Biol. Chem.* (1991) 266: pp. 21903-21910.

[17] Kuninger DT, Izumi T, Papaconstantinou J & Mitra S. Human AP-endonuclease 1 and hnRNP-L interact with a nCaRE-like repressor element in the AP-endonuclease 1 promoter. *Nucleic Acids Res.* (2002) 30: p. 823–829.

[18] Chung U, Igarashi T, Nishishita T, Iwanari H, Iwamatsu A, Suwa A, Mimori T, Hata K, Ebisu S, Ogata E, Fujita T & Okazaki T. The interaction between Ku antigen and REF1 protein mediates negative gene regulation by extracellular calcium. *J. Biol. Chem.* (1996) 271: pp. 8593-8598.

[19] Bhattacharyya A, Chattopadhyay R, Burnette BR, Cross JV, Mitra S, Ernst PB, Bhakat KK & Crowe SE. Acetylation of apurinic/apyrimidinic endonuclease-1 regulates Helicobacter pylori-mediated gastric epithelial cell apoptosis. *Gastroenterology* (2009) 136: p. 2258–22698.

[20] Bhakat KK, Izumi T, Yang S, Hazra TK & Mitra S. Role of acetylated human AP-endonuclease (APE1/Ref-1) in regulation of the parathyroid hormone gene. *EMBO J.* (2003) 22: p. 6299–6309.

[21] Busso CS, Lake MW & Izumi T. Posttranslational modification of mammalian AP endonuclease (APE1). *Cell. Mol. Life Sci.* (2010) 67: pp. 3609-3620.

[22] Mitra S, Izumi T, Boldogh I, Bhakat KK, Chattopadhyay R & Szczesny B. Intracellular trafficking and regulation of mammalian AP-endonuclease 1 (APE1), an essential DNA repair protein. *DNA Repair (Amst.)* (2007) 6: p. 461–469.

[23] Luo M, He H, Kelley MR & Georgiadis MM. Redox regulation of DNA repair: implications for human health and cancer therapeutic development. *Antioxid. Redox Signal.* (2010) 12: pp. 1247-1269.

[24] De Bont R & van Larebeke N. Endogenous DNA damage in humans: a review of quantitative data. *Mutagenesis* (2004) 19: pp. 169-185.

[25] Christmann M, Tomicic MT, Roos WP & Kaina B. Mechanisms of human DNA repair: an update. *Toxicology* (2003) 193: pp. 3-34.

[26] Kelley MR & Fishel ML. DNA repair proteins as molecular targets for cancer therapeutics. *Anticancer Agents Med Chem* (2008) 8: pp. 417-425.

[27] Hoeijmakers JH. DNA repair mechanisms. *Maturitas* (2001) 38: p. 17-22; discussion 22-3.

[28] Hoeijmakers JH. Genome maintenance mechanisms for preventing cancer. *Nature* (2001) 411: pp. 366-374.

[29] Wood RD, Mitchell M & Lindahl T. Human DNA repair genes, 2005. *Mutat. Res.* (2005) 577: pp. 275-283.

[30] Lehmann AR. DNA repair-deficient diseases, xeroderma pigmentosum, Cockayne syndrome and trichothiodystrophy. *Biochimie* (2003) 85: pp. 1101-1111.

[31] Sengupta S & Harris CC. p53: traffic cop at the crossroads of DNA repair and recombination. *Nat. Rev. Mol. Cell Biol.* (2005) 6: pp. 44-55.

[32] Eker APM, Quayle C, Chaves I & van der Horst GTJ. DNA repair in mammalian cells: Direct DNA damage reversal: elegant solutions for nasty problems. *Cell. Mol. Life Sci.* (2009) 66: pp. 968-980.

[33] Kunz C, Saito Y & Schär P. DNA Repair in mammalian cells: Mismatched repair: variations on a theme. *Cell. Mol. Life Sci.* (2009) 66: pp. 1021-1038.

[34] Nouspikel T. DNA repair in mammalian cells: So DNA repair really is that important?. *Cell. Mol. Life Sci.* (2009) 66: pp. 965-967.

[35] Nouspikel T. DNA repair in mammalian cells : Nucleotide excision repair: variations on versatility. *Cell. Mol. Life Sci.* (2009) 66: pp. 994-1009.

[36] Pardo B, Gómez-González B & Aguilera A. DNA repair in mammalian cells: DNA double-strand break repair: how to fix a broken relationship. *Cell. Mol. Life Sci.* (2009) 66: pp. 1039-1056.

[37] Robertson AB, Klungland A, Rognes T & Leiros I. DNA repair in mammalian cells: Base excision repair: the long and short of it. *Cell. Mol. Life Sci.* (2009) 66: pp. 981-993.

[38] Tornaletti S. DNA repair in mammalian cells: Transcription-coupled DNA repair: directing your effort where it's most needed. *Cell. Mol. Life Sci.* (2009) 66: pp. 1010-1020.

[39] Evans AR, Limp-Foster M & Kelley MR. Going APE over ref-1. *Mutat. Res.* (2000) 461: p. 83–108.

[40] Dawson TL, Gores GJ, Nieminen AL, Herman B & Lemasters JJ. Mitochondria as a source of reactive oxygen species during reductive stress in rat hepatocytes. *Am. J. Physiol.* (1993) 264: p. C961-7.

[41] Griendling KK, Sorescu D & Ushio-Fukai M. NAD(P)H oxidase: role in cardiovascular biology and disease. *Circ. Res.* (2000) 86: pp. 494-501.

[42] Scandalios JG. Oxidative stress: molecular perception and transduction of signals triggering antioxidant gene defenses. *Braz. J. Med. Biol. Res.* (2005) 38: pp. 995-1014.

[43] Mikkelsen RB & Wardman P. Biological chemistry of reactive oxygen and nitrogen and radiation-induced signal transduction mechanisms. *Oncogene* (2003) 22: pp. 5734-5754.

[44] Marnett LJ. Oxyradicals and DNA damage. *Carcinogenesis* (2000) 21: pp. 361-370.

[45] Lindahl T. Instability and decay of the primary structure of DNA. *Nature* (1993) 362: p. 709–715.

[46] Mitra S, Hazra TK, Roy R, Ikeda S, Biswas T, Lock J, Boldogh I & Izumi T. Complexities of DNA base excision repair in mammalian cells. *Mol. Cells* (1997) 7: pp. 305-312.

[47] David SS & Williams SD. Chemistry of Glycosylases and Endonucleases Involved in Base-Excision Repair. *Chem. Rev.* (1998) 98: pp. 1221-1262.

[48] Chen DS, Herman T & Demple B. Two distinct human DNA diesterases that hydrolyze 3'-blocking deoxyribose fragments from oxidized DNA. *Nucleic Acids Res.* (1991) 19: p. 5907–5914.

[49] Caldecott KW, Aoufouchi S, Johnson P & Shall S. XRCC1 polypeptide interacts with DNA polymerase beta and possibly poly (ADP-ribose) polymerase, and DNA ligase III is a novel molecular 'nick-sensor' in vitro. *Nucleic Acids Res.* (1996) 24: pp. 4387-4394.

[50] Fromme JC, Banerjee A & Verdine GL. DNA glycosylase recognition and catalysis. *Curr. Opin. Struct. Biol.* (2004) 14: pp. 43-49.

[51] Demple B, Herman T & Chen DS. Cloning and expression of APE, the cDNA encoding the major human apurinic endonuclease: definition of a family of DNA repair enzymes. *Proc. Natl. Acad. Sci. U.S.A.* (1991) 88: pp. 11450-11454.

[52] Ludwig DL, MacInnes MA, Takiguchi Y, Purtymun PE, Henrie M, Flannery M, Meneses J, Pedersen RA & Chen DJ. A murine AP-endonuclease gene-targeted deficiency with post-implantation embryonic progression and ionizing radiation sensitivity. *Mutat. Res.* (1998) 409: p. 17–29.

[53] Vascotto C, Cesaratto L, Zeef LAH, Deganuto M, D'Ambrosio C, Scaloni A, Romanello M, Damante G, Taglialatela G, Delneri D, Kelley MR, Mitra S, Quadrifoglio F & Tell G. Genome-wide analysis and proteomic studies reveal APE1/Ref-1 multifunctional role in mammalian cells. *Proteomics* (2009) 9: p. 1058–1074.

[54] Myles GM & Sancar A. DNA repair. *Chem. Res. Toxicol.* (1989) 2: pp. 197-226.

[55] Wong D & Demple B. Modulation of the 5'-deoxyribose-5-phosphate lyase and DNA synthesis activities of mammalian DNA polymerase beta by apurinic/apyrimidinic endonuclease 1. *J. Biol. Chem.* (2004) 279: pp. 25268-25275.

[56] Kumar A, Widen SG, Williams KR, Kedar P, Karpel RL & Wilson SH. Studies of the domain structure of mammalian DNA polymerase beta. Identification of a discrete template binding domain. *J. Biol. Chem.* (1990) 265: pp. 2124-2131.

[57] Gu H, Marth JD, Orban PC, Mossmann H & Rajewsky K. Deletion of a DNA polymerase beta gene segment in T cells using cell type-specific gene targeting. *Science* (1994) 265: pp. 103-106.

[58] Cabelof DC, Raffoul JJ, Yanamadala S, Guo Z & Heydari AR. Induction of DNA polymerase beta-dependent base excision repair in response to oxidative stress in vivo. *Carcinogenesis* (2002) 23: pp. 1419-1425.

[59] Klungland A & Lindahl T. Second pathway for completion of human DNA base excision-repair: reconstitution with purified proteins and requirement for DNase IV (FEN1). *EMBO J.* (1997) 16: pp. 3341-3348.

[60] Tomkinson AE, Vijayakumar S, Pascal JM & Ellenberger T. DNA ligases: structure, reaction mechanism, and function. *Chem. Rev.* (2006) 106: pp. 687-699.

[61] Levin DS, Bai W, Yao N, O'Donnell M & Tomkinson AE. An interaction between DNA ligase I and proliferating cell nuclear antigen: implications for Okazaki fragment synthesis and joining. *Proc. Natl. Acad. Sci. U.S.A.* (1997) 94: pp. 12863-12868.

[62] Levin DS, McKenna AE, Motycka TA, Matsumoto Y & Tomkinson AE. Interaction between PCNA and DNA ligase I is critical for joining of Okazaki fragments and long-patch base-excision repair. *Curr. Biol.* (2000) 10: pp. 919-922.

[63] Barnes DE, Tomkinson AE, Lehmann AR, Webster AD & Lindahl T. Mutations in the DNA ligase I gene of an individual with immunodeficiencies and cellular hypersensitivity to DNA-damaging agents. *Cell* (1992) 69: pp. 495-503.

[64] Prigent C, Satoh MS, Daly G, Barnes DE & Lindahl T. Aberrant DNA repair and DNA replication due to an inherited enzymatic defect in human DNA ligase I. *Mol. Cell. Biol.* (1994) 14: pp. 310-317.

[65] Caldecott KW, McKeown CK, Tucker JD, Ljungquist S & Thompson LH. An interaction between the mammalian DNA repair protein XRCC1 and DNA ligase III. *Mol. Cell. Biol.* (1994) 14: pp. 68-76.

[66] Cappelli E, Taylor R, Cevasco M, Abbondandolo A, Caldecott K & Frosina G. Involvement of XRCC1 and DNA ligase III gene products in DNA base excision repair. *J. Biol. Chem.* (1997) 272: pp. 23970-23975.

[67] Tebbs RS, Flannery ML, Meneses JJ, Hartmann A, Tucker JD, Thompson LH, Cleaver JE & Pedersen RA. Requirement for the Xrcc1 DNA base excision repair gene during early mouse development. *Dev. Biol.* (1999) 208: pp. 513-529.

[68] Rouleau M, Aubin RA & Poirier GG. Poly(ADP-ribosyl)ated chromatin domains: access granted. *J. Cell. Sci.* (2004) 117: pp. 815-825.

[69] Maga G & Hubscher U. Proliferating cell nuclear antigen (PCNA): a dancer with many partners. *J. Cell. Sci.* (2003) 116: pp. 3051-3060.

[70] Das S, Chattopadhyay R, Bhakat KK, Boldogh I, Kohno K, Prasad R, Wilson SH & Hazra TK. Stimulation of NEIL2-mediated oxidized base excision repair via YB-1 interaction during oxidative stress. *J. Biol. Chem.* (2007) 282: pp. 28474-28484.

[71] Chattopadhyay R, Das S, Maiti AK, Boldogh I, Xie J, Hazra TK, Kohno K, Mitra S & Bhakat KK. Regulatory role of human AP-endonuclease (APE1/Ref-1) in YB-1-mediated activation of the multidrug resistance gene MDR1. *Mol. Cell. Biol.* (2008) 28: p. 7066–7080.

[72] Banerjee D, Mandal SM, Das A, Hegde ML, Das S, Bhakat KK, Boldogh I, Sarkar PS, Mitra S & Hazra TK. Preferential repair of oxidized base damage in the transcribed genes of mammalian cells. *J. Biol. Chem.* (2011) 286: pp. 6006-6016.

[73] Liu Y, Prasad R & Wilson SH. HMGB1: roles in base excision repair and related function. *Biochim. Biophys. Acta* (2010) 1799: pp. 119-130.

[74] Zhou J, Ahn J, Wilson SH & Prives C. A role for p53 in base excision repair. *EMBO J.* (2001) 20: pp. 914-923.

[75] Hegde ML, Hazra TK & Mitra S. Functions of disordered regions in mammalian early base excision repair proteins. *Cell. Mol. Life Sci.* (2010) 67: pp. 3573-3587.

[76] Ju B, Solum D, Song EJ, Lee K, Rose DW, Glass CK & Rosenfeld MG. Activating the PARP-1 sensor component of the groucho/ TLE1 corepressor complex mediates a CaMKinase IIdelta-dependent neurogenic gene activation pathway. *Cell* (2004) 119: pp. 815-829.

[77] Kim MY, Mauro S, Gévry N, Lis JT & Kraus WL. NAD+-dependent modulation of chromatin structure and transcription by nucleosome binding properties of PARP-1. *Cell* (2004) 119: pp. 803-814.

[78] Pavri R, Lewis B, Kim T, Dilworth FJ, Erdjument-Bromage H, Tempst P, de Murcia G, Evans R, Chambon P & Reinberg D. PARP-1 determines specificity in a retinoid signaling pathway via direct modulation of mediator. *Mol. Cell* (2005) 18: pp. 83-96.

[79] Tulin A, Stewart D & Spradling AC. The Drosophila heterochromatic gene encoding poly(ADP-ribose) polymerase (PARP) is required to modulate chromatin structure during development. *Genes Dev.* (2002) 16: pp. 2108-2119.

[80] Szántó M, Brunyánszki A, Kiss B, Nagy L, Gergely P, Virág L & Bai P. Poly(ADP-ribose) polymerase-2: emerging transcriptional roles of a DNA-repair protein. *Cell. Mol. Life Sci.* (2012) 69: pp. 4079-4092.

[81] Izumi T, Brown DB, Naidu CV, Bhakat KK, Macinnes MA, Saito H, Chen DJ & Mitra S. Two essential but distinct functions of the mammalian abasic endonuclease. *Proc. Natl. Acad. Sci. U.S.A.* (2005) 102: p. 5739–5743.

[82] Xanthoudakis S & Curran T. Identification and characterization of Ref-1, a nuclear protein that facilitates AP-1 DNA-binding activity. *EMBO J.* (1992) 11: p. 653–665.

[83] Gorman MA, Morera S, Rothwell DG, Fortelle EDL, Mol CD, Tainer JA, Hickson ID & Freemont PS. The crystal structure of the human DNA repair endonuclease HAP1 suggests the recognition of extra-helical deoxyribose at DNA abasic sites. *EMBO J.* (1997) 16: p. 6548–6558.

[84] Vascotto C, Fantini D, Romanello M, Cesaratto L, Deganuto M, Leonardi A, Radicella JP, Kelley MR, D'Ambrosio C, Scaloni A, Quadrifoglio F & Tell G. APE1/Ref-1 interacts with NPM1 within nucleoli and plays a role in the rRNA quality control process. *Mol. Cell. Biol.* (2009) 29: pp. 1834-1854.

[85] Fantini D, Vascotto C, Marasco D, D'Ambrosio C, Romanello M, Vitagliano L, Pedone C, Poletto M, Cesaratto L, Quadrifoglio F, Scaloni A, Radicella JP & Tell G. Critical lysine residues within the overlooked N-terminal domain of human APE1 regulate its biological functions. *Nucleic Acids Res.* (2010) 38(22) : p. 8239-8256.

[86] Georgiadis MM, Luo M, Gaur RK, Delaplane S, Li X & Kelley MR. Evolution of the redox function in mammalian apurinic/apyrimidinic endonuclease. *Mutat. Res.* (2008) 643: p. 54–63.

[87] Mol CD, Izumi T, Mitra S & Tainer JA. DNA-bound structures and mutants reveal abasic DNA binding by APE1 and DNA repair coordination [corrected]. *Nature* (2000) 403: p. 451–456.

[88] Barzilay G, Mol CD, Robson CN, Walker LJ, Cunningham RP, Tainer JA & Hickson ID. Identification of critical active-site residues in the multifunctional human DNA repair enzyme HAP1. *Nat. Struct. Biol.* (1995) 2: p. 561–568.

[89] Huang LE, Arany Z, Livingston DM & Bunn HF. Activation of hypoxia-inducible transcription factor depends primarily upon redox-sensitive stabilization of its alpha subunit. *J. Biol. Chem.* (1996) 271: pp. 32253-32259.

[90] Nishi T, Shimizu N, Hiramoto M, Sato I, Yamaguchi Y, Hasegawa M, Aizawa S, Tanaka H, Kataoka K, Watanabe H & Handa H. Spatial redox regulation of a critical cysteine residue of NF-kappa B in vivo. *J. Biol. Chem.* (2002) 277: pp. 44548-44556.

[91] Xanthoudakis S, Miao G, Wang F, Pan YC & Curran T. Redox activation of Fos-Jun DNA binding activity is mediated by a DNA repair enzyme. *EMBO J.* (1992) 11: p. 3323–3335.

[92] Jayaraman L, Murthy KG, Zhu C, Curran T, Xanthoudakis S & Prives C. Identification of redox/repair protein Ref-1 as a potent activator of p53. *Genes Dev.* (1997) 11: p. 558–570.

[93] Ordway JM, Eberhart D & Curran T. Cysteine 64 of Ref-1 is not essential for redox regulation of AP-1 DNA binding. *Mol. Cell. Biol.* (2003) 23: p. 4257–4266.

[94] Hegde ML, Izumi T & Mitra S. Oxidized base damage and single-strand break repair in mammalian genomes: role of disordered regions and posttranslational modifications in early enzymes. *Prog Mol Biol Transl Sci* (2012) 110: pp. 123-153.

[95] Tóth-Petróczy A, Simon I, Fuxreiter M & Levy Y. Disordered tails of homeodomains facilitate DNA recognition by providing a trade-off between folding and specific binding. *J. Am. Chem. Soc.* (2009) 131: pp. 15084-15085.

[96] Vuzman D, Azia A & Levy Y. Searching DNA via a "Monkey Bar" mechanism: the significance of disordered tails. *J. Mol. Biol.* (2010) 396: pp. 674-684.

[97] Tell G, Fantini D & Quadrifoglio F. Understanding different functions of mammalian AP endonuclease (APE1) as a promising tool for cancer treatment. *Cell. Mol. Life Sci.* (2010) 67: pp. 3589-3608.

[98] Demple B & Harrison L. Repair of oxidative damage to DNA: enzymology and biology. *Annu. Rev. Biochem.* (1994) 63: p. 915–948.

[99] Sobol RW & Wilson SH. Mammalian DNA beta-polymerase in base excision repair of alkylation damage. *Prog. Nucleic Acid Res. Mol. Biol.* (2001) 68: pp. 57-74.

[100] Krokan HE, Standal R & Slupphaug G. DNA glycosylases in the base excision repair of DNA. *Biochem. J.* (1997) 325 (Pt 1): p. 1–16.

[101] Izumi T, Hazra TK, Boldogh I, Tomkinson AE, Park MS, Ikeda S & Mitra S. Requirement for human AP endonuclease 1 for repair of 3'-blocking damage at DNA single-strand breaks induced by reactive oxygen species. *Carcinogenesis* (2000) 21: pp. 1329-1334.

[102] Loeb LA & Preston BD. Mutagenesis by apurinic/apyrimidinic sites. *Annu. Rev. Genet.* (1986) 20: pp. 201-230.

[103] Wiederhold L, Leppard JB, Kedar P, Karimi-Busheri F, Rasouli-Nia A, Weinfeld M, Tomkinson AE, Izumi T, Prasad R, Wilson SH, Mitra S & Hazra TK. AP endonuclease-independent DNA base excision repair in human cells. *Mol. Cell* (2004) 15: pp. 209-220.

[104] Hazra TK, Kow YW, Hatahet Z, Imhoff B, Boldogh I, Mokkapati SK, Mitra S & Izumi T. Identification and characterization of a novel human DNA glycosylase for repair of cytosine-derived lesions. *J. Biol. Chem.* (2002) 277: pp. 30417-30420.

[105] Dianova II, Bohr VA & Dianov GL. Interaction of human AP endonuclease 1 with flap endonuclease 1 and proliferating cell nuclear antigen involved in long-patch base excision repair. *Biochemistry* (2001) 40: pp. 12639-12644.

[106] Fan J & Wilson DM3. Protein-protein interactions and posttranslational modifications in mammalian base excision repair. *Free Radic. Biol. Med.* (2005) 38: pp. 1121-1138.

[107] Izumi T, Wiederhold LR, Roy G, Roy R, Jaiswal A, Bhakat KK, Mitra S & Hazra TK. Mammalian DNA base excision repair proteins: their interactions and role in repair of oxidative DNA damage. *Toxicology* (2003) 193: pp. 43-65.

[108] Akamatsu Y, Ohno T, Hirota K, Kagoshima H, Yodoi J & Shigesada K. Redox regulation of the DNA binding activity in transcription factor PEBP2. The roles of two conserved cysteine residues. *J. Biol. Chem.* (1997) 272: p. 14497–14500.

[109] Ema M, Hirota K, Mimura J, Abe H, Yodoi J, Sogawa K, Poellinger L & Fujii-Kuriyama Y. Molecular mechanisms of transcription activation by HLF and HIF1alpha in response to hypoxia: their stabilization and redox signal-induced interaction with CBP/p300. *EMBO J.* (1999) 18: p. 1905–1914.

[110] Nakshatri H, Bhat-Nakshatri P & Currie RA. Subunit association and DNA binding activity of the heterotrimeric transcription factor NF-Y is regulated by cellular redox. *J. Biol. Chem.* (1996) 271: p. 28784–28791.

[111] Cesaratto L, Calligaris SD, Vascotto C, Deganuto M, Bellarosa C, Quadrifoglio F, Ostrow JD, Tiribelli C & Tell G. Bilirubin-induced cell toxicity involves PTEN activation through an APE1/Ref-1-dependent pathway. *J Mol Med (Berl)* (2007) 85: pp. 1099-1112.

[112] Hanson S, Kim E & Deppert W. Redox factor 1 (Ref-1) enhances specific DNA binding of p53 by promoting p53 tetramerization. *Oncogene* (2005) 24: p. 1641–1647.

[113] Seo YR, Kelley MR & Smith ML. Selenomethionine regulation of p53 by a ref1-dependent redox mechanism. *Proc. Natl. Acad. Sci. U.S.A.* (2002) 99: p. 14548–14553.

[114] Cao X, Kambe F, Ohmori S & Seo H. Oxidoreductive modification of two cysteine residues in paired domain by Ref-1 regulates DNA-binding activity of Pax-8. *Biochem. Biophys. Res. Commun.* (2002) 297: pp. 288-293.

[115] Tell G, Scaloni A, Pellizzari L, Formisano S, Pucillo C & Damante G. Redox potential controls the structure and DNA binding activity of the paired domain. *J. Biol. Chem.* (1998) 273: pp. 25062-25072.

[116] Tell G, Zecca A, Pellizzari L, Spessotto P, Colombatti A, Kelley MR, Damante G & Pucillo C. An 'environment to nucleus' signaling system operates in B lymphocytes: redox status modulates BSAP/Pax-5 activation through Ref-1 nuclear translocation. *Nucleic Acids Res.* (2000) 28: p. 1099–1105.

[117] Hirota K, Matsui M, Iwata S, Nishiyama A, Mori K & Yodoi J. AP-1 transcriptional activity is regulated by a direct association between thioredoxin and Ref-1. *Proc. Natl. Acad. Sci. U.S.A.* (1997) 94: p. 3633–3638.

[118] Qin J, Clore GM, Kennedy WP, Kuszewski J & Gronenborn AM. The solution structure of human thioredoxin complexed with its target from Ref-1 reveals peptide chain reversal. *Structure* (1996) 4: pp. 613-620.

[119] Ueno M, Masutani H, Arai RJ, Yamauchi A, Hirota K, Sakai T, Inamoto T, Yamaoka Y, Yodoi J & Nikaido T. Thioredoxin-dependent redox regulation of p53-mediated p21 activation. *J. Biol. Chem.* (1999) 274: pp. 35809-35815.

[120] Wei SJ, Botero A, Hirota K, Bradbury CM, Markovina S, Laszlo A, Spitz DR, Goswami PC, Yodoi J & Gius D. Thioredoxin nuclear translocation and interaction with redox factor-1 activates the activator protein-1 transcription factor in response to ionizing radiation. *Cancer Res.* (2000) 60: pp. 6688-6695.

[121] Walker LJ, Robson CN, Black E, Gillespie D & Hickson ID. Identification of residues in the human DNA repair enzyme HAP1 (Ref-1) that are essential for redox regulation of Jun DNA binding. *Mol. Cell. Biol.* (1993) 13: p. 5370–5376.

[122] Ando K, Hirao S, Kabe Y, Ogura Y, Sato I, Yamaguchi Y, Wada T & Handa H. A new APE1/Ref-1-dependent pathway leading to reduction of NF-kappaB and AP-1, and activation of their DNA-binding activity. *Nucleic Acids Res.* (2008) 36: p. 4327–4336.

[123] Angkeow P, Deshpande SS, Qi B, Liu Y, Park YC, Jeon BH, Ozaki M & Irani K. Redox factor-1: an extra-nuclear role in the regulation of endothelial oxidative stress and apoptosis. *Cell Death Differ.* (2002) 9: p. 717–725.

[124] Ozaki M, Suzuki S & Irani K. Redox factor-1/APE suppresses oxidative stress by inhibiting the rac1 GTPase. *FASEB J.* (2002) 16: pp. 889-890.

[125] Babior BM. NADPH oxidase: an update. *Blood* (1999) 93: pp. 1464-1476.

[126] Bokoch GM & Diebold BA. Current molecular models for NADPH oxidase regulation by Rac GTPase. *Blood* (2002) 100: pp. 2692-2696.

[127] Patil S, Bunderson M, Wilham J & Black SM. Important role for Rac1 in regulating reactive oxygen species generation and pulmonary arterial smooth muscle cell growth. *Am. J. Physiol. Lung Cell Mol. Physiol.* (2004) 287: p. L1314-22.

[128] Rinckel LA, Faris SL, Hitt ND & Kleinberg ME. Rac1 disrupts p67phox/p40phox binding: a novel role for Rac in NADPH oxidase activation. *Biochem. Biophys. Res. Commun.* (1999) 263: pp. 118-122.

[129] Fishel ML & Kelley MR. The DNA base excision repair protein Ape1/Ref-1 as a therapeutic and chemopreventive target. *Mol. Aspects Med.* (2007) 28: pp. 375-395.

[130] Zou G & Maitra A. Small-molecule inhibitor of the AP endonuclease 1/REF-1 E3330 inhibits pancreatic cancer cell growth and migration. *Mol. Cancer Ther.* (2008) 7: pp. 2012-2021.

[131] Lee JK, Edderkaoui M, Truong P, Ohno I, Jang K, Berti A, Pandol SJ & Gukovskaya AS. NADPH oxidase promotes pancreatic cancer cell survival via inhibiting JAK2 dephosphorylation by tyrosine phosphatases. *Gastroenterology* (2007) 133: pp. 1637-1648.

[132] Barzilay G, Walker LJ, Robson CN & Hickson ID. Site-directed mutagenesis of the human DNA repair enzyme HAP1: identification of residues important for AP endonuclease and RNase H activity. *Nucleic Acids Res.* (1995) 23: p. 1544–1550.

[133] Hofer T, Badouard C, Bajak E, Ravanat J, Mattsson A & Cotgreave IA. Hydrogen peroxide causes greater oxidation in cellular RNA than in DNA. *Biol. Chem.* (2005) 386: pp. 333-337.

[134] Shan X, Chang Y & Lin CG. Messenger RNA oxidation is an early event preceding cell death and causes reduced protein expression. *FASEB J.* (2007) 21: pp. 2753-2764.

[135] Mallette LE. Regulation of blood calcium in humans. *Endocrinol. Metab. Clin. North Am.* (1989) 18: pp. 601-610.

[136] Okazaki T, Chung U, Nishishita T, Ebisu S, Usuda S, Mishiro S, Xanthoudakis S, Igarashi T & Ogata E. A redox factor protein, ref1, is involved in negative gene regulation by extracellular calcium. *J. Biol. Chem.* (1994) 269: p. 27855–27862.

[137] Yamamoto M, Igarashi T, Muramatsu M, Fukagawa M, Motokura T & Ogata E. Hypocalcemia increases and hypercalcemia decreases the steady-state level of parathyroid hormone messenger RNA in the rat. *J. Clin. Invest.* (1989) 83: pp. 1053-1056.

[138] Fuchs S, Philippe J, Corvol P & Pinet F. Implication of Ref-1 in the repression of renin gene transcription by intracellular calcium. *J. Hypertens.* (2003) 21: p. 327–335-327–335.

[139] Izumi T, Henner WD & Mitra S. Negative regulation of the major human AP-endonuclease, a multifunctional protein. *Biochemistry* (1996) 35: p. 14679–14683.

[140] Harrison L, Ascione G, Menninger JC, Ward DC & Demple B. Human apurinic endonuclease gene (APE): structure and genomic mapping (chromosome 14q11.2-12). *Hum. Mol. Genet.* (1992) 1: p. 677–680.

[141] Harrison L, Ascione AG, Wilson DM & Demple B. Characterization of the promoter region of the human apurinic endonuclease gene (APE). *J. Biol. Chem.* (1995) 270: p. 5556–5564.

[142] Konecki DS, Wang Y, Trefz FK, Lichter-Konecki U & Woo SL. Structural characterization of the 5' regions of the human phenylalanine hydroxylase gene. *Biochemistry* (1992) 31: pp. 8363-8368.

[143] Zhao B, Grandy DK, Hagerup JM, Magenis RE, Smith L, Chauhan BC & Henner WD. The human gene for apurinic/apyrimidinic endonuclease (HAP1): sequence and localization to chromosome 14 band q12. *Nucleic Acids Res.* (1992) 20: pp. 4097-4098.

[144] Akiyama K, Seki S, Oshida T & Yoshida MC. Structure, promoter analysis and chromosomal assignment of the human APEX gene. *Biochim. Biophys. Acta* (1994) 1219: p. 15–25.

[145] Rivkees SA & Kelley MR. Expression of a multifunctional DNA repair enzyme gene, apurinic/apyrimidinic endonuclease (APE; Ref-1) in the suprachiasmatic, supraoptic and paraventricular nuclei. *Brain Res.* (1994) 666: pp. 137-142.

[146] Fung H, Bennett RA & Demple B. Key role of a downstream specificity protein 1 site in cell cycle-regulated transcription of the AP endonuclease gene APE1/APEX in NIH3T3 cells. *J. Biol. Chem.* (2001) 276: pp. 42011-42017.

[147] Zaky A, Busso C, Izumi T, Chattopadhyay R, Bassiouny A, Mitra S & Bhakat KK. Regulation of the human AP-endonuclease (APE1/Ref-1) expression by the tumor suppressor p53 in response to DNA damage. *Nucleic Acids Res.* (2008) 36: p. 1555–1566.

[148] Asai T, Kambe F, Kikumori T & Seo H. Increase in Ref-1 mRNA and protein by thyrotropin in rat thyroid FRTL-5 cells. *Biochem. Biophys. Res. Commun.* (1997) 236: pp. 71-74.

[149] Ramana CV, Boldogh I, Izumi T & Mitra S. Activation of apurinic/apyrimidinic endonuclease in human cells by reactive oxygen species and its correlation with their

adaptive response to genotoxicity of free radicals. *Proc. Natl. Acad. Sci. U.S.A.* (1998) 95: p. 5061–5066.

[150] Grösch S, Fritz G & Kaina B. Apurinic endonuclease (Ref-1) is induced in mammalian cells by oxidative stress and involved in clastogenic adaptation. *Cancer Res.* (1998) 58: pp. 4410-4416.

[151] Tell G, Pellizzari L, Pucillo C, Puglisi F, Cesselli D, Kelley MR, Di Loreto C & Damante G. TSH controls Ref-1 nuclear translocation in thyroid cells. *J. Mol. Endocrinol.* (2000) 24: pp. 383-390.

[152] Grösch S & Kaina B. Transcriptional activation of apurinic/apyrimidinic endonuclease (Ape, Ref-1) by oxidative stress requires CREB. *Biochem. Biophys. Res. Commun.* (1999) 261: pp. 859-863.

[153] Pines A, Bivi N, Romanello M, Damante G, Kelley MR, Adamson ED, D'Andrea P, Quadrifoglio F, Moro L & Tell G. Cross-regulation between Egr-1 and APE/Ref-1 during early response to oxidative stress in the human osteoblastic HOBIT cell line: evidence for an autoregulatory loop. *Free Radic. Res.* (2005) 39: p. 269–281.

[154] Yacoub A, Kelley MR & Deutsch WA. The DNA repair activity of human redox/repair protein APE/Ref-1 is inactivated by phosphorylation. *Cancer Res.* (1997) 57: pp. 5457-5459.

[155] Fritz G & Kaina B. Phosphorylation of the DNA repair protein APE/REF-1 by CKII affects redox regulation of AP-1. *Oncogene* (1999) 18: p. 1033–1040.

[156] Hsieh MM, Hegde V, Kelley MR & Deutsch WA. Activation of APE/Ref-1 redox activity is mediated by reactive oxygen species and PKC phosphorylation. *Nucleic Acids Res.* (2001) 29: p. 3116–3122.

[157] Yamamori T, DeRicco J, Naqvi A, Hoffman TA, Mattagajasingh I, Kasuno K, Jung S, Kim C & Irani K. SIRT1 deacetylates APE1 and regulates cellular base excision repair. *Nucleic Acids Res.* (2010) 38: pp. 832-845.

[158] Pickart CM. Ubiquitin enters the new millennium. *Mol. Cell* (2001) 8: pp. 499-504.

[159] Hicke L. Protein regulation by monoubiquitin. *Nat. Rev. Mol. Cell Biol.* (2001) 2: pp. 195-201.

[160] Busso CS, Iwakuma T & Izumi T. Ubiquitination of mammalian AP endonuclease (APE1) regulated by the p53-MDM2 signaling pathway. *Oncogene* (2009) 28: pp. 1616-1625.

[161] Minsky N & Oren M. The RING domain of Mdm2 mediates histone ubiquitylation and transcriptional repression. *Mol. Cell* (2004) 16: pp. 631-639.

[162] Haley B, Paunesku T, Protić M & Woloschak GE. Response of heterogeneous ribonuclear proteins (hnRNP) to ionising radiation and their involvement in DNA damage repair. *Int. J. Radiat. Biol.* (2009) 85: pp. 643-655.

[163] Brenkman AB, de Keizer PLJ, van den Broek NJF, Jochemsen AG & Burgering BMT. Mdm2 induces mono-ubiquitination of FOXO4. *PLoS ONE* (2008) 3: p. e2819.

[164] Meisenberg C, Tait PS, Dianova II, Wright K, Edelmann MJ, Ternette N, Tasaki T, Kessler BM, Parsons JL, Kwon YT & Dianov GL. Ubiquitin ligase UBR3 regulates cellular levels of the essential DNA repair protein APE1 and is required for genome stability. *Nucleic Acids Res.* (2012) 40: pp. 701-711.

[165] Yoshida A, Pourquier P & Pommier Y. Purification and characterization of a Mg2+-dependent endonuclease (AN34) from etoposide-treated human leukemia HL-60 cells undergoing apoptosis. *Cancer Res.* (1998) 58: pp. 2576-2582.

[166] Yoshida A, Urasaki Y, Waltham M, Bergman A, Pourquier P, Rothwell DG, Inuzuka M, Weinstein JN, Ueda T, Appella E, Hickson ID & Pommier Y. Human apurinic/apyrimidinic endonuclease (Ape1) and its N-terminal truncated form (AN34) are involved in DNA fragmentation during apoptosis. *J. Biol. Chem.* (2003) 278: pp. 37768-37776.

[167] Bots M & Medema JP. Granzymes at a glance. *J. Cell. Sci.* (2006) 119: pp. 5011-5014.

[168] Chowdhury D, Beresford PJ, Zhu P, Zhang D, Sung J, Demple B, Perrino FW & Lieberman J. The exonuclease TREX1 is in the SET complex and acts in concert with NM23-H1 to degrade DNA during granzyme A-mediated cell death. *Mol. Cell* (2006) 23: pp. 133-142.

[169] Fan Z, Beresford PJ, Zhang D, Xu Z, Novina CD, Yoshida A, Pommier Y & Lieberman J. Cleaving the oxidative repair protein Ape1 enhances cell death mediated by granzyme A. *Nat. Immunol.* (2003) 4: pp. 145-153.

[170] Yan N, Cherepanov P, Daigle JE, Engelman A & Lieberman J. The SET complex acts as a barrier to autointegration of HIV-1. *PLoS Pathog.* (2009) 5: p. e1000327.

[171] Jackson EB, Theriot CA, Chattopadhyay R, Mitra S & Izumi T. Analysis of nuclear transport signals in the human apurinic/apyrimidinic endonuclease (APE1/Ref1). *Nucleic Acids Res.* (2005) 33: p. 3303–3312.

[172] Marshall HE, Merchant K & Stamler JS. Nitrosation and oxidation in the regulation of gene expression. *FASEB J.* (2000) 14: pp. 1889-1900.

[173] Jaiswal M, LaRusso NF, Burgart LJ & Gores GJ. Inflammatory cytokines induce DNA damage and inhibit DNA repair in cholangiocarcinoma cells by a nitric oxide-dependent mechanism. *Cancer Res.* (2000) 60: pp. 184-190.

[174] Hara MR, Agrawal N, Kim SF, Cascio MB, Fujimuro M, Ozeki Y, Takahashi M, Cheah JH, Tankou SK, Hester LD, Ferris CD, Hayward SD, Snyder SH & Sawa A. S-nitrosylated GAPDH initiates apoptotic cell death by nuclear translocation following Siah1 binding. *Nat. Cell Biol.* (2005) 7: pp. 665-674.

[175] Qu J, Liu G, Huang B & Chen C. Nitric oxide controls nuclear export of APE1/Ref-1 through S-nitrosation of cysteines 93 and 310. *Nucleic Acids Res.* (2007) 35: pp. 2522-2532.

[176] Kelley MR & Parsons SH. Redox regulation of the DNA repair function of the human AP endonuclease Ape1/ref-1. *Antioxid. Redox Signal.* (2001) 3: pp. 671-683.

[177] Xanthoudakis S, Smeyne RJ, Wallace JD & Curran T. The redox/DNA repair protein, Ref-1, is essential for early embryonic development in mice. *Proc Natl Acad Sci USA* (1996) 93: pp. 8919-8923.

[178] Tell G, Damante G, Caldwell D & Kelley MR. The intracellular localization of APE1/Ref-1: more than a passive phenomenon?. *Antioxid. Redox Signal.* (2005) 7: pp. 367-384.

[179] Fishel ML, He Y, Smith ML & Kelley MR. Manipulation of base excision repair to sensitize ovarian cancer cells to alkylating agent temozolomide. *Clin. Cancer Res.* (2007) 13: pp. 260-267.

[180] Fishel ML, He Y, Reed AM, Chin-Sinex H, Hutchins GD, Mendonca MS & Kelley MR. Knockdown of the DNA repair and redox signaling protein Ape1/Ref-1 blocks ovarian cancer cell and tumor growth. *DNA Repair (Amst.)* (2008) 7: pp. 177-186.

[181] Lau JP, Weatherdon KL, Skalski V & Hedley DW. Effects of gemcitabine on APE/ref-1 endonuclease activity in pancreatic cancer cells, and the therapeutic potential of antisense oligonucleotides. *Br. J. Cancer* (2004) 91: pp. 1166-1173.

[182] Wang D, Luo M & Kelley MR. Human apurinic endonuclease 1 (APE1) expression and prognostic significance in osteosarcoma: enhanced sensitivity of osteosarcoma to DNA damaging agents using silencing RNA APE1 expression inhibition. *Mol. Cancer Ther.* (2004) 3: pp. 679-686.

[183] Yang Z, Chen X & Wang D. Experimental study enhancing the chemosensitivity of multiple myeloma to melphalan by using a tissue-specific APE1-silencing RNA expression vector. *Clin Lymphoma Myeloma* (2007) 7: pp. 296-304.

[184] Vascotto C & Fishel ML. Blockade of Base Excision Repair: Inhibition of Small Lesions Results in Big Consequences to Cancer Cells. Academic Press (Ed.). Elsevier, 2012.

[185] Hiramoto M, Shimizu N, Sugimoto K, Tang J, Kawakami Y, Ito M, Aizawa S, Tanaka H, Makino I & Handa H. Nuclear targeted suppression of NF-kappa B activity by the novel quinone derivative E3330. *J. Immunol.* (1998) 160: pp. 810-819.

[186] Luo M, Delaplane S, Jiang A, Reed A, He Y, Fishel M, Nyland RL, Borch RF, Qiao X, Georgiadis MM & Kelley MR. Role of the multifunctional DNA repair and redox signaling protein Ape1/Ref-1 in cancer and endothelial cells: small-molecule inhibition of the redox function of Ape1. *Antioxid. Redox Signal.* (2008) 10: p. 1853–1867.

[187] Zhang Y, Wang J, Xiang D, Wang D & Xin X. Alterations in the expression of the apurinic/apyrimidinic endonuclease-1/redox factor-1 (APE1/Ref-1) in human ovarian cancer and indentification of the therapeutic potential of APE1/Ref-1 inhibitor. *Int. J. Oncol.* (2009) 35: pp. 1069-1079.

[188] Khan N, Afaq F & Mukhtar H. Cancer chemoprevention through dietary antioxidants: progress and promise. *Antioxid. Redox Signal.* (2008) 10: pp. 475-510.

[189] Singh-Gupta V, Zhang H, Banerjee S, Kong D, Raffoul JJ, Sarkar FH & Hillman GG. Radiation-induced HIF-1alpha cell survival pathway is inhibited by soy isoflavones in prostate cancer cells. *Int. J. Cancer* (2009) 124: pp. 1675-1684.

[190] Raffoul JJ, Banerjee S, Singh-Gupta V, Knoll ZE, Fite A, Zhang H, Abrams J, Sarkar FH & Hillman GG. Down-regulation of apurinic/apyrimidinic endonuclease 1/redox factor-1 expression by soy isoflavones enhances prostate cancer radiotherapy in vitro and in vivo. *Cancer Res.* (2007) 67: pp. 2141-2149.

[191] Yang S, Irani K, Heffron SE, Jurnak F & Meyskens FLJ. Alterations in the expression of the apurinic/apyrimidinic endonuclease-1/redox factor-1 (APE/Ref-1) in human melanoma and identification of the therapeutic potential of resveratrol as an APE/Ref-1 inhibitor. *Mol. Cancer Ther.* (2005) 4: pp. 1923-1935.

[192] Yang Z, Yang S, Misner BJ, Chiu R, Liu F & Meyskens FLJ. Nitric oxide initiates progression of human melanoma via a feedback loop mediated by apurinic/apyrimidinic endonuclease-1/redox factor-1, which is inhibited by resveratrol. *Mol. Cancer Ther.* (2008) 7: pp. 3751-3760.

[193] Messina M, Kucuk O & Lampe JW. An overview of the health effects of isoflavones with an emphasis on prostate cancer risk and prostate-specific antigen levels. *J AOAC Int* (2006) 89: pp. 1121-1134.

[194] Okazaki T, Ando K, Igarashi T, Ogata E & Fujita T. Conserved mechanism of negative gene regulation by extracellular calcium. Parathyroid hormone gene versus atrial natriuretic polypeptide gene. *J. Clin. Invest.* (1992) 89: p. 1268–1273.

[195] Potter LR, Yoder AR, Flora DR, Antos LK & Dickey DM. Natriuretic peptides: their structures, receptors, physiologic functions and therapeutic applications. *Handb Exp Pharmacol* (2009) : pp. 341-366.

[196] Hackenthal E, Paul M, Ganten D & Taugner R. Morphology, physiology, and molecular biology of renin secretion. *Physiol. Rev.* (1990) 70: pp. 1067-1116.

[197] McHaffie GS & Ralston SH. Origin of a negative calcium response element in an ALU-repeat: implications for regulation of gene expression by extracellular calcium. *Bone* (1995) 17: p. 11–14.

[198] Ullu E & Tschudi C. Alu sequences are processed 7SL RNA genes. *Nature* (1984) 312: pp. 171-172.

[199] Kriegs JO, Churakov G, Jurka J, Brosius J & Schmitz J. Evolutionary history of 7SL RNA-derived SINEs in Supraprimates. *Trends Genet.* (2007) 23: pp. 158-161.

[200] Shen MR, Batzer MA & Deininger PL. Evolution of the master Alu gene(s). *J. Mol. Evol.* (1991) 33: pp. 311-320.

[201] Jurka J & Milosavljevic A. Reconstruction and analysis of human Alu genes. *J. Mol. Evol.* (1991) 32: pp. 105-121.

[202] Shankar R, Grover D, Brahmachari SK & Mukerji M. Evolution and distribution of RNA polymerase II regulatory sites from RNA polymerase III dependant mobile Alu elements. *BMC Evol. Biol.* (2004) 4: pp. 37-37.

[203] Lander ES, Linton LM, Birren B, Nusbaum C, Zody MC, Baldwin J, Devon K, Dewar K, Doyle M, FitzHugh W, Funke R, Gage D, Harris K, Heaford A, Howland J, Kann L, Lehoczky J, LeVine R, McEwan P, McKernan K, Meldrim J, Mesirov JP, Miranda C, Morris W, Naylor J, Raymond C, Rosetti M, Santos R, Sheridan A, Sougnez C, Stange-Thomann N, Stojanovic N, Subramanian A, Wyman D, Rogers J, Sulston J, Ainscough R, Beck S, Bentley D, Burton J, Clee C, Carter N, Coulson A, Deadman R, Deloukas P, Dunham A, Dunham I, Durbin R, French L, Grafham D, Gregory S, Hubbard T, Humphray S, Hunt A, Jones M, Lloyd C, McMurray A, Matthews L, Mercer S, Milne S, Mullikin JC, Mungall A, Plumb R, Ross M, Shownkeen R, Sims S, Waterston RH, Wilson RK, Hillier LW, McPherson JD, Marra MA, Mardis ER, Fulton LA, Chinwalla AT, Pepin KH, Gish WR, Chissoe SL, Wendl MC, Delehaunty KD, Miner TL, Delehaunty A, Kramer JB, Cook LL, Fulton RS, Johnson DL, Minx PJ, Clifton SW, Hawkins T, Branscomb E, Predki P, Richardson P, Wenning S, Slezak T, Doggett N, Cheng JF, Olsen A, Lucas S, Elkin C, Uberbacher E, Frazier M, Gibbs RA, Muzny DM, Scherer SE, Bouck JB, Sodergren EJ, Worley KC, Rives CM, Gorrell JH, Metzker ML, Naylor SL, Kucherlapati RS, Nelson DL, Weinstock GM, Sakaki Y, Fujiyama A, Hattori M, Yada T, Toyoda A, Itoh T, Kawagoe C, Watanabe H, Totoki Y, Taylor T, Weissenbach J, Heilig R, Saurin W, Artiguenave F, Brottier P, Bruls T, Pelletier E, Robert C, Wincker P, Smith DR, Doucette-Stamm L, Rubenfield M, Weinstock K, Lee HM, Dubois J, Rosenthal A, Platzer M, Nyakatura G, Taudien S, Rump A, Yang H, Yu J, Wang J, Huang G, Gu J, Hood L, Rowen L, Madan A, Qin S, Davis RW, Federspiel NA, Abola AP, Proctor MJ, Myers RM, Schmutz J, Dickson M, Grimwood J, Cox DR, Olson MV, Kaul R, Raymond C, Shimizu N, Kawasaki K, Minoshima S, Evans GA, Athanasiou M, Schultz R, Roe BA, Chen F, Pan H, Ramser J, Lehrach H, Reinhardt R, McCombie WR, Bastide MDL, Dedhia N, Blöcker H, Hornischer K, Nordsiek G, Agarwala R, Aravind L, Bailey JA, Bateman A, Batzoglou S, Birney E, Bork P, Brown DG, Burge CB, Cerutti L, Chen HC, Church D, Clamp M, Copley RR, Doerks T, Eddy SR, Eichler EE, Furey TS, Galagan J, Gilbert JG, Harmon C, Hayashizaki Y, Haussler D, Hermjakob H, Hokamp K, Jang W, Johnson LS, Jones TA, Kasif S, Kaspryzk A, Kennedy S, Kent WJ, Kitts P, Koonin EV, Korf I, Kulp D, Lancet D, Lowe TM, McLysaght A, Mikkelsen T, Moran JV, Mulder N, Pollara VJ, Ponting CP, Schuler G, Schultz J, Slater G, Smit AF, Stupka E, Szustakowski J, Thierry-Mieg D, Thierry-Mieg J, Wagner L, Wallis J, Wheeler R, Williams A, Wolf YI, Wolfe KH, Yang SP, Yeh RF, Collins F, Guyer MS, Peterson J, Felsenfeld A, Wetterstrand KA, Patrinos A, Morgan MJ, Jong PD, Catanese JJ, Osoegawa K, Shizuya H, Choi S, Chen YJ & Szustakowki J. Initial sequencing and analysis of the human genome. *Nature* (2001) 409: p. 860–921.

[204] Korenberg JR & Rykowski MC. Human genome organization: Alu, lines, and the molecular structure of metaphase chromosome bands. *Cell* (1988) 53: pp. 391-400.

[205] Filatov LV, Mamayeva SE & Tomilin NV. Non-random distribution of Alu-family repeats in human chromosomes. *Mol. Biol. Rep.* (1987) 12: pp. 117-122.

[206] Finnie NJ, Gottlieb TM, Blunt T, Jeggo PA & Jackson SP. DNA-dependent protein kinase activity is absent in xrs-6 cells: implications for site-specific recombination

and DNA double-strand break repair. *Proc. Natl. Acad. Sci. U.S.A.* (1995) 92: pp. 320-324.

[207] Nussenzweig A, Chen C, da Costa Soares V, Sanchez M, Sokol K, Nussenzweig MC & Li GC. Requirement for Ku80 in growth and immunoglobulin V(D)J recombination. *Nature* (1996) 382: pp. 551-555.

[208] Gu Y, Jin S, Gao Y, Weaver DT & Alt FW. Ku70-deficient embryonic stem cells have increased ionizing radiosensitivity, defective DNA end-binding activity, and inability to support V(D)J recombination. *Proc. Natl. Acad. Sci. U.S.A.* (1997) 94: pp. 8076-8081.

[209] Bailey SM, Meyne J, Chen DJ, Kurimasa A, Li GC, Lehnert BE & Goodwin EH. DNA double-strand break repair proteins are required to cap the ends of mammalian chromosomes. *Proc. Natl. Acad. Sci. U.S.A.* (1999) 96: pp. 14899-14904.

[210] Dreyfuss G, Swanson MS & Piñol-Roma S. Heterogeneous nuclear ribonucleoprotein particles and the pathway of mRNA formation. *Trends Biochem. Sci.* (1988) 13: pp. 86-91.

[211] Weighardt F, Biamonti G & Riva S. The roles of heterogeneous nuclear ribonucleoproteins (hnRNP) in RNA metabolism. *Bioessays* (1996) 18: pp. 747-756.

[212] Ladomery M. Multifunctional proteins suggest connections between transcriptional and post-transcriptional processes. *Bioessays* (1997) 19: pp. 903-909.

[213] Xanthoudakis S, Miao GG & Curran T. The redox and DNA-repair activities of Ref-1 are encoded by nonoverlapping domains. *Proc. Natl. Acad. Sci. U.S.A.* (1994) 91: pp. 23-27.

[214] Lando D, Pongratz I, Poellinger L & Whitelaw ML. A redox mechanism controls differential DNA binding activities of hypoxia-inducible factor (HIF) 1alpha and the HIF-like factor. *J. Biol. Chem.* (2000) 275: p. 4618–4627.

[215] Konturek PC, Pierzchalski P, Konturek SJ, Meixner H, Faller G, Kirchner T & Hahn EG. Helicobacter pylori induces apoptosis in gastric mucosa through an upregulation of Bax expression in humans. *Scand. J. Gastroenterol.* (1999) 34: pp. 375-383.

[216] Uemura N, Okamoto S, Yamamoto S, Matsumura N, Yamaguchi S, Yamakido M, Taniyama K, Sasaki N & Schlemper RJ. Helicobacter pylori infection and the development of gastric cancer. *N. Engl. J. Med.* (2001) 345: pp. 784-789.

[217] Pearson WR. Flexible sequence similarity searching with the FASTA3 program package. *Methods Mol. Biol.* (2000) 132: pp. 185-219.

[218] Poletto M, Vascotto C, Scognamiglio PL, Marasco D & Tell G. Role of the N-terminal tail of the human Apurinic/Apyrimidinic Endonuclease 1 (hAPE1) in the modulation of its interaction with nucleic acids and NPM1. *Biochemical Journal*, under revision.

[219] Fan J, Matsumoto Y & Wilson DM3. Nucleotide sequence and DNA secondary structure, as well as replication protein A, modulate the single-stranded abasic endonuclease activity of APE1. *J. Biol. Chem.* (2006) 281: pp. 3889-3898.

[220] Parkinson MJ & Lilley DM. The junction-resolving enzyme T7 endonuclease I: quaternary structure and interaction with DNA. *J. Mol. Biol.* (1997) 270: pp. 169-178.

[221] Déclais A, Fogg JM, Freeman ADJ, Coste F, Hadden JM, Phillips SEV & Lilley DMJ. The complex between a four-way DNA junction and T7 endonuclease I. *EMBO J.* (2003) 22: pp. 1398-1409.

[222] Amosova O, Kumar V, Deutsch A & Fresco JR. Self-catalyzed site-specific depurination of G residues mediated by cruciform extrusion in closed circular DNA plasmids. *J. Biol. Chem.* (2011) 286: pp. 36322-36330.

[223] Scaloni A, Miraglia N, Orrù S, Amodeo P, Motta A, Marino G & Pucci P. Topology of the calmodulin-melittin complex. *J. Mol. Biol.* (1998) 277: pp. 945-958.

[224] Renzone G, Vitale RM, Scaloni A, Rossi M, Amodeo P & Guagliardi A. Structural characterization of the functional regions in the archaeal protein Sso7d. *Proteins* (2007) 67: pp. 189-197.

[225] Scaloni A, Monti M, Acquaviva R, Tell G, Damante G, Formisano S & Pucci P. Topology of the thyroid transcription factor 1 homeodomain-DNA complex. *Biochemistry* (1999) 38: pp. 64-72.

[226] Beernink PT, Segelke BW, Hadi MZ, Erzberger JP, Wilson DM3 & Rupp B. Two divalent metal ions in the active site of a new crystal form of human apurinic/apyrimidinic endonuclease, Ape1: implications for the catalytic mechanism. *J. Mol. Biol.* (2001) 307: pp. 1023-1034.

[227] Izumi T, Malecki J, Chaudhry MA, Weinfeld M, Hill JH, Lee JC & Mitra S. Intragenic suppression of an active site mutation in the human apurinic/apyrimidinic endonuclease. *J. Mol. Biol.* (1999) 287: p. 47–57.

[228] Kim E & Um S. SIRT1: roles in aging and cancer. *BMB Reports* (2008) 41: p. 751–756.

[229] Cohen HY, Miller C, Bitterman KJ, Wall NR, Hekking B, Kessler B, Howitz KT, Gorospe M, de Cabo R & Sinclair DA. Calorie restriction promotes mammalian cell survival by inducing the SIRT1 deacetylase. *Science* (2004) 305: pp. 390-392.

[230] Kaina B, Ochs K, Grösch S, Fritz G, Lips J, Tomicic M, Dunkern T & Christmann M. BER, MGMT, and MMR in defense against alkylation-induced genotoxicity and apoptosis. *Prog. Nucleic Acid Res. Mol. Biol.* (2001) 68: pp. 41-54.

[231] Wilson DM3 & Simeonov A. Small molecule inhibitors of DNA repair nuclease activities of APE1. *Cell. Mol. Life Sci.* (2010) 67: pp. 3621-3631.

[232] Guarente L. Sirtuins, aging, and metabolism. *Cold Spring Harb. Symp. Quant. Biol.* (2011) 76: pp. 81-90.

[233] Deininger PL, Jolly DJ, Rubin CM, Friedmann T & Schmid CW. Base sequence studies of 300 nucleotide renatured repeated human DNA clones. *J. Mol. Biol.* (1981) 151: pp. 17-33.

[234] Nishihara H, Terai Y & Okada N. Characterization of novel Alu- and tRNA-related SINEs from the tree shrew and evolutionary implications of their origins. *Mol. Biol. Evol.* (2002) 19: pp. 1964-1972.

[235] Krayev AS, Kramerov DA, Skryabin KG, Ryskov AP, Bayev AA & Georgiev GP. The nucleotide sequence of the ubiquitous repetitive DNA sequence B1 complementary to the most abundant class of mouse fold-back RNA. *Nucleic Acids Res.* (1980) 8: pp. 1201-1215.

[236] Murphy WJ, Eizirik E, O'Brien SJ, Madsen O, Scally M, Douady CJ, Teeling E, Ryder OA, Stanhope MJ, de Jong WW & Springer MS. Resolution of the early placental mammal radiation using Bayesian phylogenetics. *Science* (2001) 294: pp. 2348-2351.

[237] Lieber MR. The mechanism of double-strand DNA break repair by the nonhomologous DNA end-joining pathway. *Annu. Rev. Biochem.* (2010) 79: pp. 181-211.

[238] Walker JR, Corpina RA & Goldberg J. Structure of the Ku heterodimer bound to DNA and its implications for double-strand break repair. *Nature* (2001) 412: pp. 607-614.

[239] Postow L. Destroying the ring: Freeing DNA from Ku with ubiquitin. *FEBS Lett.* (2011) 585: pp. 2876-2882.

[240] Adelmant G, Calkins AS, Garg BK, Card JD, Askenazi M, Miron A, Sobhian B, Zhang Y, Nakatani Y, Silver PA, Iglehart JD, Marto JA & Lazaro J. DNA ends alter the molecular composition and localization of Ku multicomponent complexes. *Mol. Cell Proteomics* (2012) 11: pp. 411-421.

[241] Giffin W, Torrance H, Rodda DJ, Préfontaine GG, Pope L & Hache RJ. Sequence-specific DNA binding by Ku autoantigen and its effects on transcription. *Nature* (1996) 380: pp. 265-268.

[242] Mo X & Dynan WS. Subnuclear localization of Ku protein: functional association with RNA polymerase II elongation sites. *Mol. Cell. Biol.* (2002) 22: pp. 8088-8099.

[243] Dvir A, Peterson SR, Knuth MW, Lu H & Dynan WS. Ku autoantigen is the regulatory component of a template-associated protein kinase that phosphorylates RNA polymerase II. *Proc. Natl. Acad. Sci. U.S.A.* (1992) 89: pp. 11920-11924.

[244] Chibazakura T, Watanabe F, Kitajima S, Tsukada K, Yasukochi Y & Teraoka H. Phosphorylation of human general transcription factors TATA-binding protein and transcription factor IIB by DNA-dependent protein kinase--synergistic stimulation of RNA polymerase II basal transcription in vitro. *Eur. J. Biochem.* (1997) 247: pp. 1166-1173.

[245] Sartorius CA, Takimoto GS, Richer JK, Tung L & Horwitz KB. Association of the Ku autoantigen/DNA-dependent protein kinase holoenzyme and poly(ADP-ribose) polymerase with the DNA binding domain of progesterone receptors. *J. Mol. Endocrinol.* (2000) 24: pp. 165-182.

[246] Mayeur GL, Kung W, Martinez A, Izumiya C, Chen DJ & Kung H. Ku is a novel transcriptional recycling coactivator of the androgen receptor in prostate cancer cells. *J. Biol. Chem.* (2005) 280: pp. 10827-10833.

[247] Kurahashi H, Inagaki H, Yamada K, Ohye T, Taniguchi M, Emanuel BS & Toda T. Cruciform DNA structure underlies the etiology for palindrome-mediated human chromosomal translocations. *J. Biol. Chem.* (2004) 279: pp. 35377-35383.

[248] Cunningham LA, Coté AG, Cam-Ozdemir C & Lewis SM. Rapid, stabilizing palindrome rearrangements in somatic cells by the center-break mechanism. *Mol. Cell. Biol.* (2003) 23: pp. 8740-8750.

[249] Pearson CE, Ruiz MT, Price GB & Zannis-Hadjopoulos M. Cruciform DNA binding protein in HeLa cell extracts. *Biochemistry* (1994) 33: pp. 14185-14196.

[250] Alvarez D, Novac O, Callejo M, Ruiz MT, Price GB & Zannis-Hadjopoulos M. 14-3-3sigma is a cruciform DNA binding protein and associates in vivo with origins of DNA replication. *J. Cell. Biochem.* (2002) 87: pp. 194-207.

[251] Shlyakhtenko LS, Hsieh P, Grigoriev M, Potaman VN, Sinden RR & Lyubchenko YL. A cruciform structural transition provides a molecular switch for chromosome structure and dynamics. *J. Mol. Biol.* (2000) 296: pp. 1169-1173.

[252] Perillo B, Ombra MN, Bertoni A, Cuozzo C, Sacchetti S, Sasso A, Chiariotti L, Malorni A, Abbondanza C & Avvedimento EV. DNA oxidation as triggered by H3K9me2 demethylation drives estrogen-induced gene expression. *Science* (2008) 319: pp. 202-206.

[253] Amente S, Bertoni A, Morano A, Lania L, Avvedimento EV & Majello B. LSD1-mediated demethylation of histone H3 lysine 4 triggers Myc-induced transcription. *Oncogene* (2010) 29: pp. 3691-3702.

[254] Ju B, Lunyak VV, Perissi V, Garcia-Bassets I, Rose DW, Glass CK & Rosenfeld MG. A topoisomerase IIbeta-mediated dsDNA break required for regulated transcription. *Science* (2006) 312: pp. 1798-1802.

[255] Spudich G, Fernández-Suárez XM & Birney E. Genome browsing with Ensembl: a practical overview. *Brief Funct Genomic Proteomic* (2007) 6: pp. 202-219.

[256] Altschul SF. Amino acid substitution matrices from an information theoretic perspective. *J. Mol. Biol.* (1991) 219: pp. 555-565.

[257] Corà D, Cunto FD, Provero P, Silengo L & Caselle M. Computational identification of transcription factor binding sites by functional analysis of sets of genes sharing overrepresented upstream motifs. *BMC Bioinformatics* (2004) 5: pp. 57-57.

[258] Carmona-Saez P, Chagoyen M, Tirado F, Carazo JM & Pascual-Montano A. GENECODIS: a web-based tool for finding significant concurrent annotations in gene lists. *Genome Biol.* (2007) 8: p. R3.

[259] Nogales-Cadenas R, Carmona-Saez P, Vazquez M, Vicente C, Yang X, Tirado F, Carazo JM & Pascual-Montano A. GeneCodis: interpreting gene lists through enrichment

analysis and integration of diverse biological information. *Nucleic Acids Res.* (2009) 37: p. W317-22.

[260] Tabas-Madrid D, Nogales-Cadenas R & Pascual-Montano A. GeneCodis3: a non-redundant and modular enrichment analysis tool for functional genomics. *Nucleic Acids Res.* (2012) 40: p. W478-83.

[261] Ziel KA, Grishko V, Campbell CC, Breit JF, Wilson GL & Gillespie MN. Oxidants in signal transduction: impact on DNA integrity and gene expression. *The FASEB Journal: Official Publication of the Federation of American Societies for Experimental Biology* (2005) 19: p. 387–394.

9 Appendix

Supplementary Table 4

Significant GO terms associated to genes bearing nCaRE elements and present in expression profile data obtained from experiment in which APE1 was knocked down.

Here we are reported only the most significant GO annotation terms obtained when performing the exact Fisher's test. The column titled "n_annotation" correspond to the total number of genes associated to that GO term in Gene Ontology database; instead, column "n_both" represents the amount of genes in our dataset associated to the same GO term. "Expect" column reports for all GO terms the number of genes expected by chance in a set made of the same number of dataset genes, but selected at random from database. The columns titled "C", "F" and "P" correspond to the three branches of the Gene Ontology: cellular component, molecular function and biological process respectively.

GO ID	n_annotation	n_both	expect	pv	-	
GO:0044424	10446	291	187.2580	8.69E-028	intracellular part	C
GO:0005622	10863	296	194.7340	7.22E-027	intracellular	C
GO:0043229	8870	260	159.0070	8.72E-026	intracellular organelle	C
GO:0043226	8885	260	159.2750	1.18E-025	organelle	C
GO:0005515	8150	238	146.1000	9.42E-022	protein binding	F
GO:0043231	7836	232	140.4710	1.03E-021	intracellular membrane-bounded organelle	C
GO:0043227	7845	232	140.6320	1.22E-021	membrane-bounded organelle	C
GO:0044464	14446	334	258.9640	4.67E-019	cell part	C
GO:0005623	14447	334	258.9820	4.74E-019	cell	C
GO:0005634	5052	168	90.5638	1.39E-018	nucleus	C
GO:0044446	3929	139	70.4326	5.42E-017	intracellular organelle part	C
GO:0044422	3957	139	70.9345	1.00E-016	organelle part	C
GO:0044428	1616	79	28.9690	1.56E-016	nuclear part	C
GO:0005737	7181	206	128.7290	2.43E-016	cytoplasm	C
GO:0005575	15609	344	279.8120	3.50E-016	cellular_component	C
GO:0006139	1842	82	33.0203	7.61E-015	nucleobase, nucleoside, nucleotide and nucleic acid metabolic process	P
GO:0009987	10893	267	195.2720	5.09E-014	cellular process	P
GO:0005488	12806	298	229.5650	6.67E-014	binding	F
GO:0006807	2248	90	40.2984	1.42E-013	nitrogen compound metabolic process	P
GO:0044260	3877	129	69.5004	1.61E-013	cellular macromolecule metabolic process	P
GO:0043232	2536	97	45.4612	1.91E-013	intracellular non-membrane-bounded organelle	C
GO:0043228	2536	97	45.4612	1.91E-013	non-membrane-bounded organelle	C
GO:0044237	5431	162	97.3579	2.93E-013	cellular metabolic process	P
GO:0031981	1231	60	22.0673	1.44E-012	nuclear lumen	C
GO:0016070	938	51	16.8149	1.57E-012	RNA metabolic process	P

GO ID	n_annotation	n_both	expect	pv	-	
GO:0008150	14455	319	259.1250	2.69E-012	biological_process	P
GO:0031974	1610	69	28.8614	9.32E-012	membrane-enclosed lumen	C
GO:0043233	1575	68	28.2340	9.77E-012	organelle lumen	C
GO:0070013	1539	67	27.5886	9.91E-012	intracellular organelle lumen	C
GO:0044238	5664	161	101.5350	2.39E-011	primary metabolic process	P
GO:0043170	4436	135	79.5212	2.73E-011	macromolecule metabolic process	P
GO:0043067	740	42	13.2655	4.62E-011	regulation of programmed cell death	P
GO:0010941	742	42	13.3013	5.02E-011	regulation of cell death	P
GO:0042981	731	41	13.1042	1.15E-010	regulation of apoptosis	P
GO:0003674	15294	327	274.1650	1.17E-010	molecular_function	F
GO:0032991	3223	106	57.7766	1.29E-010	macromolecular complex	C
GO:0008152	6464	173	115.8760	4.09E-010	metabolic process	P
GO:0005654	857	42	15.3629	3.91E-009	nucleoplasm	C
GO:0048519	1704	63	30.5465	2.85E-008	negative regulation of biological process	P
GO:0048523	1550	59	27.7858	3.06E-008	negative regulation of cellular process	P
GO:0005856	1386	54	24.8459	6.01E-008	cytoskeleton	C
GO:0006996	1386	54	24.8459	6.01E-008	organelle organization	P
GO:0044444	4724	129	84.6840	1.06E-007	cytoplasmic part	C
GO:0010467	1326	51	23.7703	2.18E-007	gene expression	P
GO:0044248	1081	44	19.3784	3.53E-007	cellular catabolic process	P
GO:0034645	1164	46	20.8663	4.30E-007	cellular macromolecule biosynthetic process	P
GO:0022402	542	28	9.7161	6.19E-007	cell cycle process	P
GO:0009059	1182	46	21.1889	6.59E-007	macromolecule biosynthetic process	P
GO:0044430	893	38	16.0082	8.12E-007	cytoskeletal part	C
GO:0044249	2001	66	35.8706	8.52E-007	cellular biosynthetic process	P
GO:0016043	2593	79	46.4830	1.37E-006	cellular component organization	P
GO:0044265	783	34	14.0363	2.04E-006	cellular macromolecule catabolic process	P
GO:0044267	2446	75	43.8478	2.15E-006	cellular protein metabolic process	P
GO:0016071	359	21	6.4356	2.39E-006	mRNA metabolic process	P
GO:0009058	2062	66	36.9641	2.40E-006	biosynthetic process	P
GO:0043234	2546	77	45.6404	2.55E-006	protein complex	C
GO:0034660	248	17	4.4457	2.70E-006	ncRNA metabolic process	P
GO:0005730	429	23	7.6904	3.44E-006	nucleolus	C
GO:0007010	439	23	7.8697	5.04E-006	cytoskeleton organization	P
GO:0006259	538	26	9.6444	5.27E-006	DNA metabolic process	P
GO:0006396	540	26	9.6802	5.63E-006	RNA processing	P
GO:0000278	352	20	6.3101	6.40E-006	mitotic cell cycle	P

GO ID	n_annotation	n_both	expect	pv	-	
GO:0006403	95	10	1.7030	7.96E-006	RNA localization	P
GO:0043065	360	20	6.4535	8.92E-006	positive regulation of apoptosis	P
GO:0042802	624	28	11.1860	9.19E-006	identical protein binding	F
GO:0043068	363	20	6.5073	1.01E-005	positive regulation of programmed cell death	P
GO:0016874	426	22	7.6366	1.01E-005	ligase activity	F
GO:0010942	365	20	6.5431	1.09E-005	positive regulation of cell death	P
GO:0007049	738	31	13.2296	1.13E-005	cell cycle	P
GO:0005200	83	9	1.4879	1.78E-005	structural constituent of cytoskeleton	F
GO:0015629	347	19	6.2204	1.83E-005	actin cytoskeleton	C
GO:0005916	10	4	0.1793	1.96E-005	fascia adherens	C
GO:0008092	516	24	9.2500	2.27E-005	cytoskeletal protein binding	F
GO:0015931	108	10	1.9360	2.48E-005	nucleobase, nucleoside, nucleotide and nucleic acid transport	P
GO:0003723	704	29	12.6201	3.11E-005	RNA binding	F
GO:0003779	330	18	5.9157	3.18E-005	actin binding	F
GO:0019538	2968	82	53.2054	3.42E-005	protein metabolic process	P
GO:0043038	70	8	1.2548	3.55E-005	amino acid activation	P
GO:0006418	70	8	1.2548	3.55E-005	tRNA aminoacylation for protein translation	P
GO:0043039	70	8	1.2548	3.55E-005	tRNA aminoacylation	P
GO:0044085	1133	40	20.3105	3.56E-005	cellular component biogenesis	P
GO:0022403	399	20	7.1526	3.90E-005	cell cycle phase	P
GO:0004812	71	8	1.2728	3.94E-005	aminoacyl-tRNA ligase activity	F
GO:0016876	71	8	1.2728	3.94E-005	ligase activity, forming aminoacyl-tRNA and related compounds	F
GO:0016875	71	8	1.2728	3.94E-005	ligase activity, forming carbon-oxygen bonds	F
GO:0051236	92	9	1.6492	4.08E-005	establishment of RNA localization	P
GO:0050657	92	9	1.6492	4.08E-005	nucleic acid transport	P
GO:0050658	92	9	1.6492	4.08E-005	RNA transport	P
GO:0000049	23	5	0.4123	4.65E-005	tRNA binding	F
GO:0006399	142	11	2.5455	5.22E-005	tRNA metabolic process	P
GO:0006950	2005	60	35.9423	5.46E-005	response to stress	P
GO:0043632	548	24	9.8236	5.90E-005	modification-dependent macromolecule catabolic process	P
GO:0019941	548	24	9.8236	5.90E-005	modification-dependent protein catabolic process	P
GO:0030529	550	24	9.8595	6.24E-005	ribonucleoprotein complex	C
GO:0006402	39	6	0.6991	6.31E-005	mRNA catabolic process	P
GO:0065009	933	34	16.7253	7.66E-005	regulation of molecular function	P
GO:0006261	58	7	1.0397	7.71E-005	DNA-dependent DNA replication	P
GO:0006401	59	7	1.0577	8.62E-005	RNA catabolic process	P
GO:0000184	26	5	0.4661	8.70E-005	nuclear-transcribed mRNA catabolic process, nonsense-mediated decay	P

GO ID	n_annotation	n_both	expect	pv	-	
GO:0006520	263	15	4.7146	8.76E-005	cellular amino acid metabolic process	P
GO:0005625	325	17	5.8261	8.79E-005	soluble fraction	C
GO:0015630	527	23	9.4472	8.84E-005	microtubule cytoskeleton	C
GO:0005829	1141	39	20.4539	8.93E-005	cytosol	C
GO:0007067	205	13	3.6749	8.95E-005	mitosis	P
GO:0000280	205	13	3.6749	8.95E-005	nuclear division	P

Supplementary Table 5

The final 57 genes extracted from the application of Gene Ontology and phylogentic footprinting analysis that can be considered *bona fide* as bearing the candidate nCaRE sequences within their regulatory elements and potentially regulated by APE1.

Ensembl ID	Gene title	Gene symbol	Chr. location
ENSG00000090861	alanyl-tRNA synthetase	AARS	chr16q22
ENSG00000100823	APEX nuclease (multifunctional DNA repair enzyme) 1	APEX1	chr14q11.2-q12
ENSG00000062725	amyloid beta precursor protein (cytoplasmic tail) binding protein 2	APPBP2	chr17q21-q23
ENSG00000162704	actin related protein 2/3 complex, subunit 5, 16kDa	ARPC5	chr1q25.3
ENSG00000113732	ATPase, H+ transporting, lysosomal 9kDa, V0 subunit e	ATP6V0E	chr5q35.1
ENSG00000156735	BCL2-associated athanogene 4	BAG4	chr8p12
ENSG00000060762	brain protein 44-like	BRP44L	chr6q27
ENSG00000130303	bone marrow stromal cell antigen 2	BST2	chr19p13.2
ENSG00000164941	chromosome 8 open reading frame 52	C8orf52	chr8q22.1
ENSG00000110619	cysteinyl-tRNA synthetase	CARS	chr11p15.5
ENSG00000160200	cystathionine-beta-synthase	CBS	chr21q22.3
ENSG00000117877	CD3E antigen, epsilon polypeptide associated protein	CD3EAP	chr19q13.3
ENSG00000010278	CD9 antigen (p24)	CD9	chr12p13.3
ENSG00000153774	craniofacial development protein 1	CFDP1	chr16q22.2-q22.3
ENSG00000149600	COMM domain containing 7	COMMD7	chr20q11.21
ENSG00000175215	CTD (carboxy-terminal domain, RNA polymerase II, polypeptide A) small phosphatase 2	CTDSP2	chr12q13-q15
ENSG00000143079	CTTNBP2 N-terminal like	CTTNBP2NL	chr1p13.2
ENSG00000108406	DEAH (Asp-Glu-Ala-His) box polypeptide 40	DHX40	chr17q23.2
ENSG00000120738	Early growth response 1	EGR1	chr5q31.1
ENSG00000147677	eukaryotic translation initiation factor 3, subunit 3 gamma, 40kDa	EIF3S3	chr8q24.11
ENSG00000187840	eukaryotic translation initiation factor 4E binding protein 1	EIF4EBP1	chr8p12
ENSG00000136628	glutamyl-prolyl-tRNA synthetase	EPRS	chr1q41-q42
ENSG00000147874	family with sequence similarity 29, member A	FAM29A	chr9p22.1
ENSG00000104872	hypothetical protein FLJ20643	FLJ20643	chr19q13.33
ENSG00000143575	HCLS1 associated protein X-1	HAX1	chr1q21.3
ENSG00000185359	hepatocyte growth factor-regulated tyrosine kinase substrate	HGS	chr17q25
ENSG00000189159	hematological and neurological expressed 1	HN1	chr17q25.1
ENSG00000131373	2-hydroxyphytanoyl-CoA lyase	HPCL2	chr3p25.1
ENSG00000166411	isocitrate dehydrogenase 3 (NAD+) alpha	IDH3A	chr15q25.1-q25.2
ENSG00000130522	jun D proto-oncogene	JUND	chr19p13.2
ENSG00000145725	KIAA0433 protein	KIAA0433	chr5q21.1
ENSG00000052749	KIAA0690	KIAA0690	chr10q24.1
ENSG00000112200	KIAA1702 protein	KIAA1702	chr6p11
ENSG00000118193	kinesin family member 14	KIF14	chr1pter-q31.3

Ensembl ID	Gene title	Gene symbol	Chr. location
ENSG00000109790	kelch-like 5 (Drosophila)	KLHL5	chr4p14
ENSG00000126214	kinesin 2	KNS2	chr14q32.3
ENSG00000130164	low density lipoprotein receptor (familial hypercholesterolemia)	LDLR	chr19p13.3
ENSG00000133895	multiple endocrine neoplasia I	MEN1	chr11q13
ENSG00000109919	mitochondrial carrier homolog 2 (C. elegans)	MTCH2	chr11p11.2
ENSG00000102908	nuclear factor of activated T-cells 5, tonicity-responsive	NFAT5	chr16q22.1
ENSG00000171246	neuronal pentraxin I	NPTX1	chr17q25.1-q25.2
ENSG00000135318	5'-nucleotidase, ecto (CD73)	NT5E	chr6q14-q21
ENSG00000025293	PHD finger protein 20	PHF20	chr20q11.22-q11.23
ENSG00000149547	translokin	PIG8	chr11q21
ENSG00000198056	primase, polypeptide 1, 49kDa	PRIM1	chr12q13
ENSG00000034677	ring finger protein 19	RNF19	chr8q22
ENSG00000096717	sirtuin (silent mating type information regulation 2 homolog) 1 (S. cerevisiae)	SIRT1	chr10q21.3
ENSG00000105281	solute carrier family 1 (neutral amino acid transporter), member 5	SLC1A5	chr19q13.3
ENSG00000127616	SWI/SNF related, matrix associated, actin dependent regulator of chromatin, subfamily a, member 4	SMARCA4	chr19p13.2
ENSG00000163029	SMC6 structural maintenance of chromosomes 6-like 1 (yeast)	SMC6L1	chr2p24.2
ENSG00000197694	spectrin, alpha, non-erythrocytic 1 (alpha-fodrin)	SPTAN1	chr9q33-q34
ENSG00000173465	Sjogren's syndrome/scleroderma autoantigen 1	SSSCA1	chr11q13.1
ENSG00000144043	testis expressed sequence 261	TEX261	chr2p13.3
ENSG00000035862	TIMP metallopeptidase inhibitor 2	TIMP2	chr17q25
ENSG00000198211	tubulin, beta 3	TUBB3	chr16q24.3
ENSG00000165280	valosin-containing protein	VCP	chr9p13.3
ENSG00000134684	tyrosyl-tRNA synthetase	YARS	chr1p35.1

Supplementary Table 6

Complete data reporting all the significant functional enrichments obtained performing GeneCodis analysis.

'GO term ID' and 'Annotations' columns represent the Gene Ontology codes of annotations and the textual description of annotations, respectively. BP refers to 'biological process' category of Gene Ontology annotation. Third and fourth columns represent the number of genes in the input list and the reference list for a given annotation, respectively. P-values calculated using hypergeometric distribution and its correction using the stimulation-based approach are reported. The 'Genes' column identifies the set of genes in the input list showing a given annotation.

GO term ID	Annotations	# of annotated genes in the input list (Total # of genes in the input list)	# of annotated genes in the reference list (Total # of genes in the reference list)	Hypergeometric Distribution (Fisher's exact test)	Corrected Hypergeometric Dist. (Fisher's exact test)	Genes
GO:0010467	gene expression (BP)	6(57)	408(34208)	6,02E-05	9,97E-03	EIF4EBP1 YARS AARS EPRS CARS EIF3H
GO:0045944	positive regulation of transcription from RNA polymerase II promoter (BP)	6(57)	578(34208)	3,96E-04	1,87E-02	SIRT1 EGR1 JUND SMARCA4 MEN1 NFAT5
GO:0006281	DNA repair (BP)	5(57)	285(34208)	1,14E-04	1,26E-02	SIRT1 SMC6 VCP MEN1 APEX1
GO:0006810	transport (BP)	5(57)	604(34208)	3,32E-03	2,89E-02	VCP LDLR NPTX1 ATP6V0E1 MTCH2
GO:0006418	tRNA aminoacylation for protein translation (BP)	4(57)	43(34208)	8,14E-07	2,70E-04	YARS AARS EPRS CARS
GO:0008285	negative regulation of cell proliferation (BP)	4(57)	341(34208)	2,53E-03	2,46E-02	HGS MEN1 CD9 TIMP2
GO:0045892	negative regulation of transcription, DNA-dependent (BP)	4(57)	401(34208)	4,50E-03	2,37E-02	SIRT1 SMARCA4 MEN1 COMMD7

GO term ID	Annotations	# of annotated genes in the input list (Total # of genes in the input list)	# of annotated genes in the reference list (Total # of genes in the reference list)	Hypergeometric Distribution (Fisher's exact test)	Corrected Hypergeometric Dist. (Fisher's exact test)	Genes
GO:0000122	negative regulation of transcription from RNA polymerase II promoter (BP)	4(57)	416(34208)	5,13E-03	2,23E-02	SIRT1 EGR1 SMARCA4 MEN1
GO:0007018	microtubule-based movement (BP)	3(57)	90(34208)	4,65E-04	1,92E-02	KLC1 KIF14 TUBB3
GO:0030308	negative regulation of cell growth (BP)	3(57)	113(34208)	9,02E-04	2,71E-02	SIRT1 SMARCA4 EI24
GO:0006974	response to DNA damage stimulus (BP)	3(57)	129(34208)	1,32E-03	3,12E-02	SIRT1 VCP MEN1
GO:0043065	positive regulation of apoptotic process (BP)	3(57)	178(34208)	3,30E-03	3,03E-02	TEX261 SIRT1 MEN1
GO:0006457	protein folding (BP)	3(57)	182(34208)	3,51E-03	1,94E-02	AARS BAG4 TUBB3
GO:0044267	cellular protein metabolic process (BP)	3(57)	284(34208)	1,19E-02	3,40E-02	EIF4EBP1 TUBB3 EIF3H
GO:0060766	negative regulation of androgen receptor signaling pathway (BP)	2(57)	10(34208)	1,22E-04	1,01E-02	SIRT1 SMARCA4
GO:0060135	maternal process involved in female pregnancy (BP)	2(57)	14(34208)	2,45E-04	1,62E-02	MEN1 CBS
GO:0002076	osteoblast development (BP)	2(57)	16(34208)	3,22E-04	1,78E-02	JUND MEN1

GO term ID	Annotations	# of annotated genes in the input list (Total # of genes in the input list)	# of annotated genes in the reference list (Total # of genes in the reference list)	Hypergeometric Distribution (Fisher's exact test)	Corrected Hypergeometric Dist. (Fisher's exact test)	Genes
GO:0045739	positive regulation of DNA repair (BP)	2(57)	23(34208)	6,75E-04	2,48E-02	SIRT1 APEX1
GO:0030968	endoplasmic reticulum unfolded protein response (BP)	2(57)	25(34208)	7,98E-04	2,64E-02	VCP AARS
GO:0043280	positive regulation of cysteine-type endopeptidase activity involved in apoptotic process (BP)	2(57)	27(34208)	9,32E-04	2,57E-02	SIRT1 MEN1
GO:0071356	cellular response to tumor necrosis factor (BP)	2(57)	28(34208)	1,00E-03	2,55E-02	SIRT1 BAG4
GO:0045768	positive regulation of anti-apoptosis (BP)	2(57)	41(34208)	2,15E-03	2,22E-02	SIRT1 APEX1
GO:0045669	positive regulation of osteoblast differentiation (BP)	2(57)	42(34208)	2,25E-03	2,26E-02	JUND MEN1
GO:0032088	negative regulation of NF-kappaB transcription factor activity (BP)	2(57)	46(34208)	2,69E-03	2,55E-02	SIRT1 COMMD7
GO:0042632	cholesterol homeostasis (BP)	2(57)	51(34208)	3,30E-03	2,95E-02	SIRT1 LDLR
GO:0043161	proteasomal ubiquitin-dependent protein catabolic process (BP)	2(57)	52(34208)	3,43E-03	1,92E-02	SIRT1 VCP
GO:0043433	negative regulation of sequence-specific DNA binding transcription factor activity (BP)	2(57)	54(34208)	3,69E-03	1,97E-02	SIRT1 MEN1

Annotations	# of annotated genes in the input list (Total # of genes in the input list)	# of annotated genes in the reference list (Total # of genes in the reference list)	Hypergeometric Distribution (Fisher's exact test)	Corrected Hypergeometric Dist. (Fisher's exact test)	Genes	
chromatin remodeling (BP)	2(57)	54(34208)	3,69E-03	1,97E-02	SMARCA4 MEN1	
response to insulin stimulus (BP)	2(57)	62(34208)	4,84E-03	2,50E-02	SIRT1 EGR1	
DNA recombination (BP)	2(57)	86(34208)	9,12E-03	3,05E-02	SMC6 APEX1	
cellular component movement (BP)	2(57)	95(34208)	1,10E-02	3,35E-02	CD9 ARPC5	
regulation of cell proliferation (BP)	2(57)	101(34208)	1,24E-02	3,51E-02	SIRT1 CFDP1	
insulin receptor signaling pathway (BP)	2(57)	139(34208)	2,26E-02	4,89E-02	EIF4EBP1 ATP6V0E1	
homocysteine catabolic process (BP)	1(57)	1(34208)	1,67E-03	1,78E-02	CBS	
cysteine biosynthetic process via cystathionine (BP)	1(57)	1(34208)	1,67E-03	1,78E-02	CBS	
transsulfuration (BP)	1(57)	1(34208)	1,67E-03	1,78E-02	CBS	
cysteine biosynthetic process from serine (BP)	1(57)	1(34208)	1,67E-03	1,78E-02	CBS	
tyrosyl-tRNA aminoacylation (BP)	1(57)	1(34208)	1,67E-03	1,78E-02	YARS	
positive regulation of histone methylation (BP)	1(57)	1(34208)	1,67E-03	1,78E-02	MEN1	
adenosine biosynthetic process (BP)	1(57)	1(34208)	1,67E-03	1,78E-02	NT5E	

GO term ID	Annotations	# of annotated genes in the input list (Total # of genes in the input list)	# of annotated genes in the reference list (Total # of genes in the reference list)	Hypergeometric Distribution (Fisher's exact test)	Corrected Hypergeometric Dist. (Fisher's exact test)	Genes
GO:0072303	positive regulation of glomerular metanephric mesangial cell proliferation (BP)	1(57)	1(34208)	1,67E-03	1,78E-02	EGR1
GO:0072110	glomerular mesangial cell proliferation (BP)	1(57)	1(34208)	1,67E-03	1,78E-02	EGR1
GO:0033233	regulation of protein sumoylation (BP)	1(57)	1(34208)	1,67E-03	1,78E-02	EGR1
GO:2000655	negative regulation of cellular response to testosterone stimulus (BP)	1(57)	1(34208)	1,67E-03	1,78E-02	SIRT1
GO:2000480	negative regulation of cAMP-dependent protein kinase activity (BP)	1(57)	1(34208)	1,67E-03	1,78E-02	SIRT1
GO:0006343	establishment of chromatin silencing (BP)	1(57)	1(34208)	1,67E-03	1,78E-02	SIRT1
GO:2000757	negative regulation of peptidyl-lysine acetylation (BP)	1(57)	1(34208)	1,67E-03	1,78E-02	SIRT1
GO:0034391	regulation of smooth muscle cell apoptosis (BP)	1(57)	1(34208)	1,67E-03	1,78E-02	SIRT1
GO:0031937	positive regulation of chromatin silencing (BP)	1(57)	1(34208)	1,67E-03	1,78E-02	SIRT1

GO term ID	Annotations	# of annotated genes in the input list (Total # of genes in the input list)	# of annotated genes in the reference list (Total # of genes in the reference list)	Hypergeometric Distribution (Fisher's exact test)	Corrected Hypergeometric Dist. (Fisher's exact test)	Genes
GO:0031393	negative regulation of prostaglandin biosynthetic process (BP)	1(57)	1(34208)	1,67E-03	1,78E-02	SIRT1
GO:0060385	axonogenesis involved in innervation (BP)	1(57)	2(34208)	3,33E-03	1,90E-02	NPTX1
GO:2000481	positive regulation of cAMP-dependent protein kinase activity (BP)	1(57)	2(34208)	3,33E-03	1,90E-02	SIRT1
GO:2000773	negative regulation of cellular senescence (BP)	1(57)	2(34208)	3,33E-03	1,90E-02	SIRT1
GO:0035617	stress granule disassembly (BP)	1(57)	2(34208)	3,33E-03	1,90E-02	KLC1
GO:0006424	glutamyl-tRNA aminoacylation (BP)	1(57)	2(34208)	3,33E-03	1,90E-02	EPRS
GO:0016239	positive regulation of macroautophagy (BP)	1(57)	2(34208)	3,33E-03	1,90E-02	SIRT1
GO:0006433	prolyl-tRNA aminoacylation (BP)	1(57)	2(34208)	3,33E-03	1,90E-02	EPRS
GO:0006423	cysteinyl-tRNA aminoacylation (BP)	1(57)	2(34208)	3,33E-03	1,90E-02	CARS
GO:0043506	regulation of JUN kinase activity (BP)	1(57)	2(34208)	3,33E-03	1,90E-02	CBS

GO term ID	Annotations	# of annotated genes in the input list (Total # of genes in the input list)	# of annotated genes in the reference list (Total # of genes in the reference list)	Hypergeometric Distribution (Fisher's exact test)	Corrected Hypergeometric Dist. (Fisher's exact test)	Genes
GO:0030823	regulation of cGMP metabolic process (BP)	1(57)	2(34208)	3,33E-03	1,90E-02	CBS
GO:0070814	hydrogen sulfide biosynthetic process (BP)	1(57)	2(34208)	3,33E-03	1,90E-02	CBS
GO:0019448	L-cysteine catabolic process (BP)	1(57)	2(34208)	3,33E-03	1,90E-02	CBS
GO:0010899	regulation of phosphatidylcholine catabolic process (BP)	1(57)	2(34208)	3,33E-03	1,90E-02	LDLR
GO:0018394	peptidyl-lysine acetylation (BP)	1(57)	2(34208)	3,33E-03	1,90E-02	SIRT1
GO:0080134	regulation of response to stress (BP)	1(57)	2(34208)	3,33E-03	1,90E-02	SIRT1
GO:0002051	osteoblast fate commitment (BP)	1(57)	2(34208)	3,33E-03	1,90E-02	MEN1
GO:0006196	AMP catabolic process (BP)	1(57)	2(34208)	3,33E-03	1,90E-02	NT5E
GO:0000720	pyrimidine dimer repair by nucleotide-excision repair (BP)	1(57)	2(34208)	3,33E-03	1,90E-02	SIRT1
GO:0071506	cellular response to mycophenolic acid (BP)	1(57)	2(34208)	3,33E-03	1,90E-02	EGR1
GO:0032071	regulation of endodeoxyribonuclease activity (BP)	1(57)	2(34208)	3,33E-03	1,90E-02	SIRT1
GO:0000492	box C/D snoRNP assembly (BP)	1(57)	3(34208)	4,99E-03	2,20E-02	PIH1D1
GO:0006565	L-serine catabolic process (BP)	1(57)	3(34208)	4,99E-03	2,20E-02	CBS

GO term ID	Annotations	# of annotated genes in the input list (Total # of genes in the input list)	# of annotated genes in the reference list (Total # of genes in the reference list)	Hypergeometric Distribution (Fisher's exact test)	Corrected Hypergeometric Dist. (Fisher's exact test)	Genes
GO:0030814	regulation of cAMP metabolic process (BP)	1(57)	4(34208)	6,65E-03	2,45E-02	TIMP2
GO:0007035	vacuolar acidification (BP)	1(57)	4(34208)	6,65E-03	2,45E-02	ATP6V0E1
GO:0006020	inositol metabolic process (BP)	1(57)	4(34208)	6,65E-03	2,45E-02	PPIP5K2
GO:0070842	aggresome assembly (BP)	1(57)	4(34208)	6,65E-03	2,45E-02	VCP
GO:0034983	peptidyl-lysine deacetylation (BP)	1(57)	4(34208)	6,65E-03	2,45E-02	SIRT1
GO:0006868	glutamine transport (BP)	1(57)	4(34208)	6,65E-03	2,45E-02	SLC1A5
GO:0050667	homocysteine metabolic process (BP)	1(57)	4(34208)	6,65E-03	2,45E-02	CBS
GO:0070857	regulation of bile acid biosynthetic process (BP)	1(57)	4(34208)	6,65E-03	2,45E-02	SIRT1
GO:0070932	histone H3 deacetylation (BP)	1(57)	4(34208)	6,65E-03	2,45E-02	SIRT1
GO:0033158	regulation of protein import into nucleus, translocation (BP)	1(57)	4(34208)	6,65E-03	2,45E-02	SIRT1
GO:0006346	methylation-dependent chromatin silencing (BP)	1(57)	5(34208)	8,30E-03	2,80E-02	SIRT1
GO:0030913	paranodal junction assembly (BP)	1(57)	5(34208)	8,30E-03	2,80E-02	CD9
GO:0006563	L-serine metabolic process (BP)	1(57)	5(34208)	8,30E-03	2,80E-02	CBS
GO:0001678	cellular glucose homeostasis (BP)	1(57)	5(34208)	8,30E-03	2,80E-02	SIRT1
GO:0071504	cellular response to heparin (BP)	1(57)	5(34208)	8,30E-03	2,80E-02	EGR1

GO term ID	Annotations	# of annotated genes in the input list (Total # of genes in the input list)	# of annotated genes in the reference list (Total # of genes in the reference list)	Hypergeometric Distribution (Fisher's exact test)	Corrected Hypergeometric Dist. (Fisher's exact test)	Genes
GO:0030970	retrograde protein transport, ER to cytosol (BP)	1(57)	5(34208)	8,30E-03	2,80E-02	VCP
GO:0043039	tRNA aminoacylation (BP)	1(57)	5(34208)	8,30E-03	2,80E-02	AARS
GO:0032925	regulation of activin receptor signaling pathway (BP)	1(57)	5(34208)	8,30E-03	2,80E-02	MEN1
GO:0008088	axon cargo transport (BP)	1(57)	6(34208)	9,96E-03	3,05E-02	KLC1
GO:0046628	positive regulation of insulin receptor signaling pathway (BP)	1(57)	6(34208)	9,96E-03	3,05E-02	SIRT1
GO:0021587	cerebellum morphogenesis (BP)	1(57)	6(34208)	9,96E-03	3,05E-02	CBS
GO:0003407	neural retina development (BP)	1(57)	6(34208)	9,96E-03	3,05E-02	SMARCA4
GO:0001561	fatty acid alpha-oxidation (BP)	1(57)	6(34208)	9,96E-03	3,05E-02	HACL1
GO:0046426	negative regulation of JAK-STAT cascade (BP)	1(57)	6(34208)	9,96E-03	3,05E-02	HGS
GO:0006642	triglyceride mobilization (BP)	1(57)	6(34208)	9,96E-03	3,05E-02	SIRT1
GO:0046621	negative regulation of organ growth (BP)	1(57)	6(34208)	9,96E-03	3,05E-02	MEN1
GO:0006102	isocitrate metabolic process (BP)	1(57)	6(34208)	9,96E-03	3,05E-02	IDH3A
GO:0071480	cellular response to gamma radiation (BP)	1(57)	7(34208)	1,16E-02	3,34E-02	EGR1
GO:0010867	positive regulation of triglyceride biosynthetic process (BP)	1(57)	7(34208)	1,16E-02	3,34E-02	LDLR

GO term ID	Annotations	# of annotated genes in the input list (Total # of genes in the input list)	# of annotated genes in the reference list (Total # of genes in the reference list)	Hypergeometric Distribution (Fisher's exact test)	Corrected Hypergeometric Dist. (Fisher's exact test)	Genes
GO:0051974	negative regulation of telomerase activity (BP)	1(57)	7(34208)	1,16E-02	3,34E-02	MEN1
GO:0000183	chromatin silencing at rDNA (BP)	1(57)	7(34208)	1,16E-02	3,34E-02	SIRT1
GO:0060351	cartilage development involved in endochondral bone morphogenesis (BP)	1(57)	7(34208)	1,16E-02	3,34E-02	CBS
GO:0006734	NADH metabolic process (BP)	1(57)	7(34208)	1,16E-02	3,34E-02	IDH3A
GO:0031929	TOR signaling cascade (BP)	1(57)	8(34208)	1,33E-02	3,48E-02	EIF4EBP1
GO:0006835	dicarboxylic acid transport (BP)	1(57)	8(34208)	1,33E-02	3,48E-02	SLC1A5
GO:0000012	single strand break repair (BP)	1(57)	8(34208)	1,33E-02	3,48E-02	SIRT1
GO:0055089	fatty acid homeostasis (BP)	1(57)	8(34208)	1,33E-02	3,48E-02	SIRT1
GO:0034383	low-density lipoprotein particle clearance (BP)	1(57)	8(34208)	1,33E-02	3,48E-02	LDLR
GO:0006400	tRNA modification (BP)	1(57)	8(34208)	1,33E-02	3,48E-02	AARS
GO:0030299	intestinal cholesterol absorption (BP)	1(57)	8(34208)	1,33E-02	3,48E-02	LDLR
GO:0045348	positive regulation of MHC class II biosynthetic process (BP)	1(57)	8(34208)	1,33E-02	3,48E-02	SIRT1
GO:0006342	chromatin silencing (BP)	1(57)	8(34208)	1,33E-02	3,48E-02	SIRT1
GO:0021680	cerebellar Purkinje cell layer development (BP)	1(57)	9(34208)	1,49E-02	3,68E-02	AARS

GO term ID	Annotations	# of annotated genes in the input list (Total # of genes in the input list)	# of annotated genes in the reference list (Total # of genes in the reference list)	Hypergeometric Distribution (Fisher's exact test)	Corrected Hypergeometric Dist. (Fisher's exact test)	Genes
GO:0015804	neutral amino acid transport (BP)	1(57)	9(34208)	1,49E-02	3,68E-02	SLC1A5
GO:0007342	fusion of sperm to egg plasma membrane (BP)	1(57)	9(34208)	1,49E-02	3,68E-02	CD9
GO:0001542	ovulation from ovarian follicle (BP)	1(57)	9(34208)	1,49E-02	3,68E-02	SIRT1
GO:0070498	interleukin-1-mediated signaling pathway (BP)	1(57)	9(34208)	1,49E-02	3,68E-02	EGR1
GO:0051593	response to folic acid (BP)	1(57)	9(34208)	1,49E-02	3,68E-02	CBS
GO:0031333	negative regulation of protein complex assembly (BP)	1(57)	9(34208)	1,49E-02	3,68E-02	EIF4EBP1
GO:0045749	negative regulation of S phase of mitotic cell cycle (BP)	1(57)	9(34208)	1,49E-02	3,68E-02	SMARCA4
GO:0000731	DNA synthesis involved in DNA repair (BP)	1(57)	10(34208)	1,65E-02	3,97E-02	SIRT1
GO:0034968	histone lysine methylation (BP)	1(57)	10(34208)	1,65E-02	3,97E-02	MEN1
GO:0043923	positive regulation by host of viral transcription (BP)	1(57)	10(34208)	1,65E-02	3,97E-02	SMARCA4
GO:0043518	negative regulation of DNA damage response, signal transduction by p53 class mediator (BP)	1(57)	10(34208)	1,65E-02	3,97E-02	SIRT1
GO:0006195	purine nucleotide catabolic process (BP)	1(57)	11(34208)	1,82E-02	4,15E-02	NT5E

GO term ID	Annotations	# of annotated genes in the input list (Total # of genes in the input list)	# of annotated genes in the reference list (Total # of genes in the reference list)	Hypergeometric Distribution (Fisher's exact test)	Corrected Hypergeometric Dist. (Fisher's exact test)	Genes
GO:0045947	negative regulation of translational initiation (BP)	1(57)	11(34208)	1,82E-02	4,15E-02	EIF4EBP1
GO:0043488	regulation of mRNA stability (BP)	1(57)	11(34208)	1,82E-02	4,15E-02	APEX1
GO:0010875	positive regulation of cholesterol efflux (BP)	1(57)	11(34208)	1,82E-02	4,15E-02	SIRT1
GO:0043408	regulation of MAPK cascade (BP)	1(57)	11(34208)	1,82E-02	4,15E-02	TIMP2
GO:0031334	positive regulation of protein complex assembly (BP)	1(57)	11(34208)	1,82E-02	4,15E-02	VCP
GO:0006476	protein deacetylation (BP)	1(57)	11(34208)	1,82E-02	4,15E-02	SIRT1
GO:0016180	snRNA processing (BP)	1(57)	12(34208)	1,98E-02	4,37E-02	INTS8
GO:0050872	white fat cell differentiation (BP)	1(57)	12(34208)	1,98E-02	4,37E-02	SIRT1
GO:0080111	DNA demethylation (BP)	1(57)	12(34208)	1,98E-02	4,37E-02	APEX1
GO:0032007	negative regulation of TOR signaling cascade (BP)	1(57)	12(34208)	1,98E-02	4,37E-02	SIRT1
GO:0046135	pyrimidine nucleoside catabolic process (BP)	1(57)	12(34208)	1,98E-02	4,37E-02	NT5E
GO:0030301	cholesterol transport (BP)	1(57)	13(34208)	2,15E-02	4,67E-02	LDLR
GO:0030833	regulation of actin filament polymerization (BP)	1(57)	13(34208)	2,15E-02	4,67E-02	ARPC5

GO term ID	Annotations	# of annotated genes in the input list (Total # of genes in the input list)	# of annotated genes in the reference list (Total # of genes in the reference list)	Hypergeometric Distribution (Fisher's exact test)	Corrected Hypergeometric Dist. (Fisher's exact test)	Genes
GO:0042176	regulation of protein catabolic process (BP)	1(57)	14(34208)	2,31E-02	4,90E-02	HGS
GO:0009303	rRNA transcription (BP)	1(57)	14(34208)	2,31E-02	4,90E-02	CD3EAP
GO:0050880	regulation of blood vessel size (BP)	1(57)	14(34208)	2,31E-02	4,90E-02	CBS

Supplementary Table 7

Results from time-course limited proteolysis experiments as determined by parallel reactions with the indicated proteases on non-complexed recombinant APE1, recombinant APE1-SIRT1 nCaRE-B complex or recombinant APE1-PTH nCaRE complex. Shown are the proteases/protein (w/w) values used for each experiment as well as the measured/theoretical mass values and the deduced primary cleavage sites in the recombinant APE1 product. In parenthesis are reported the corresponding cleavage sites in the native protein, which differs from the recombinant one for the lack of three amino acids at protein N-terminus. Mi, monoisotopic; av, average.

				APE1	APE1-SIRT1 nCaRE complex	APE1-PTH nCaRE complex	
Enzyme	**Time (min)**	**Peptide**	**Theoretical mass**	**Experimental mass**	**Experimental mass**	**Experimental mass**	**Primary cleavage site**
Trypsin/APE1 1:5000 (w/w)	**5**	**1-9**	1041.62$_{mi}$	1041.60 $_{mi}$			K9 (K6)
		1-10	1169.72 $_{mi}$	1169.68 $_{mi}$			K10 (K7)
		10-321	34856.56$_{av}$	34854.12 $_{av}$			K9 (K6)
		11-321	34727.40$_{av}$	34726.80 $_{av}$			K10 (K7)
		1-321	35880.86$_{av}$	35879.87 $_{av}$	35879.5$_{av}$	35880.22 $_{av}$	
	15	**1-9**	1041.62 $_{mi}$	1041.58 $_{mi}$			K9 (K6)
		1-10	1169.72 $_{mi}$	1169.67 $_{mi}$			K10 (K7)
		10-321	34856.56$_{av}$	34856.70 $_{av}$			K9 (K6)

		11-321	34727.40 $_{av}$	34726.50 $_{av}$			K10 (K7)
		11-27	1785.84 $_{mi}$	1785.81 $_{mi}$			
		11-30	2129.06 $_{mi}$	2128.96 $_{mi}$			
		31-321	32615.10 $_{av}$	32613.80$_{av}$			
		1-321	35880.86 $_{av}$	35879.46 $_{av}$	35879.9$_{av}$	35879.95$_{av}$	
	30	**1-9**	1041.62 $_{mi}$	1041.59 $_{mi}$			K9 (K6)
		1-10	1169.72 $_{mi}$	1169.70 $_{mi}$			K10 (K7)
		10-321	34856.56$_{av}$	34858.76 $_{av}$			K9 (K6)
		11-321	34727.40$_{av}$	34726.72 $_{av}$			K10 (K7)
		11-27	1785.84 $_{mi}$	1785.82 $_{mi}$			
		11-30	2129.06 $_{mi}$	2128.03 $_{mi}$			
		31-321	32615.10$_{av}$	32613.75 $_{av}$			
		1-321	35880.86$_{av}$	35879.92 $_{av}$	35879.50 $_{av}$	35880.02 $_{av}$	
	60	**1-9**	1041.62 $_{mi}$	1041.57 $_{mi}$	1041.58 $_{mi}$	1041.60 $_{mi}$	K9 (K6)
		1-10	1169.72 $_{mi}$	1169.65 $_{mi}$			K10 (K7)

		10-321	34856.56 $_{av}$	34858.83 $_{av}$	34857.66 $_{av}$	34858.23 $_{av}$	K9 (K6)
		11-321	34727.40$_{av}$	34726.51 $_{av}$			K10 (K7)
		11-27	1785.84$_{mi}$	1785.79 $_{mi}$	1785.80 $_{mi}$	1785.80 $_{mi}$	
		11-30	2129.06$_{mi}$	2128.95 $_{mi}$		2129.10 $_{mi}$	
		31-321	32615.1$_{av}$	32613.28 $_{av}$	32614.13 $_{av}$	32614.58 $_{av}$	
		1-321	35880.86$_{av}$		35879.70 $_{av}$	35879.30 $_{av}$	
Endoprotease AspN/APE1 1:500 (w/w)	**5**	**1-17**	1768.97 $_{mi}$	1768.95 $_{mi}$			D18 (D15)
		18-321	34128.79 $_{av}$	34127.5 $_{av}$			D18 (D15)
		1-321	35880.96 $_{av}$	35878.6 $_{av}$	35879.10 $_{av}$	35877.50 $_{av}$	
	15	**1-17**	1768.97 $_{mi}$				D18 (D15)
		18-321	34128.79 $_{av}$	34127.4 $_{av}$			D18 (D15)
		1-321	35880.96 $_{av}$	35878.9 $_{av}$	35878.40 $_{av}$	35879.20 $_{av}$	
	30	**1-17**	1768.97 $_{mi}$	1768.96 $_{mi}$			D18 (D15)
		18-321	34128.79 $_{av}$	34126.9 $_{av}$			D18 (D15)
		1-321	35880.96 $_{av}$	35878.6 $_{av}$	35878.90 $_{av}$	35878.10 $_{av}$	

	60	**1-17**	1768.97 $_{mi}$	1798.94 $_{mi}$		1798.95 $_{mi}$	D18 (D15)
		18-321	34128.79 $_{av}$	34127.9 $_{av}$		34126.20 $_{av}$	D18 (D15)
		1-321	35880.96 $_{av}$	35879.02 $_{av}$	35875.60 $_{av}$	35877.70 $_{av}$	
Chimotrypsin/APE1 1:1000 (w/w)	**5**	**1-114**	12501.23 $_{av}$	12501.02 $_{av}$	12500.28 $_{av}$		L114 (L111)
		115-321	23397.64 $_{av}$	23396.86 $_{av}$	23395.16 $_{av}$		L114 (L111)
		1-321	35880.86 $_{av}$	35878.9 $_{av}$	35878.10 $_{av}$	35878.40 $_{av}$	
	15	**1-114**	12501.23 $_{av}$	12501.02 $_{av}$	12500.67 $_{av}$	12500.50 $_{av}$	L114 (L111)
		8-114	11662.74 $_{av}$	11662.28 $_{av}$			
		115-198	9535.62 $_{av}$	9535.21 $_{av}$			
		115-321	23397.64 $_{av}$	23396.86 $_{av}$	23395.43 $_{av}$	23396.90 $_{av}$	L114 (L111)
		1-321	35880.86 $_{av}$	35879.50 $_{av}$	35878.67 $_{av}$	35879.30 $_{av}$	
	30	**1-114**	12501.23 $_{av}$	12500.86 $_{av}$	12500.80 $_{av}$	12501.00 $_{av}$	L114 (L111)

		8-114	11662.74 av	11662.11 av			
		115-198	9535.62 av	9534.35 av			
		115-321	23397.64 av	23395.91 av	23395.60 av	23396.73 av	L114 (L111)
		1-321	35880.86 av	35878.5 av	35878.40 av	35879.72 av	
		1-114	12501.23 av	12500.20 av	12500.10 av	12500.50 av	L114 (L111)
		8-114	11662.74 av	11661.99 av			
		21-114	10391.8 av	10391.27 av			
	60	**115-198**	9535.62 av	9535.12 av			
		115-321	23397.64 av	23395.8 av	23395.80 av	23396.80 av	L114 (L111)
		1-321	35880.86 av	35878.70 av	35878.60 av	35879.15 av	
1 **1:10**	**5**	**1-12**	1297.78 mi	1297.76 mi			A12 (A9)

		1-14	1467.88 mi	1467.85 mi			A14 (A11)
		13-321	34600.25 av	34597.6 av			A12 (A9)
		15-321	34430.43 av	34428.2 av			A14 (A11)
		1-321	35880.86 av	35877.5 av	35877.10 av	35876.90 av	
	15	**1-12**	1297.78 mi	1297.75 mi			A12 (A9)
		1-14	1467.88 mi	1467.87 mi			A14 (A11)
		1-20	2126.13 mi	2126.10 mi			L20 (L17)
		13-321	34600.25 av	34598.3 av			A12 (A9)
		15-321	34430.43 av	34429.0 av			A14 (A11)
		21-321	33771.43 av	33768.5 av			L20 (L17)
		1-321	35880.86 av	35878.6 av	35878.30 av	35879.10 av	
	30	**1-12**	1297.78 mi	1297.77 mi			A12 (A9)
		1-14	1467.88 mi	1467.86 mi			A14 (A11)
		1-20	2126.13 mi	2126.11 mi	2126.20 mi	2126.14 mi	L20 (L17)
		13-321	34600.25 av	34596.8 av			A12 (A9)

		15-321	34430.43 $_{av}$	34427.4 $_{av}$			A14 (A11)
		21-321	33771.43 $_{av}$	33767.9 $_{av}$	33769.20 $_{av}$	33768.50 $_{av}$	L20 (L17)
		1-321	35880.86 $_{av}$	35876.9 $_{av}$	35878.50 $_{av}$	35877.60 $_{av}$	
		1-12	1297.78 $_{mi}$	1297.80 $_{mi}$			A12 (A9)
		1-14	1467.88 $_{mi}$	1467.87 $_{mi}$			A14 (A11)
		1-20	2126.13 $_{mi}$	2126.12 $_{mi}$	2125.99 $_{mi}$	2126.10 $_{mi}$	L20 (L17)
	60	**13-321**	34600.25 $_{av}$	34599.1 $_{av}$			A12 (A9)
		15-321	34430.43 $_{av}$	34429.5 $_{av}$			A14 (A11)
		21-321	33771.43 $_{av}$	33770 $_{av}$	33768.90 $_{av}$	33770.80 $_{av}$	L20 (L17)
		1-321	35880.86 $_{av}$		35877.80 $_{av}$	35880.20 $_{av}$	

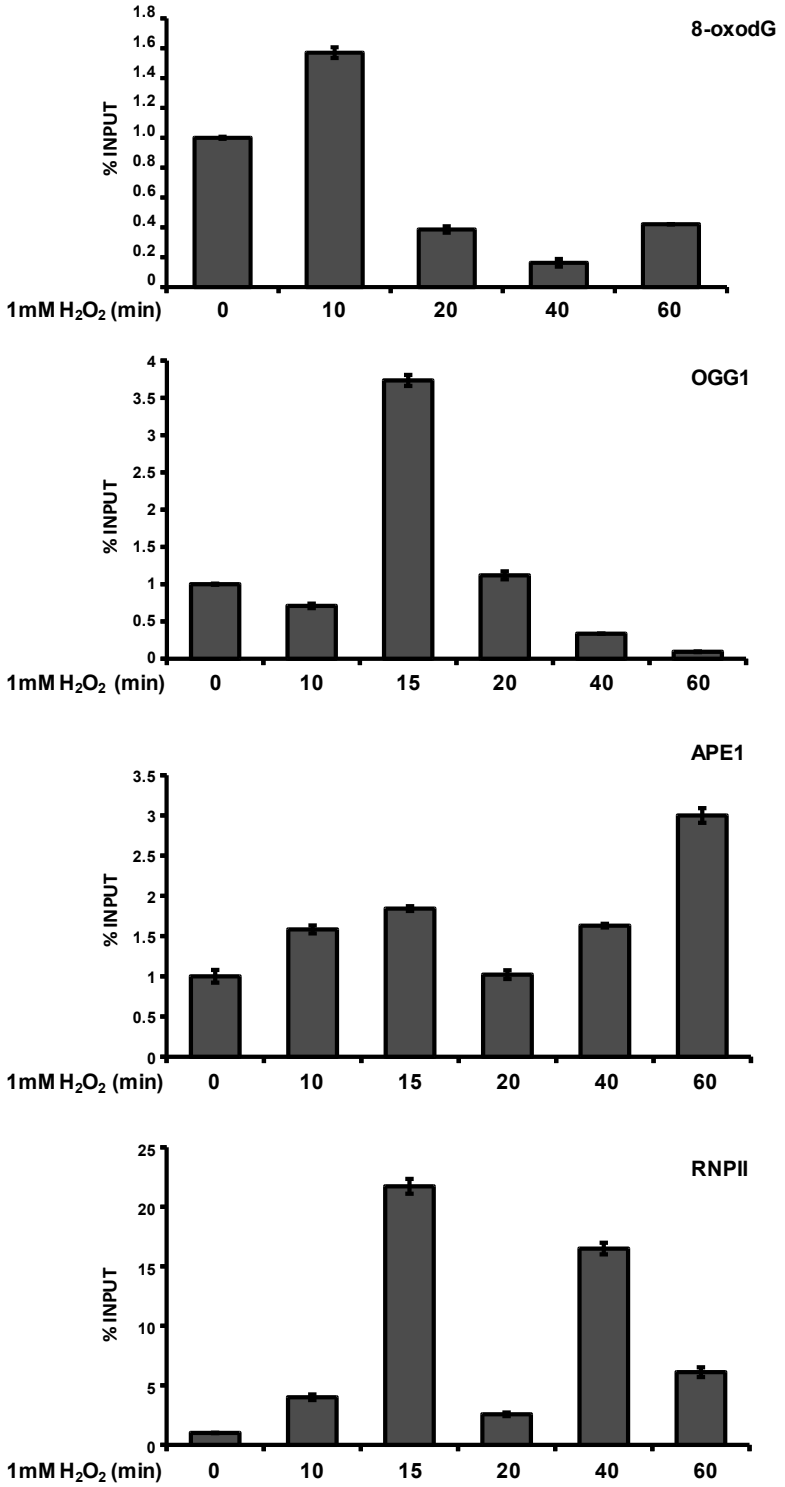

Supplementary Figure 33 - Recruitment of BER enzymes on hSIRT1 promoter after oxidative condition.
HeLa cells treated with 1 mM H_2O_2 for 10, 15, 20, 40, 60 minutes, were analyzed by qChIP using specific antibodies recognizing 8-oxodG, OGG1 and APE1. The histogram represents the amount of hSIRT1 promoter sequence immunoprecipitated. Data were presented as percent of input and normalized to the quantity of DNA immunoprecipitated by α-tubulin (α-tub) and further normalized on the amount of immunoprecipitated protein.

10 Abbreviations

8-oxoG, 8-oxoguanine

AcAPE1, acetylated apurinic/apyrimidinic endonuclease-1

ANP Atrial natriuretic peptide

AP, abasic site

AP-1, activating protein-1

APE1, apurinic/apyrimidinic endonuclease-1

$APE1^{WT}$, wild type APE1

$APE1^{N\Delta 33}$, N-terminal APE1 deletion mutant

hAPE1, human APE1

zAPE1, zebrafish APE1

BER, base excision repair

Bax, Bcl-2–associated X

CAT, chloramphenicol acetyltransferase

ChIP, chromatin immunoprecipitation

CREB, cAMP-responsible element binding protein

DR, direct repair

Ds, double stranded

E3330, 2E-3-[5-(2, 3 dimethoxy-6- methyl-1, 4-benzoquinolyl)]-2-nonyl-2- propenoic acid

Egr-1, early growth response protein-1

EMSA, electromobility shift assay

GEC, gastric epithelial cell

GO, gene ontology

HAT, histone acetyltransferase

HDAC, histone deacetylase

hnRNP-L, Heterogeneous nuclear ribonucleoprotein L

HR, homologous recombination

KuAg, Ku antigen

LC-ESI-MS, liquid chromatography-electrospray ionization-mass spectrometry

LP-BER, long-patch base excision repair

MDM2, murine double minute 2

MMR, mismatch repair

MMS, Methylmethanesulfonate

nCaRE, Negative calcium responsive element

NER, nucleotide-excision repair

NF-κB, nuclear factor-kappaB

NHEJ, nonhomologous end joining

PARP-1, Poly (adenosine diphosphate-ribose) polymerase 1

PCNA, proliferating cell nuclear antigen

PTM, post-translational modification

PTH, parathyroid hormone

Rac1, ras-related C3 botulinum toxin substrate 1

RAS, Renin-angiotensin system

RNA pol II/III, RNA polymerase

ROS, reactive oxygen species

SINE, short interspersed nucleotide elements

SIRT1, sirtuin 1

SP-BER, short-patch base excision repair

SPR, surface Plasmon resonance

SSB, single strand break

TF, transcription factor

THF, tetrahydrofuran

Trx, thioredoxin

XRCC1, X-ray cross-species complementing 1

11 List of papers published during the PhD course (2010-2012)

Lirussi L., Antoniali G., Vascotto C., D'Ambrosio C., Poletto M., Romanello M., Marasco D., Leone M., Quadrifoglio F., Bhakat K.K., Scaloni A., Tell G. “Nucleolar accumulation of APE1 depends on charged lysine residues that undergo acetylation upon genotoxic stress and modulate its BER activity in cells”. Mol Biol Cell. 2012 Oct; 23(20):4079-96

The work described in this thesis is included in:

Antoniali G., D’Ambrosio C., Lirussi L., Dal Piaz F., Vascotto C., Marasco D., Scaloni A., Fogolari F., Tell G. “SIRT1 gene expression upon genotoxic damage is regulated by APE1 through nCaRE-promoter elements”
Submitted

During my PhD I have been involved in additional projects that are not presented in this thesis but are part of the following manuscript:

Romanello M., Piatkowska E., Antoniali G., Cesaratto L., Vascotto C., Iozzo R., Delneri D., Brancia F. “Osteoblastic cell secretome: a novel role for progranulin during risedronate treatment”
Manuscript in preparation

Codarin E., Antoniali G., Cesaratto L., Vascotto C., Arena S., Bortolussi G., Calligaris R., Gustincich S., Tiribelli C., Scaloni A., Muro A., Tell G. “Proteomic analysis and Transcript Profiling of Ugt1 Mutant Mouse Cerebellum identify new targets of Bilirubin cytotoxicity”
Manuscript in preparation

Nucleolar accumulation of APE1 depends on charged lysine residues that undergo acetylation upon genotoxic stress and modulate its BER activity in cells

Lisa Lirussi[a,*], Giulia Antoniali[a,*], Carlo Vascotto[a], Chiara D'Ambrosio[b], Mattia Poletto[a], Milena Romanello[a], Daniela Marasco[c,d], Marilisa Leone[d], Franco Quadrifoglio[a], Kishor K. Bhakat[e], Andrea Scaloni[b], and Gianluca Tell[a]

[a]Department of Medical and Biological Sciences, University of Udine, 33100 Udine, Italy; [b]Proteomics and Mass Spectrometry Laboratory, Istituto di Ricerche per il Sistema Produzione Animale in Ambiente Mediterraneo, National Research Council, 80147 Naples, Italy; [c]Department of Biological Sciences, University of Naples "Federico II," 80134 Naples, Italy; [d]Institute of Biostructures and Bioimaging, National Research Council, 80134 Naples, Italy; [e]Department of Biochemistry and Molecular Biology, University of Texas Medical Branch, Galveston, TX 77555

ABSTRACT **Apurinic/apyrimidinic endonuclease 1 (APE1) is the main abasic endonuclease in the base excision repair (BER) pathway of DNA lesions caused by oxidation/alkylation in mammalian cells; within nucleoli it interacts with nucleophosmin and rRNA through N-terminal Lys residues, some of which ($K^{27}/K^{31}/K^{32}/K^{35}$) may undergo acetylation in vivo. Here we study the functional role of these modifications during genotoxic damage and their in vivo relevance. We demonstrate that cells expressing a specific K-to-A multiple mutant are APE1 nucleolar deficient and are more resistant to genotoxic treatment than those expressing the wild type, although they show impaired proliferation. Of interest, we find that genotoxic treatment induces acetylation at these K residues. We also find that the charged status of $K^{27}/K^{31}/K^{32}/K^{35}$ modulates acetylation at K^{6}/K^{7} residues that are known to be involved in the coordination of BER activity through a mechanism regulated by the sirtuin 1 deacetylase. Of note, structural studies show that acetylation at $K^{27}/K^{31}/K^{32}/K^{35}$ may account for local conformational changes on APE1 protein structure. These results highlight the emerging role of acetylation of critical Lys residues in regulating APE1 functions. They also suggest the existence of cross-talk between different Lys residues of APE1 occurring upon genotoxic damage, which may modulate APE1 subnuclear distribution and enzymatic activity in vivo.**

Monitoring Editor
Karsten Weis
University of California, Berkeley

Received: Apr 17, 2012
Revised: Jul 25, 2012
Accepted: Aug 16, 2012

This article was published online ahead of print in MBoC in Press (http://www.molbiolcell.org/cgi/doi/10.1091/mbc.E12-04-0299) on August 23, 2012.

*These authors contributed equally to this work

The authors declare that they have no conflict of interests.

Address correspondence to: Gianluca Tell (gianluca.tell@uniud.it).

Abbreviations used: APE1/Ref-1, apurinic/apyrimidinic endonuclease/redox effector factor 1; BER, base excision repair; MMS, methyl methanesulfonate; MTS, 3-(4-5-dimethylthiazol-2-yl)-5-(3-carboxymethoxyphenyl)-2-(4-sulfophenyl)-2H-tetrazolium salt; NPM1, nucleophosmin 1; SIRT1, sirtuin 1; TBHP, *tert*-butyl hydroperoxide.

INTRODUCTION

Apurinic/apyrimidinic endonuclease 1/redox effector factor-1 (APE1) plays a central role in the maintenance of genome stability and redox signaling (Bapat *et al.*, 2009, 2010; Tell *et al.*, 2010a; Wilson and Simeonov, 2010). Through its C-terminal domain (residues 61–318), it acts as an essential enzyme in the base excision repair (BER) pathway of DNA damages caused by both endogenous and exogenous oxidizing/alkylating agents, including many chemotherapeutic drugs. In combination with thioredoxin (Ueno *et al.*, 1999; Seemann and Hainaut, 2005) and through its N-terminal domain (residues 1–127), it also functions as a regulatory redox agent to maintain cancer-related transcription factors (Egr-1, NF-κB, p53, HIF-1α, AP-1, and Pax proteins) in an active reduced state (Hirota *et al.*, 1997;

Wei *et al.*, 2000; Ziel *et al.*, 2004; Gray *et al.*, 2005; Pines *et al.*, 2005; Tell *et al.*, 2005, 2010a). APE1 can also act as a transcriptional repressor through indirect binding to negative Ca^{2+}-response elements (nCaRE), which are regulated by K^6/K^7 acetylation (Bhakat *et al.*, 2003). Recently APE1 was demonstrated to bind/cleave abasic RNA (Vascotto *et al.*, 2009b; Fantini *et al.*, 2010; Tell *et al.*, 2010b) and to control *c-Myc* expression by cleaving its mRNA (Barnes *et al.*, 2009). These discoveries pointed to a new function of APE1 in regulating gene expression through posttranscriptional mechanisms and brought to light the fact that this protein is a possible target for anticancer therapy.

In this context, we showed that the first 35 amino acids in the nonstructured N-terminal domain of APE1 are required for a stable interaction with rRNA, nucleophosmin 1 (NPM1), and other proteins involved in ribosome biogenesis/RNA processing (Vascotto *et al.*, 2009b; Tell *et al.*, 2010b). In particular, K residues within the protein region spanning amino acids 24–35 are involved in the interaction of APE1 with both rRNA and NPM1 and also regulate its in vitro enzymatic activity (Fantini *et al.*, 2010). Of interest, some of these critical K residues, namely $K^{27}/K^{31}/K^{32}/K^{35}$, undergo in vivo acetylation. These results suggest that protein–protein interactions and/or posttranslational modifications (PTMs) involving the APE1 N-terminal domain may play important roles in vivo in coordinating and fine-tuning the protein's BER activity and functions on rRNA metabolism. Recently it was also demonstrated that APE1 K^6/K^7 may undergo acetylation during cell response to genotoxic treatment (Fantini *et al.*, 2008) and that the acetylation status of these K residues, controlled by the sirtuin 1 (SIRT1) deacetylase activity, should be important in modulating protein DNA-repair function by regulating the kinetics of its interaction with other enzymes involved in BER, for example, XRCC1 (Yamamori *et al.*, 2010).

APE1 is mainly a nuclear protein and is critical for controlling cellular proliferative rates (Fung and Demple, 2005; Izumi *et al.*, 2005; Vascotto *et al.*, 2009b). We also showed that a considerable amount of APE1 is accumulated within the nucleoli of different cell lines (Vascotto *et al.*, 2009b; Fantini *et al.*, 2010), but its role within this compartment is unknown. Cytoplasmic, mitochondrial, and endoplasmic reticulum localizations have also been ascertained (Tell *et al.*, 2001; Szczesny and Mitra, 2005; Chattopadhyay *et al.*, 2006; Grillo *et al.*, 2006; Mitra *et al.*, 2007). APE1 is an abundant and relatively stable protein in mammalian cells (Tell *et al.*, 2009, 2010a). Fine-tuning of the multiple APE1 functions may therefore depend on the modulation of its PTMs and, eventually, on its interactome. Although a functional role has been determined for some PTMs (K^6/K^7 acetylation and $K^{24}/K^{25}/K^{27}$ ubiquitination; Bhakat *et al.*, 2003; Fantini *et al.*, 2008; Busso *et al.*, 2009), the identity and importance of various interacting partners in modulating APE1 biological functions are still under investigation (Parlanti *et al.*, 2007; Busso *et al.*, 2009; Vascotto *et al.*, 2009b). APE1 may affect cell growth by directly acting on rRNA quality control mechanisms; in particular, APE1 interaction with NPM1 may affect its activity over rRNA molecules. However, many aspects of this new function are undefined (Vascotto *et al.*, 2009b; Tell *et al.*, 2010b).

In this study, we address the biological role of APE1 acetylation at $K^{27}/K^{31}/K^{32}/K^{35}$ and, in light of recent evidence showing the emerging function of the nucleolus as a central sensor of protein trafficking during DNA repair after genotoxic treatment (Nalabothula *et al.*, 2010), the role of the nucleolus itself on the APE1 protective function toward genotoxic damage. We used a reconstitution strategy with APE1 mutants in which the charged Lys residues were replaced by either Ala or Arg to mimic constitutive acetylated ($APE1^{K4pleA}$) and nonacetylatable ($APE1^{K4pleR}$) protein forms, respectively. These mutants are reintroduced into APE1-silenced cell clones to determine the role of these crucial amino acids during cell response to genotoxic treatment.

RESULTS

Positively charged $K^{27}/K^{31}/K^{32}/K^{35}$ residues are essential for APE1 nucleolar accumulation through stabilization of protein interaction with NPM1 and rRNA

We previously demonstrated that charged K residues, located within the unstructured APE1 N-terminal domain (i.e., $K^{24}/K^{25}/K^{27}/K^{31}/K^{32}$), are crucial for APE1 interaction with rRNA and NPM1 and for modulating its catalytic activity on abasic DNA through regulation of product binding. Of interest, some of these critical amino acids (i.e., $K^{27}/K^{31}/K^{32}$ in addition to K^{35}) may undergo in vivo acetylation under basal conditions (Fantini *et al.*, 2010). We hypothesized that the degree of positive charges, modified by acetylation at these residues, may modulate APE1's different functions through its redirection to different substrates and/or stimulation of its DNA-repair enzymatic activity (Fantini *et al.*, 2010). To address this issue, we inspected the role of the positively charged residues within the region 27–35 in modulating the interaction between APE1 and NPM1. Colocalization experiments in HeLa cells transiently transfected with either FLAG-tagged, wild-type APE1 ($APE1^{WT}$), a K-to-A mutant ($APE1^{K4pleA}$) in which the positive charges have been removed as in the case of constitutive acetylation, or a nonacetylatable K-to-R APE1 mutant ($APE1^{K4pleR}$) showed that $APE1^{K4pleA}$ mutant has a marked exclusion from the nucleoli apparent in all expressing cells (Figure 1A). Silencing of the endogenous APE1 protein did not alter either the ability of the $APE1^{WT}$ and $APE1^{K4pleR}$ proteins to accumulate within the nucleolar compartment or the inability of the $APE1^{K4pleA}$ to accumulate within the nucleolus (unpublished data). These data thus demonstrate that $APE1^{WT}$ and $APE1^{K4pleR}$ nucleolar accumulation is not the consequence of their overexpression.

To complement these observations and also to exclude a possible contribution of the FLAG tag used to generate recombinant ectopic proteins, we exploited a live-cell imaging system as suggested by Schnell *et al.* (2012). APE1 cDNA was cloned into a pDendra2 vector to express APE1 in fusion with the green photoconvertible fluorophore Dendra (Chudakov *et al.*, 2007). As reported in Figure 1B, the fluorophore alone is present in both the cytoplasm and the nuclear compartment, but it is completely excluded from the nucleoli, as demonstrated by quantitative fluorescence signal analyses. In contrast, whereas the expression of Dendra in fusion with $APE1^{WT}$ and $APE1^{K4pleR}$ results in an efficient accumulation of the protein within the nucleolar compartment, the Dendra-$APE1^{K4pleA}$ mutant displays a homogeneous nuclear distribution. This approach confirms immunofluorescence-based data on the reduced accumulation of FLAG-tagged $APE1^{K4pleA}$ within the nucleoli and supports the evidence that the nucleolar accumulation of APE1 protein does not depend on the protein abundance nor does it depend on the specific tag used to generate the ectopic recombinant proteins (see also Supplemental Figure S1).

We supported our immunofluorescence data with biochemical interaction experiments. Coimmunoprecipitation analysis showed that the $APE1^{K4pleA}$ mutant has a significantly reduced interaction with NPM1 (Figure 2A), in accordance with its impaired nucleolar accumulation. The altered electrophoretic mobility observed for the $APE1^{K4pleA}$ mutant (Figure 2A) was further confirmed by SDS–PAGE analysis of recombinant proteins expressed in *Escherichia coli* and purified by chromatography. The effect is likely due to alteration of its overall charge, since electrospray ionization mass spectrometry analysis confirmed the correctness of protein mass values, and the

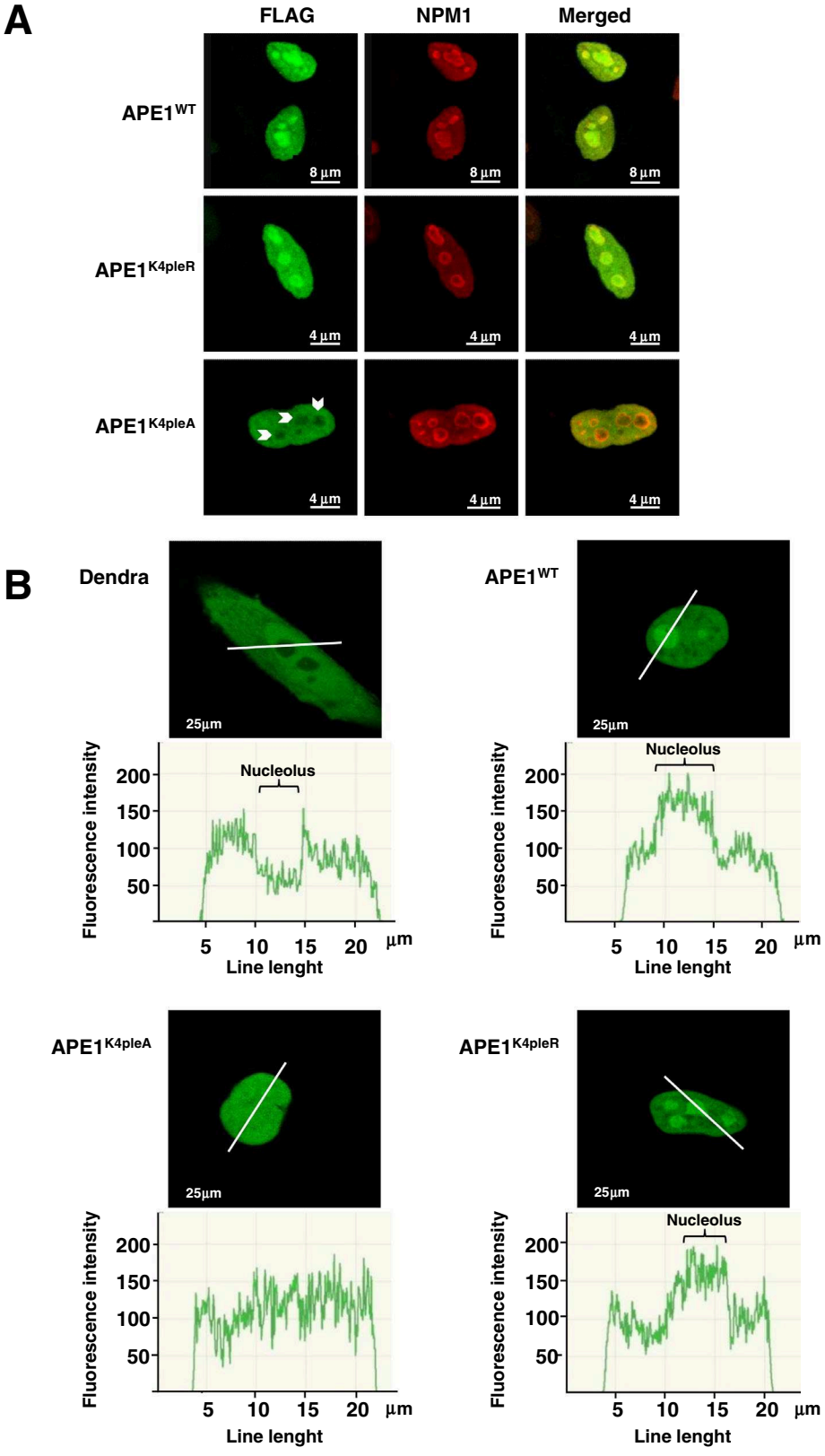

FIGURE 1: Positively charged $K^{27}/K^{31}/K^{32}/K^{35}$ residues are required for APE1 nucleolar accumulation. (A) Confocal microscopy of HeLa cells transfected with $APE1^{WT}$, $APE1^{K4pleA}$, or $APE1^{K4pleR}$ FLAG-tagged proteins and stained with antibodies against NPM1 (red) and ectopic FLAG-APE1 (green). Overlap of staining (yellow) demonstrated colocalization of the two proteins. Of note, the $APE1^{K4pleA}$ mutant was completely excluded from nucleoli (white arrowheads), whereas both $APE1^{WT}$ and the $APE1^{K4pleR}$ were accumulated within. Images are representative of 100% of transfected cells. (B) HeLa cells transfected with pDendra2-N empty vector or encoding APE1 (wild-type and mutants) in fusion with Dendra fluorophore were analyzed with a live confocal microscopy workstation. Cells transfected with empty vector (Dendra) showed diffuse green fluorescence within cytoplasm and nucleus, with exclusion of the nucleolar compartment. $APE1^{WT}$ and $APE1^{K4pleR}$ mutant mainly localized within the nuclear compartment and accumulated within nucleoli. In contrast, $APE1^{K4pleA}$ did not show any nucleolar accumulation. Images were captured by using the same settings (488-nm laser at 10% of intensity and PMT at 760 V). Fluorescence intensity analysis was carried out on a 25-µm-long line (white). Graphs represent the fluorescence intensity measured through a cross section of the nucleus and demonstrate an incremental fluorescence in corresponding nucleoli only in the case of $APE1^{WT}$ and $APE1^{K4pleR}$-Dendra fusion protein–expressing cells.

difference in their apparent mobility observed in SDS–PAGE was abolished when separating various mutants in urea-containing denaturing gels (Supplemental Figure S2 and unpublished data). It was also observed for other K-to-A mutants of APE1 (Fantini *et al.*, 2010). We then evaluated the contribution of the single K residues to the extent of APE1 nucleolar localization (Supplemental Figure S3) and the ability to interact with NPM1 (Figure 2B). Double mutants $APE1^{K27/35A}$, $APE1^{K31/32A}$, $APE1^{K27/35R}$, and $APE1^{K31/32R}$ and a deletion mutant lacking 33 amino acids at the protein N-terminus ($APE1^{N\Delta33}$) were compared with $APE1^{WT}$. Whereas $APE1^{WT}$, $APE1^{K27/35R}$, and $APE1^{K31/32R}$ displayed a nucleolar and nucleoplasmic staining, $APE1^{K27/35A}$ and $APE1^{K31/32A}$ showed two alternative stainings, exhibiting nucleolar/nucleoplasmic or only nucleoplasmic positivity, respectively (Supplemental Figure S3). Coimmunoprecipitation experiments (Figure 2B) were in accordance with immunofluorescence analyses and showed a substantial reduction of the interaction in the case of $APE1^{K4pleA}$ and $APE1^{N\Delta33}$ mutants and a moderate impairment for $APE1^{K27/35A}$ and $APE1^{K31/32A}$ mutants. Glutathione *S*-transferase (GST) pull-down assays with recombinant purified proteins confirmed that these results were due to effects on direct interaction between APE1 and NPM1 (Figure 2C). This confirmed previous hypotheses (Fantini *et al.*, 2010). We also checked the effect of the K-to-A mutation on the ability of APE1 to bind nucleolar rRNA (Vascotto *et al.*, 2009b). As expected, rRNA–chromatin immunoprecipitation (ChIP) analyses showed that K-to-A mutations significantly alter APE1 binding to

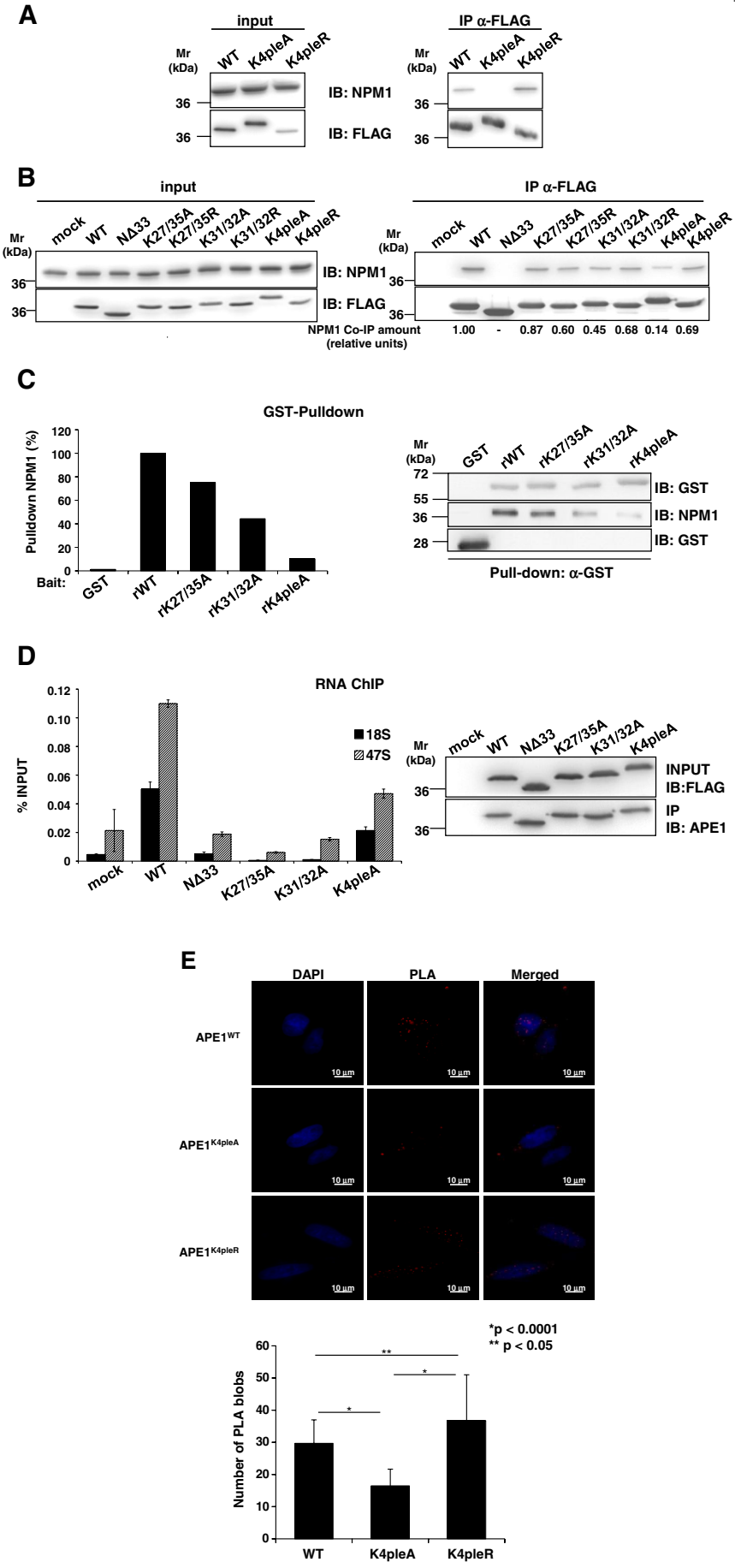

FIGURE 2: Positively charged $K^{27}/K^{31}/K^{32}/K^{35}$ residues are required for NPM1 interaction. (A) The $APE1^{K4pleA}$ mutant shows impaired interaction with NPM1. Coimmunoprecipitation (CoIP) analysis on HeLa cells transfected with $APE1^{WT}$, $APE1^{K4pleA}$, or $APE1^{K4pleR}$ FLAG-tagged proteins with endogenous NPM1. Western blot analysis was used to quantify the interaction among the different APE1 forms and NPM1 by using specific antibodies. IB, immunoblot. (B) $K^{27}/K^{31}/K^{32}/K^{35}$ residues are responsible for proper interaction of APE1 with NPM1. CoIP analysis on HeLa cells transfected with FLAG-tagged $APE1^{WT}$, $APE1^{N\Delta33}$, or the APE1 double ($APE1^{K27/35A}$, $APE1^{K31/32A}$, $APE1^{K27/35R}$, and $APE1^{K31/32R}$) or quadruple ($APE1^{K4pleA}$ and $APE1^{K4pleR}$) K-to-A or K-to-R mutants. Western blot analysis was performed on total cell extracts (left) and on immunoprecipitated material (right) with specific antibody for endogenous NPM1. Normalized coimmunoprecipitated amounts of NPM1 are indicated under each relative bar. Anti-FLAG staining was used as loading control. (C) Interaction of K-to-A APE1 mutants with NPM1 and rRNA. A 150-pmol amount of each bait GST-APE1 recombinant purified protein (rAPE1) was incubated with an equimolar amount of recombinant NPM1, as described in *Materials and Methods*. After GST pull-down, samples underwent Western blot analysis by using the indicated antibodies (right). NPM1 band intensities were normalized vs. those of GST-APE1 proteins, and the resulting values, expressed as percentage of bound with respect to $APE1^{WT}$, were plotted in the histogram (left). Each bar represents the mean of two independent experiments whose variation was <10%. (D) Interaction of K-to-A APE1 mutants with NPM1 and rRNA. After transfection of HeLa cells, total cell lysates were prepared as described in *Materials and Methods*, and an RNA-ChIP assay was performed to measure the rRNA-binding activity of the different APE1 mutants. Immunoprecipitated samples underwent either Western blot analysis (right) or RNA extraction and quantification by reverse transcription and quantitative PCR analysis, using 18S and 47S rRNA–specific primers. Data are presented as a fold percentage of the amount of total 18S or 47S rRNA with respect to the amount of immunoprecipitated FLAG-tagged APE1 protein, respectively. The resulting values are plotted in the histograms (left), showing the average values with SD of three independent experiments. (E) Nucleoplasmic interaction between APE1 and NPM1 is affected by K-to-A mutation on APE1. PLA technology was used to evaluate in vivo the effect of positively charged $K^{27}/K^{31}/K^{32}/K^{35}$ residues on APE1 interaction with NPM1 in the nuclear compartment. Stable HeLa clones expressing $APE1^{WT}$, $APE1^{K4pleA}$, or $APE1^{K4pleR}$ FLAG-tagged proteins were seeded on a glass coverslip, and PLA reaction was carried out using anti-FLAG and anti-NPM1 antibodies. 4′,6-Diamidino-2-phenylindole staining is used as a reference for the nuclei. The histogram represents the average number of PLA blobs scored for at least 30 cells per slide. Asterisks represent a significant difference between $APE1^{WT}$ and mutants.

rRNA molecules (Figure 2D) and that a partial removal of positive charges in the region 27–35 strongly affects the protein binding to rRNA molecules.

Interaction between APE1 and NPM1 may also occur in the nucleoplasmic compartment of cells. We measured the effect of the K-to-A mutation on the nucleoplasmic interaction of APE1 with NPM1 through proximity ligation assay (PLA) analysis, which allows in situ detection of two proteins that are at interacting distance of <40 nm (Weibrecht *et al.*, 2010). Data displayed in Figure 2E show that nucleoplasmic interaction between APE1 and NPM1 was significantly affected by the K-to-A mutation. Taken together, these data demonstrate that charged lysines within the 27–35 region are essential for APE1 maintenance within the nucleoli and for a proper/stable interaction of this protein with NPM1 or rRNA molecules. Moreover, our data suggest that APE1 must lose the positive charge at more than two K residues (among $K^{27}/K^{31}/K^{32}/K^{35}$) to get a significant reduction of the APE1/NPM1 interaction in the nucleus and loss of APE1 nucleolar accumulation.

Loss of APE1 nucleolar accumulation causes impairment of cell proliferation

APE1 protects cells against genotoxic damaging agents (Tell and Wilson, 2010). To clarify the biological relevance of the APE1 nucleolar accumulation, we estimated the effect of the expression of the nucleolar-deficient form of APE1 (i.e., $APE1^{K4pleA}$) on cell viability with respect to $APE1^{WT}$ and $APE1^{K4pleR}$ mutant. To test the effects of the mutant proteins and exclude the contribution of the endogenous one, we used inducible APE1-silenced (through small interfering RNA [siRNA] technology) HeLa cells, which were reconstituted with siRNA-resistant APE1 ectopic proteins in place of the endogenous one (Figure 3A; Vascotto *et al.*, 2009a). The levels of the ectopic proteins expressed by the different cell clones used for the following experiments were comparable to that of the wild-type endogenous one before silencing, as demonstrated by quantitative Western blot analysis (Supplemental Figure S4); the extent of the residual endogenous protein was <10%. Quantification of the nuclear amount of ectopic proteins after doxycycline treatment, demonstrated by Western blot analysis with a calibration curve, gave the following results (expressed as nanograms of APE1 per microgram of nuclear extract): 23.22 ± 6.04 for $APE1^{WT}$, 18.63 ± 4.84 for $APE1^{K4pleA}$, and 17.69 ±4.60 for $APE1^{K4pleR}$ (Supplemental Figure S4B). Therefore these cell lines represent a reliable system for testing our hypothesis. On the basis of previous data showing that nucleolar APE1 may act as a cleansing factor in rRNA quality control, possibly affecting cellular proliferation through an impairment of the overall protein synthesis machinery (Vascotto *et al.*, 2009b; Tell *et al.*, 2010b), we investigated the effect of the nucleolar-deficient form $APE1^{K4pleA}$ on cell proliferation rate under basal conditions. Of interest, by cell counting assays performed on reconstituted cell clones, we obtained proof that $APE1^{K4pleA}$ acts as a loss-of-function mutation in terms of cell proliferation, whereas $APE1^{K4pleR}$ behaves similarly to $APE1^{WT}$ (Figure 3B). These data, confirmed by using at least two different clones for each mutant cell line, suggest that nucleolar APE1 is required for appropriate control of cell proliferation, perhaps through its role in rRNA metabolism (Tell *et al.*, 2010b). Colony formation assays confirmed cell proliferation data (Figure 3C). However, although the cell number in each colony of $APE1^{K4pleR}$-expressing cells was always similar to that expressing $APE1^{WT}$, these cells grew in a more widespread manner, possibly due to an altered migrating phenotype and/or an intercellular adhesion pattern. These data were indicative that abolition of the acetylatable residues of APE1 at $K^{27}/K^{31}/K^{32}/K^{35}$ may significantly affect cell biology, even though it is also possible that the lower expression level of the $APE1^{K4pleR}$ (~76%) with respect to $APE1^{WT}$ may also have an effect on this phenotype.

Increased APE1 acetylation at $K^{27}/K^{31}/K^{32}/K^{35}$ residues upon genotoxic damage

APE1 acetylation at K^6/K^7 is known to be enhanced after genotoxic insult by methyl methanesulfonate (MMS) and it has been shown to play a role in modulating APE1 interaction with XRCC1, possibly coordinating different enzymatic steps in the BER pathway (Yamamori *et al.*, 2010). We therefore tested whether MMS treatment, which promotes generation of DNA damage specifically repaired through BER, may also induce APE1 acetylation at $K^{27}/K^{31}/K^{32}/K^{35}$ residues. Immunopurified APE1 samples from control and MMS-treated cells were separated by SDS–PAGE and excised bands and then analyzed by peptide mapping experiments. Semiquantitative nano–electrospray linear ion trap tandem mass spectrometry (nanoLC-ESI-LIT-MS/MS) analysis was performed on identical quantities of immunopurified $APE1^{WT}$-FLAG protein samples obtained from HeLa cells before and after MMS treatment (Supplemental Figure S5). In particular, we evaluated the amount of the peptides (15–33)Ac_3 and (15–35)Ac_4 in each APE1 endoprotease AspN digest and compared them to that of the nonmodified counterparts. Analysis was performed by extracting and integrating the corresponding nanoLC-ESI-LIT-MS peak areas equivalent to the assigned *m/z* values for the acetylated and nonacetylated peptides in the same total ion chromatogram. After MMS treatment, the amount of the peptide (15–33)Ac_3 was significantly increased, and the peptide (15–35)Ac_4 was almost doubled as compared with that of the nonmodified counterparts (Figure 4A). The MMS-induced acetylation on the aforementioned residues was further demonstrated by Western blotting using a commercial anti–Ac-Lys antibody on immunopurified proteins from HeLa cells transiently transfected with the FLAG-tagged $APE1^{WT}$ and the nonacetylatable $APE1^{K4pleR}$ forms. It is striking that a significant increase of APE1 acetylation was observed after MMS treatment but mainly for $APE1^{WT}$ rather than for $APE1^{K4pleR}$ (Supplemental Figure S6). These data show that, besides increasing the acetylation status of K^6/K^7 (see later discussion and Yamamori *et al.*, 2010), MMS treatment also promotes acetylation at $K^{27}/K^{31}/K^{32}/K^{35}$ residues. The mild increase of Lys acetylation level in the mutant $APE1^{K4pleR}$ may possibly be ascribed to K^6/K^7 acetylation (see later discussion).

We then investigated the cellular distribution pattern of acetylated APE1 at $K^{27}/K^{31}/K^{32}/K^{35}$ residues by using an ad hoc–developed antibody that specifically recognized the peptide 25–38 fully acetylated at $K^{27}/K^{31}/K^{32}/K^{35}$, hereafter referred to as anti-$APE1^{K27\text{-}35Ac}$ (Poletto *et al.*, 2012). This antibody was particularly efficient in recognizing acetylation at K^{35} with a measured affinity in the nanomolar range (196 nM for the tetra-acetylated stretch vs. 26,800 nM for the nonacetylated one, as assessed by surface plasmon resonance (SPR; Poletto *et al.*, 2012). Preincubation of the antibody with the acetylated and nonacetylated peptides confirmed the specificity of the antibody (Poletto *et al.*, 2012). The distribution pattern of $APE1^{WT}$, $APE1^{K4pleA}$, and $APE1^{K4pleR}$ was compared by using anti-FLAG and anti-$APE1^{K27\text{-}35Ac}$ antibodies. Of interest, staining with the anti-$APE1^{K27\text{-}35Ac}$ antibody gave a pattern quite similar (i.e., nucleolar exclusion) to that of the anti-FLAG antibody but only in the case of the $APE1^{K4pleA}$ mutant (Figure 4B). PLA was also carried out to demonstrate the in vivo occurrence of acetylation on endogenous APE1 by using either the anti-$APE1^{K27\text{-}35Ac}$ antibody alone (as a control) or together with an anti-APE1 antibody (Figure 4C). This assay clearly highlighted the proximity between the target of both

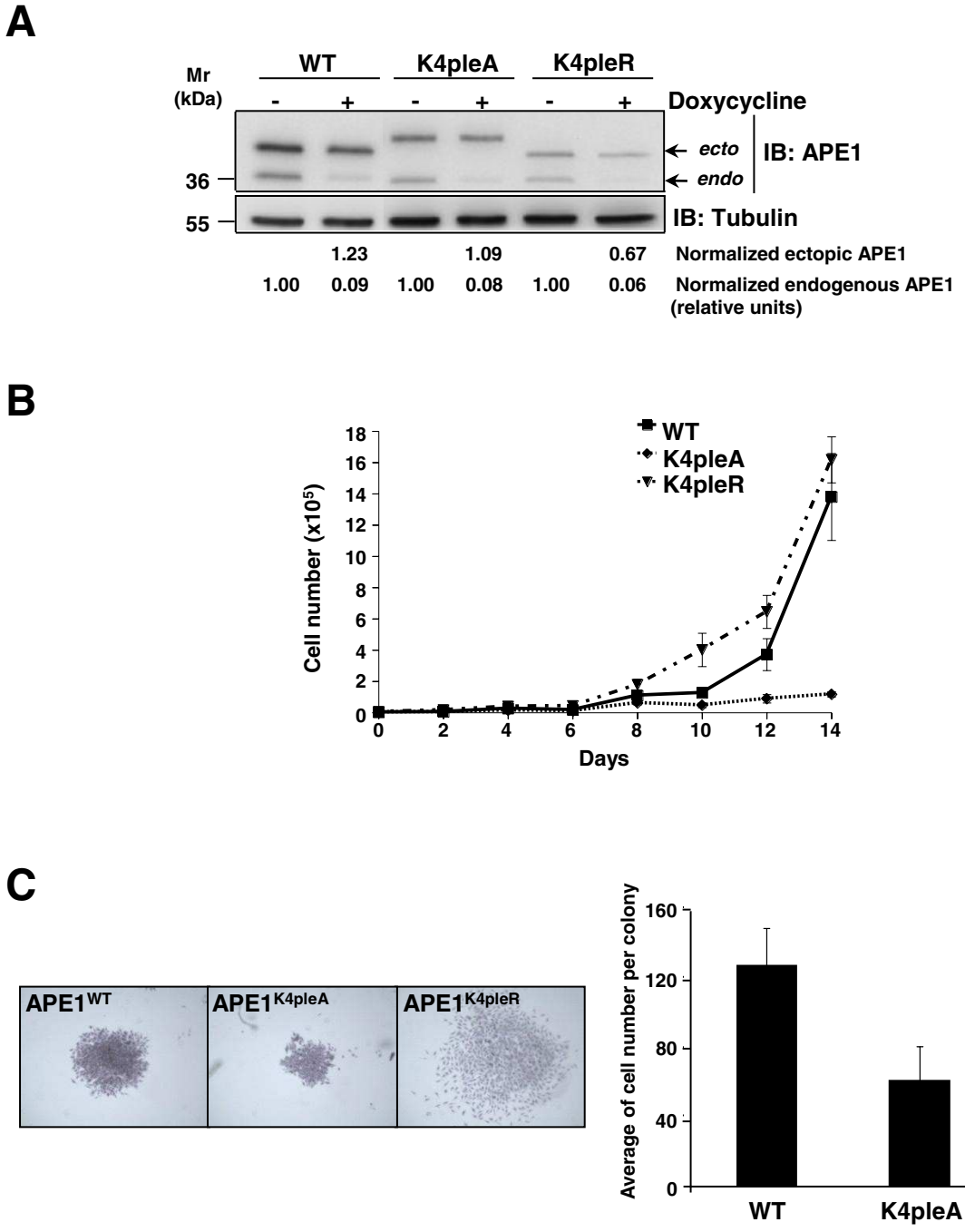

FIGURE 3: Expression of the nucleolus-deficient APE1 mutant causes impaired cell proliferation. (A) Generation of reconstituted cell lines expressing APE1^{K4pleA} and APE1^{K4pleR} mutants. HeLa cells were stably transfected with the inducible siRNA vectors and siRNA resistant APE1^{WT}, APE1^{K4pleA}, and APE1^{K4pleR}–expressing vectors, as previously described (Vascotto *et al.*, 2009a; Fantini *et al.*, 2010). Expression of ectopic APE1 forms without silencing and after the suppression of endogenous APE1 expression after 10 d of treatment with doxycycline (Doxy) was assayed by Western blotting on total cellular extracts with an anti-APE1 antibody. Normalized expression levels for each clone of ectopic and endogenous APE1 protein after the silencing are indicated under each relative band. β-Tubulin was used as loading control. (B) Cell proliferation assays for APE1-reconstituted cell lines. APE1-expressing cell clones were seeded in 60-mm Petri dishes. Growth was followed by measuring cell numbers at various times upon doxycycline treatment, as indicated. Cells were harvested at the indicated times, stained with trypan blue, and counted in triplicate. Data, expressed as cell number, are the mean ± SD of three independent experiments. (C) Colony formation assays for APE1-reconstituted cell lines. After 8 d of doxycycline treatment, 200 cells of APE1^{WT} and the indicated APE1 mutants were seeded in 60-mm Petri dishes and grown for 8 d in medium supplemented with doxycycline to promote endogenous APE1 silencing. Then cells were stained with crystal violet and images captured by using a Leica S8 microscope with 80× magnification. Data, expressed as number of cells per colony, are the mean ± SD of 10 colonies for each clone.

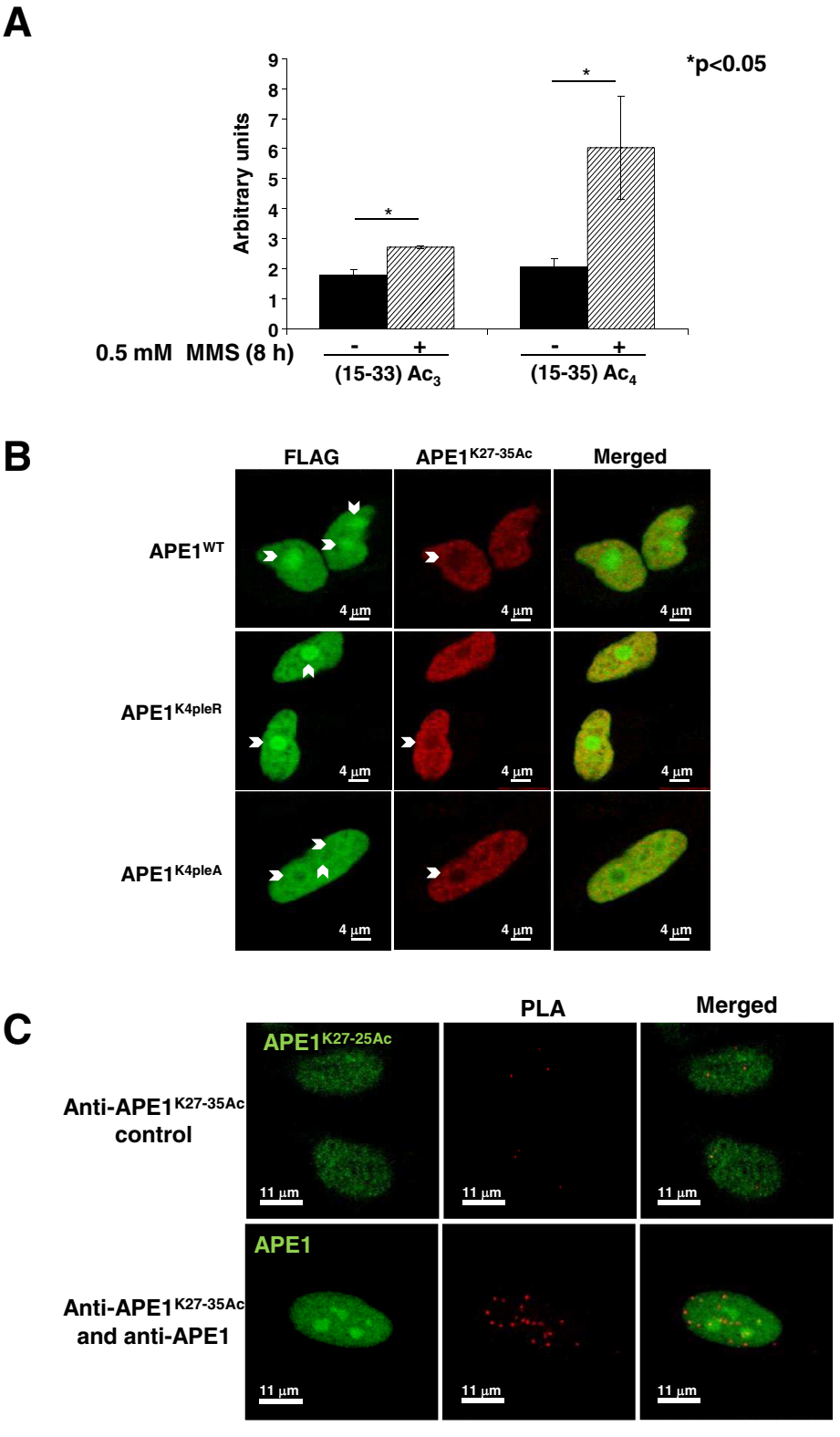

FIGURE 4: Genotoxic treatment promotes APE1 acetylation at $K^{27}/K^{31}/K^{32}/K^{35}$ residues. (A) Relative quantitative changes of APE1 acetylation at $K^{27}/K^{31}/K^{32}/K^{35}$ after MMS treatment. Mass spectrometry analysis of acetylated peptides present in the endoprotease AspN digest of FLAG-tagged $APE1^{WT}$ purified from HeLa cells (see *Materials and Methods* for details). Histograms indicate the relative amounts of the peptides (15–33)Ac_3 and (15–35)Ac_4 with respect to their nonmodified counterparts before and after MMS treatment. Identical ionization tendencies were assumed for each peptide pair. Each bar represents the mean of three independent experiments. (B) Acetylated APE1 at $K^{27}/K^{31}/K^{32}/K^{35}$ residues is present within cell nucleoplasm but is excluded from nucleoli. Confocal microscopy of HeLa cells transfected with $APE1^{WT}$, $APE1^{K4pleA}$, or $APE1^{K4pleR}$ FLAG-tagged proteins and stained with antibodies against endogenous $APE1^{K27–35Ac}$ (anti-$APE1^{K27–35Ac}$, red) and ectopic APE1 FLAG-tagged (green). Overlap of staining (yellow) demonstrated the codetection of the two protein forms. Images are representative of 100% of transfected cells. (C) APE1 acetylation at $K^{27}/K^{31}/K^{32}/K^{35}$ occurs in vivo. PLA signal obtained using the anti-$APE1^{K27–35Ac}$ antibody together with the anti-APE1 antibody on fixed HeLa cells. A technical control, using the anti-$APE1^{K27–35Ac}$ antibody alone, was introduced (top). Nuclei were counterstained using an Alexa Fluor 488–conjugated secondary anti-rabbit (recognizing the endogenous $APE1^{K27–35Ac}$, in the control reaction) or anti-mouse antibody (recognizing the endogenous APE1 protein in the PLA reaction; green).

antibodies, further suggesting that, in vivo, APE1 is acetylated at $K^{27}/K^{31}/K^{32}/K^{35}$ residues and that these acetylated forms are excluded from the nucleoli. Taken together, these data suggest that acetylation at these charged amino acids may control the nucleolar/nucleoplasmic distribution of APE1 within cells.

Removal of positively charged $K^{27}/K^{31}/K^{32}/K^{35}$ residues increases APE1 DNA-repair activity in vivo

We tested whether abolition of positive charges on acetylatable residues may affect the APE1 DNA repair function in cells, as previously demonstrated in vitro by using recombinant purified proteins bearing two different clusters of K-to-A mutation (i.e., on residues 24/25/27 and on residues 24/25/27/31/32; Fantini *et al.*, 2010). For this purpose we used nuclear extracts from reconstituted cell clones after precise normalization for the APE1 ectopic nuclear content with a titration curve (as shown in Supplemental Figure S4). This normalization for APE1 ectopic protein expression allowed comparison of the enzymatic activities of the different protein mutants in the nuclear fractions from each clone. Figure 5A shows that the AP-endonuclease activity of the $APE1^{K4pleA}$ mutant, measured through cleavage assays performed with nuclear extracts, was significantly increased with respect to $APE1^{WT}$-and $APE1^{K4pleR}$-expressing cells. Moreover, Figure 5B shows a lower amount of abasic DNA lesions accumulated after MMS treatment by the $APE1^{K4pleA}$- as compared with the $APE1^{WT}$-expressing cells. These results suggest that removal of positive charges at Lys 27–35, as exerted by acetylation, may result in a more enzymatically active protein.

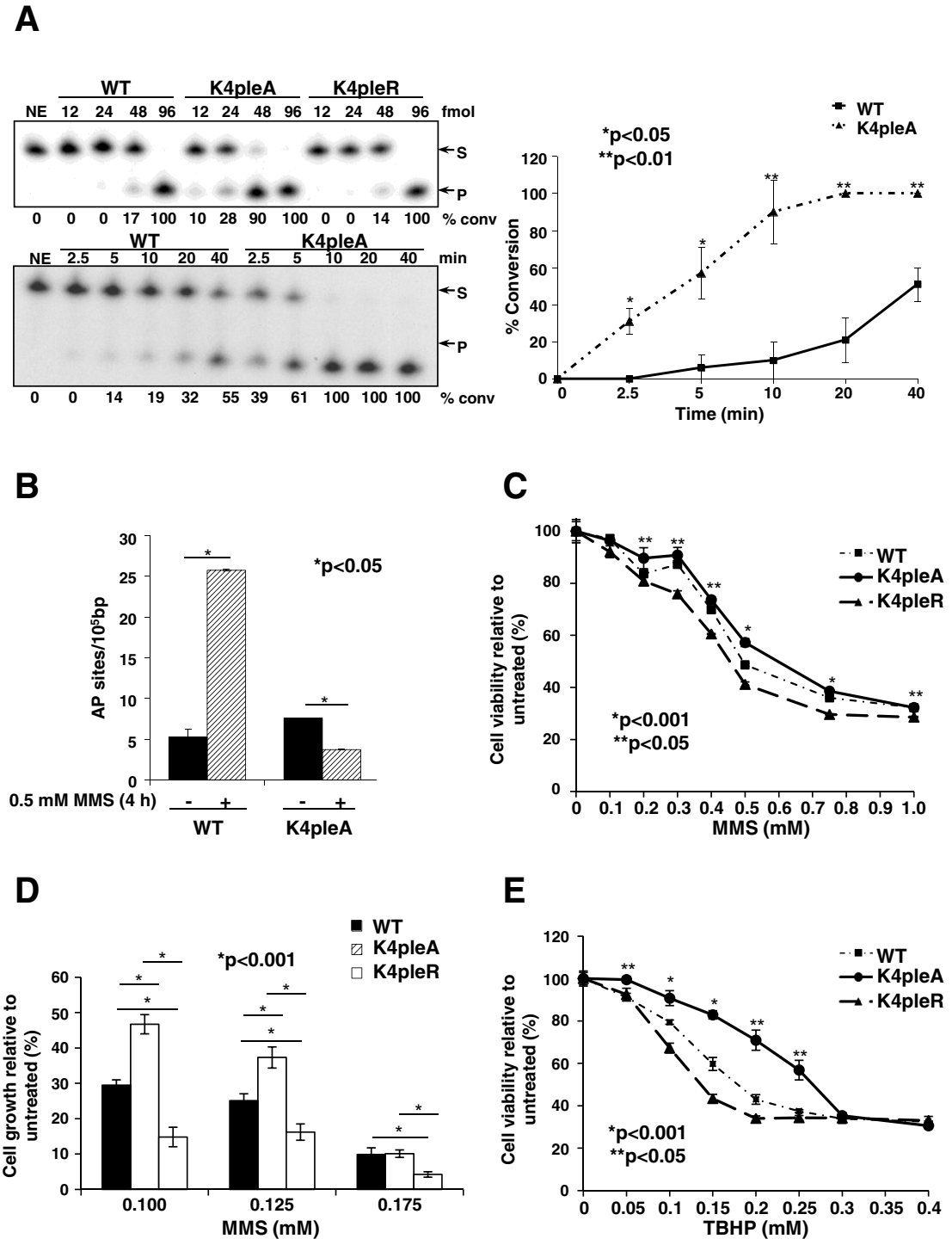

FIGURE 5: Abolition of positively charges $K^{27}/K^{31}/K^{32}/K^{35}$ residues increases APE1 DNA-repair activity. (A) Nuclear extracts from $APE1^{K4pleA}$ mutant present an increased AP endonuclease activity on abasic DNA. AP-site incision activity of the nuclear extracts from HeLa-reconstituted cell clones was tested using an AP endonuclease activity assay as described in *Material and Methods*. The nuclear APE1 content in each clone was precisely quantified through a titration curve obtained using purified recombinant APE1 (Supplemental Figure S4). Nuclear ectopic APE1 protein levels were then normalized between the different cell clones in order to compare their relative enzymatic activities. Top left, concentration-dependent conversion of an AP site–containing DNA substrate (S) to the incised product (P). A representative image of the denaturing polyacrylamide gel of the enzymatic reactions is shown. The amounts (femtomoles) of APE1 used in the reaction and the percentage of substrate converted into product, as determined by standard phosphorimager analysis, are indicated. NE, no cell extract control. Bottom left, time-dependent kinetics of APE1 (2.15 ng) endonuclease activity from nuclear extracts of the different reconstituted cell clones. The image of a representative gel analysis is shown (bottom). Right, graph depicting the time-course kinetics of APE1 from incision results shown on the left. Average values are plotted ± SD of three independent experiments. Asterisks represent a

Cell viability experiments, after MMS treatment, were carried out to verify the enzymatic data. Thus, the effect of $K^{27}/K^{31}/K^{32}/K^{35}$ mutation on cell viability after MMS treatment was measured by 3-(4-5-dimethylthiazol-2-yl)-5-(3-carboxymethoxyphenyl)-2-(4-sulfophenyl)-2H-tetrazolium salt (MTS) and clonogenic assays using the reconstituted cell clones. The MTS data (Figure 5C) showed that the $APE1^{K4pleA}$-mutant–expressing cells were significantly more resistant to MMS treatment than those expressing the nonacetylatable $APE1^{K4pleR}$ mutant. Of note, clonogenic assay experiments (Figure 5D) confirmed these results and highlighted the relevant acetylation occurring at the K residues, as demonstrated by the higher sensitivity of $APE1^{K4pleR}$-expressing cells after MMS treatment. We extended our observations on the protective function of the $APE1^{K4pleA}$ mutant by using *tert*-butyl-hydroperoxide (TBHP) as a reactive oxygen species (ROS) generator (Lazzé *et al.*, 2003). We recently demonstrated that APE1 knockdown sensitizes HeLa cells to TBHP treatment (Li *et al.*, 2012). Therefore we now measured the sensitivity of the different reconstituted cell clones to TBHP in a dose–response experiment (Figure 5E). As in the case of MMS treatment, expression of the $APE1^{K4pleA}$ mutant exerted a protective function with regard to TBHP treatment with respect to $APE1^{WT}$-expressing cells. Similarly to MMS treatment, the $APE1^{K4pleR}$-mutant–expressing clone evidenced even more sensitivity than the $APE1^{WT}$-expressing one. Taken together, these data show that acetylation at residues $K^{27}/K^{31}/K^{32}/K^{35}$ is associated with cell response to DNA damage and confers protection to genotoxic treatment. The increased activity of the $APE1^{K4pleA}$ mutant may explain its proficient protective effect in vivo against genotoxic treatment, even though further explanatory mechanisms, such as its altered protein association in the cell or its possible higher stability (Vascotto *et al.*, 2011), could also be invoked.

K^6/K^7 deacetylation by SIRT1 is modulated by the charged status of $K^{27}/K^{31}/K^{32}/K^{35}$residues

It was recently demonstrated that APE1 K^6/K^7 may undergo acetylation during cell response to genotoxic treatment (Fantini *et al.*, 2008; Yamamori *et al.*, 2010) and that modulation of the acetylation status of these residues through SIRT1 deacetylase activity is important for the regulation of APE1 DNA-repair function after MMS treatment (Yamamori *et al.*, 2010). However, the molecular mechanism regulating the SIRT1-mediated modification at these amino acids during MMS treatment is unknown. We thus checked whether the charged status of $K^{27}/K^{31}/K^{32}/K^{35}$ residues might play a role in modulating the acetylation status of K^6/K^7 through the contribution of SIRT1. First, we evaluated the effect of the modification at $K^{27}/K^{31}/K^{32}/K^{35}$ on the ability of SIRT1 to deacetylate K^6/K^7 in APE1. We found that recombinant purified APE1 protein is nonenzymatically acetylated after incubation with acetyl-CoA, as demonstrated for other proteins (Garbutt and Abraham, 1981). Thus, to obtain a significant amount of acetylated recombinant APE1 protein on K^6/K^7 residues, we treated purified recombinant rAPE1 obtained from *E. coli* with acetyl-CoA, as described in the Supplemental Information. Then we treated in vitro–acetylated $rAPE1^{WT}$, $rAPE1^{K4pleA}$, $rAPE1^{K27/35A,}$ or $rAPE1^{K31/32A}$ with purified recombinant SIRT1 protein and measured the acetylation level on K^6/K^7 through a specific antibody that recognizes only acetylation at these residues (Fantini *et al.*, 2008; Sengupta *et al.*, 2011). Of interest, although $APE1^{WT}$ was efficiently deacetylated by SIRT1 at K^6/K^7 (Figure 6A), the $APE1^{K4pleA}$ mutant did not show any deacetylation in this region; concomitant K-to-A substitutions at positions 27 and 35 ($APE1^{K27/35A}$ mutant) or at positions 31 and 32 ($APE1^{K31/32A}$ mutant) caused an intermediate effect.

We then verified the ability of SIRT1 to directly deacetylate APE1 at $K^{27}/K^{31}/K^{32}/K^{35}$ residues through in vitro deacetylation assays carried out on acetylated purified recombinant $rAPE1^{WT}$ or mutant proteins as substrates (Supplemental Figure S7). Protein acetylation level was monitored by using the anti-$APE1^{K27\text{-}35Ac}$ (Figure 6B). Incubation with recombinant-purified SIRT1 protein revealed a marked decrease in acetyl-APE1 signal but only when $APE1^{WT}$ was used. These data were corroborated by qualitative peptide mapping experiments on in vitro–acetylated $rAPE1^{WT}$ before and after incubation with SIRT1. This analysis demonstrated that SIRT1 was indeed able to deacetylate in vitro–acetylated $rAPE1^{WT}$ at least at $K^{25}/K^{27}/K^{32}$ residues (Supplemental Table S1).

The ability of SIRT1 to deacetylate in vitro APE1 at $K^{27}/K^{31}/K^{32}/K^{35}$ was also analyzed on APE1 (25–38) peptides (Figure 6C), which were chemically synthesized either in their nonacetylated or tetra-acetylated form at these K residues. These peptides were used in a competitive fluorescence-based assay in which a fluorogenic p53 acetylated peptide was used as SIRT1 substrate (Marcotte *et al.*, 2004). As expected, we observed a dose-dependent decrease in the

significant difference between $APE1^{WT}$ and $APE1^{K4pleA}$. (B) Accumulation of genomic abasic (AP) lesions after MMS treatment (0.5 mM, 4 h) of reconstituted cell clones with $APE1^{WT}$ and $APE1^{K4pleA}$ mutant as measured by an aldehyde-reactive probe. $APE1^{WT}$ and $APE1^{K4pleA}$-expressing HeLa cells were grown in medium supplemented with Doxy (10 d) to silence endogenous APE1 expression and were treated with 0.5 mM MMS for 4 h. Counting at the AP sites was performed by using the AP-site quantification kit, as described in *Materials and Methods*. In the histogram, data are expressed as number of AP sites per 10^5 base pairs and represent the mean ± SD of four independent experiments. Asterisks represent a significant difference between the two conditions (untreated and MMS-treated cells). (C) Effects of APE1 acetylation mutants on cell viability after MMS treatment in reconstituted cells. $APE1^{WT}$, $APE1^{K4pleA}$-, and $APE1^{K4pleR}$-expressing cells were grown in medium supplemented with Doxy to silence APE1 endogenous protein and treated with increasing concentrations of MMS for 8 h; the cytotoxic effect of this compound was determined by the MTS assay (see *Materials and Methods* for details). Each point, shown as percentage viability with respect to untreated clones, represents the mean ± SD of four observations, repeated in at least two independent assays. Asterisks represent a significant difference between $APE1^{K4pleA}$ and $APE1^{K4pleR}$ mutants. (D) Cell growth as measured by colony survival assay. One thousand cells of $APE1^{WT}$-, $APE1^{K4pleA}$-, and $APE1^{K4pleR}$-expressing clones treated with increasing concentrations of MMS for 8 h were seeded in Petri dishes and then treated with Doxy for 10 d to silence endogenous APE1. Data, expressed as the percentage of change with respect to untreated clones, are the mean ± SD of three independent experiments. (E) Effects of APE1 acetylation mutants on cell viability after TBHP treatment in $APE1^{WT}$-, $APE1^{K4pleA}$-, and $APE1^{K4pleR}$-expressing cells grown in medium supplemented with Doxy to silence APE1 endogenous protein. Cells were treated with increasing concentrations of TBHP for 6 h, and the cytotoxic effects were determined by the MTS assay. Each point, shown as percentage viability with respect to untreated clones, represents the mean ± SD of four observations, repeated in at least two independent assays. Asterisks represent a significant difference between $APE1^{K4pleA}$ and $APE1^{K4pleR}$ mutants.

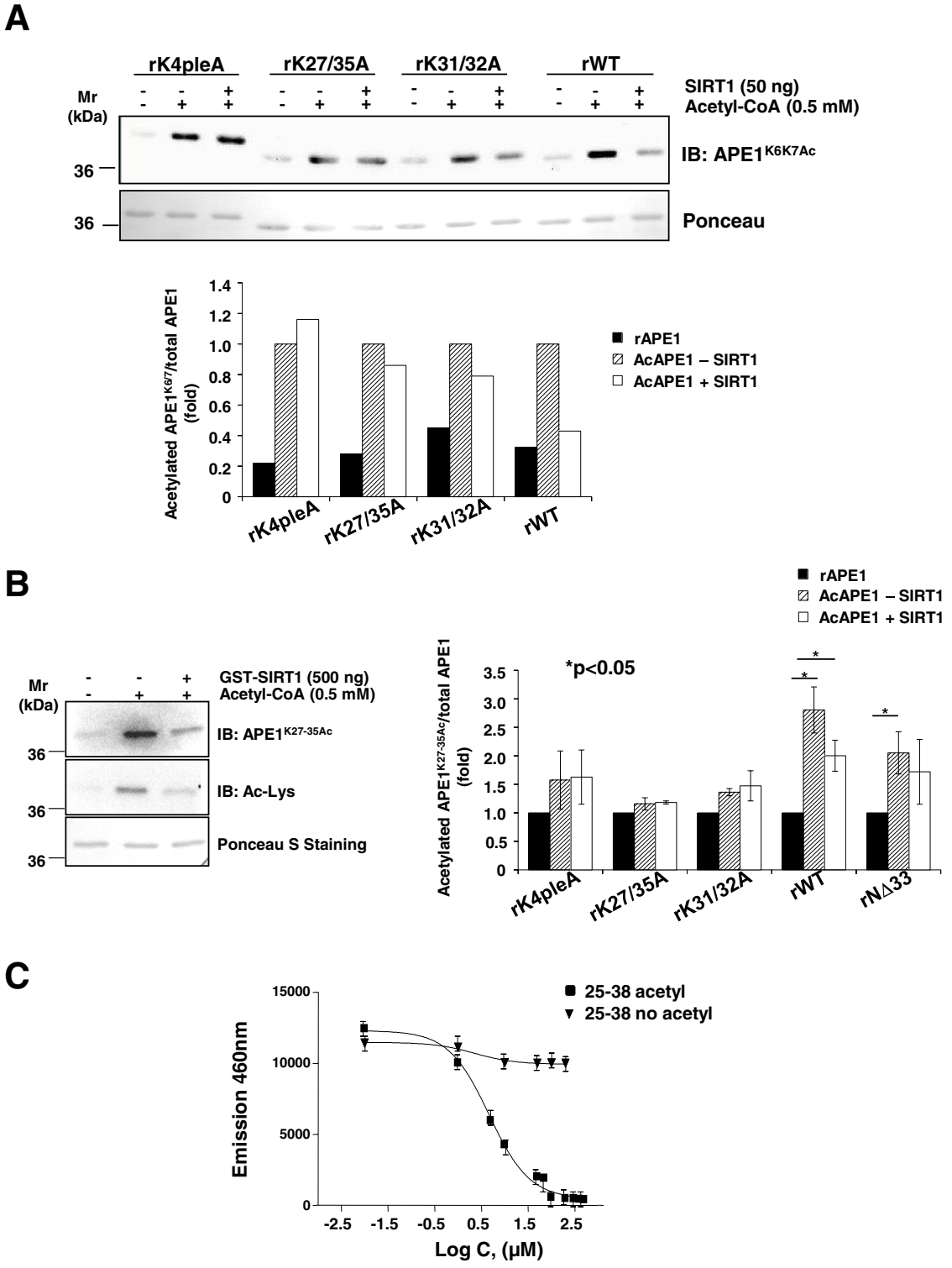

FIGURE 6: SIRT1 deacetylase activity on K^6/K^7 depends on the charged status of $K^{27}/K^{31}/K^{32}/K^{35}$ residues. (A) K^6/K^7 acetylation, modulated by SIRT1, depends on the charged status of $K^{27}/K^{31}/K^{32}/K^{35}$ residues. Western blot analysis on purified recombinant APE1 proteins in vitro acetylated with acetyl-CoA and then incubated in the presence/absence of recombinant GST-SIRT1, as indicated. The analysis was carried out using an antibody specific for acetylated K^6/K^7 APE1 (top). The histogram reports data obtained from densitometric quantification of the bands for each APE1 protein after normalization on Ponceau S staining (bottom). Data shown are the mean of two independent experimental sets whose variation was <10%. (B) SIRT1 deacetylates rAPE1 at $K^{27}/K^{31}/K^{32}/K^{35}$. Left, Western blot analysis on the in vitro–acetylated and deacetylated purified recombinant APE1, further subjected to MS analysis (Supplemental Table S1). $rAPE1^{WT}$ was incubated with 0.5 mM acetyl-CoA and then with recombinant SIRT1 protein, as shown. Samples were separated onto 10% SDS–PAGE, and Western blot analysis was performed by using the anti-$APE1^{K27-35Ac}$ antibody. Ponceau S staining was used as loading control. Right, the histogram shows the densitometric quantification of the

fluorescence signal by using different amounts of the tetra-acetylated peptide (25–38); the nonacetylated counterpart was used as a negative control substrate. Best data fitting was observed with a one-site competition equation, which provided an IC_{50} value of 4.6 ± 0.3 μM. These data support the conclusion that the acetylated APE1 region spanning amino acids 27–35 is a substrate for SIRT1 deacetylase activity. Taken together, these results demonstrate that SIRT1's ability to efficiently deacetylate APE1 at K^6/K^7 residues relies on the presence of positive charges at $K^{27}/K^{31}/K^{32}/K^{35}$. Moreover, SIRT1 is also able to bind and possibly deacetylate in vitro–acetylated APE1 $K^{27}/K^{31}/K^{32}/K^{35}$ residues.

Cross-talk between the charged state of $K^{27}/K^{31}/K^{32}/K^{35}$ and the acetylation status of K^6/K^7 residues through SIRT1

To understand whether SIRT1 activity on acetylated K^6/K^7 residues might be modulated in vivo by MMS as a function of the charged status of $K^{27}/K^{31}/K^{32}/K^{35}$, we performed coimmunoprecipitation experiments on transiently transfected HeLa cells. As shown in Figure 7A, an intact N-terminal domain is required for stable APE1 binding to SIRT1. The APE1/SIRT1 association was induced after MMS treatment and was abolished in the case of both $APE1^{N\Delta33}$ and $APE1^{K4pleA}$ mutants. Substitution of $K^{27}/K^{31}/K^{32}/K^{35}$ residues with nonacetylatable R residues was ineffective, suggesting that SIRT1 binding depends on the presence of positively charged amino acids spanning the APE1 region 27–35. Measurements of K^6/K^7 acetylation status with the specific antibody (performed on the same samples) clearly showed that, in agreement with the binding data, K^6/K^7 residues resulted in more acetylation both under basal and after MMS treatment but only in the case of the $APE1^{K4pleA}$ mutant. In addition, the acetylation status of $APE1^{WT}$ and $APE1^{K4pleR}$, both under basal conditions and after MMS treatment, was comparable (Figure 7B), supporting the existence of cross-talk between the charged status of $K^{27}/K^{31}/K^{32}/K^{35}$ and the acetylation level of K^6/K^7.

We then investigated the cross-talk between K^6/K^7 and $K^{27}/K^{31}/K^{32}/K^{35}$ acetylation status through siRNA experiments. HeLa cell lines stably expressing both endogenous APE1 and $APE1^{WT}$, $APE1^{K4pleA}$, and $APE1^{K4pleR}$ ectopic forms were silenced for SIRT1 expression as described in *Materials and Methods*. The acetylation level of K^6/K^7 was then measured through Western blotting. Data shown in Figure 7C demonstrate that the K^6/K^7 acetylation level of the ectopic APE1 forms was increased ~30–40% upon SIRT1 silencing but only in the case of $APE1^{WT}$- and $APE1^{K4pleR}$-expressing cells, whereas acetylation of K^6/K^7 of $APE1^{K4pleA}$ was <10%. As a control, the acetylation level of endogenous APE1 always increased (~60–70%) upon SIRT1 silencing in all the cell lines tested (unpublished data). Taken together, these data demonstrate that the acetylation/charged status of $K^{27}/K^{31}/K^{32}/K^{35}$ residues controls the stability of the SIRT1/APE1 complex, thus playing a role in the acetylation level of K^6/K^7.

Possible relevance of acetylation for APE1 subnuclear distribution and protein local conformation

The data suggest that a coordinated acetylation/deacetylation dynamic modulated by SIRT1 may occur within the cell nucleus and could be responsible for APE1 subnuclear trafficking. Thus, we examined the subnuclear distribution of SIRT1 on c-myc-SIRT1–transfected cells through immunofluorescence analysis. We found that transiently transfected c-myc-SIRT1 mainly localized in the nucleoplasmic compartment and was not found in the nucleoli (Figure 8A, left); quantification of the endogenous SIRT1 protein in biochemically purified nucleoli confirmed its absence from this subnuclear compartment (Figure 8A, right). Evaluation of the acetylation status of APE1 present in nucleolar or nucleoplasmic fractions under basal conditions showed that APE1 acetylated at K^6/K^7 is mainly present within the nucleoplasm but almost absent in the nucleolus (Figure 8B). Of note, these findings may have important implications for SIRT1-mediated deacetylation at K^6/K^7 and demonstrate the possibility that APE1 acetylation modulates the protein's subnuclear distribution and enzymatic functions, corroborating our previous work (Fantini *et al.*, 2010).

It is known that Lys acetylation may control local conformational stability of proteins, thus affecting their activity, subcellular distribution, and protein–protein interaction network. To examine the effect of acetylation on the local structure of the N-terminal APE1 region, we analyzed the conformational behavior of the protein portion of residues 14–38, which contain $K^{27}/K^{31}/K^{32}/K^{35}$ residues acetylatable in vivo. To this end, we chemically synthesized and purified four peptides bearing differential acetylation at positions 27, 31, 32, and 35 (Supplemental Table S2). To evaluate the effect of acetylation on peptide conformation, we undertook structural analysis of these peptides in solution by far-ultraviolet (UV) circular dichroism (CD) and nuclear magnetic resonance (NMR) spectroscopy. Figure 8C shows the overlay of CD spectra of APE1(14–38) and $APE1(14–38)^{K27/31/32/35Ac}$ in aqueous buffer, indicating a minimum at ~200 nm and a shoulder at ~220 nm. These features suggest the presence of mixed conformational states in which an unfolded state coexists with a certain helical content. The propensity of this domain to adopt helical conformation was also confirmed by trifluoroethanol (TFE) titration experiments (Supplemental Figure S8A). In particular, the CD spectrum of the tetra-acetylated peptide showed a minimum at 220 nm that was deeper than that of the nonacetylated counterpart, suggesting a role for the acetyl groups in determining structural changes in this protein region. An intermediate behavior was observed for the monoacetylated and triacetylated peptides, confirming the role of this K modification in modulating the conformation of the N-terminal APE1 region (unpublished data).

To further address this point, we carried out additional NMR experiments. In aqueous buffer, the one-dimensional (1D) spectra presented poor signal dispersion (Figure 8D, left), confirming a rather disordered state for both the tetra-acetylated and nonacetylated peptides. This observation was further strengthened by the analysis of two-dimensional (2D) [^{1}H, ^{1}H] total correlation spectroscopy (TOCSY) spectra (Griesinger *et al.*, 1988; Figure 8D, middle), and 2D [^{1}H, ^{1}H] rotating frame nuclear Overhauser effect spectroscopy (ROESY) spectra (Bax and Davis, 1985; Figure 8D, right). In the latter case, the presence of a restricted set of cross-peaks in the $_N$H-aliphatic side-chain proton correlation region made unfeasible the process of sequential resonance assignments, as often occurs for small, flexible

band intensities, after normalization to the nonacetylated APE1 form, of the in vitro–acetylated and deacetylated purified APE1 mutants. Data are the mean ± SD of three independent replicates. Asterisks represent a significant difference. (C) The acetylated APE1 25–38 peptide is a substrate of SIRT1 activity. Purified APE1 peptides (25–38) either in fully acetylated form at $K^{27}/K^{31}/K^{32}/K^{35}$ residues or not acetylated were analyzed as competitors in an in vitro deacetylase SIRT1 assay based on a fluorogenic acetylated peptide derived from p53 (region 379–382). Dose–response signals allowed an estimated IC_{50} value of 4.6 ± 0.3 μM of the acetylated APE1 25–38 region with respect to the p53 peptide.

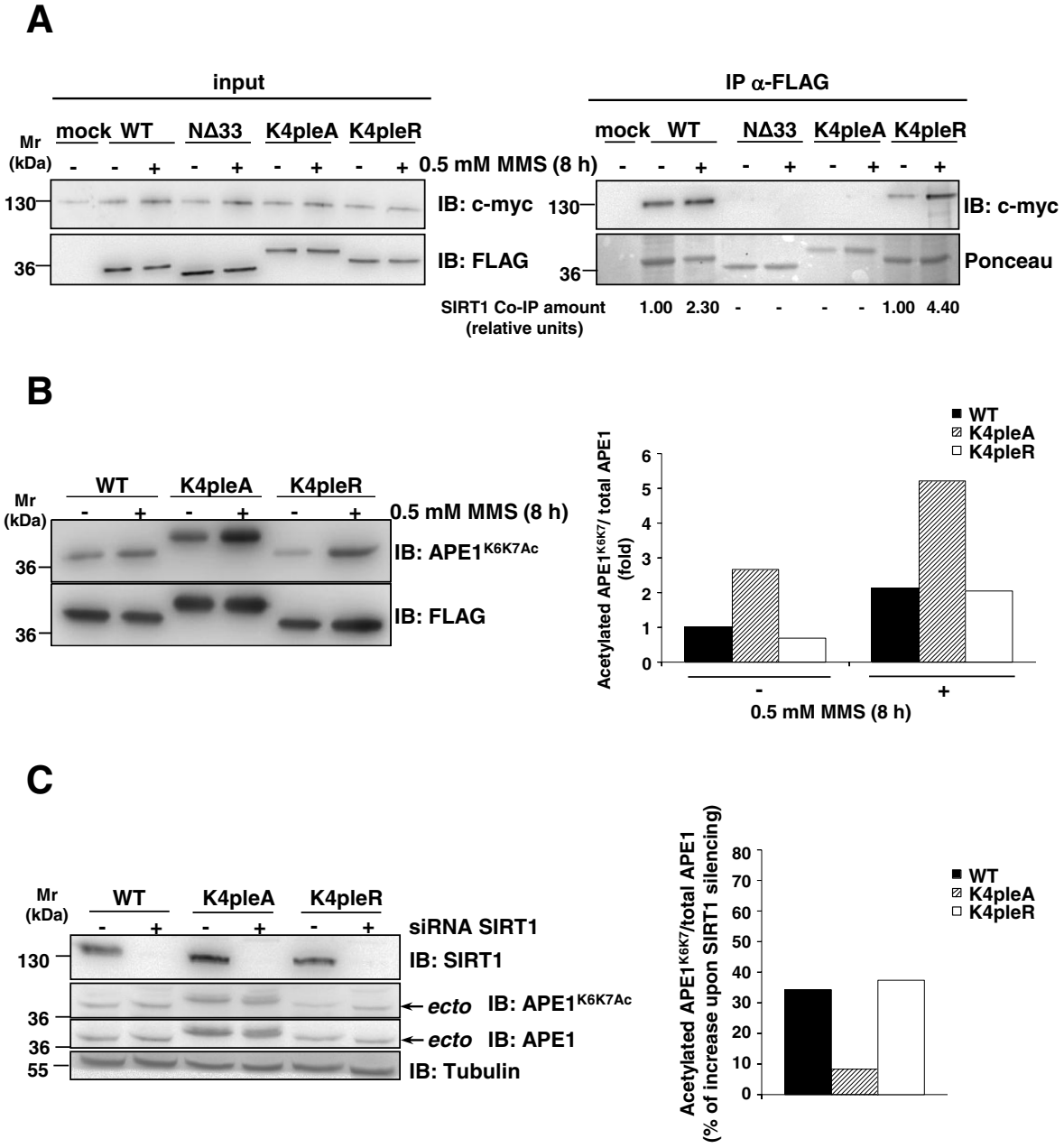

FIGURE 7: Cross-talk between the acetylation status of $K^{27}/K^{31}/K^{32}/K^{35}$ and K^6/K^7 residues through SIRT1. (A) Positive charges at $K^{27}/K^{31}/K^{32}/K^{35}$ residues strongly influence the stability of SIRT1 binding to APE1. Western blot analysis performed on total cell extracts (left) and on immunoprecipitated material (right) from HeLa cells cotransfected with c-myc–tagged SIRT1 and $APE1^{WT}$, $APE1^{N\Delta33}$, $APE1^{K4pleA}$, or $APE1^{K4pleR}$ FLAG-tagged proteins and treated with 0.5 mM MMS for 8 h. Coimmunoprecipitated amounts of SIRT1 normalized with respect to $APE1^{WT}$ or $APE1^{K4pleR}$, respectively, are indicated under each relative bar. Ponceau S staining was used as loading control. (B) Acetylation level of K^6/K^7 in $APE1^{K4pleA}$ mutant is higher than that of $APE1^{WT}$ both under basal conditions and after MMS treatment. Western blot analysis on CoIP material after MMS treatment from HeLa cells transfected with $APE1^{WT}$ and FLAG-tagged mutants is shown. The histogram indicates the relative amount of acetylated $APE1^{K6/K7}$ in the different clones obtained from the densitometric quantification of acetylated APE1 bands, normalized with respect to the amount of APE1 FLAG-tagged immunopurified protein. Data shown are the mean of two independent experimental sets whose variation was <10%. (C) SIRT1 siRNA knockdown increases APE1 K^6/K^7 acetylation. HeLa stable clones expressing $APE1^{WT}$, $APE1^{K4pleA}$, and $APE1^{K4pleR}$ were transfected with siRNA against SIRT1 protein or control siRNA. Western blot analysis was performed to detect differential amount of the acetylated K^6/K^7 APE1 after SIRT1 silencing. Arrows highlight bands of ectopic APE1 protein form; β-tubulin was used as a loading control. The histogram shows densitometric quantification of acetylated K^6/K^7 APE1 form. Data are expressed as percentage of induction of the acetylated K^6/K^7 APE1 after SIRT1 silencing after normalization for the total APE1 protein levels. Data shown are the mean of two independent experimental sets whose variation was <10%.

peptides that tumble very rapidly in solution. On the other hand, a detailed comparison of the 1D NMR data for the nonacetylated and tetra-acetylated APE1 peptides (Figure 8D, left) indicated that acetylation causes a small but clear improvement of spectral dispersion, which can be particularly appreciated in the $_N$H region (Figure 8D, top left). Moreover, the intensity of ROE cross-peaks is increased in the spectra of APE1(14-38)$^{K27/31/32/35Ac}$ peptide as compared with the nonmodified counterpart (Figure 8D, right). This evidence, together with small chemical shift changes, point toward the presence of more organized conformations for the tetra-acetylated peptide in aqueous solution, in agreement with CD data. Similar conclusions are drawn from the analysis of NMR data for APE1(14–38) and APE1(14–38)$^{K27/31/32/35Ac}$ peptides in phosphate:TFE solution (Supplemental Figure S8B), which suggested again the higher propensity of this domain in its acetylated form to adopt a more ordered conformation in contrast to the nonmodified counterpart. Also in this case, monoacetylated and triacetylated peptides showed an intermediate behavior (unpublished data). These data suggest that acetylation may account for local conformational changes on APE1 structure that may modulate its binding ability to different substrates.

DISCUSSION

APE1 is an unusually abundant DNA-repair protein in mammalian cells, with a wide nuclear distribution and an essential role in the BER pathway of DNA lesions (Tell and Wilson, 2010). We calculated that HeLa cells express ~4 × 10^7 molecules per cell (Supplemental Figure S4A), whereas other enzymes of the BER pathway, such as Pol β or XRCC1, are present at an extent of <1/10 (Demple and DeMott, 2002; Parsons *et al.*, 2008). Therefore APE1 involvement in preformed DNA-repair complexes may only partially explain the energy cost used to maintain such high protein concentration within the cells. Recently we found that APE1 may interact with rRNA and with proteins involved in RNA metabolism and is associated with nucleolar structures through its interaction with NPM1 (Vascotto *et al.*, 2009b; Tell *et al.*, 2010b). Interaction with rRNA and NPM1 strictly depends on the positive charge of K residues within the APE1 region 24–35 placed within the unstructured protein N-terminal domain, as demonstrated by the inability of the corresponding K-to-A mutants (resembling constitutive acetylation at these residues) to stably bind both rRNA and NPM1 (Fantini *et al.*, 2010). Of interest, some of these amino acids (i.e., $K^{27}/K^{31}/K^{32}/K^{35}$), which have been acquired during evolution, may undergo in vivo acetylation (Fantini *et al.*, 2010). We conjectured that, under physiological conditions, nonacetylated APE1 may be stored in the nucleolar compartment through its binding to NPM1 and rRNA, but the in vivo relevance of APE1 nucleolar accumulation was still unclear. This study was aimed at addressing this issue.

We also found that APE1^{K4pleA} binds poorly to NPM1 and rRNA in vivo and as a result is unable to accumulate within the nucleoli, whereas it is present in the nucleoplasm. Moreover, reconstitution of HeLa cells with this mutant gave improved protection from genotoxic damage induced by alkylating agents, such as MMS, and oxidative stress-generating compounds, such as TBHP, through increased DNA-repair activity. As expected for a regulated phenomenon such as the response to a genome insult, an in vivo–augmented acetylation at $K^{27}/K^{31}/K^{32}/K^{35}$ residues was observed during cell response to genotoxic damage. Furthermore, cross-talk involving the SIRT1 deacetylase occurred within cells between acetylation at $K^{27}/K^{31}/K^{32}/K^{35}$ and at K^6/K^7 residues. Therefore we hypothesized that genotoxic stress may shift the equilibrium between the nonacetylated and acetylated APE1 forms toward the latter, which would result in the most enzymatically active one on abasic DNA. This also corresponds to our previous data obtained in vitro with recombinant purified proteins (Fantini *et al.*, 2010). In many cases, the presence of the unstructured N-terminal domain of APE1 seemed essential for interaction of APE1 with different substrates (i.e., nucleic acids or proteins). Interaction also increased after histone deacetylase (HDAC) inhibition, which promotes APE1 acetylation at K^6/K^7 residues (Bhakat *et al.*, 2003; Yamamori *et al.*, 2010). This evidence strongly support the notion that this unstructured domain is responsible for the modulation of APE1's different functions through the recruitment of APE1 in different protein complexes by means of various amino acid side-chain modification events. From an evolutionary perspective, it can be hypothesized that mammalian APE1 activity was made adjustable (through PTMs and/or interaction with other proteins), or expanded toward other substrates, with the acquisition of a protein N-terminus containing positively charged residues, without major modifications on the enzyme catalytic site, which retained the "canonical" function toward abasic DNA. The existence of such an N-terminal extension in only mammals may suggest its evolutionary significance in the face of increased functional complexity. For the noncomplexed protein in solution, the intrinsic lack of a secondary structure associated with this domain can confer functional advantages to mammalian APE1, including the ability to bind to different protein targets (e.g., NPM1, XRCC1, CSB, RNA, etc.; Vidal *et al.*, 2001; Wong *et al.*, 2007; Vascotto *et al.*, 2009a; Tell *et al.*, 2010a), thus allowing efficient control over the thermodynamics in the binding process to different substrates. Because the protein's N-terminus is required for the stabilization of APE1 interaction with NPM1 or rRNA and for the control of the overall endonuclease activity (possibly decreasing the rate of product release once in the positively charged state; Fantini *et al.*, 2010; Figure 5), this region-specific multitasking function can provide a "trigger" for molecular regulation with important biological significance. This should be regarded, however, in light of BER coordination to prevent formation of harmful, unprotected DNA strand breaks. Therefore subcellular distribution of APE1 and its enzymatic activity seem to be finely tuned to demand and in a time-dependent manner through multiple interactions with various protein partners and the coordinated occurrence of different PTMs, such as acetylation and ubiquitination (Busso *et al.*, 2009, 2011). The observation that acetylation at $K^{27}/K^{31}/K^{32}/K^{35}$ residues may favor a transition toward a more organized conformation (Supplemental Figure S8) would support the notion that this modification may significantly modulate the interaction with several protein partners on a structural basis. In addition, acetylation at the mentioned K residues may profoundly affect APE1 protein stability, based on a recent report showing that the same K residues can be also polyubiquitinated by UBR3, targeting the protein for degradation by the proteasome (Meisenberg *et al.*, 2011). Given that acetylation competes with ubiquitination for the same K residues, it may represent the switch for controlling protein turnover rate. In this context, the acetylation at these residues that we observed during cell response to genotoxicants may stabilize protein half-life, thus preventing its degradation.

Few studies have reported on the effect of acetylation on the structure of small, ordered (Hughes and Waters, 2006; Liu and Duan, 2008) and disordered (Smet-Nocca *et al.*, 2010) peptides. Molecular dynamic simulations carried out on a peptide from the histone H3 N-terminal tail in the nonacetylated and doubly acetylated forms revealed that acetylation, although not appreciably disturbing the overall structure of the most-populated states, influenced peptide stability (Liu and Duan, 2008). The effect of acetylation at K residues on the conformational properties of small random-coil peptides from the histone H4 N-terminal tail and from nonhistone thymine DNA glycosylase indicated that acetylation had little effect on the

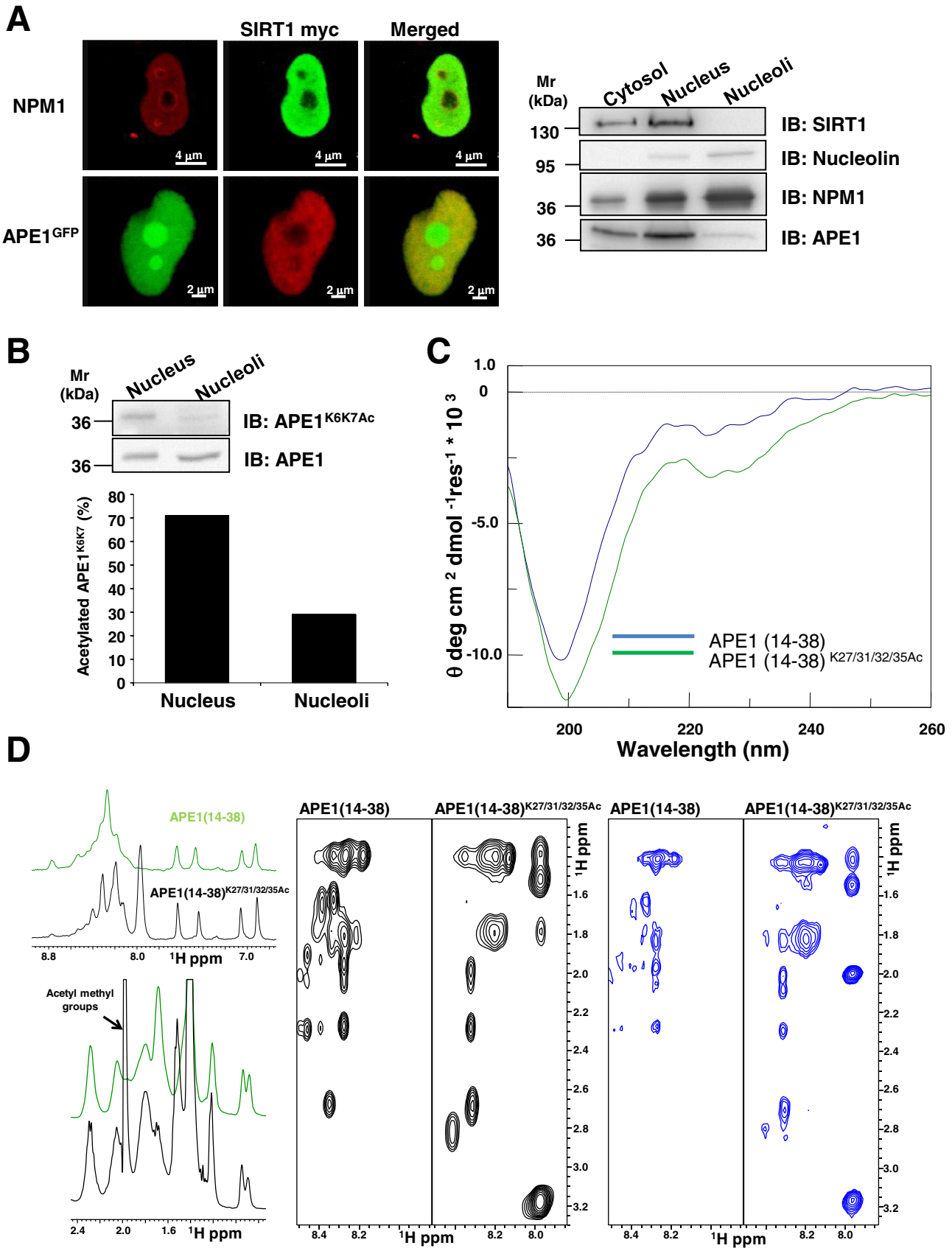

FIGURE 8: Nucleolar APE1 hypoacetylated on K^6/K^7 and conformational impact of acetylation at $K^{27}/K^{31}/K^{32}/K^{35}$ on APE1 local structure. (A) SIRT1 resides within the nucleoplasm of HeLa cells. Left, confocal microscopy of HeLa cells cotransfected with green fluorescent protein–fused APE1 ($APE1^{GFP}$) and c-myc-SIRT1 after fixing and staining with antibodies against NPM1 (red) and c-myc-SIRT1 (top, green; bottom, red). SIRT1, clearly excluded from nucleoli,

overall polypeptide structure, while inducing local conformational changes (Smet-Nocca *et al.*, 2010). In agreement with these studies, APE1(14–38) and APE1(14–38)$^{K27/31/32/35Ac}$ became disordered, as shown by the lack of ROE (Bax and Davis, 1985) cross-peak patterns, which are characteristic of ordered secondary structure elements. However, small differences in the NMR spectra (Figure 8 and Supplemental Figure S8), concerning both chemical shift values and signal intensities, seem to indicate that at least local conformational changes may occur following acetylation. We cannot ignore that these changes may be important for the interaction of APE1 with SIRT1 deacetylase and with NPM1; they highlight the role that the charged status of K residues within this region may play at the protein structural level. Based on our data, it can be speculated that full acetylation of $K^{27–35}$ may reduce SIRT1 binding to APE1, thus delaying its enzymatic activity on K^6/K^7. This mechanism could represent a way to coordinate the kinetics of the overall acetylation status of the protein. According to this hypothesis, SIRT1 should first deacetylate $K^{27–35Ac}$ before deacetylating K^6/K^{7Ac}. Our ability to identify APE1 peptides with varying amounts of acetylation on $K^{27–35}$ supports the existence of a dynamic equilibrium between multiple acetylated forms of the protein within cells and thus its functional regulatory role. Moreover, the presence of SIRT1, found exclusively in the nucleoplasm but not in the nucleoli (similar to the APE1 acetylated on $K^{27–35}$ and the reduced nucleolar presence of APE1 acetylated on K^6/K^7; Figure 8, A and B), suggests that acetylation of APE1 may force its exit from nucleoli to nucleoplasm, where it can be deacetylated by SIRT1. This model is further supported by the significantly reduced interaction of AcAPE1K^{27-35} with NPM1 (Figure 2). Further studies to identify the acetyltransferase able to acetylate APE1 within the nucleoli are in progress. Furthermore, this work supports findings by Yu *et al.* (2010), who demonstrated that these K residue conformational adjustments were concomitant with DNA binding and catalysis or with interaction with Pol β.

The nucleolar role of APE1 storage and regulation, as described here, may have profound biological consequences during cell response to stressor signals, especially in light of recent evidence pointing to the nucleolus as a central hub in DNA damage (Nalabothula *et al.*, 2010). Accordingly, the nucleolus seems responsible for actively transmitting signals to the molecular complex regulating p53 activity mediated by ARF–NPM1 interaction (Colombo *et al.*, 2002; Lee *et al.*, 2005; Nalabothula *et al.*, 2010), and thus it is involved in the maintenance of genome stability. A careful elucidation of the NPM1-ARF-p53 signaling networks and their involvement in the DNA-repair pathway coordinated by APE1 is an important subject for molecular carcinogenesis and deserves further study. This is also underway in our laboratory. Of note, data obtained in this work not only show that nucleoli may act as a storage site so that an appropriate amount of APE1 is readily available for maintenance of genome stability, but also emphasize that nucleolar accumulation of APE1 controls cell proliferation, possibly through its rRNA cleansing function. Compatible with this, APE1^{K4pleA}-expressing cells, under basal conditions, showed impairment in proliferation rate with respect to APE^{WT}-expressing ones (Figure 3). Therefore it can be speculated that nucleolar APE1 is responsible for functional activity of the nucleolus in ribosome biogenesis. APE1 release from the nucleoli after genotoxic treatment may constitute a signal to block active protein synthesis and allow activation of the proper DNA-repair mechanisms. Experiments are in progress along these lines to address this in light of the possibility that acetylation may control the APE1 trafficking from nucleoli to nucleoplasm.

In conclusion, our data shed light on novel molecular aspects highlighting the multifunctional nature of APE1 in regulating different biological outcomes and point to acetylation as an important mechanism for the fine-tuning of protein functions, subcellular distribution, and stability. They also emphasize the need for additional investigation of the APE1 N-terminal domain in order to understand the structural details of the regulatory mechanisms for this multifunctional protein. In addition, recent evidence on APE1 acetylation pattern in triple-negative breast cancer reveals that, concomitantly with total APE1 overexpression, a profound deregulation of APE1 acetylation status occurs under pathological conditions (Poletto *et al.*, 2012). This underscores the biological relevance of our findings and the need for future investigation.

MATERIALS AND METHODS

Inducible APE1 knockdown and generation of APE1 knock-in cell lines

Inducible silencing of endogenous APE1 and reconstitution with mutant proteins in HeLa cell clones was performed as described (Vascotto *et al.*, 2009a,b) and as reported in the Supplemental Information. For inducible shRNA experiments, doxycycline (1 μg/ml; Sigma-Aldrich, St. Louis, MO) was added to the cell culture medium, and cells were grown for 10 d. All biological data were reproduced in at least two different cell clones for each model.

Cell culture and transient transfection with plasmids or siRNA knockdown

HeLa cells were grown in DMEM (Invitrogen, Carlsbad, CA) supplemented with 10% fetal bovine serum (EuroClone, Milan, Italy), 100 U/ml penicillin, and 100 μg/ml streptomycin sulfate. One day

colocalizes with APE1 in the nucleoplasm. The inner part of nucleoli, marked in the granular zone by NPM1, is negative for SIRT1. Right, biochemical isolation of nucleoli confirms that SIRT1 localizes in the nucleoplasmic fraction and it is excluded from nucleoli, where nucleolin, NPM1, and APE1 reside (see *Materials and Methods* for details). Nucleolin was used as a positive control for nuclear and nucleolar compartment. (B) Acetylated K^6/K^7-containing APE1 is enriched within the nucleoplasmic compartment with respect to nucleoli. After normalization for total APE1 protein amount, the levels of acetylated APE1 in nucleolar and nucleoplasmic fractions were analyzed through Western blotting. APE1 acetylated at K^6/K^7 residues is predominately present within the nucleoplasmic fraction, whereas it is reduced in the nucleolar fraction. The histogram indicates the relative percentage amount of acetylated APE1 obtained from the densitometric quantification of acetylated APE1 bands normalized with respect to the amount of total APE1 in each fraction. Each bar represents the mean of two independent experiments whose variation was <10%. (C) CD spectra of the APE1(14–38) and APE1(14–38)$^{K27/31/32/35Ac}$ peptides in 10 mM phosphate buffer, pH 7. (D) Comparison of 1D (left), 2D [^{1}H, ^{1}H] TOCSY (middle), and 2D [^{1}H, ^{1}H] ROESY (right) spectra of APE1(14–38) and APE1(14–38)$^{K27/31/32/35Ac}$ peptides in 10 mM phosphate buffer, pH 7.0. Two different expansions of the proton 1D spectrum are shown; the region between 0.8 and 2.4 ppm, in the lower inset, contains signals from side-chain protons. Acetyl methyl groups originate a peak around 2 ppm, which can be clearly seen in the spectrum of the acetylated peptide; peaks of backbone and side-chain $_N$H atoms appear between 7.0 and 8.8 ppm in the upper inset. For 2D [^{1}H, ^{1}H] TOCSY and 2D [^{1}H, ^{1}H] ROESY experiments the H_N-aliphatic protons correlation region of the spectra are reported.

before transfection, cells were seeded in 10-cm plates at a density of 3.0×10^6 cells/plate. Cells were then transiently transfected with the indicated plasmids using the Lipofectamine 2000 reagent (Invitrogen), according to the manufacturer's instructions. Cells were harvested either 24 or 48 h after transfection, as indicated.

For SIRT1-knockdown experiments, HeLa clones were transfected with 150 nM siRNA siGENOME SMART pool or negative control siRNA 5′-CCAUGAGGUCAUGGUCUGdTdT-3′ (Dharmacon, Lafayette, CO), using Oligofectamine (Invitrogen). After 72 h the cells were harvested.

Preparation of total cell extracts and anti-FLAG coimmunoprecipitation

Preparation of total cell lysates and coimmunoprecipitation analyses were performed as described (Vascotto *et al.*, 2009a,b).

Determination of AP endonuclease activity and abasic site assay

Determination of APE1 AP endonuclease activity was performed using an oligonucleotide cleavage assay, as described previously (Vascotto *et al.*, 2009b) and detailed in the Supplemental Information.

Mass spectrometric analysis of APE1 acetylation

Characterization of APE1 acetylation was performed on the immunopurified protein obtained from APE1-FLAG–expressing HeLa cells (Vascotto *et al.*, 2009b). APE1 was resolved by SDS–PAGE; corresponding protein bands were excised, S-alkylated, and digested with endoprotease AspN (Fantini *et al.*, 2010). Digest aliquots were directly analyzed by nanoLC-ESI-LIT-MS/MS using an LTQ XL mass spectrometer (ThermoFisher Scientific, Waltham, MA) equipped with a Proxeon nanospray source connected to an Easy-nanoLC (ThermoFisher Scientific; Arena *et al.*, 2010; Scippa *et al.*, 2010), and analysis of APE1 acetylation was performed as described (D'Ambrosio *et al.*, 2006) and detailed in the Supplemental Information. A semiquantitative measurement of the amino acid modification was obtained by extracting and integrating nanoLC-ESI-LIT-MS peak areas corresponding to *m/z* values of the modified and nonmodified peptides in the same total ion chromatogram (Salzano *et al.*, 2011). Modification extent was then assayed by evaluating the peak area of the modified peptide with respect to that of the modified peptide plus that of the nonmodified peptide, assuming identical ionization properties for modified and nonmodified species. All these analyses were performed in triplicate.

Antibodies for immunofluorescence and immunoblotting

Antibodies used were anti-NPM1 monoclonal, anti-nucleolin monoclonal (Zymed, Invitrogen), anti-FLAG peroxidase-conjugated, anti-GST peroxidase-conjugated, anti-SIRT1 polyclonal (Abcam, Cambridge, MA), anti–c-myc (Santa Cruz Biotechnology, Santa Cruz, CA), and anti–β-tubulin monoclonal (Sigma-Aldrich). Anti-APE1 monoclonal (Vascotto *et al.*, 2009a) and anti-APE1^{K6K7Ac} (Bhakat *et al.*, 2003) were described previously. Anti-APE1$^{K27\text{-}35Ac}$ polyclonal antibody was generated by PRIMM (Milan, Italy; Poletto *et al.*, 2012).

Western blot analyses

For Western blot analyses, the indicated amounts of cell extracts were resolved in 12% SDS–PAGE and transferred to nitrocellulose membranes (Schleicher & Schuell BioScience, Dassel, Germany). Membranes were blocked with 5% (wt/vol) nonfat dry milk in phosphate-buffered saline (PBS) containing 0.1% (vol/vol) Tween 20 and probed with the indicated antibodies; blots were developed by using the ECL enhanced chemiluminescence procedure (GE Healthcare Piscataway, NJ) or Western Lightning Ultra (PerkinElmer, Waltham, MA). Normalization was performed by using a monoclonal anti-tubulin antibody (Sigma-Aldrich). Blots were quantified by using a Chemidoc XRS video densitometer (Bio-Rad, Hercules, CA).

Plasmids and expression of recombinant proteins

Expression and purification of recombinant proteins from *E. coli* were performed as previously described (Vascotto *et al.*, 2009b; Fantini *et al.*, 2010). Where recombinant proteins were used for in vitro assays, the acronym rAPE1 is used.

GST pull-down assay

A 150-pmol amount of either GST-tagged rAPE1^{WT} or mutant proteins was added to 15 μl of glutathione–Sepharose 4B beads (GE Healthcare), together with equimolar amounts of recombinant NPM1. Binding was performed in PBS, supplemented with 1 mM dithiothreitol (DTT) and 0.5 mM phenylmethylsulfonyl fluoride (PMSF) for 2 h, under rotation, at 4°C. Beads were washed three times with PBS, supplemented with 0.1% (vol/vol) Igepal CA-630 (Sigma-Aldrich), 1 mM DTT, and 0.5 mM PMSF and resuspended in Laemmli sample buffer for Western blot analysis.

DNA–RNA ChIP assays

DNA–RNA ChIP assays were carried out by using a modified version of a protocol described earlier (Gilbert *et al.*, 2000) and as detailed in the Supplemental Information.

Enzymatic fluorescence assays

To examine in vitro deacetylase activity on the acetylated APE1 region 25–38, we used the SIRT Fluorescent Activity Assay Kit (Biomol, Plymouth, PA). Optimizing manufacturer's instructions, we used white plates (OPTI PLATE; PerkinElmer) with 384 wells at reduced volume (total reaction volume, 20 μl). Purified peptides were incubated in 25 mM Tris-HCl, pH 8.0, 2.7 mM KCl, 137 mM NaCl, 1 mM $MgCl_2$, and 1 mg/ml bovine serum albumin containing the enzyme (0.04 U/μl) and 25 μM Fluor de Lys-p53 peptide substrate (Arg-His-Lys-Lys [Ac], from region 379–382 of human p53) in the presence/absence of 250 μM NAD^+ for 30 min at 37°C. Deacetylase activity was measured in arbitrary fluorescence units at 460 nm. Dose–response experiments were carried out by using a 0–500 μM range of peptide concentration. Data fitting was performed using the GraphPad Prism 4 software, version 4.02 (GraphPad, La Jolla, CA). Data were in triplicate/duplicate from three independent assays.

Immunofluorescence confocal and proximity ligation analyses

Immunofluorescence procedures and PLA were carried out as described earlier (Vascotto *et al.*, 2009b, 2011). To study the interaction between APE1 and NPM1 in vivo, we used the in situ Proximity Ligation Assay technology (Olink Bioscience, Uppsala, Sweden). After incubation with monoclonal anti-APE1 (1:50) or anti-FLAG antibody (1:200) for 3 h at 37°C, cells were incubated with polyclonal anti-NPM1 (1:200) overnight at 4°C. PLA was performed following manufacturer's instructions. Technical controls, represented by the omission of anti-NPM1 primary antibody, resulted in the complete loss of PLA signal. Cells were visualized through a Leica TCS SP laser-scanning confocal microscope (Leica Microsystems, Wetzlar, Germany). Determination of PLA signals was performed using BlobFinder software (Center for Image Analysis, Uppsala University, Uppsala, Sweden). PLA technology was also used to detect acetylated APE1 at $K^{27}/K^{31}/K^{32}/K^{35}$ residues. Cells were incubated with the

anti-APE1$^{K27–35Ac}$ rabbit-polyclonal antibody diluted 1:1500 and then with a mouse-monoclonal anti-APE1 antibody (1:27). PLA was subsequently carried out following manufacturer's instructions.

Confocal analyses of APE1-Dendra fusion protein through in vivo live imaging

For in vivo APE1-Dendra trafficking studies, HeLa cells were seated on glass-bottom Petri dishes (thickness #1.5; WillCo Wells, Amsterdam, Netherlands), transfected with APE1-Dendra constructs, and grown in the presence of DMEM without phenol red. A Leica TCS SP laser-scanning confocal microscope was equipped with a heating system (Incubator S) and a CO_2 controller (CTI Controller 3700 digital) to maintain cells in optimal growing conditions. Images were captured 24 h after transfection using a 63× oil fluorescence objective. For Dendra green fluorescence acquisition a 488-nm argon laser was regulated at 10% of power with PTM 750 V.

Cell viability, cell growth, and clonogenic assays

Cell viability was measured by using the MTS assay (Celltiter 96 Aqueous One solution cell proliferation assay; Promega, Madison, WI) on HeLa cells stably expressing APE1^{WT}, APE1^{K4pleA}, and APE1^{K4pleR} proteins grown in 96-well plates. After MMS (Sigma-Aldrich) treatment or TBHP (Sigma-Aldrich), the MTS solution was added to each well and the plates were incubated for 2 h. Absorbance was measured at 490 nm by using a multiwell plate reader. The values were standardized to wells containing media alone.

Cell growth assays were performed as described (Vascotto *et al.*, 2009a,b) and detailed in the Supplemental Information, and clonogenic assays were performed according to Plumb (1999) and essentially as described previously (Vascotto *et al.*, 2009a,b).

Circular dichroism spectroscopy

CD spectra were recorded on a Jasco J-810 spectropolarimeter (Jasco, Tokyo, Japan) at 25°C in the far-UV region from 190 to 260 nm. Each spectrum was obtained by averaging three scans, subtracting contributions from the corresponding blanks, and converting the signal to mean residue ellipticity in units of deg-cm^2 dmol^{-1} res^{-1}. Other experimental settings were 20 nm/min scan speed, 2.0 nm bandwidth, 0.2 nm resolution, 50 mdeg sensitivity, and 4 s response. Peptide concentration was kept at 100 μM, and a 0.1 cm path-length quartz cuvette was used. Spectra were acquired in 10 mM phosphate buffer, pH 7.0, containing various percentages of TFE.

NMR spectroscopy

NMR samples were prepared by dissolving APE1 peptides (1.5–2 mg) either in 600 μl of a 10 mM phosphate buffer, pH 7, containing 10% (vol/vol) D_2O or in a mixture of 10 mM phosphate buffer:2-2-2 trifluorethanol-d3 (98% deuterium; Armar Chemicals, Döttingen, Switzerland) 70:30 (vol/vol). The 2D [^{1}H, ^{1}H] TOCSY spectra (1024 × 256 total data points, 32 scans per t1 increment, 70 ms mixing time; Griesinger *et al.*, 1988) were recorded at 298 K on a Varian ^{UNITY}INOVA 600 spectrometer (Palo Alto, CA) equipped with a cold-probe. The 1D proton (128 scans and a relaxation delay of 1.5 s) and 2D [^{1}H, ^{1}H] ROESY (2048 × 256 total data points, 64 scans per t1 increment, 200 ms mixing time) spectra were acquired at 298 K on a Varian ^{UNITY}INOVA 400 spectrometer provided with *z*-axis pulsed-field gradients and a triple-resonance probe. Water signal was suppressed by means of either double pulsed field gradient selective echo techniques (Dalvit, 1998) or continuous wave irradiation. Varian software VNMRJ 1.1D was implemented for spectral processing. The programs MestRe-C2.3a (Universidade de Santiago de Compostela, Santiago de Compostela, Spain) and NEASY (Bartels *et al.*, 1995; www.nmr.ch) were used for analysis of 1D and 2D NMR data, respectively.

Statistical analyses

Statistical analyses were performed by using the Excel (Microsoft, Redmond, WA) data analysis program for Student's *t* test. $p < 0.05$ was considered as statistically significant.

ACKNOWLEDGMENTS

We thank Paolo Peruzzo for generation of mutant recombinant proteins, K. Irani for providing SIRT1-encoding plasmids, and Pablo Radicella for helpful comments on the manuscript. We also thank Julie Driscol for excellent help in editing the manuscript. This work was supported by the Associazione Italiana per la Ricerca sul Cancro (IG10269) and the Ministero dell'Istruzione, dell'Università e della Ricerca (FIRB_RBRN07BMCT and PRIN2008_CCPKRP_003 to G.T.; PRIN2008_CCPKRP_002 and FIRB2008_RBNE08YFN3_003 to A.S.). This work was also supported by a UICC Yamagiwa-Yoshida Memorial International Cancer Study Grant to G.T. and by the Regione Friulia Venezia Giulia for the Project MINA under the Programma per la Cooperazione Transfrontaliera Italia-Slovenia 2007–2013.

REFERENCES

Arena S, Renzone G, Novi G, Paffetti A, Bernardini G, Santucci A, Scaloni A (2010). Modern proteomic methodologies for the characterization of lactosylation protein targets in milk. Proteomics 10, 3414–3434.

Bapat A, Fishel ML, Kelley MR (2009). Going Ape as an approach to cancer therapeutics. Antioxid Redox Signal 11, 651–668.

Bapat A, Glass LS, Luo M, Fishel ML, Long EC, Georgiadis MM, Kelley MR (2010). Novel small-molecule inhibitor of apurinic/apyrimidinic endonuclease 1 blocks proliferation and reduces viability of glioblastoma cells. J Pharmacol Exp Ther 334, 988–998.

Barnes T, Kim WC, Mantha AK, Kim SE, Izumi T, Mitra S, Lee CH (2009). Identification of apurinic/apyrimidinic endonuclease 1 (APE1) as the endoribonuclease that cleaves c-myc mRNA. Nucleic Acids Res 37, 3946–3958.

Bartels C, Xia T, Billeter M, Gunthert P, Wüthrich K (1995). The program XEASY for computer-supported NMR spectral analysis of biological macromolecules. J Biomol NMR 6, 1–10.

Bax A, Davis DG (1985). Practical aspects of two-dimensional transverse NOE spectroscopy. J Magn Reson 63, 207–213.

Bhakat KK, Izumi T, Yang SH, Hazra TK, Mitra S (2003). Role of acetylated human AP-endonuclease (APE1/Ref-1) in regulation of the parathyroid hormone gene. EMBO J 1, 6299–6309.

Busso CS, Iwakuma T, Izumi T (2009). Ubiquitination of mammalian AP endonuclease (APE1) regulated by the p53-MDM2 signaling pathway. Oncogene 28, 1616–1625.

Busso CS, Wedgeworth CM, Izumi T (2011). Ubiquitination of human AP-endonuclease 1 (APE1) enhanced by T233E substitution and by CDK5. Nucleic Acids Res 39, 8017–8028.

Chattopadhyay R, Wiederhold L, Szczesny B, Boldogh I, Hazra TK, Izumi T, Mitra S (2006). Identification and characterization of mitochondrial abasic (AP)-endonuclease in mammalian cells. Nucleic Acids Res 34, 2067–2076.

Chudakov DM, Lukyanov S, Lukyanov KA (2007). Tracking intracellular protein movements using photoswitchable fluorescent protein PS-CFP2 and Dendra2. Nat Protoc 2, 2024–2032.

Colombo E, Marine JC, Danovi D, Falini B, Pelicci PG (2002). Nucleophosmin regulates the stability and transcriptional activity of p53. Nat Cell Biol 4, 529–533.

Dalvit C (1998). Efficient multiple-solvent suppression for the study of the interaction of organic solvents with biomolecules. J Biomol NMR 11, 437–444.

D'Ambrosio C, Arena S, Fulcoli G, Scheinfeld MH, Zhou D, D'Adamio L, Scaloni A (2006). Hyperphosphorylation of JNK-interacting protein 1, a protein associated with Alzheimer disease. Mol Cell Proteomics 5, 97–113.

Demple B, DeMott MS (2002). Dynamics and diversions in base excision DNA repair of oxidized abasic lesions. Oncogene 21, 8926–8934.

Fantini D *et al.* (2008). APE1/Ref-1 regulates PTEN expression mediated by Egr1. Free Radic Res 42, 20–29.

Fantini D *et al*. (2010). Critical lysine residues within the overlooked N-terminal domain of human APE1 regulate its biological functions. Nucleic Acids Res 38, 8239–8256.
Fung H, Demple B (2005). A vital role for APE1/Ref1 protein in repairing spontaneous DNA damage in human cells. Mol Cell 17, 463–470.
Garbutt GJ, Abraham EC (1981). Non-enzymatic acetylation of human hemoglobins. Biochim Biophys Acta 670, 190–194.
Gilbert SL, Pehrson JR, Sharp PA (2000). XIST RNA associates with specific regions of the inactive X chromatin. J Biol Chem 275, 36491–36494.
Gray MJ, Zhang J, Ellis LM, Semenza GL, Evans DB, Watowich SS, Gallick GE (2005). HIF-1alpha, STAT3, CBP/p300 and Ref-1/APE are components of a transcriptional complex that regulates Src-dependent hypoxia-induced expression of VEGF in pancreatic and prostate carcinomas. Oncogene 24, 3110–3120.
Griesinger C, Otting G, Wüthrich K, Ernst RR (1988). Clean TOCSY for 1H spin system identification in macromolecules. J Am Chem Soc 110, 7870–7872.
Grillo C, D'Ambrosio C, Scaloni A, Maceroni M, Merluzzi S, Turano C, Altieri F (2006). Cooperative activity of Ref-1/APE and ERp57 in reductive activation of transcription factors. Free Radic Biol Med 41, 1113–1123.
Hirota K, Matsui M, Iwata Z, Nishiyama A, Mori K, Yodoi J (1997). AP-1 transcriptional activity is regulated by a direct association between thioredoxin and Ref-1. Proc Natl Acad Sci USA 94, 3633–3638.
Hughes RM, (2006). Effects of lysine acetylation in a beta-hairpin peptide: comparison of an amide-pi and a cation-pi interaction. J Am Chem Soc 128, 13586–13591.
Izumi T, Brown DB, Naidu CV, Bhakat KK, Macinnes V, Saito H, Chen DJ, Mitra S (2005). Two essential but distinct functions of the mammalian abasic endonuclease. Proc Natl Acad Sci USA 102, 5739–5743.
Lazzé MC, Pizzala R, Savio M, Stivala LA, Prosperi E, Bianchi L (2003). Anthocyanins protect against DNA damage induced by tert-butyl-hydroperoxide in rat smooth muscle and hepatoma cells. Mutat Res 535, 103–115.
Lee C, Smith BA, Bandyopadhway K, Gjerset RA (2005). DNA damage disrupts the p14ARF-B23(nucleophosmin) interaction and triggers a transient subnuclear redistribution of p14ARF. Cancer Res 65, 9834–9842.
Li M, Vascotto C, Xu S, Dai N, Qing Y, Zhong Z, Tell G, Wang D (2012). Human AP endonuclease/redox factor APE1/ref-1modulates mitochondrial function after oxidative stress by regulating the transcriptional activity of NRF1. Free Radic Biol Med 53, 237–248.
Liu H, Duan Y (2008). Effects of posttranslational modifications on the structure and dynamics of histone H3 N-terminal Peptide. Biophys J 94, 4579–4585.
Marcotte PA, Richardson PL, Guo J, Barrett LW, Xu N, Gunasekera A, Glaser KB (2004). Fluorescence assay of SIRT protein deacetylases using an acetylated peptide substrate and a secondary trypsin reaction. Anal Biochem 332, 90–99.
Meisenberg C *et al*. (2011). Ubiquitin ligase UBR3 regulates cellular levels of the essential DNA repair protein APE1 and is required for genome stability. Nucleic Acids Res 40, 701–711.
Mitra S, Izumi T, Boldogh I, Bhakat KK, Chattopadhyay R, Szczesny B (2007). Intracellular trafficking and regulation of mammalian AP-endonuclease 1 (APE1), an essential DNA repair protein. DNA Repair 6, 461–469.
Nalabothula N, Indig FE, Carrier F (2010). The nucleolus takes control of protein trafficking under cellular stress. Mol Cell Pharmacol 2, 203–212.
Parlanti E, Locatelli G, Maga G, Dogliotti E (2007). Human base excision repair complex is physically associated to DNA replication and cell cycle regulatory proteins. Nucleic Acids Res 35, 1569–1577.
Parsons JL, Tait PS, Finch D, Dianova II, Allinson SL, Dianov GL (2008). CHIP-mediated degradation and DNA damage-dependent stabilization regulate base excision repair proteins. Mol Cell 29, 477–487.
Pines A, Bivi N, Romanello M, Damante G, Kelley MR, Adamson ED, D'Andrea P, Quadrifoglio F, Moro L, Tell G (2005). Cross-regulation between Egr-1 and APE/Ref-1 during early response to oxidative stress in the human osteoblastic HOBIT cell line: evidence for an autoregulatory loop. Free Radic Res 39, 269–281.
Poletto M, Loreto CD, Marasco D, Poletto E, Puglisi F, Damante G, Tell G (2012). Acetylation on critical lysine residues of apurinic/apyrimidinic endonuclease 1 (APE1) in triple negative breast cancers. Biochem Biophys Res Commun 424, 34–39.
Plumb JA (1999). Cell sensitivity assays: clonogenic assay. Methods Mol 28, 17–23.
Salzano AM, Renzone G, Scaloni A, Torreggiani A, Ferreri C, Chatgilialoglu C (2011). Human serum albumin modifications associated with reductive radical stress. Mol Biosyst 7, 889–898.
Schnell U, Dijk F, Sjollema KA, Giepmans BN (2012). Immunolabeling artifacts and the need for live-cell imaging. Nat Methods 9, 152–158.
Scippa GS, Rocco M, Ialicicco M, Trupiano D, Viscosi V, Di Michele M, Arena S, Chiatante D, Scaloni A (2010). The proteome of lentil (*Lens culinaris* Medik.) seeds: discriminating between landraces. Electrophoresis 31, 497–506.
Seemann S, Hainaut P (2005). Roles of thioredoxin reductase 1 and APE/Ref-1 in the control of basal p53 stability and activity. Oncogene 24, 3853–3863.
Sengupta S, Mantha AK, Mitra S, Bhakat KK (2011). Human AP endonuclease (APE1/Ref-1) and its acetylation regulate YB-1-p300 recruitment and RNA polymerase II loading in the drug-induced activation of multidrug resistance gene MDR1. Oncogene 30, 482–493.
Smet-Nocca C, Wieruszeski JM, Melnyk O, Benecke A (2010). NMR-based detection of acetylation sites in peptides. J Pept Sci 16, 414–423.
Szczesny B, Mitra S (2005). Effect of aging on intracellular distribution of abasic (AP) endonuclease 1 in the mouse liver. Mech Ageing Dev 126, 1071–1078.
Tell G, Crivellato E, Pines A, Paron I, Pucillo C, Manzini G, Bandiera A, Kelley MR, Di Loreto C, Damante G (2001). Mitochondrial localization of APE/Ref-1 in thyroid cells. Mutat Res 485, 143–152.
Tell G, Damante G, Caldwell D, Kelley MR (2005). The intracellular localization of APE1/Ref-1: more than a passive phenomenon. Antioxid Redox Signal 7, 367–384.
Tell G, Fantini D, Quadrifoglio F (2010a). Understanding different functions of mammalian AP endonuclease (APE1) as a promising tool for cancer treatment. Cell Mol Life Sci 67, 3589–3608.
Tell G, Quadrifoglio F, Tiribelli C, Kelley MR (2009). The many functions of APE1/Ref-1: not only a DNA-repair enzyme. Antioxid Redox Signal 11, 601–620.
Tell G, Wilson DM 3rd (2010). Targeting DNA repair proteins for cancer treatment. Cell Mol Life Sci 67, 3569–3572.
Tell G, Wilson DM 3rd, Lee CH (2010b). Intrusion of a DNA repair protein in the RNome world: is this the beginning of a new era. Mol Cell Biol 30, 366–371.
Ueno M, Masutani H, Arai RJ, Yamauchi A, Hirota K, Sakai T, Inamoto T, Yamaoka Y, Yodoi J, Nikaido T (1999). Thioredoxin-dependent redox regulation of p53-mediated p21 activation. J Biol Chem 274, 35809–35815.
Vascotto C *et al*. (2011). Knock-in reconstitution studies reveal an unexpected role of Cys-65 in regulating APE1/Ref-1 subcellular trafficking and function. Mol Biol Cell 22, 3887–3901.
Vascotto C *et al*. (2009a). Genome-wide analysis and proteomic studies reveal APE1/Ref-1 multifunctional role in mammalian cells. Proteomics 9, 1058–1074.
Vascotto C *et al*. (2009b). APE1/Ref-1 interacts with NPM1 within nucleoli and plays a role in the rRNA quality control process. Mol Cell Biol 29, 1834–1854.
Vidal AE, Boiteux S, Hickson ID, Radicella JP (2001). XRCC1 coordinates the initial and late stages of DNA abasic site repair through protein-protein interactions. EMBO J 20, 6530–6539.
Wei SJ, Botero A, Hirota K, Bradbury CM, Markovina S, Laszlo A, Spitz DR, Goswami PC, Yodoi J, Gius D (2000). Thioredoxin nuclear translocation and interaction with redox factor-1 activates the activator protein-1 transcription factor in response to ionizing radiation. Cancer Res 60, 6688–6695.
Weibrecht I, Leuchowius KJ, Clausson CM, Conze T, Jarvius M, Howell WM, Kamali-Moghaddam M, Söderberg O (2010). Proximity ligation assays: a recent addition to the proteomics toolbox. Expert Rev Proteomics 7, 401–409.
Wilson DM 3rd, (2010). Small molecule inhibitors of DNA repair nuclease activities of APE1. Cell Mol Life Sci 67, 3621–3631.
Wong HK, Muftuoglu M, Beck G, Imam SZ, Bohr VA, Wilson DM 3rd (2007). Cockayne syndrome B protein stimulates apurinic endonuclease 1 activity and protects against agents that introduce base excision repair intermediates. Nucleic Acids Res 35, 4103–4113.
Yacoub A, Kelley MR, Deutsch WA (1997). The DNA repair activity of human redox/repair protein APE/Ref-1 is inactivated by phosphorylation. Cancer Res 57, 5457–5459.
Yamamori T, DeRicco J, Naqvi A, Hoffman TA, Mattagajasingh I, Kasuno K, Jung SB, Kim CS, Irani K (2010). SIRT1 deacetylates APE1 and regulates cellular base excision repair. Nucleic Acids Res 38, 832–845.
Yu E, Gaucher SP, Hadi MZ (2010). Probing conformational changes in Ape1 during the progression of base excision repair. Biochemistry 49, 3786–3796.
Ziel KA, Campbell CC, Wilson GL, Gillespie MN (2004). Ref-1/Ape is critical for formation of the hypoxia-inducible transcriptional complex on the hypoxic response element of the rat pulmonary artery endothelial cell VEGF gene. FASEB J 18, 986–988.

Acknowledgment - Ringraziamenti

Rare sono le persone che usano la mente. Poche coloro
che usano il cuore e uniche coloro che usano entrambi.
Rita Levi Montalcini

Desidero innanzitutto esprimere un sentito ringraziamento al prof. Gianluca Tell per avermi accolto e dato la possibilità di svolgere il dottorato presso il suo laboratorio ma soprattutto per aver creduto nelle mie capacità.

Ringrazio inoltre tutte le persone che hanno collaborato alla realizzazione dello studio proposto:
dott. Andrea Scaloni, ISPAAM CNR, Napoli;
dott.ssa Chiara D'ambrosio, ISPAAM CNR, Napoli;
dott.ssa Daniela Marasco, Dipartimento di Scienze Biologiche, Università "Federico II" di Napoli;
prof. Federico Fogolari, Università degli Studi di Udine;
prof. Tadahide Izumi, Graduate Center for Toxicology, Università del Kentucky.

Un profondo ringraziamento a tutti i miei colleghi, sia passati che presenti: la dott.ssa Milena Romanello, il dott. Damiano Fantini, il dott. Carlo Vascotto, la dott.ssa Erika Codarin e la dott.ssa Laura Cesaratto per la professionalità e la competenza dimostrata.

Un sincero grazie ai miei compagni di laboratorio, Lisa, Mattia ed Elena perché la loro compagnia e allegria hanno reso piacevoli le intense giornate di lavoro.

Un grazie agli amici di vecchia data e a quelli nuovi che mi fanno sempre ritrovare il sorriso.

Inoltre, ringrazio con affetto i miei familiari per avermi sempre sostenuto e incoraggiato durante tutti questi lunghi anni di studio.

Un ringraziamento speciale, infine, a Christian perché senza la sua pazienza e il suo prezioso aiuto tutto ciò non sarebbe stato possibile.